Bulletin No. 5 (2020–2021)

Global Glacier Change Bulletin

A contribution to

the Global Terrestrial Network for Glaciers (GTN-G) as part of the Global Climate Observing System (GCOS) and its Terrestrial Observation Panel for Climate (TOPC),

the Science Division and the Global Environment Outlook as part of the United Nations Environment Programme (Science Division and GEO, UNEP),

and the International Hydrological Programme of the United Nations Educational, Scientific and Cultural Organization (IHP, UNESCO)

Compiled by
the World Glacier Monitoring Service (WGMS)

ISC (WDS) – IUGG (IACS) – UNEP – UNESCO – WMO | 2023

GLOBAL GLACIER CHANGE BULLETIN

No. 5 (2020–2021)

A contribution to

the Global Terrestrial Network for Glaciers (GTN-G)
as part of the Global Climate Observing System (GCOS)
and its Terrestrial Observation Panel for Climate (TOPC),

the Science Division and the Global Environment Outlook as part of the
United Nations Environment Programme (Science Division and GEO, UNEP),

and the International Hydrological Programme of the United Nations Educational,
Scientific and Cultural Organization (IHP, UNESCO)

Compiled by
the World Glacier Monitoring Service (WGMS)

wgms

Edited by

Michael Zemp, Isabelle Gärtner-Roer, Samuel U. Nussbaumer,
Ethan Z. Welty, Inès Dussaillant, Jacqueline Bannwart

World Glacier Monitoring Service
Department of Geography
University of Zurich
Switzerland

ISC (WDS) – IUGG (IACS) – UNEP – UNESCO – WMO

2023

Imprint

World Glacier Monitoring Service
c/o Department of Geography
University of Zurich
Winterthurerstrasse 190
CH-8057 Zurich
Switzerland
https://www.wgms.ch
wgms@geo.uzh.ch

Contributors

Principal Investigators (see pages 111 ff): data measurements, submission, and review of press proof
National Correspondents (see pages 129 ff): data compilation, submission, and review of press proof
Dilara Kim (Julius-Maximilians-Universität Würzburg, Germany): editing of maps
Susan Braun-Clarke (Translations & Proofreading, Eichenau, Germany): language editing

Printed by

Staffel Medien AG
CH-8045 Zurich
Switzerland

Citation

WGMS 2023. *Global Glacier Change Bulletin No. 5 (2020–2021)*. Zemp, M., Gärtner-Roer, I., Nussbaumer, S.U., Welty, E.Z., Dussaillant, I. and Bannwart, J., (eds.), ISC(WDS)/IUGG(IACS)/UNEP/UNESCO/WMO, World Glacier Monitoring Service, Zurich, Switzerland, 134 pp., publication based on database version: doi:10.5904/wgms-fog-2023-09.

Cover page

Aerial view from the south towards Hofsjökull (photograph taken by Thorsteinn Thorsteinsson on August 20, 2020).

Preface by IACS (IUGG)

The International Association of Cryospheric Sciences (IACS) was established in 2007 as the youngest of eight Associations within the International Union of Geodesy and Geophysics (IUGG). As a service of IACS and several other organizations, WGMS works to assemble and disseminate information on global glacier change and has established itself as the global go-to organization for glacier fluctuation data. These data form a critical component of cryospheric and climate-system monitoring, are indispensable for the expanding suite of large-scale glacier-evolution models and serve as a nucleus for internationally coordinated research efforts. The datasets compiled and maintained by the WGMS enable contributions to ongoing IACS Working Groups, including:

- ‘Regional Assessments of Glacier Mass Change (RAGMAC)’ whose aim is to introduce a new consensus estimate of global glacier mass changes and related uncertainties
- ‘Randolph Glacier Inventory (RGI) and its role in future glacier monitoring and GLIMS’ whose aims are to maintain and further develop the Randolph Glacier Inventory.

The WGMS also contributes information on glacier fluctuations to reports of the Intergovernmental Panel on Climate Change (IPCC), including the Special Report on the Ocean and Cryosphere in a Changing Climate (SROCC 2019), and the Sixth Assessment Report (AR6 2021).

A notable success from this past year was the completion of the eight-year evaluation of the Global Terrestrial Network for Glaciers (GTN-G). The GTN-G is the framework for the internationally coordinated monitoring of glaciers, jointly run by several organizations, including the WGMS. It plays a prominent and respected leadership role in the glaciological community by promoting the democratization of data, facilitating data sharing and exchange, and exercising sound data standardization, curation and management. The 2023 evaluation highlighted strengths of the GTN-G, including keeping up with the increase in quantity and quality of data, which can be accessed through their improved data portal and browser. A major achievement with the increase in data has been the data management and stewardship of the GTN-G. The officers strengthen international collaboration, highlighting the work of the GTN-G as important to researchers, as well as policymakers, stakeholders and the public.

We acknowledge and appreciate the ongoing efforts of the contributors, Principal Investigators and National Correspondents, and applaud their commitment to making observations publicly available through the WGMS. On behalf of the scientific community, we commend the WGMS for its longstanding leadership in the sphere of open data, and for the vital role it continues to play in a rapidly evolving data landscape.

Gwenn Flowers, Prof Dr
Head, Division of Glaciers
IACS

Lauren Vargo, Dr
Deputy Head, Division of Glaciers
IACS

Liss Andreassen, Dr
President
IACS

Preface by IHP, UNESCO

Melting glaciers and ice sheets are the biggest cause of sea level rise in recent decades. Glacier loss is a serious threat to natural and human water supplies in many parts of the world. According to IPCC 2021, risks in physical water availability and water-related hazards will continue to increase by the mid- to long-term in all assessed regions, with greater risk at higher global warming levels.

50 UNESCO World Heritage sites are home to glaciers (a total of 18,600 glaciers have been identified in these 50 sites, covering around 66,000 km²), representing almost 10% of the Earth's total glacierized area. A recent study by UNESCO (UNESCO, IUCN, 2022) highlights the accelerated melting of glaciers in World Heritage sites, with glaciers in a third of sites expected to disappear by 2050.

The need for a worldwide inventory of existing perennial ice and snow masses was first considered during the International Hydrological Decade, declared by UNESCO for 1965–1974 (UNESCO, 1970). However, there still remain deep gaps in monitoring the glacier system in all mountainous regions.

UNESCO's Intergovernmental Hydrological Programme (IHP) plays a key role, as a platform for scientific networking and cooperation, to contribute to assessing and monitoring changes in snow, glaciers and water resources and as well to propose options for adaptation. This role is recognized by the adopted resolution on glaciers preservation by the UN General Assembly (A/RES/77/158) and invites UNESCO to support countries in addressing issues related to accelerated melting of glaciers and its consequences.

The regular publication of Global Glacier Change Bulletins by the World Glacier Monitoring Services (WGMS) is very commendable, the bulletin is produced based on the internationally coordinated systematic observations on glacier fluctuations, which provide a valuable and increasingly important data on glacier changes. The knowledge generated through the monitoring of glacier changes is also a contribution to IHP IX (2022–2029) "Science for a water secure world in a changing environment". The publication is very relevant to the recent UNESCO IHP Projects "Strengthening the resilience of Central Asian countries by enabling regional cooperation to assess high altitude glacio-nival systems to develop integrated methods for sustainable development" and "Adaptation to climate change reducing vulnerabilities of populations in the Central Asia region from glacier lake outburst floods in changing climate".

The periodical publication will also make a contribution to the 2025 the International Year of Glaciers' Preservation and to the World Day for Glaciers on 21 March of each year, adopted by UN General Assembly (A/RES/77/158) to be observed starting in 2025. UNESCO commends WGMS for its ongoing leadership and efforts towards closing the gaps in monitoring the glacier system in all regions.

Abou Amani, Dr
Director Division of Water Sciences, Intergovernmental Hydrological Programme (IHP), UNESCO

Preface by MeteoSwiss

The cryosphere builds an important part of the climate system. Its systematic observation is essential as changes in polar and high mountain areas affect the whole globe. In this regard, the year 2022 was an extreme example, illustrating the impact of rising temperatures on the mass balance of Alpine glaciers. According to observations by Glacier Monitoring Switzerland (GLAMOS), in 2022, Swiss glaciers have lost 6% of their total volume. Never before has such a dramatic glacier melt been observed in Switzerland.

Peak values, such as these, demonstrate the importance of high quality, systematic and long-term climate observations. Without the collection and sharing of these observations, the ability to predict, understand, mitigate, and adapt to changes in the climate system would be limited. Therefore, very recently, at its 19th congress in May 2023, the World Meteorological Organization (WMO) endorsed a resolution addressing the rapid changes in cryosphere by calling for urgent action through coordinated observations and predictions, data exchange, research, and services.

In line with this recent resolution, one purpose of the Global Climate Observing System (GCOS) is to promote the unrestricted distribution of accurate and sustained observations of all components of the climate system. According to the 2022 GCOS Implementation Plan, "ensuring that Global Data Centres exist for all in situ observations of Essential Climate Variables ECVs" is one priority of GCOS. In this context, the importance of the cooperation between GCOS and WGMS is explicitly recognized. While WGMS has been playing an important role in ensuring access to glacier observations since 1894, this illustrates that over the past decades, WGMS has established itself as an outstanding international data centre not only at Swiss but also at global level.

In the framework of GCOS Switzerland, the Federal Office of Meteorology and Climatology MeteoSwiss has been one of the funding agencies for WGMS since over a decade. Today WGMS provides a significant contribution to the international GCOS programme and serves as role model for other data centres. MeteoSwiss is a proud partner of this service and remains strongly committed to continue its engagement to WGMS and GCOS and thereby to the coordinated observation of the climate system.

Bertrand Calpini, Prof Dr
Deputy Director
MeteoSwiss

Michelle Stalder
Head of Swiss GAW/GCOS Office
MeteoSwiss

Foreword by the WGMS Director

Glaciers around the globe continue to melt at rapid rates. In the time period covered by the present bulletin, the glaciers observed lost about 0.75 m water equivalent per year which corresponds to a loss of 750 litres of water reserve per square meter of ice cover and year. With this, glaciers are continuing the historically unprecedented ice loss observed since the turn of the century and amounting to double the ice loss rates of the 1990s (based on the 'reference' glacier sample). Glaciers are indeed key indicators and a unique mean of displaying ongoing climate change. Their rapid decline not only alters the visual landscape of mountain and polar regions, it also has a very real impact on local hazard situations, regional water cycles, and global sea levels.

The present Global Glacier Change Bulletin is the fifth issue of this publication series. The primary focus is on glaciological mass-balance observations that are complemented by geodetic volume changes and front variation series. It serves as an authoritative source of illustrated and commentated information on global glacier changes based on the latest observations from the scientific collaboration network of the WGMS. The present bulletin reports the results from the hydrological years 2019/20 and 2020/21 as well as preliminary observations for 2021/22. Since the last bulletin, we added more than 400 glaciological mass-balance and about 600 front-variation records to our database, reported from about 400 Principal Investigators from 40 countries. In addition, we added over 1 million elevation change records from over 200,000 glaciers from space-borne geodetic surveys (Hugonnet et al., 2021).

Thanks to the global observational coverage, we are now able to combine the seasonal to annual variability from glaciological observations with multi-annual to decadal geodetic elevation changes for improved regional and global estimates of glacier mass changes (Zemp et al., 2019, 2020; Dussaillant et al., 2023). The global mass loss of glacier ice has increased significantly since the 1990s and amounts to around 350 gigatonnes per year for the past decade. This corresponds to an increase in sea level of almost 1 millimetre per year. Corresponding assessments contributed to the latest state of the climate reports (e.g., IPCC AR6, 2021, C3S, 2023) and to global estimates of the Earth's ice imbalance (Slater et al. 2021), water cycle (Dorigo et al., 2021), and energy budget (von Schuckmann et al., 2023) as well as to the Glacier Mass Balance Intercomparison Exercise (https://glambie.org) funded by ESA.

While the successful boost in glacier observations from space provides new insights in global glacier changes, it also required a complete overhaul of the WGMS data infrastructure. The latest evaluation through IACS commended the WGMS to continue its current efforts in data standardization, curation, and management. It also showed the need to push the in-situ network to real-time monitoring and to rethink the concept of the present publication series in view of increasing data volumes and diverging user needs.

Sincere thanks are extended to WGMS co-workers, National Correspondents, and Principal Investigators around the world and their sponsoring agencies at national and international levels for their long-term commitment to building up an unrivalled database which, despite its limitations, undoubtedly remains an indispensable treasury of international snow and ice research, readily available to the scientific community and to the public.

Michael Zemp, Prof Dr
Director, WGMS

TABLE OF CONTENTS

TABLE OF CONTENTS

Please note: This bulletin is published and made available in digital format. A limited edition is printed for the WGMS library. Open access to the data related to this bulletin is provided through the WGMS website: https://www.wgms.ch.

1 INTRODUCTION

Internationally coordinated glacier monitoring began in 1894, with the periodic publication of compiled information on glacier fluctuations starting one year later (Forel, 1895; Allison et al., 2019). In the beginning, glacier monitoring focused mainly on observations of glacier front variations and after the late 1940s on glacierwide mass-balance measurements (Haeberli, 1998). Beginning with the introduction of the Fluctuations of Glaciers (FoG) series in the late 1960s (PSFG, 1967; WGMS, 2012, and volumes in between), standardized data on changes in glacier length, area, volume and mass have been published at pentadal intervals. At the beginning of the 1990s, the Glacier Mass Balance Bulletin series (WGMS, 1991; WGMS, 2013, and issues in between) was designed to speed up access to information on glacier mass balance at two-year intervals. Since the late 1980s, glacier fluctuation data have been organized in a relational database (Hoelzle & Trindler, 1998) and are available in electronic form through websites of the WGMS (https://www.wgms.ch) and GTN-G (https://www.gtn-g.org). The Fluctuations of Glaciers web browser provides easy access to global glacier change data and helps to increase the visibility of related observers, their sponsoring agencies, and the internationally coordinated glacier monitoring network.

In the 1990s, an international glacier monitoring strategy was drawn up for providing quantitative, comprehensive, and easily understandable information relating to questions about process understanding, change detection, model validation and environmental impacts with an interdisciplinary knowledge transfer to the scientific community as well as to policymakers, the media and the public (Haeberli et al., 2000; Haeberli, 1998).

This strategy has five tiers:

1. organizing glacier monitoring as a multi-component system across environmental gradients, thereby integrating glacier-wide observations at the following levels:
2. extensive glacier mass balance and flow studies within major climatic zones for improved process understanding and calibration of numerical models;
3. determination of glacier mass balance using cost-saving methodologies within major mountain systems to assess the regional variability;
4. long-term observations of glacier length changes and remotely sensed volume changes for large glacier samples within major mountain ranges for assessing the representativeness of mass-balance measurement series; and
5. glacier inventories repeated at time intervals of a few decades by using remotely sensed data.

Based on this strategy, the monitoring of glaciers has been internationally coordinated within the framework of GTN-G under the Global Climate Observing System (GCOS) in support of the United Nations Framework Convention on Climate Change (UNFCCC). The GTN-G is run by the WGMS in close collaboration with the U.S. National Snow and Ice Data Center (NSIDC) and the Global Land Ice Measurements from Space (GLIMS) initiative. The WGMS is a permanent service of the International Association of Cryospheric Sciences of the International Union of Geodesy and Geophysics (IACS/IUGG) and of the World Data System within the International Science Council (WDS/ISC) and operates under the auspices of the United Nations Environment Programme (UNEP), United Nations Educational, Scientific and Cultural Organization (UNESCO), and the World Meteorological Organization (WMO).

To further document the evolution and to clarify the physical processes and relationship involved in global glacier changes, the WGMS collects standardized information on changes in glacier length, area, volume, and mass through annual calls-for-data. In 2022, the near-time reporting was extended to all glaciers, after consultation with the WGMS National Correspondents and Principal Investigators, replacing the earlier one-year retention period. This allows the WGMS to report preliminary mass-balance estimates as soon as a few months after the end of the corresponding observation period. In this way, we are responding to the international organisation's increasing need for timely contributions to the various climate status reports and have been able to greatly increase the visibility of the internationally coordinated glacier measurement network. All submitted data are considered public domain and are made available in print and digital form through the WGMS at no cost under the requirement of appropriate citation.

The Global Glacier Change Bulletin series merges the former Fluctuations of Glaciers (Vol. I–X) and Glacier Mass Balance Bulletin (No. 1–12) series. It aims to provide an integrative assessment of global glacier changes every two years. In this process, the main focus is on mass-balance measurements based on the glaciological method (cf. Cogley et al., 2011). This method provides quantitative results at high temporal resolution, which are essential for understanding climate-glacier processes and for allowing the spatial and temporal variability of the glacier mass balance to be captured, even with only a small sample of observation points. The glaciological observations are complemented by results from the geodetic method (cf. Cogley et al., 2011) to extend the glaciological sample in space and time. The geodetic method provides overall glacier volume changes over a longer time period by repeat mapping from ground, air- or space-borne surveys and subsequent differencing of glacier surface elevations. It is recommended to periodically validate and calibrate annual glaciological mass-balance series with decadal geodetic balances to detect and remove systematic biases (Zemp et al., 2013). Meanwhile, geodetic observations from space-borne surveys allow to compute elevation and volume changes for all glaciers in the world (Hugonnet et al. 2021). Related error bars are still relatively large for individual glaciers but the data allow to credibly assess glacier mass-changes at decadal and regional to global scale. In addition, glacier front-variation series are reported for the documentation of clearly visibly glacier reactions to mass changes and for extending observations of glacier fluctuations backward in time.

The Global Glacier Change Bulletin No. 5 is organized in three main sections: global summary, regional summaries, and detailed information for selected glaciers. The global summary provides an overview of reported data and of glaciological balance results for the observation periods 2019/20 and 2020/21, including preliminary values based on the near-time reporting for 2021/22. This first section contains a global map of available glacier fluctuation data, tables with key statistics on reported data and glaciological balance results as well as a set of global figures summarizing reported data and results of changes in glacier mass, volume and length. The second section consists of standardized facts and figures on glacier changes for all glacierized regions of the world, each supplemented with mass balance and front-variation series from selected glaciers. The third section contains detailed information for selected glaciers to provide an insight into the results of the glaciological method. In addition, a list is included naming all Principal Investigators and their sponsoring agencies for the observation periods of the current bulletin as well as of all National Correspondents as of 2023. We note two major changes since the last bulletin. First, the present bulletin is only printed in a limited edition for the WGMS library and archive, and not shipped around the world anymore due to tighter customs regulations and the move away from printed products by many libraries. Second, the production of a data appendix is not practical anymore due to the large volume of now available data from spaceborne observations. However, the bulletin(s) are published and made available in digital and searchable format. And open access to the latest and earlier versions of the database is provided through the WGMS website (https://www.wgms.ch).

2 GLOBAL SUMMARY

Pioneer surveys of accumulation and ablation of snow, firn and ice at isolated points date back to the end of the 19th century and the beginning of the 20th century (e.g., Mercanton, 1916). In the 1920s and 1930s, short-term observations (up to one year) were carried out at various glaciers in the Nordic countries. Continuous, modern series of annual/seasonal measurements of glacier-wide mass balance were started in the late 1940s in Sweden, Norway, and in western North America, followed by a growing number of glaciers in the European Alps, North America, and other glacierized regions. In the meantime, more than 7,800 glaciological mass-balance observations from 490 glaciers have been collected and made available by the WGMS.

For the observation periods covering the hydrological years 2019/20 and 2020/21, 318 annual mass-balance observations were compiled based on 169 glaciers worldwide. Of these observations, 71%, 65%, and 49% were reported including seasonal mass balance, mass distribution with elevation, and point measurements, respectively. Preliminary results for 2021/22 were reported for 71% of these glaciers. In addition, more than 1 million elevation change records and 600 front variations from over 200,000 and 390 glaciers, respectively, were added since the last bulletin. The large number of geodetic observations is the result of the compilation of geodetic assessments, provided by the research community using space-borne sensors, within the framework of ESA's Climate Change Initiative (CCI, CCI+) and Europe's Copernicus Climate Change Service (C3S). A global overview of available glacier change data is shown in Figure 2.1. Reported data for the observation periods covered by the present bulletin are given in Table 2.1.

Table 2.1 Annual mass balances for the observation periods 2019/20 and 2020/21 as well as preliminary values (*) for 2021/22. Abbreviations and units: PU = political unit; B20, B21, B22* in mm w.e.; ELA = equilibrium line altitude in m a.s.l.; AAR = accumulation area ratio in %. ELA0 and AAR0 correspond to balanced-budget ELA and AAR, respectively, and are derived from linear regressions with B as independent variable (cf. Chapter 4). WGMS '**reference**' and 'benchmark' glaciers are highlighted with grey background.

PU	Glacier name	1st/last/nr years	B20	B21	B22*	ELA20	ELA21	ELA$_0$	AAR20	AAR21	AAR$_0$
AQ	Bahía del Diablo	2000/2022/23	–400	–740	–291	450	500	350	25	27	55
AQ	Hurd	2002/2021/20	–1180	–180		300	260	192	8	31	56
AQ	Johnsons	2002/2021/20	–800	210		>360	160	190	0	76	58
AR	Agua Negra	2015/2020/06	–1264			>5280			0		
AR	Brown Superior	2008/2022/15	–3826	–1106	–2026						
AR	Conconta Norte	2008/2022/15	–2887	–962	–1834						
AR	De Los Tres	1996/2020/09	–535			1470		1432	47		75
AR	Martial Este	2001/2022/22	–692	–1133	–480	1090		1067	10	0	56
AT	**Goldbergkees**	**1989/2022/34**	**–1093**	**–504**	**–2800**	**3050**	**2850**	**2892**	**10**	**35**	**44**
AT	Hallstätter Gletscher	2007/2022/16	–1440	–1228	–2602	2812		2498	14	0	62
AT	**Hintereisferner**	**1953/2022/70**	**–970**	**–668**	**–3319**	**3193**	**3095**	**2921**	**32**	**40**	**66**
AT	**Jamtalferner**	**1989/2022/34**	**–1675**	**–1000**	**–3630**		**3079**	**2769**	**0**	**8**	**56**
AT	**Kesselwandferner**	**1953/2022/70**	**–522**	**–183**	**–2800**	**3239**	**3177**	**3120**	**39**	**53**	**68**
AT	Kleinfleisskees	1999/2022/24	–738	–291	–2700	3000	2950	2866	24	51	59
AT	**Pasterze**	**1980/2022/35**	**–1011**	**-740**	**–2300**	**3025**	**2940**	**2713**	**39**	**52**	**91**
AT	Seekarles Ferner	2014/2022/09	–731	–650	–3289	3160	3160		24	37	53
AT	Stubacher Sonnblickkees[1]	1946/2021/70	–627	–688		2905	2905	2748	29	26	58
AT	Venedigerkees	2013/2022/10	–392	–248	–2208	2944	2875	2849	45	58	55
AT	**Vernagtferner**	**1965/2022/58**	**–824**	**–593**	**–3249**	**3275**	**3248**	**3084**	**24**	**23**	**65**

PU	Glacier name	1st/last/nr years	B20	B21	B22*	ELA20	ELA21	ELA$_0$	AAR20	AAR21	AAR$_0$
AT	Wurtenkees[2]	1983/2022/40	–1342	–458	–3596	>2750	>2750	2890	10	28	36
AT	Zettalunitz/ Mullwitzkees	2007/2022/16	–393	–446	–2449	3130	3122	3085	41	40	42
BO	Charquini Sur	2003/2021/19	–600	117		5234	5184	5176	17	19	36
BO	**Zongo**	**1992/2021/30**	**–334**	**119**		**5260**	**5359**	**5274**	**72**	**68**	**67**
BT	Thana	2020/2021/02	–2784	–1699		>5600			0		
CA	Athabasca	2013/2022/08		–445	–260		2680	2701		72	71
CA	Bologna	2016/2022/04			–257						
CA	**Devon Ice Cap NW**	**1961/2022/62**	**–647**	**–5**	**–508**	**1600**	**1030**	**1016**	**6**	**67**	**70**
CA	**Helm**	**1975/2022/46**	**–1470**	**–3070**	**–1002**	**>2080**	**2115**	**1994**	**2**	**2**	**35**
CA	Kokanee	2015/2022/08	–91	–1922	–80	2635	>2799	2583	39	1	56
CA	**Meighen Ice Cap**	**1960/2022/63**	**–726**	**–131**	**–451**	**>270**	**>270**		**0**	**0**	
CA	**Melville South Ice Cap**	**1963/2022/60**	**–807**	**122**	**–1077**	**>715**	**<526**		**0**	**100**	
CA	**Peyto**	**1966/2022/57**	**–474**	**–1925**	**–848**	**>2690**	**2910**	**2610**	**27**	**6**	**51**
CA	**Place**	**1965/2022/57**	**–1650**	**–2379**	**–870**	**>2450**	**2450**	**2091**	**1**	**2**	**47**
CA	**White**	**1960/2022/60**	**–552**	**–107**	**–472**	**1344**	**1083**	**939**	**24**	**62**	**70**
CH	Adler	2006/2021/16	–491	–513		3485	3505	3394	43	40	57
CH	**Allalin**	**1956/2022/67**	**–395**	**–452**	**–2372**	**3365**	**3385**	**3247**	**49**	**47**	**58**
CH	**Basòdino**	**1992/2021/30**	**–539**	**–439**		**3055**	**3065**	**2877**	**10**	**9**	**49**
CH	Claridenfirn[3]	1915/2021/107	–750	–408		2905	2885	2756	37	43	62
CH	Corbassière	1997/2021/25	–640	–729		3285	3345	2992	48	39	71
CH	Corvatsch South[4]	2014/2021/08	–881	–937		3312	3302	3269	12	15	35
CH	Findelen	2005/2021/17	–250	–531		3285	3345	3220	58	49	66
CH	**Giétro**	**1967/2022/56**	**–439**	**–556**	**–2724**	**3225**	**3285**	**3157**	**52**	**35**	**61**
CH	**Gries**	**1962/2022/61**	**–1218**	**–892**	**–3645**	**3075**	**3085**	**2821**	**16**	**15**	**56**
CH	Grosser Aletsch	1940/2021/62	–1165	–115		3125	2965	2904	51	61	65
CH	Hohlaub	1956/2021/66	–174	–183		3195	3185	3149	54	56	59
CH	Murtèl[4]	2013/2021/09	–311	–372		3202	3217	3188	43	28	52
CH	Oberaar	2021/2022/02		–300	–3000		2800			57	
CH	Otemma	2020/2021/02	–1168	–909		3165	3135		25	31	
CH	Pers	2020/2021/02	–591	–525		3015	3025		43	42	
CH	Pizol[4]	2007/2021/15	–1345	–310		2722	2712	2695	5	18	19
CH	Plaine Morte	2010/2021/12	–1443	–982		2805	2795		0	0	
CH	Rhone	1885/2021/44	–686	–102		2915	2855	2846	57	65	62
CH	Sankt Anna[4]	2012/2021/10	–766	–484		2857	2842	2781	7	11	31
CH	Schwarzbach[4]	2013/2021/09	–446	–334		2822	>2832	2784	8	0	50
CH	Schwarzberg	1956/2021/66	–517	–698		3125	3135	3018	40	37	56
CH	Sex Rouge[4]	2012/2021/10	–1811	–479		2882	2832		0	10	
CH	**Silvretta**	**1919/2022/104**	**–915**	**–868**	**–3188**	**2905**	**2925**	**2746**	**25**	**20**	**56**
CH	Tsanfleuron	2010/2021/12	–2263	–607		2975	2855		0	10	
CL	**Echaurren Norte[5]**	**1976/2022/47**	**–2430**	**–700**	**–1161**						
CL	Mocho Choshuenco SE	2004/2021/12	–800	–1615			>2400	1922			59
CN	Parlung No. 94	2006/2021/16	–1489	–2065		5458	5503	5363	14	5	46
CN	**Urumqi Glacier No. 1[6]**	**1959/2022/51**	**–230**	**–829**	**–1251**	**4020**	**4275**	**4004**	**52**	**5**	**59**
CN	Urumqi Glacier No. 1 E-Branch	1988/2022/32	–310	–824	–1315	3987	4200	3948	48	2	64

PU	Glacier name	1st/last/nr years	B20	B21	B22*	ELA20	ELA21	ELA_0	AAR20	AAR21	AAR_0
CN	Urumqi Glacier No. 1 W-Branch	1988/2022/35	–89	–837	–1134	4053	4350	4051	59	10	61
CO	Conejeras[5]	2006/2021/16	–4986	–2786		>4913	>4871		0	1	
CO	Ritacuba Blanco	2009/2021/12		367			4949	5006		82	57
EC	Antizana 15 Alpha	1995/2021/27	–930	–840		5145	5132	5067			72
ES	**Maladeta**[5]	**1992/2022/31**	**–212**	**–1939**	**–3017**	**3117**	**>3200**	**3069**	**46**	**0**	**43**
FR	**Argentière**	**1976/2022/47**	**–1030**	**–370**	**–3800**	**2900**	**2850**				
FR	Gébroulaz	1995/2022/28	–430	–1000	–2550	3000	2875	2949			
FR	Ossoue[5]	2002/2022/21	–1510	–2220	-4060	>3200			0		53
FR	**Saint Sorlin**	**1957/2022/66**	**–1140**	**–1390**	**–3810**	**2950**	**2950**	**2852**			
FR	**Sarennes**[5]	**1949/2022/74**	**–100**	**–70**	**–4260**	**>2970**			**0**		
FR	Tré-la-Tête	2014/2022/09	–1550	–210	–4560						
GL	Freya	2008/2022/15	–510	–900	–700	1100	>1300	709	10	5	59
GL	Mittivakkat	1996/2022/27	–1390	–1720	–1450	>930	>930	497	0	0	58
GL	Qasigiannguit	2013/2022/10	–643	–265	–26	908	893	831	39	37	50
IN	Batal	2017/2020/04	–160								
IN	Chhota Shigri	1987/2022/20			–1475			4974			59
IN	Hoksar	2014/2022/09	–70	–1440	–1530	4000	4110	3953	67	47	76
IN	Kolahoi	2015/2022/08	–90	–1390	–1678	4360	4440	4328	63	54	67
IN	Sutri Dhaka	2017/2020/04	–230			5279			60		
IS	**Brúarjökull**	**1993/2022/30**	**–175**	**–840**	**344**	**1220**	**1335**	**1205**	**60**	**48**	**61**
IS	Dyngjujökull	1992/2022/25	216	–710	422	1320	1465	1348	68	53	62
IS	**Eyjabakkajökull**	**1991/2022/31**	**–778**	**–1477**	**–359**	**1165**	**1215**	**1085**	**47**	**27**	**55**
IS	**Hofsjökull E**	**1989/2022/34**	**–680**	**–800**	**–190**	**1234**	**1263**	**1144**	**44**	**43**	**51**
IS	**Hofsjökull N**	**1988/2022/35**	**–390**	**–1410**	**280**	**1274**	**1381**	**1250**	**43**	**24**	**52**
IS	**Hofsjökull SW**	**1990/2022/33**	**–80**	**–480**	**460**	**1339**	**1355**	**1272**	**55**	**52**	**53**
IS	Köldukvíslarjökull	1992/2022/29	–151	–1322	386	1440	1590	1361	53	34	57
IS	Langjökull Ice Cap	1997/2022/26	–564	–1790	–50				48	15	57
IS	**Tungnárjökull**	**1986/2022/31**	**–774**	**–1611**	**–1355**	**1225**	**1350**	**1143**	**50**	**31**	**62**
IS	Vatnajökull	2020/2020/01	–300								
IT	Calderone	1995/2022/24	–496	–292	–308			2683			63
IT	Campo settentrionale[5]	2010/2022/13	–226	–350	–3130	3060	3080	3058	39	28	40
IT	**Caresèr**[5]	**1967/2022/56**	**–1371**	**–950**	**–3965**	**3114**	**3106**	**3091**	**1**	**3**	**44**
IT	**Ciardoney**[5]	**1992/2022/31**	**–780**	**–1330**	**–4000**	**3100**	**>3120**	**2980**	**<5%**	**0**	**54**
IT	Grand Etret	2000/2022/23	–333	–1715	–3662	3050	3070		37	11	
IT	Lupo	2010/2022/13	–421	–211	–4000	2600	2600	2577	25	32	46
IT	Malavalle/ Übeltalferner	2002/2022/21	–574	–420	–3174	3156	3108	3017	19	30	43
IT	Pendente/ Hangender Ferner	1996/2022/27	–1896	–1200	–3493	>2950	2934	2814	2	0	39
IT	Suretta meridionale[5]	2010/2022/13	–1323	–737	–3564	2860	2825	2769	2	19	54
IT	Timorion	2001/2020/18	–695			>3480			0		
IT	Vedretta de La Mare	2003/2021/19	–392	–64		3245	3216	3170	41	49	49
IT	Vedretta occ. di Ries/ Westlicher Rieserferner	2009/2022/14	14	–202	–2487	3000	3050	3003	44	40	48
JP	Hamaguri Yuki[4]	1968/2022/51	–1636	1029	40						
KG	**Abramov**	**1968/2022/42**	**124**	**–1296**	**–762**	**4115**	**4310**	**4156**	**71**	**48**	**65**

PU	Glacier name	1st/last/nr years	B20	B21	B22*	ELA20	ELA21	ELA_0	AAR20	AAR21	AAR_0
KG	Batysh Sook/ Syek Zapadniy	1971/2022/17	4	–362	–941	4135	4330	4212	89	38	59
KG	Bordu	2016/2022/07	–70	–650	–1270	4210	4400	4259	54	17	43
KG	Glacier No. 354 (Akshiyrak)	2011/2022/12	–35	–1100	–753	4205	4440	4143	51	6	61
KG	Glacier No. 599 (Kjungei Ala-Too)	2015/2022/08	15	–352	–1458	4004	4071	4052	65	39	53
KG	**Golubin**	**1969/2022/38**	**213**	**–194**	**–1050**	**3755**	**3840**	**3800**	**72**	**78**	**72**
KG	**Kara-Batkak**	**1957/2022/51**	**–240**	**–490**	**–810**	**3910**	**3980**	**3854**	**54**	**46**	**57**
KG	Sary Tor (Glacier No. 356)	1985/2022/13	–10	–410	–1270	4210	4320	4231	64	44	49
KG	Turgen-Aksuu	2019/2022/04	–343	–847	–1055	4040	4240		48	26	
KZ	**Ts. Tuyuksuyskiy**	**1957/2022/66**	**–287**	**–609**	**–1130**	**3800**	**3870**	**3752**	**46**	**36**	**52**
NO	**Ålfotbreen**	**1963/2022/60**	**1003**	**–1707**	**–550**	**<1000**	**>1360**	**1194**	**100**	**0**	**56**
NO	Austdalsbreen[7]	1988/2022/35	801	–1775	–50	1375	>1740	1421	82	0	69
NO	**Engabreen**	**1970/2022/53**	**1170**	**–500**	**150**	**1017**	**1234**	**1161**	**85**	**47**	**60**
NO	**Gråsubreen**	**1962/2021/60**	**–643**	**–1541**		**>2277**	**>2777**	**2100**	**0**	**0**	**36**
NO	Hansebreen	1986/2022/37	486	–2335	–1050	1065	>1303	1141	80	0	57
NO	**Hellstugubreen**	**1962/2021/60**	**–436**	**–1279**		**1935**	**2155**	**1851**	**33**	**1**	**56**
NO	**Langfjordjøkelen**	**1989/2022/32**	**–19**	**–195**	**–1900**	**830**	**780**	**768**	**59**	**65**	**62**
NO	**Nigardsbreen**	**1962/2022/61**	**1651**	**–566**	**800**	**1285**	**1645**	**1550**	**93**	**46**	**59**
NO	**Rembesdalskåka**	**1963/2022/60**	**637**	**–1529**	**100**	**1580**	**>1851**	**1667**	**86**	**0**	**71**
NO	**Storbreen**	**1949/2021/73**	**–46**	**–1672**		**1760**	**2015**	**1716**	**53**	**2**	**57**
NP	Mera	2008/2022/15	–490	290	–850	5684	5330	5532	40	86	58
NP	Pokalde	2010/2011/13	–970	–150	–840	5626	5589	5580	13	41	46
NP	Rikha Samba	1999/2021/11	–218	–218		5858	5858	5797	37	37	62
NP	West Changri Nup	2011/2022/12	–830	–350	–2500	5526	5534	5520	29	29	32
NP	Yala	2012/2022/11	–865	477	–1065	5459	5330	5382	26	63	46
NZ	Brewster	2005/2022/18	–1454	178	–1125	2225	1907	1938	7	43	45
NZ	Rolleston	2011/2022/12	–649	–993	–1065	1815	1810	1804	39	44	55
RU	**Djankuat**	**1968/2022/55**	**–1370**	**–170**	**–590**	**3470**	**3180**	**3191**	**18**	**63**	**59**
RU	**Garabashi**	**1984/2022/39**	**–1427**	**–502**	**–1153**			**3789**	**8**	**48**	**60**
RU	**Leviy Aktru**	**1977/2022/40**	**–947**	**–531**	**–603**	**3670**	**3350**	**3163**	**35**	**56**	**61**
SE	**Mårmaglaciären**	**1990/2022/32**		**–755**	**–427**	**1635**	**1617**	**1578**	**14**	**24**	**35**
SE	**Rabots glaciär**	**1946/2022/39**	**–106**	**–500**	**–943**	**1499**	**1492**	**1379**	**40**	**34**	**48**
SE	**Riukojietna**	**1986/2022/34**	**–702**	**–822**	**–795**	**1364**	**1420**	**1333**	**5**	**0**	**56**
SE	**Storglaciären**	**1946/2022/77**	**136**	**–823**	**–212**	**1402**	**1549**	**1462**	**56**	**30**	**46**
SJ	**Austre Brøggerbreen**	**1967/2022/56**	**–1744**	**–600**	**–1393**	**788**	**465**	**291**	**0**	**5**	**47**
SJ	Grønfjord E	1986/2021/09	–1965	–1680		>560	>560			0	
SJ	Hansbreen[7]	1989/2021/32		–725				311		12	56
SJ	Irenebreen	2002/2021/20	–2204	–745	-2164	886	564	305	0	0	27
SJ	Kongsvegen[7]	1987/2022/36	–1081	–160	–968	766	573	535	0	35	47
SJ	Kronebreen[7]	2003/2022/14	–1133	30	–809	941	694	676	14	38	42
SJ	**Midtre Lovénbreen**	**1968/2022/55**	**–1574**	**–540**	**–1239**	**648**	**438**	**309**	**0**	**9**	**52**
SJ	Nordenskioeldbreen	2006/2021/15		–122			691	660			50
SJ	Waldemarbreen	1995/2021/27	–2276	–947	-2198	642	493	293	0	1	31
SJ	Werenskioldbreen	1980/2020/10	–1773			618					
TJ	East Zulmart (Glacier No 139)	2019/2022/04	–210	–206	–311	5250	5300		37	36	

PU	Glacier name	1st/last/nr years	B20	B21	B22*	ELA20	ELA21	ELA$_0$	AAR20	AAR21	AAR$_0$
TJ	Glacier No 457	2021/2022/02		–353	–437		5030			50	
TJ	Glacier No 676	2020/2020/01	–98			3660			58		
TJ	Yakarcha (Glacier No 71)	2020/2020/01	139			4100			62		
US	**Columbia (2057)**	**1984/2022/39**	**–892**	**–866**	**–861**	**1640**	**1650**	**1577**	**40**	**40**	**63**
US	Daniels	1984/2022/39	–380	–2150	–1180				57	12	61
US	**Easton**	**1990/2022/33**	**–633**	**–1562**	**–1216**	**2160**	**2400**	**2066**	**48**	**23**	**66**
US	**Gulkana**	**1966/2022/57**	**–190**	**–770**	**–1160**	**1792**	**1805**	**1742**			**62**
US	Ice Worm	1984/2022/39	–620	–1450	–1260				45	31	63
US	**Lemon Creek**	**1953/2022/70**	**–950**	**–540**	**–680**	**1179**	**1093**	**1016**			**60**
US	Lower Curtis	1984/2022/39	–810	–1480	–730	1660	1680	1650	46	32	62
US	Lynch	1984/2022/39	–580	–2260	–1360				51	18	65
US	**Rainbow**	**1984/2022/39**	**–441**	**–945**	**–751**	**1950**	**1860**	**1704**	**48**	**38**	**64**
US	Sholes	1990/2022/33	–1960	–1720	–1810				21	24	62
US	**South Cascade**	**1953/2022/69**	**–150**	**–1210**	**–1260**	**1891**	**2262**	**1913**			**54**
US	Sperry	2005/2022/18	–370	–2240	–1010	2346	2576	2442			
US	Taku[8]	1946/2022/77	–180	30	–180	1086	1004	1038			
US	**Wolverine**	**1966/2022/57**	**–1810**	**–930**	**–1180**	**1335**	**1236**	**1162**			**63**
UZ	Barkrak Sredniy	2017/2022/06	–281	–671	–571	3736	3747	3706	52	51	62
UZ	Barkrak Sredniy E	2018/2022/05	–441	–662	–498	3752	3770		65	59	

1 = based on Ba-AAR regression from 1963/64 to 1979/80

2 = influenced by strong glacier disintegration and artificial snow management

3 = balances include estimates for dry calving

4 = glacieret (cf. Cogley et al., 2011)

5 = influenced by strong glacier disintegration

6 = In 1993, Urumqi Glacier No. 1 divided into two parts: the East Branch and the West Branch.

7 = glacier influenced by calving

8 = The mass balance of this tidewater glacier is determined by a combination of snow pit, ablation stake measurements, observations of the transient snowline, and the ELA.

Climate (change)-related trend analysis is, in the ideal case, based on long-term measurement series. Ongoing glaciological mass-balance records for more than 30 continuous observation years are recognized as WGMS 'reference' glaciers. These glaciers have well-documented and long-term mass-balance programmes based on the direct glaciological method (cf. Østrem & Brugman, 1991; Cogley et al., 2011), are not dominated by non-climatic drivers such as calving or surge dynamics, and fulfil a set of criteria as described on the WGMS website (https://wgms.ch/products_ref_glaciers/). It is recommended that these glaciological results be validated and, if necessary, calibrated with independent results from the geodetic method (cf. Zemp et al., 2013). In 2023, we introduced the WGMS 'benchmark' glaciers, after consultation with our international collaboration network. The label 'benchmark' glacier is awarded to selected glaciological mass-balance programmes that have not yet reached 30 years of ongoing measurements but are located in regions without 'reference' glaciers, or where existing 'reference' glaciers are about to vanish. Benchmark glaciers fulfil the preconditions as defined for the 'reference' glaciers, have a time series of more than 10 years of ongoing glaciological mass-balance measurements, and can have a maximum observational gap of one year in the past decade. The present bulletin lists 60 'reference' and 25 'benchmark' glaciers (Table 2.1). Results of the 'reference' glaciers are summarized in Table 2.2 and in Figure 2.2.

Table 2.2 Summarized mass balance data. A statistical overview of the results of the 'reference' glacier sample is given for the three recent reporting periods 2019/20, 2020/21, and 2021/22* (upper table) in comparison with corresponding values averaged for the decades 1981–1990, 1991–2000, 2001–2010, and 2011–2020 (lower table). All annual balance values in mm w.e.; * = preliminary values.

	2019/20	2020/21	2021/22*
mean specific (annual) mass balance	–600	–855	–1452
standard deviation	731	623	1315
minimum value	–2430	–3070	–4260
maximum value	1651	122	800
nr of positive/reported balances	8/61	2/60	6/56
mean AAR	36%	30%	21%

decadal averages of:	1981–1990	1991–2000	2001–2010	2011–2020
mean specific (annual) mass balance	–294	–445	–828	–832
standard deviation	721	767	835	843
minimum	–1999	–2601	–3061	–2968
maximum	1847	1353	984	1122
avg nr of positive/reported balances	13/46	15/59	9/57	9/59
mean AAR	49%	44%	33%	33%

Taking the two years of this reporting period and preliminary results for 2019/20 together (from the near-time reporting), the mean annual mass balance was –0.97 m w.e. per year. This is 17% more negative than the mean annual mass balance for the first two decades of the 21st century (Table 2.2) which were without precedent on a global scale, at least for the time period with available observations (Zemp et al., 2015). Since the turn of the century, the maximum mass loss of the 1980–2000 time period (i.e., less than –0.9 m w.e. observed in 1997/98) was reached or exceeded nine times: in 2002/03, 2004/05, 2005/06, 2009/10, 2010/11, 2014/15, 2017/18, 2018/19, and again in 2021/22. The percentage of positive annual mass balances decreased from 28% in the 1980s to 9% (2019/20–2021/22), and there have been no more years with a positive mean balance for more than five decades. The melt rate and cumulative loss in glacier thickness continues to be extraordinary. Furthermore, the analysis of mean AAR values shows that the glaciers are in strong and increasing imbalance with the climate and hence will continue to lose mass even if climate remained stable (Mernild et al., 2013). As such, mean AAR values indicate that the observed glaciers would

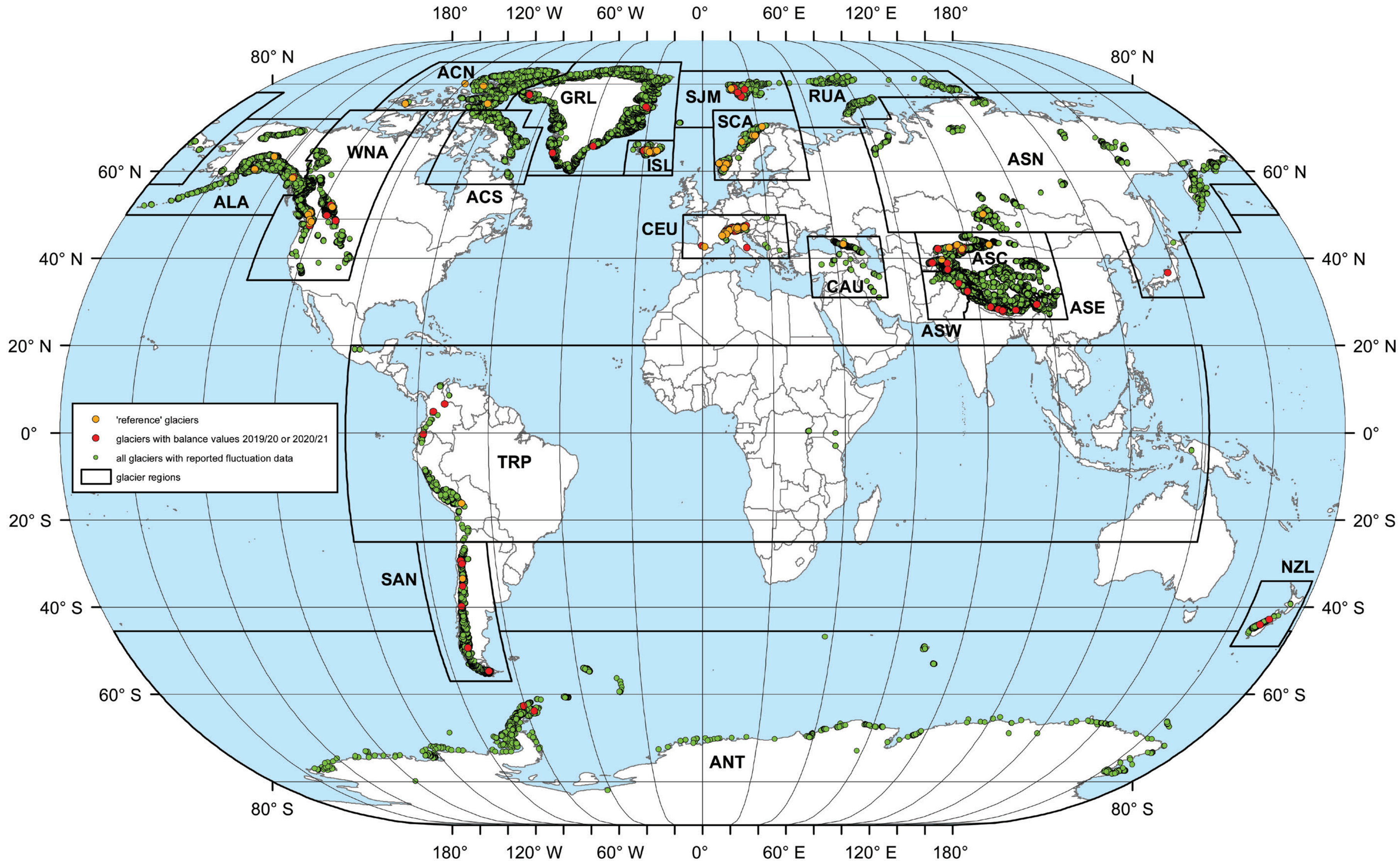

Figure 2.1 Location of all glaciers for which fluctuation data or special events are available from the WGMS. This overview includes 169 glaciers with reported mass balance data for the observation periods 2019/20 and 2020/21, and 60 'reference' glaciers with well-documented and independently calibrated, long-term mass balance programmes based on the glaciological method. The glacier regions are based on GTN-G (2017).

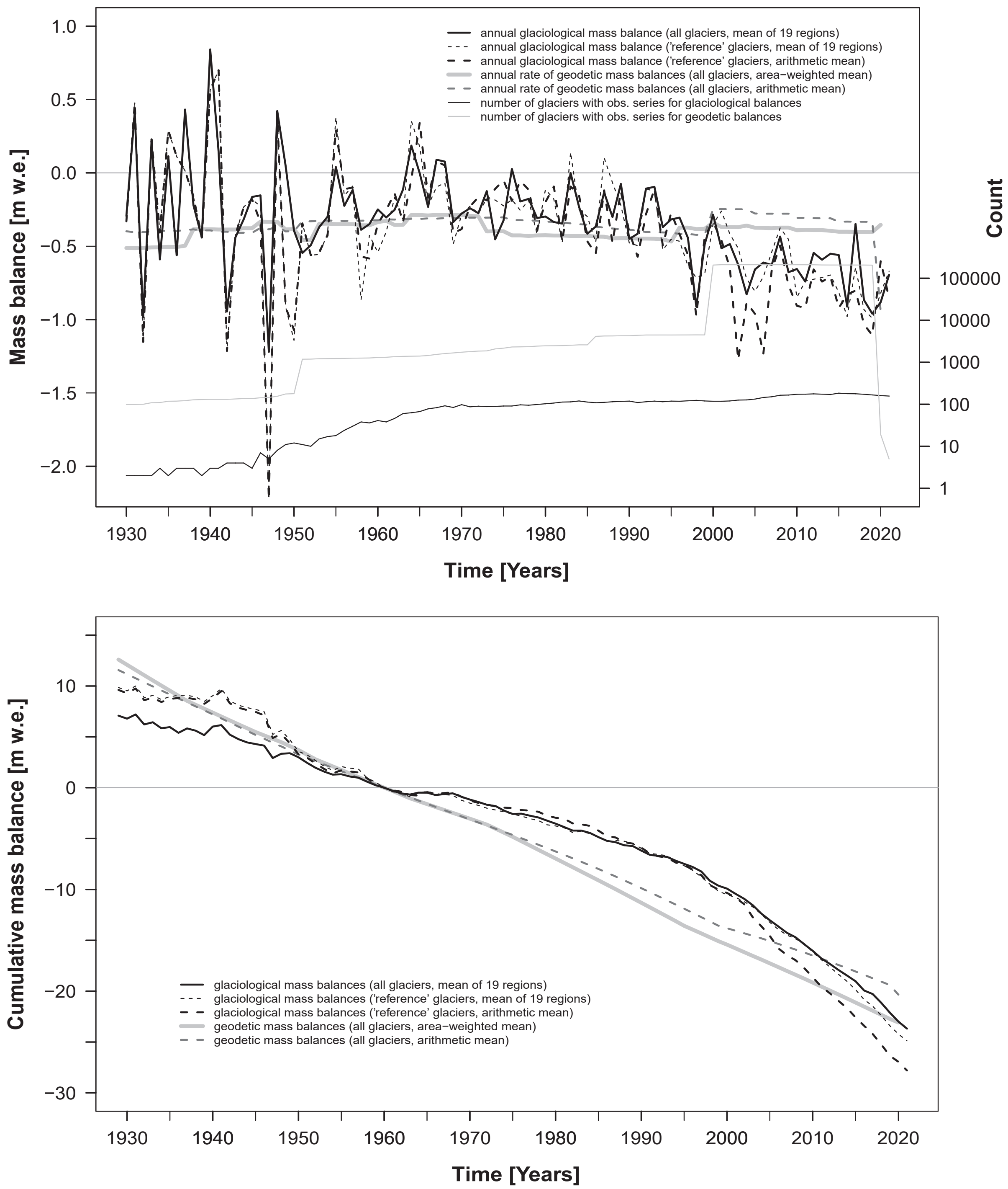

Figure 2.2 Global averages of observed mass balances from 1930 to 2021. Annual glaciological balances (m w.e.) and annual rates of geodetic balances (m w.e. a^{-1}) are shown together with the corresponding number of observed glaciers (upper graph). Cumulative annual averages relative to 1960 (lower graph). Geodetic balances were calculated assuming a glacier-wide average density of 850 kg m^{-3}. Note that the strong variability in the glaciolgocal data before 1960 is due to the small sample size.

be committed to an average area loss of 41% under the climatic conditions of the reporting period.

The arithmetic mean of the 'reference' glaciers included in the analysis is based on a relatively small sample and influenced by the large proportion of Alpine and Scandinavian glaciers. Therefore, mean values are also calculated for (i) all mass balances available, independent of record length, and (ii) using only one single value (averaged) for each of the 19 regions (cf. GTN-G, 2017). Looking at the regional average of the 'reference' glaciers, the mean annual balance of the current reporting period (incl. preliminary estimates of 2021/22) resulted in –0.85 m w.e. per year, which is slightly less negative than the arithmetic mean. Since

2010, 9 out of 13 years ranked in the top 10 with respect to glacier mass loss since 1960. Note that the balance variability before 1960 is strongly influenced by the very small sample size. Figure 2.2 shows the number of reported observation series as well as annual and cumulative results for all three means. In their general trend and magnitude, all three averages relate quite closely to each other and are in good agreement with the results from a moving-sample averaging of all available data (cf. Kaser et al., 2006; Zemp et al., 2009; Zemp et al., 2015). The global average cumulative mass balance indicates a strong mass loss in the first decade after the start of measurements in 1946 (though based on few observation series only), slowing down in the second decade (1956–1965; based on observations above 30° N only), followed by a moderate ice loss between 1966 and 1985 (with data from the Southern Hemisphere only since 1976) and a subsequent acceleration of mass loss to the present time (2019).

The geodetic method (cf. Cogley et al., 2011) provides overall glacier-volume changes over a longer time period by repeat mapping from ground, air- or spaceborne surveys and subsequent differencing of glacier surface elevations. The geodetic results - shown as arithmetic and area-weighted means - allow the glaciological sample to be extended in both space and time (Figures 2.2, 2.3). Over the past decade, we were able to boost the geodetic sample by integration of results from large assessments (e.g., Gardelle et al., 2013, Fischer et al., 2015; Le Bris and Paul, 2015; Vijay and Braun 2016; Brun et al., 2017; Falaschi et al., 2019; Braun et al., 2019; Dussaillant et al., 2019; Seehaus et al., 2019; Huber et al., 2020; Hugonnet et al., 2021) to global coverage with more than one million observations from over 200,000 glaciers. The difference in survey periods between the glaciological and the geodetic data becomes manifest in the variability of the two graphs: a smooth line with mean balance between –0.25 and –0.5 m w.e. with steps due to changes in the observed sample, i.e. a few hundred until 1950, a few thousands between 1950 and 2000, and over 200,000 glaciers from 2000 to 2020. The observation period from 2000 to 2020 shows a less negative geodetic balance (Figs. 2.2 and 2.3) and indicates a negative bias in the glaciological sample. The mean balance of the geodetic sample basically follows the trend of the glaciological sample but would require a sample correction for trend analysis.

Zemp et al. (2019) combined glaciological and geodetic (from DEM differencing) datasets to a global assessment and show that glaciers alone lost 9,625 billion tons of ice between 1961 and 2016, corresponding to a sea-level equivalent of 27 millimetres. The global mass loss of glacier ice has increased significantly in the last 30 years and currently amounts to 335 billion tons of lost ice each year. This corresponds to an increase in sea levels of almost 1 millimetre per year. Zemp et al. (2020) presented a new approach to estimate and correct for the bias in the glaciological sample. These ad hoc estimates for the latest years (2016/17–2021/22) indicate that global glacier mass loss has further increased with sea-level rise contributions exceeding 1 mm per year, which corresponds to more than a quarter of the currently observed sea-level rise (cf. IPCC, 2019). This ice loss of all glaciers roughly corresponds to the mass loss of Greenland's Ice Sheet, and clearly exceeds that of the Antarctic Ice Sheet.

Direct observations of glacier-front positions extend back into the 19th century. This data sample has been extended in space based on remotely sensed length change observations and continued back in time by reconstructed front variations. Overall, the database contains more than 49,000 observations which allow the front variations of about 2,500 glaciers to be illustrated and quantified back into the 19th century. Reconstruction series from 40 glaciers extend far into the Little Ice Age (LIA) period, i.e., to the 16th century. The global compilation of front-variation data, as qualitatively summarized in Figure 2.4, shows that glacier retreat has been dominant for the past two centuries, with LIA maximum extents reached (in some regions several times) between the mid-16th and the late 19th centuries. The qualitative summary of cumulative mean annual front variations (Fig. 2.4) reveals a distinct trend toward global centennial glacier retreat, with the early 21st century marking the historical minimum extent in all regions (except New Zealand (NZL) and Antarctic and Sub Antarctic Islands (ANT), where few observations are available) at least for the time period of documented front variations. Intermittent periods of glacier re-advance, such as those in the European Alps around the 1920s and 1970s or in Scandinavia in the 1990s, are barely to be found in Figure 2.4a because they do not even come close to achieving LIA maximum extents. Figure 2.4b provides a better overview of these readvance periods by highlighting the years with a larger ratio of advancing glaciers. A qualitative overview of regional changes from both the glaciological and the geodetic method is given in Figure 2.3 and discussed in more detail in Section 3 on regional summaries.

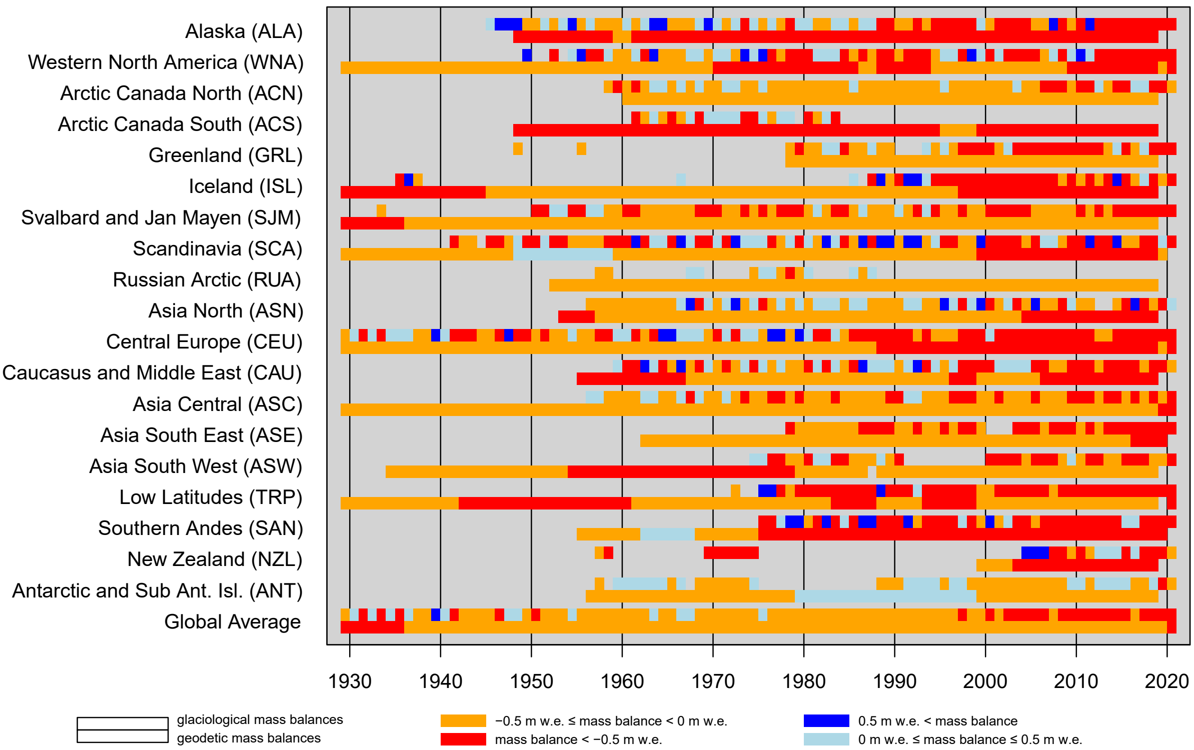

Figure 2.3 Regional mass balances from 1930 to 2021. Annual glaciological balances (m w.e.) and annual rates of geodetic balances (area-weighted means, m w.e. a^{-1}) are shown for 19 glacier regions and for the global average. Geodetic mass balances were calculated assuming a glacier-wide average density of 850 kg m^{-3}.

Fluctuations of Glaciers database contains more than 1.25 million observations from over 200,000 glaciers (Table 2.3). Regional and global overviews of the observational data samples are given in Figures 2.5–2.7. A look at the glaciological sample reveals a steady increase over the past 25 years (Fig. 2.6). This reflects the successful efforts of the observers to continue and extend their monitoring programmes in several regions as well as of the WGMS to compile these results through its collaboration network. The geodetic sample could be greatly increased in many regions, reaching global coverage in the period 2000–2020 (Fig. 2.7). The decline in the geodetic sample over the last few years has to do with the typically decadal time period and the normal post-processing character of geodetic surveys. In the case of the observational front-variation sample (Fig. 2.5), the decrease in observations is reported to be caused mainly by the abandonment of in-situ programmes without remote-sensing compensation.

Table 2.3 Database statistics and increase from current observation periods.

Dataset	Number of glaciers	Number of observations	Increment since WGMS (2021)
Front variations (from observations)	2,569	47,273	–12/+595
Front variations (from reconstructions)	40	1,884	+1/+5
Mass Balance (glacier-wide)	492	7,821	+10/+435
Mass balance (point information)	157	52,297	+16/+5,942
Volume/thickness change (geodetic method)	210,480	1,143,173	+173,034/+1,031,289
Special events	2,749	4,789	+2/–29
Glacier maps	101	157	0/0

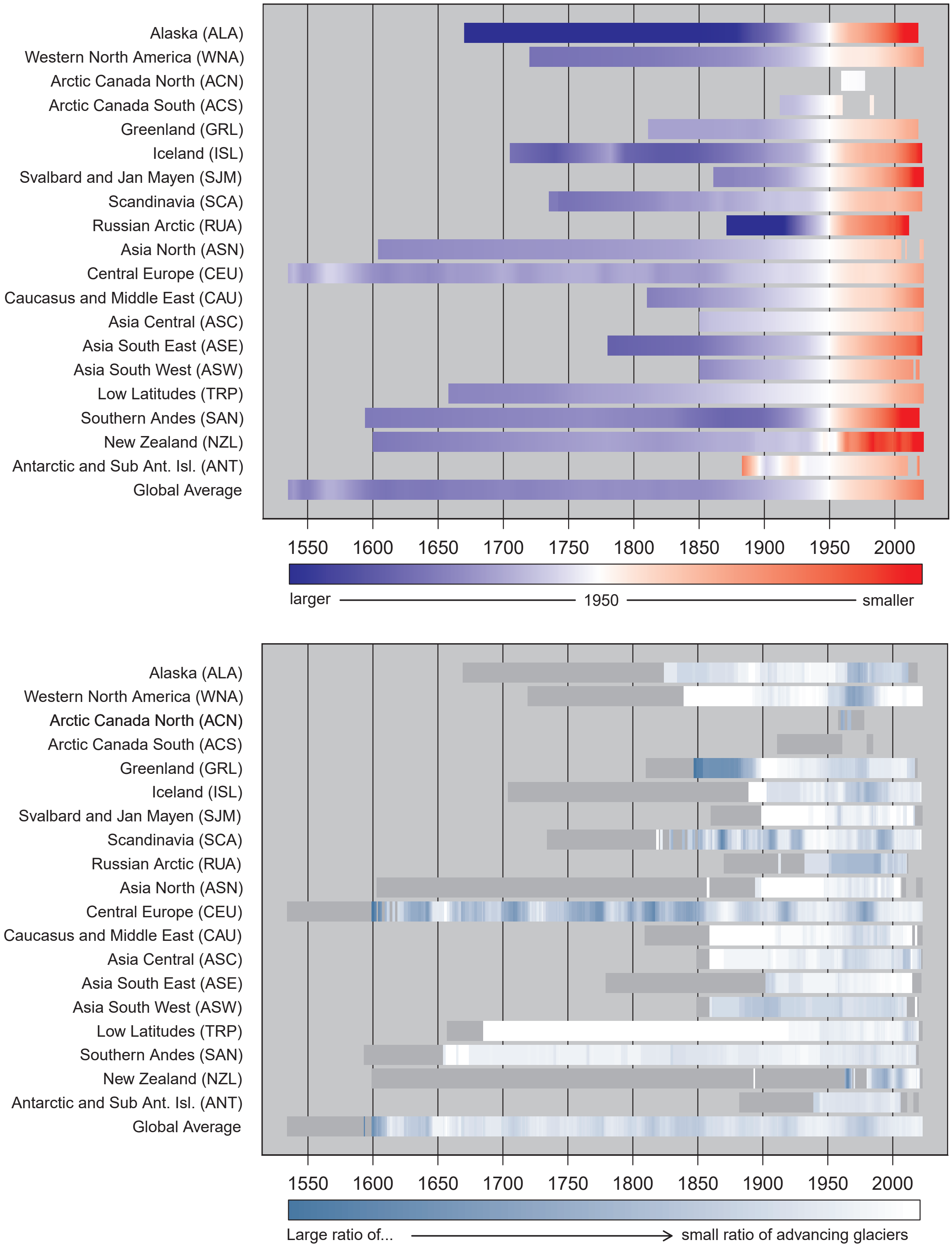

Figure 2.4 Global front variation observations from 1535 to 2021. Upper Figure: Qualitative summary of cumulative mean annual front variations. The colours range from dark blue for maximum extents (+2.5 km) to dark red for minumum extents (–1.6 km) relative to the extent in 1950 as a common reference (i.e. 0 km in white). Lower Figure: Qualitative summary of the ratio of advancing glaciers. The colours range from white for years with no reported advances to dark blue for years with a large ratio of advancing glaciers. Periods with very small data samples ($n < 6$) are masked in dark grey. The figure is based on all available front variation observations and reconstructions, excluding absolute annual front variations larger than 210 m a^{-1} in order to reduce the effects of calving and surging glaciers.

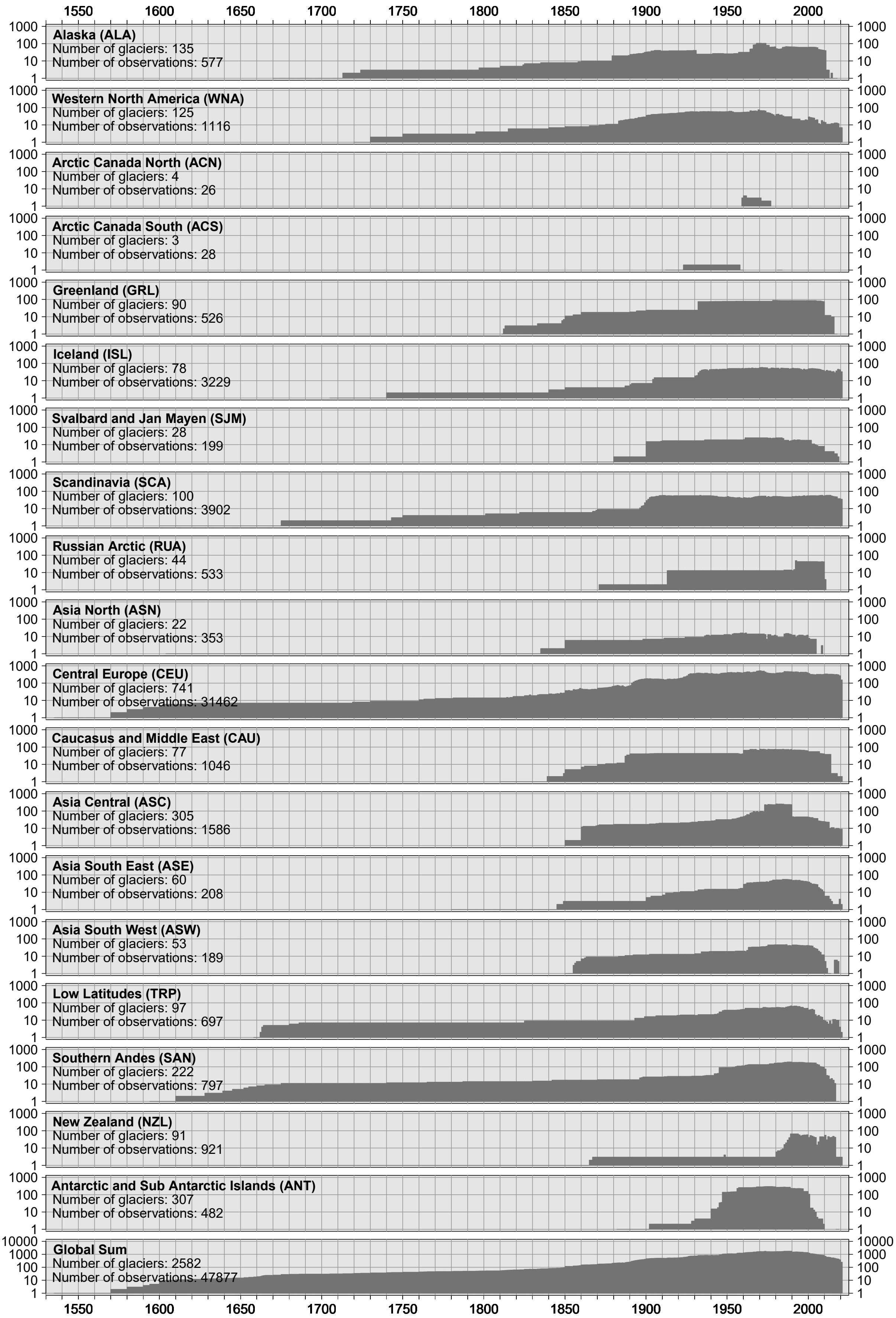

Figure 2.5 Regional and global number of glaciers with front-variation data from 1535–2021.

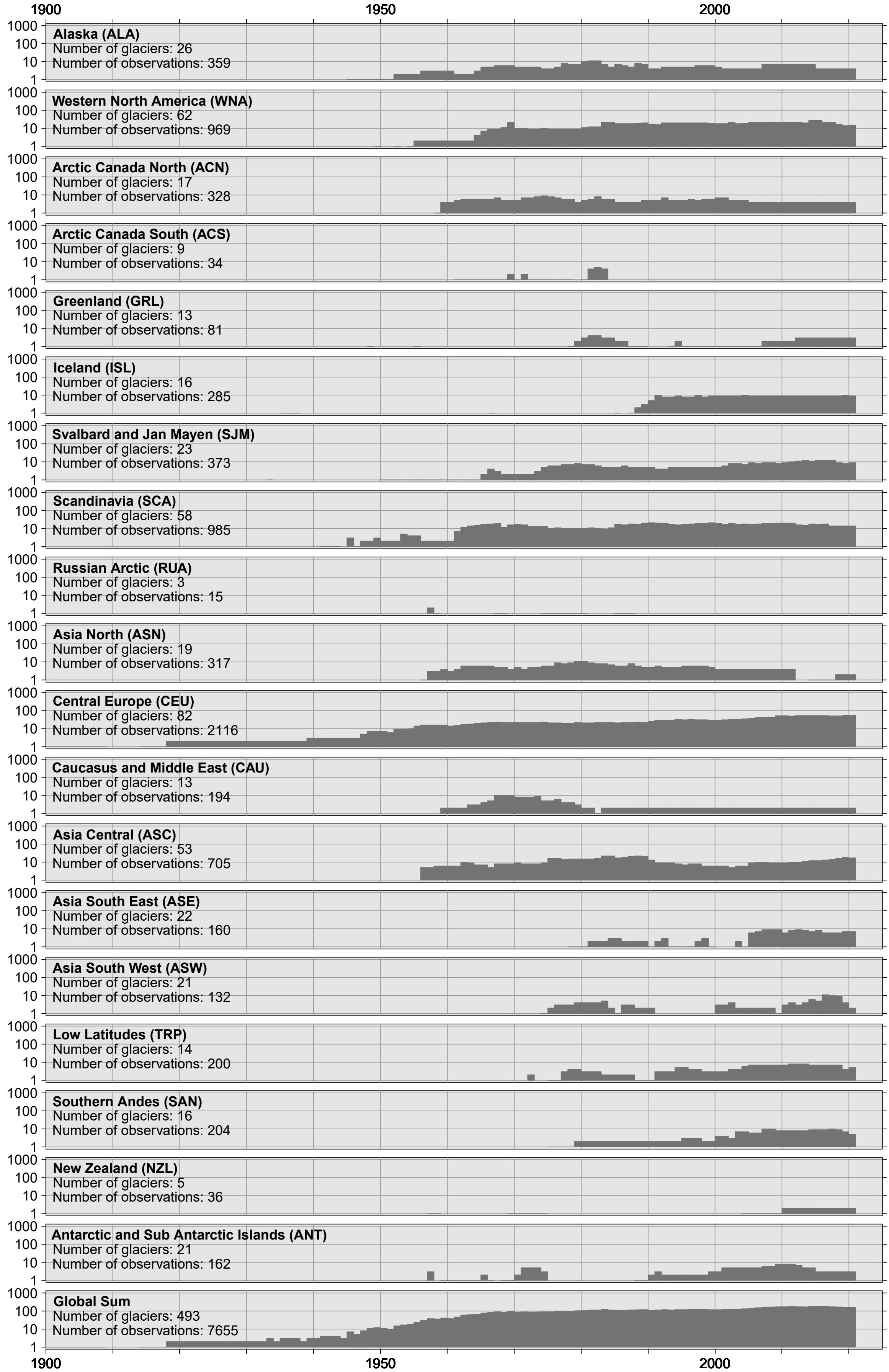

Figure 2.6 Regional and global number of glaciers with glaciological mass-balance data from 1900–2021.

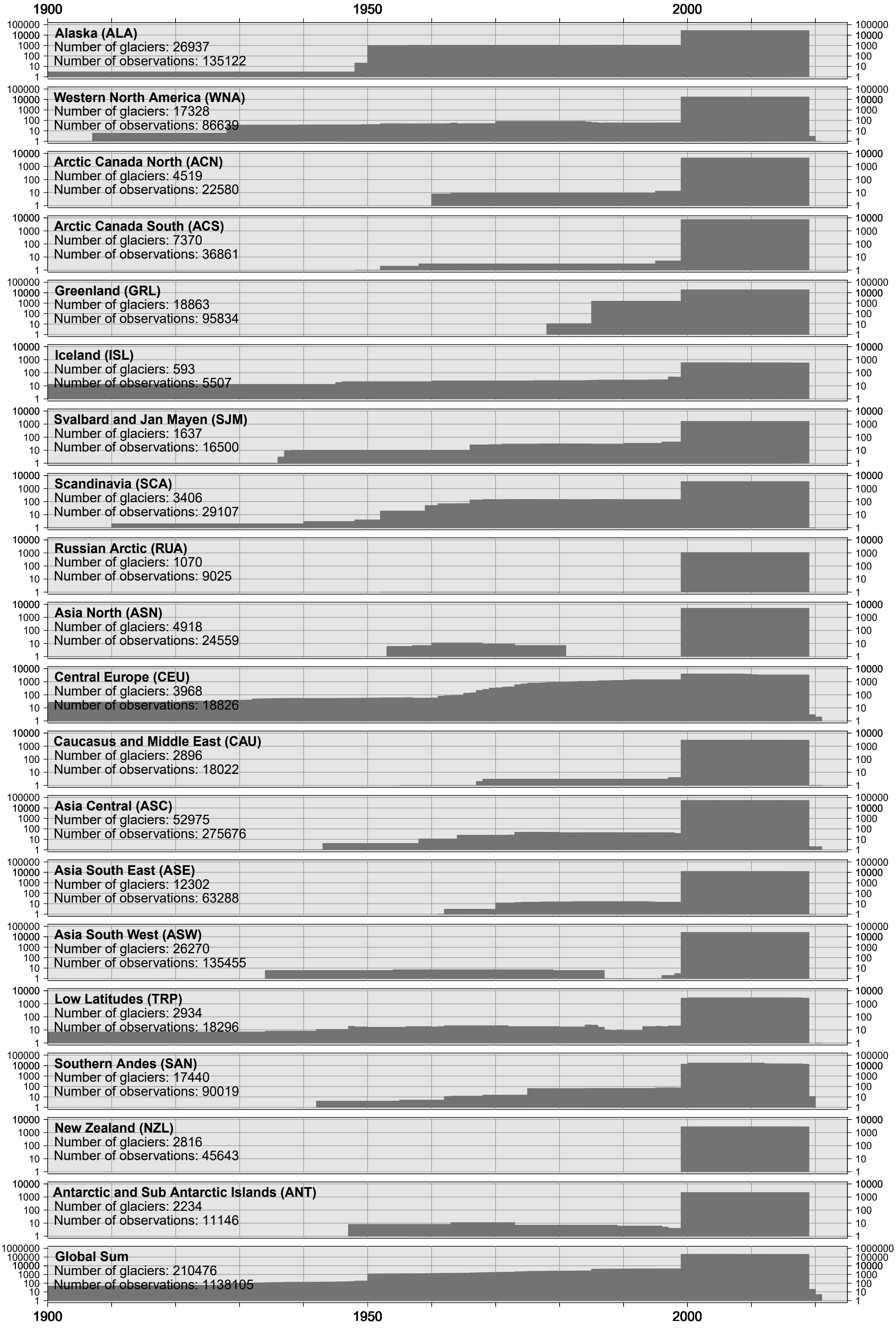

Figure 2.7 Regional and global number of glaciers with geodetic mass-change data from 1900–2021.

3 REGIONAL INFORMATION

Fluctuations of glaciers (not influenced by surge or calving dynamics) are recognized as high-confidence climate indicators and as an important element in early detection strategies within the international climate monitoring programmes (GCOS, 2010; GTOS, 2009). Their fluctuations can be analyzed on global and regional scales, but also on the local scale, where topographic effects may lead to different reactions of two adjacent glaciers (Kuhn et al., 1985). The sensitivity of a glacier to climatic change is strongly related to the climate regime in which the glacier resides. The mass balance of temperate glaciers in the mid-latitudes is mainly dependent on winter precipitation, summer temperature and summer snowfalls (temporally reducing the melt due to the increased albedo; Kuhn et al., 1999). In contrast, the glaciers in low latitudes, where ablation occurs throughout the year and multiple accumulation seasons exist, are strongly influenced by variations in the atmospheric moisture content which affects incoming solar radiation, precipitation and albedo, atmospheric long-wave emission, and sublimation (Wagnon et al., 2001; Kaser & Osmaston, 2002). In the Himalaya, which is influenced by the monsoon, most of the accumulation and ablation occurs during the summer (Ageta & Fujita, 1996; Fujita & Ageta, 2000). Glaciers at high altitudes and in polar regions can experience accumulation in any season (Chinn, 1985). The challenges of fieldwork in these different regions and climate regimes are summarized and contrasted by Stumm et al. (2017).

For regional analysis and comparison of glacier fluctuation data, it is convenient to group glaciers by proximity. We refer to the glacier regions as jointly defined by the GTN-G Advisory Board, GLIMS, the Randolph Glacier Inventory Working Group of IACS, and the WGMS (GTN-G, 2017). For global studies of mass balance, these glacier regions seem to be appropriate because of their manageable number and their geographical extent, which is close to the spatial correlation distance of glacier mass-balance variability in most regions (several hundred kilometres; cf. Letreguilly & Reynaud, 1990; Cogley & Adams, 1998). For every region, all data records are aggregated at the annual time resolution to give consideration to the corresponding observational peculiarities, i.e., for multi-annual survey periods, the annual change rate is calculated and assigned to each year of the survey period. For quantitative comparisons over time and between regions, decadal mean mass balances can be used to reduce the influence of meteorological extremes and of density conversion issues (cf. Huss, 2013). For regional and global studies, arithmetic mean balances are suitable for assessing the state of the average glacier, whereas area-weighted mean balances reflect the total mass change, as relevant for sea-level contributions.

This chapter provides regional overviews including a figure showing regional averages of glaciological and geodetic mass balances. Glaciological balances are shown as arithmetic means, and geodetic balances both as arithmetic and area-weighted means. Glaciological observations were reported by the Principal Investigators or compiled from the literature (e.g. Cogley, 2009; Dyurgerov & Meier, 2005). Geodetic data were compiled from global (Zemp et al., 2019, Hugonnet et al. 2021) and regional assessments (as cited in the following sections) and integrated into the Fluctuations of Glaciers database with the support of corresponding researchers. Additional data were compiled from the literature. These geodetic results are shown together with the corresponding number of observations, key statistics on regional glacier distribution and available fluctuation series, as well as graphs of cumulative front variation and mass balance from selected glaciers with long-term observation series. Note that for cumulative graphs with observational gaps the absolute change over the full time period is unknown. The regions are ordered approximately from West to East and from North to South. Regional estimates of total glacier area, rounded out to the next 500 km² mark, are from the RGI 6.0 (RGI Consortium, 2017).

3.1 ALASKA

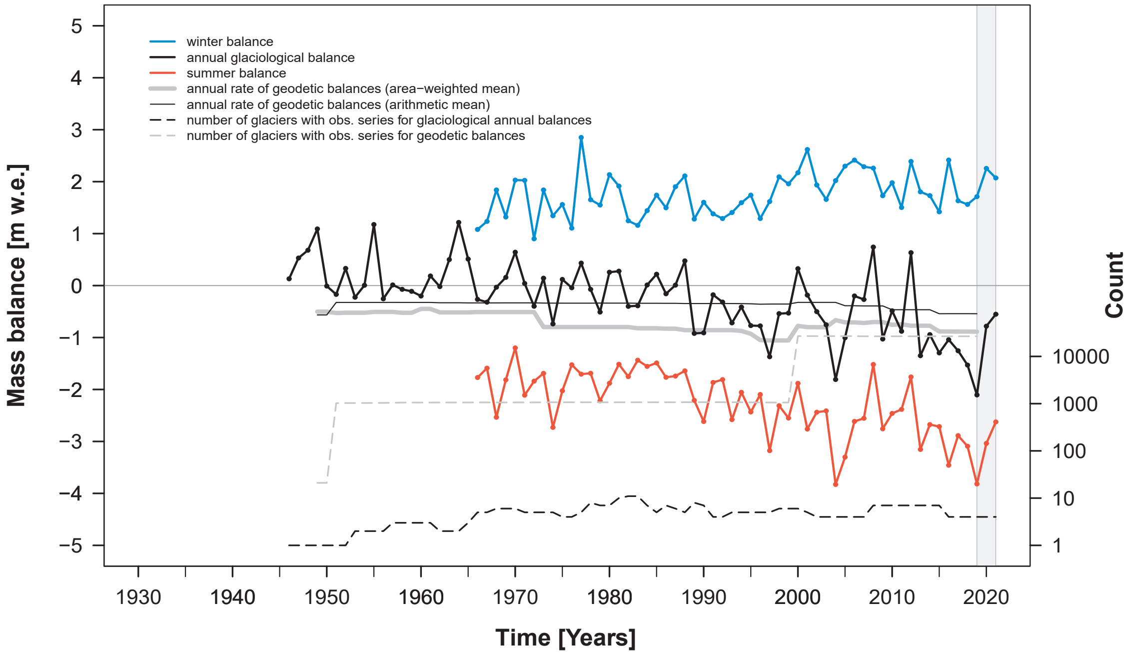

Figure 3.1.1 Regional mass balances: Annual glaciological balances (m w.e.) and annual rates of geodetic balances (m w.e. a^{-1}) are shown together with the corresponding number of glaciers with observations. Geodetic balances were calculated assuming a glacier-wide average density of 850 kg m^{-3}.

The glaciers and icefields of Alaska are located in the Brooks Range, the Alaska Range, where Mount McKinley/Denali (the highest peak of the continent) is located, and in the Coast Mountains along the Gulf of Alaska coastline. Together these glaciers cover an area of about 86,500 km². Climate conditions in this region range from very maritime conditions in the Coast Mountains to continental conditions in the Alaska Range. In Alaska, the major part of the front-variation series was discontinued at the end of the 20th century. Long-term mass-balance measurements have been reported from Gulkana and Wolverine in the Alaska Range as well as from the Juneau Icefield's Taku and Lemon Creek glaciers located in southeast Alaska.

In Alaska, glaciers reached their Little Ice Age (LIA) maxima at various times; for the northeast Brooks Range it was the late 15th century, and for the Kenai Mountains, the mid-17th century (Grove, 2004). However, most of the glaciers attained the LIA maximum extent between the early 18th and late 19th centuries (Molnia, 2007). Reported front-variation observations show a general glacier retreat from the LIA extents. Exceptions to this general trend are large tidewater glaciers with impressive frontal retreat (e.g. Columbia No 627) and advance (e.g. Harvard, Taku) cycles, mainly driven by calving dynamics. The former tidewater glacier Muir, located in the Saint Elias Mountains, became a land-terminating glacier after its last retreat phase. Observed mass-balance glaciers lost about half a metre w.e. per year during the 1990s and 2000s, with three years of positive mean balances in 1999/00, 2007/08, and 2011/12. Seasonal balance observations show the large mass turnover of the maritime glaciers. In 2019/20 the reported balance was negative with –782 mm w.e. a^{-1} followed by a less negative balance of –552 mm w.e. a^{-1} in 2020/21. The glaciological measurements are supported by results from geodetic surveys between the 1950s and the 2020s. Regional glacier change assessments were recently published by Berthier et al. (2018), Jakob et al. (2020), Larsen et al. (2015), Le Bris & Paul (2015), McNabb & Hock (2014), McNeil et al. (2020), O'Neel et al. (2019), and Yang et al. (2020).

Estimated total glacier area (km²):	86,500
Front variations	
- # of series*:	136/0
- # of obs. from stat. or adv. glaciers*:	210/0
- # of obs. from retreating glaciers*:	382/0
Glaciological balances	
- # of series*:	26/4
- # of observations*:	363/8
Geodetic balances	
- # of series°:	26,938/26,661
- # of observations°:	135,173/80,497

* (total/2020 & 2021), ° (total/>2009)

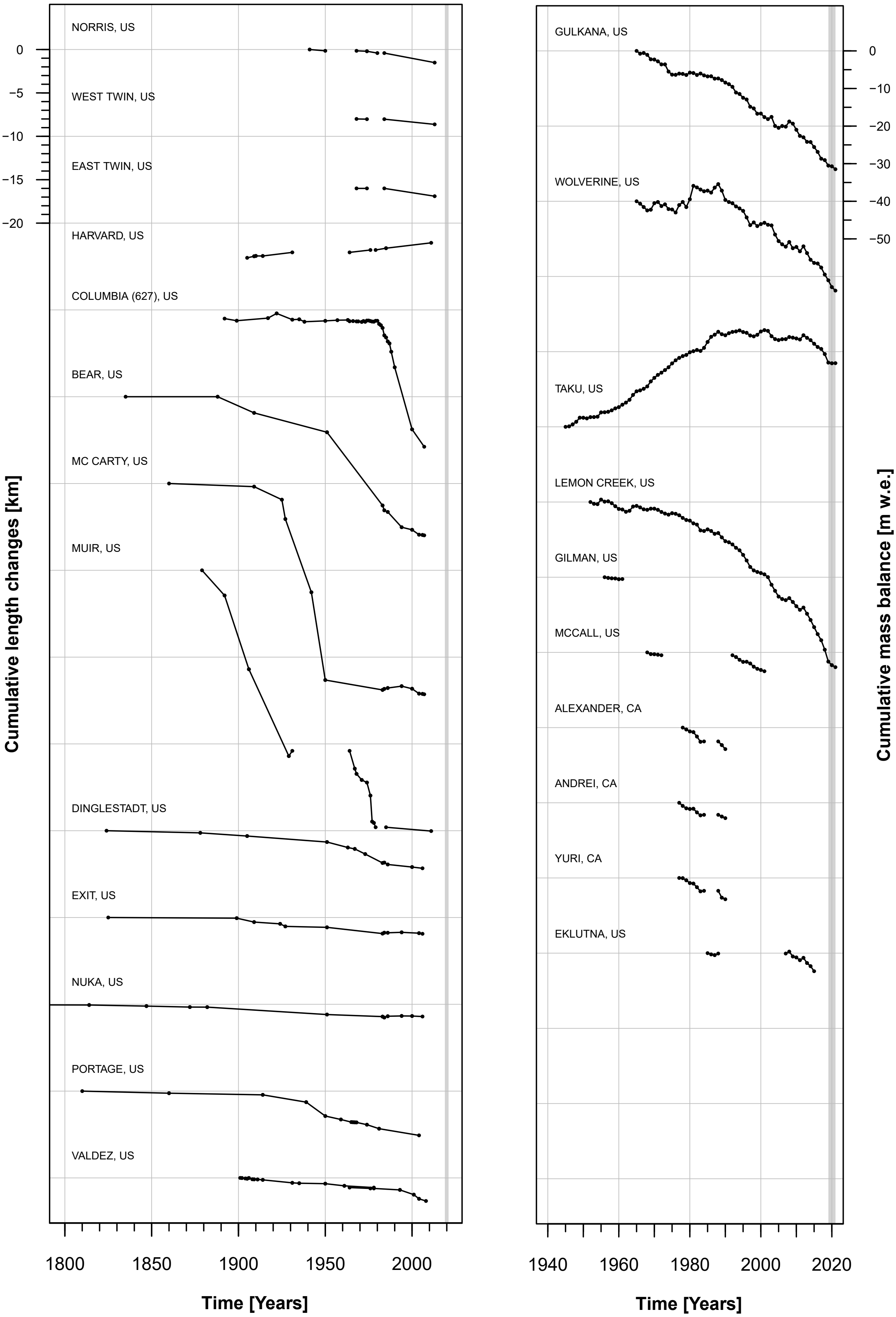

Figure 3.1.2 Cumulative length changes (left) and cumulative mass balances (right) of selected glaciers in Alaska over the entire observation period.

3.2 WESTERN NORTH AMERICA

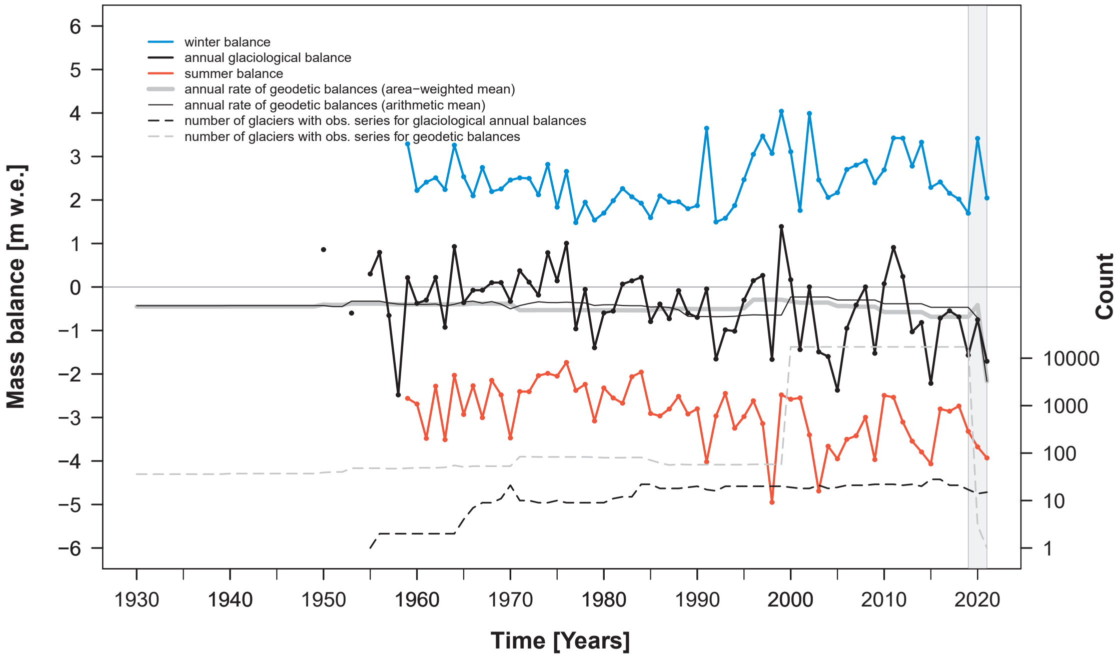

Figure 3.2.1 Regional mass balances: Annual glaciological balances (m w.e.) and annual rates of geodetic balances (m w.e. a^{-1}) are shown together with the corresponding number of glaciers with observations. Geodetic balances were calculated assuming a glacier-wide average density of 850 kg m^{-3}.

The glaciers in Western North America are located in the Pacific Coast Mountains, the Rocky Mountains, the Cascade Range, and in the Sierre Nevada. Together, the glacier area covers a total of approx. 14,500 km^2. In general, the climate of the mountain ranges shows strong variations depending on latitude, altitude and proximity to the sea. Therefore, glaciers in the south are much smaller and occur at higher elevations than in the higher latitudes, where some glaciers extend down to the coast.

From western North America more than 50 mass balance and more than 120 front-variation series are available but only half of them have been continued into the 21st century. South Cascade Glacier in the Cascade Range has the longest mass-balance record followed by Place and Helm glaciers in the Coast Mountains and Peyto Glacier in the Rocky Mountains. In conterminous USA and Canada, glaciers reached their LIA maximum extent in the mid to late 19th century (Kaufmann et al., 2004). Reported front variations show a general glacier retreat from the LIA extents with intermittent periods of glacier re-advances in the early 20th century and from the 1970s to 1980s. Since the 1990s glacier retreat has been continued.

Mean annual balance rates of the observed glaciers were between 400 and 450 mm w.e. a^{-1} in the 1980s and 1990s, and almost –1000 mm w.e. a^{-1} in the 2000s. Seasonal balance observations show the large mass turnover of the maritime glaciers. The reported mean annual balance of 2019/20 was negative with –752 mm w.e. followed by a very negative mean annual balance of –1,708 mm w.e. in 2020/21. The glaciological observations are well supported by results from geodetic surveys.

Regional glacier change assessments were recently published by Menounos et al. (2019), Pelto (2018), Pelto & Brown (2012), Shea et al. (2013), Tennant & Menounos (2013), and Tennant et al. (2012).

Estimated total glacier area (km^2):	14,500
Front variations	
- # of series*:	125/7
- # of obs. from stat. or adv. glaciers*:	284/0
- # of obs. from retreating glaciers*:	842/13
Glaciological balances	
- # of series*:	62/15
- # of observations*:	985/29
Geodetic balances	
- # of series°:	17,307/17,278
- # of observations°:	86,893/51,848

* (total/2020 & 2021), ° (total/>2009)

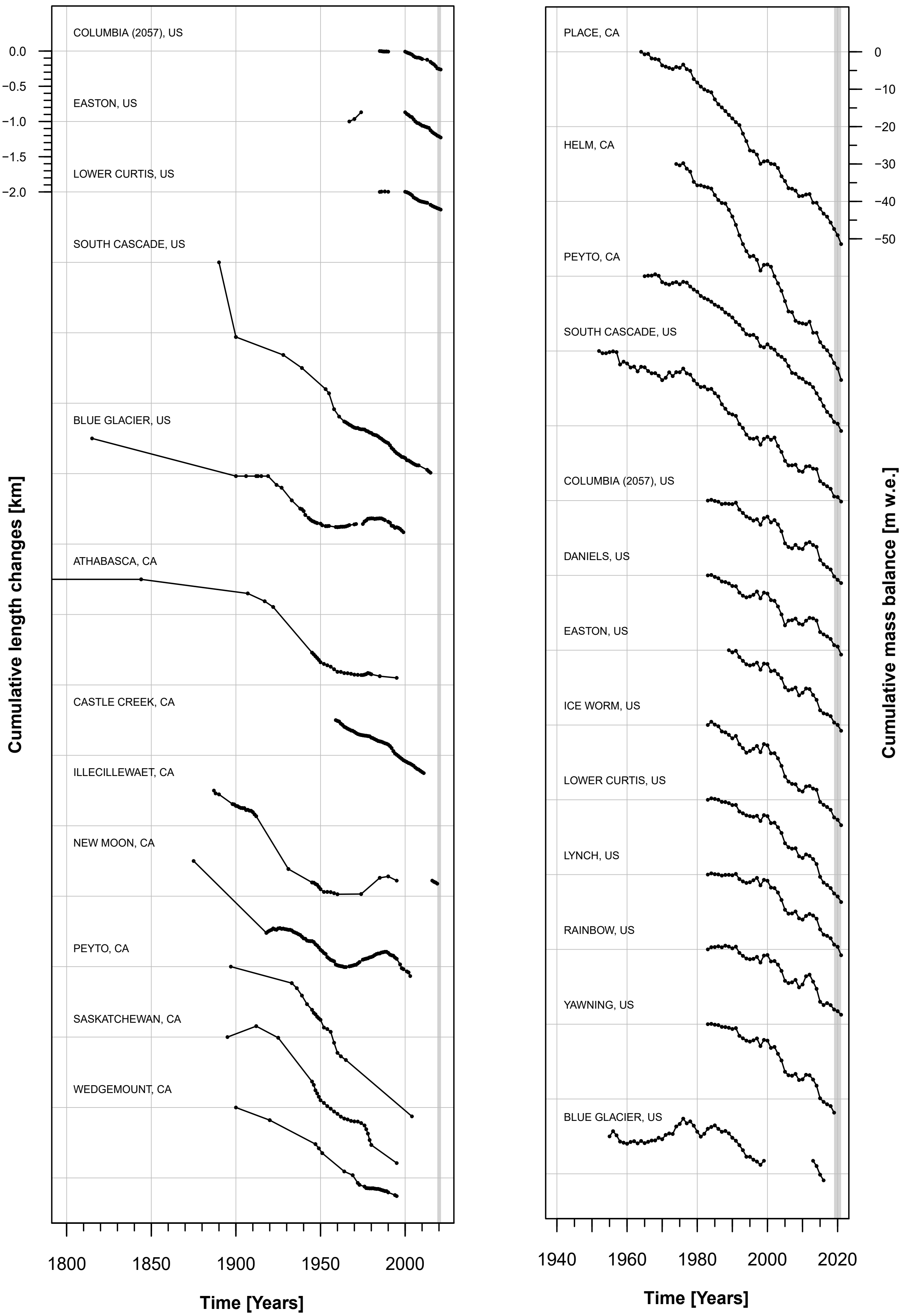

Figure 3.2.2 Cumulative length changes (left) and cumulative mass balances (right) of selected glaciers in Western North America over the entire observation period.

3.3 ARCTIC CANADA NORTH & SOUTH

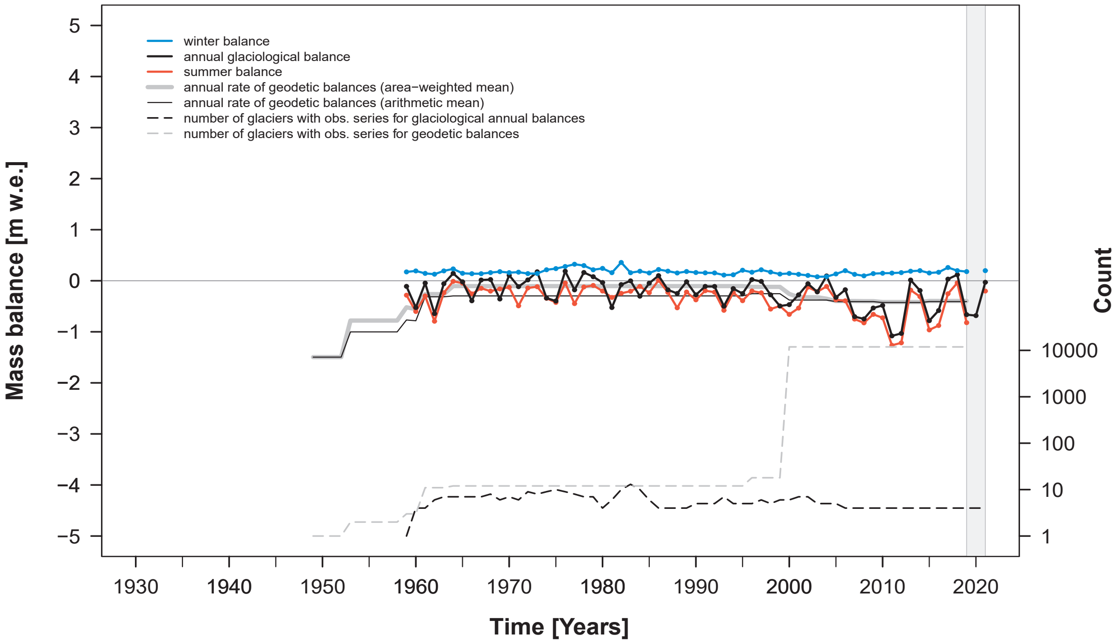

Figure 3.3.1 Regional mass balances: Annual glaciological balances (m w.e.) and annual rates of geodetic balances (m w.e. a^{-1}) are shown together with the corresponding number of glaciers with observations. Geodetic balances were calculated assuming a glacier-wide average density of 850 kg m^{-3}.

The Canadian Arctic Archipelago is a group of more than 36,000 islands and hosts a total of about 146,000 km^2 of glaciers, icefields and ice caps. The largest islands with glaciers are Baffin, Ellesmere, Devon, Axel Heiberg, and Melville. The glaciers in this high-latitude region are much influenced by the extent and distribution of sea ice which in turn depends on ocean currents and on the Arctic and North Atlantic Oscillations.

Information on glacier changes mainly stems from a few dozen mass-balance series. The longest continuous measurements are reported from Meighen, Devon and Melville Ice Caps and from White Glacier. The long-term glaciological measurement series of White Glacier has recently been homogenized and validated with geodetic surveys by Thomson et al. (2017). In addition, Burgess and Danielson (2022) used geodetic survey data to provide independent validation to the annual in-situ glaciological measurements collected over the Meighen Ice Cap since 1959.

The timing of the LIA maximum extent of glaciers in the Canadian Artic Archipelago is estimated to the end of the 19th century (Grove, 2004). The subsequent glacier retreat is clearly visible in remotely sensed images thanks to glacier moraines and trimlines. However, detailed front-variation observations are not available for this region.

The few reported mass-balance measurements indicate slightly negative balances of less than 100 mm w.e. a^{-1} between the 1960s and the 1980s and an increased mass loss between –200 and –300 mm w.e. a^{-1} in the 1990s and 2000s. Seasonal balances show the small mass turnover of the Arctic ice caps. In Arctic Canada North, the reported mean annual balance of 2019/20 was very negative with –683 mm w.e. and less negative with –30 mm w.e. in 2020/21. The available results from geodetic surveys are also indicating negative balances since the mid 20th century. Between 2000 and 2020, the geodetic sample covers both Artic Canada North and South. Regional glacier change assessments were recently published by Noël et al. (2018).

Estimated total glacier area (km^2):	146,000
Front variations	
- # of series*:	7/0
- # of obs. from stat. or adv. glaciers*:	17/0
- # of obs. from retreating glaciers*:	37/0
Glaciological balances	
- # of series*:	26/4
- # of observations*:	366/8
Geodetic balances	
- # of series°:	11,889/11,882
- # of observations°:	59,559/35,756

* (total/2020 & 2021), ° (total/>2009)

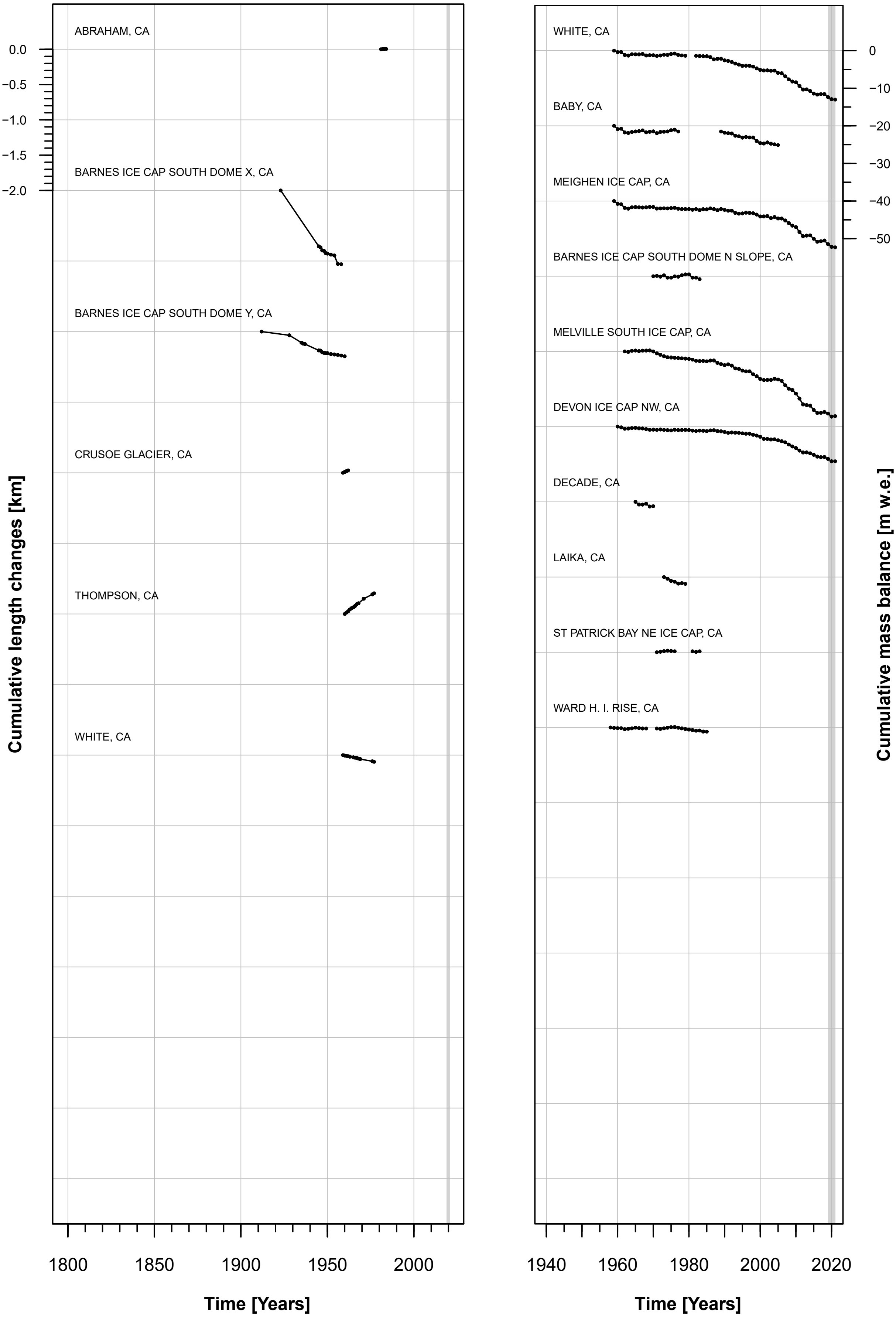

Figure 3.3.2 Cumulative length changes (left) and cumulative mass balances (right) of selected glaciers in Arctic Canada over the entire observation period.

3.4 GREENLAND

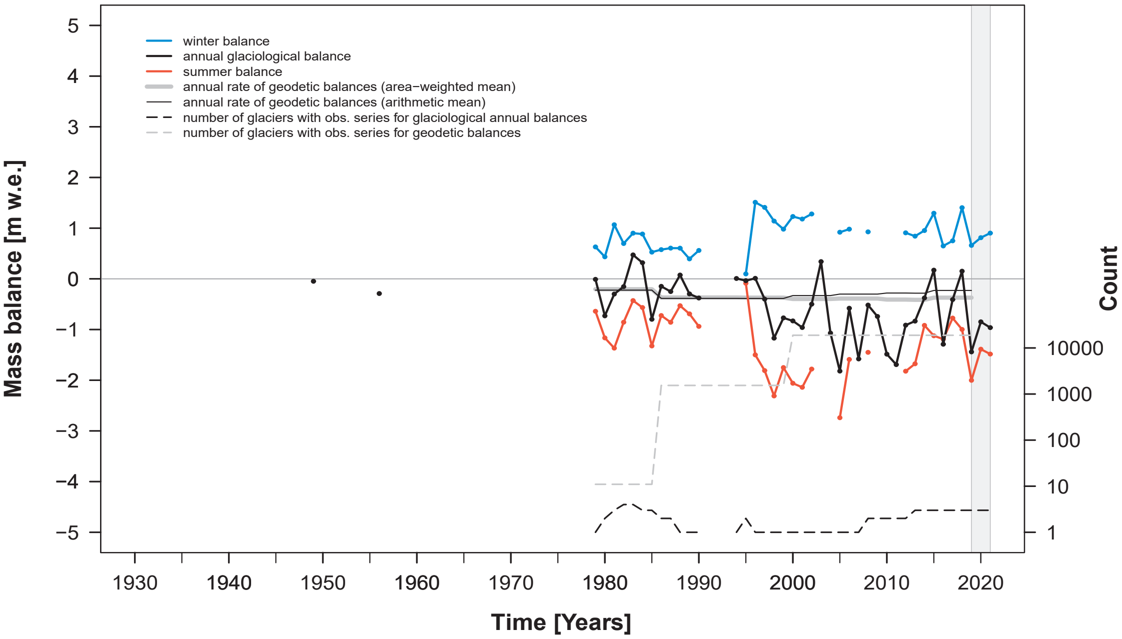

Figure 3.4.1 Regional mass balances: Annual glaciological balances (m w.e.) and annual rates of geodetic balances (m w.e. a^{-1}) are shown together with the corresponding number of glaciers with observations. Geodetic balances were calculated assuming a glacier-wide average density of 850 kg m^{-3}.

The world's largest non-continental island is covered to about 80% by the Greenland Ice Sheet. In addition, about 20,300 local glaciers cover an area between 90,000 km^2 and 130,000 km^2, depending on the counting of different connectivity levels between local glaciers and the ice sheet (Rastner et al., 2012). These glaciers range from sea level to 3,694 m a.s.l. at Gunnbjørn Fjeld – Greenland's highest mountain located in the Watkins Range on the east coast.

There exists a large variety of glacier types, from icefields and ice caps with numerous outlet glaciers, to valley, mountain and cirque glaciers. The island acts as a centre of cooling resulting in a polar to subpolar climate regime. Due to the large north-south extent, different thermal regimes can be expected for the glaciers, ranging from mostly cold in the north to polythermal in the central part to temperate in the south. About 80 front-variation series are available from the southern part. Mass-balance measurements are available from about 25 sites, but most series are discontinued after a couple of years. Recent measurements are reported from Mittivakkat and Freya, both located on the east coast and Qasigiannguit on the west coast. The few investigations from Greenland indicate that many glaciers and ice caps (e.g. on Disko Island) reached their maximum extents before the 19th century. The subsequent glacier retreat is documented at about decadal intervals for approx. 80 glaciers in the southern part of Greenland. However, observations made after 2010 have been reported only from Mittivakkat Glacier.

Mass-balance measurements indicate that the ice loss increased from –630 mm w.e. a^{-1} in the 1990s to –890 mm w.e. a^{-1} in the 2000s. The reported mean annual balance of 2019/20 was negative with –848 mm w.e. and in the same range with –962 mm w.e. for 2020/21. Geodetic estimates with a full spatial coverage between 2000 and 2020 show a more moderate mass loss than indicatec by the few glaciological observations.

Regional glacier change assessments were published by Bjørk et al. (2012), Bolch et al. (2013), Citterio et al. (2009), and Machguth et al. (2016). Huber et al. (2020) show a geodetic mass-change of –0.5 m a^{-1} for west-central Greenland from 1985 to 2012.

Estimated total glacier area (km^2):	89,500
Front variations	
- # of series*:	90/0
- # of obs. from stat. or adv. glaciers*:	124/0
- # of obs. from retreating glaciers*:	402/0
Glaciological balances	
- # of series*:	13/3
- # of observations*:	84/6
Geodetic balances	
- # of series°:	18,864/18,863
- # of observations°:	95,838/58,117

* (total/2020 & 2021), ° (total/>2009)

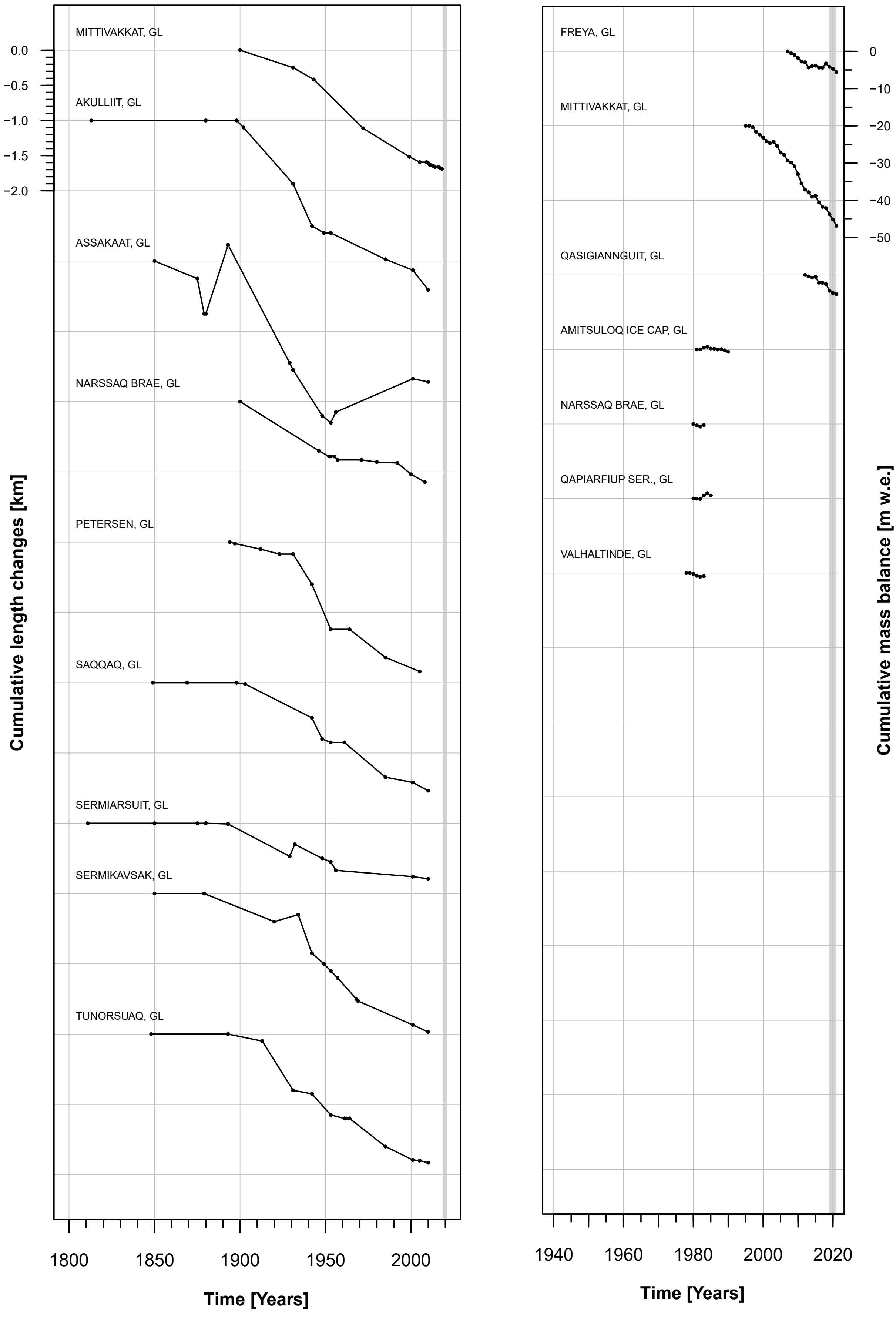

Figure 3.4.2 Cumulative length changes (left) and cumulative mass balances (right) of selected glaciers in Greenland over the entire observation period.

3.5 ICELAND

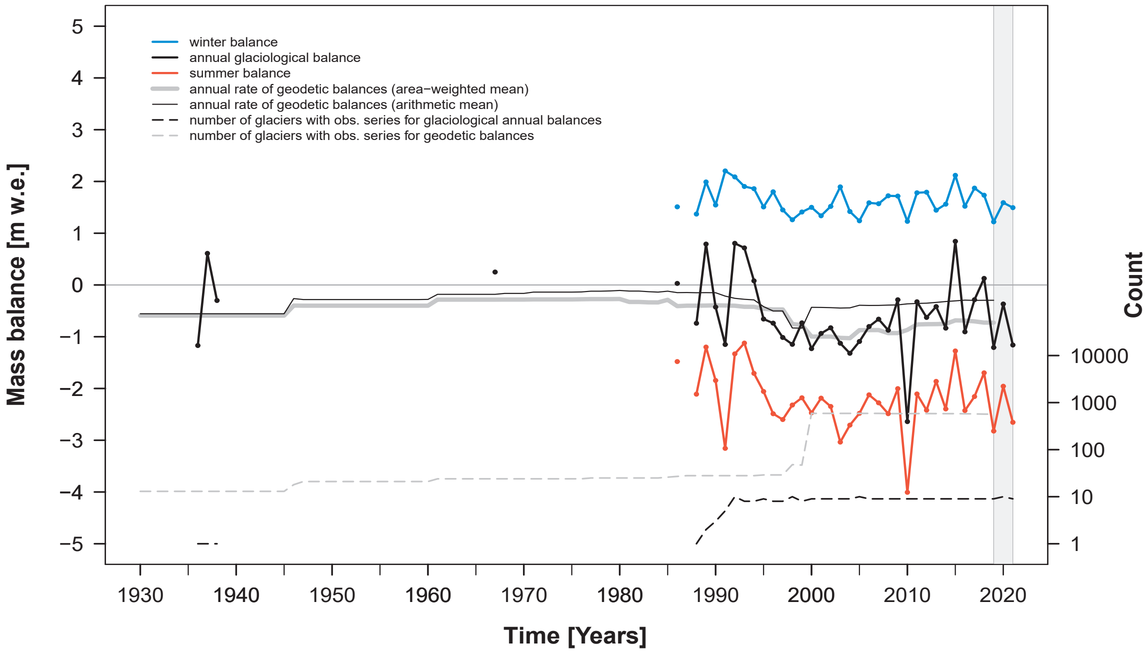

Figure 3.5.1 Regional mass balances: Annual glaciological balances (m w.e.) and annual rates of geodetic balances (m w.e. a^{-1}) are shown together with the corresponding number of glaciers with observations. Geodetic balances were calculated assuming a glacier-wide average density of 850 kg m^{-3}.

Iceland is located on the Mid-Atlantic Ridge and its ice cover is dominated by six large ice caps. Vatnajökull is the largest followed by Langjökull, Hofsjökull, Mýrdalsjökull, Drangajökull, and Eyjafjallajökull. The entire glacier cover is estimated to total slightly above 10,000 km^2 (Hannesdóttir et al. 2020).

The glaciers in Iceland are located in a region of subpolar oceanic climate. The warm North Atlantic Current ensures generally higher temperatures than in most places of similar latitude. Winter precipitation and summer ablation levels on the glaciers are comparatively high and the mass-balance sensitivity is among the highest recorded. Many ice caps and glaciers in Iceland are influenced by geothermal and volcanic activity, resulting in frequent glacier outburst floods, known in Icelandic as jökulhlaups.

Mass-balance measurements are available from a dozen glaciers. The longest series starting in 1988 is from outlet glaciers of Hofsjökull. Measurements on Vatnajökull outlets and on Langjökull were started in 1991 and 1997, respectively. Detailed front-variation series are available from over 70 glacier tongues reaching back to the 1930s, with sporadic information derived from historical sources back to the 18th century and in a few cases even further back in time.

The maximum LIA extent is estimated to have occurred close to the end of the 19th century (Thorarinsson, 1943; Sigurðsson, 2005). Detailed front-variation observations document the general retreat from the LIA maximum extent up to 1970, with a period of intermittent re-advance between 1970 and 1990 and continued retreat from 1995 to the present time. Abrupt re-advances are due to surges.

The average mass loss of glaciers has increased from about –500 mm w.e. a^{-1} in the 1990s to more than –1,000 mm w.e. a^{-1} in the 2000s. The average mass balance during the glaciological year 2019/20 was negative with –368 mm w.e., followed by a quite negative mass balance of –1,160 mm w.e. in 2020/21. Regional glacier change assessments were recently published by Aðalgeirsdóttir et al. (2020), Belart et al. (2020), Björnsson et al. (2013), Foresta et al. (2016), Hannesdóttir et al. (2015), Jóhannesson et al. (2020), and Pope et al. (2016).

Estimated total glacier area (km^2):	11,000
Front variations	
- # of series*:	77/43
- # of obs. from stat. or adv. glaciers*:	805/9
- # of obs. from retreating glaciers*:	2,447/61
Glaciological balances	
- # of series*:	16/10
- # of observations*:	294/19
Geodetic balances	
- # of series°:	593/586
- # of observations°:	5,542/4,250

* (total/2020 & 2021), ° (total/>2009)

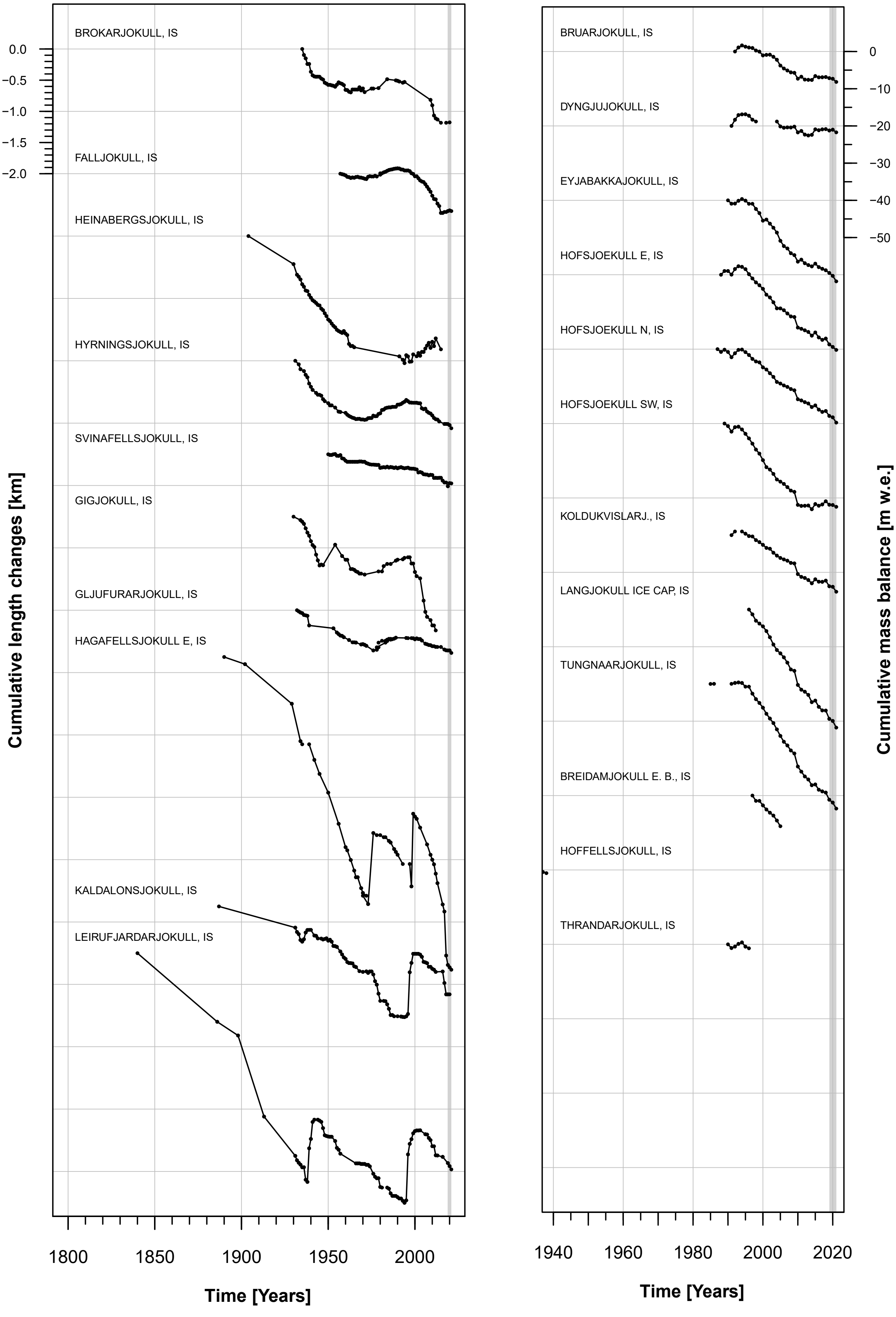

Figure 3.5.2 Cumulative length changes (left) and cumulative mass balances (right) of selected glaciers in Iceland over the entire observation period.

3.6 SVALBARD & JAN MAYEN

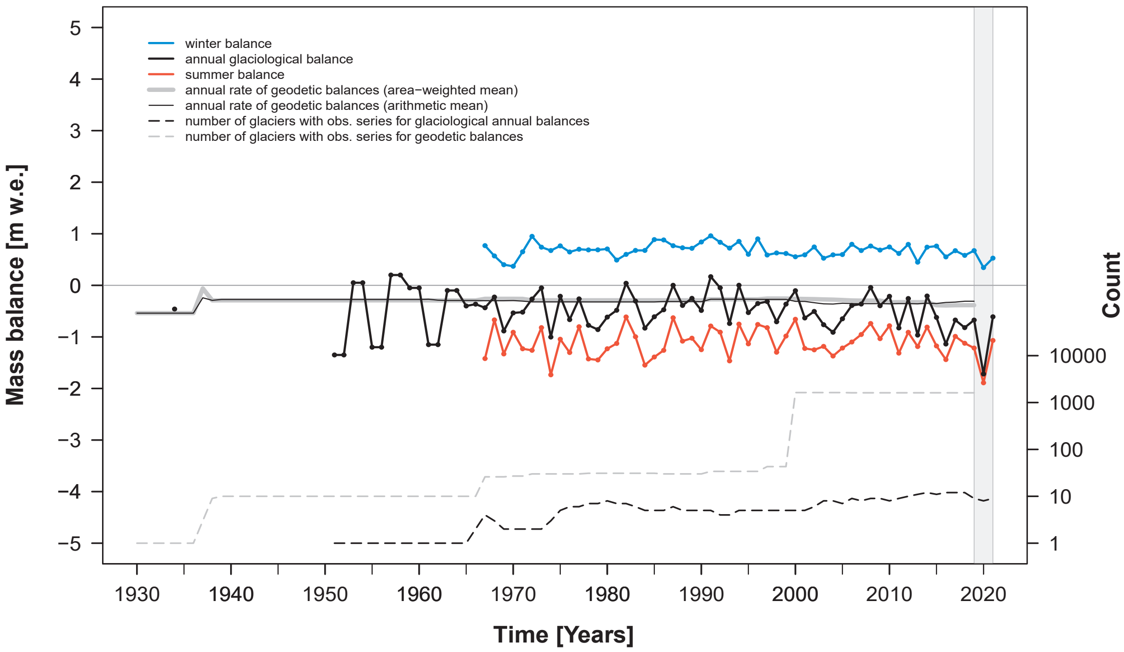

Figure 3.6.1 Regional mass balances: Annual glaciological balances (m w.e.) and annual rates of geodetic balances (m w.e. a^{-1}) are shown together with the corresponding number of glaciers with observations. Geodetic balances were calculated assuming a glacier-wide average density of 850 kg m^{-3}.

The Svalbard Archipelago is situated in the Arctic Ocean north of mainland Europe. The largest island is Spitsbergen, followed by Nordaustlandet and Edgeøya. Its topography is more than half covered by ice, and is characterized by plateau mountains and fjords. The entire glacier area totals about 34,000 km². Jan Mayen is a volcanic island in the Arctic Ocean and is part of the Kingdom of Norway, as is Svalbard. It is partly covered by glaciers, with an area of about 100 km² around the Beerenberg Volcano. Svalbard and Jan Mayen both have an arctic climate, although with much higher temperatures than other regions at the same latitude. Numerous glaciers on Svalbard are of the surge-type.

Over 20 continuous mass-balance series are reported from Svalbard, the longest ones being from Austre Brøggerbreen, Midtre Lovenbreen, Kongsvegen, Hansbreen, Waldemarbreen, and Irenebreen. Front variations are available from roughly 30 glaciers, most of them dating back to about 1900. From Jan Mayen, front variations are reported from Sorbreen.

During the LIA, glaciers in Svalbard were close to their late Holocene maximum extent and remained there until the beginning of the 20th century (Svendsen & Magerud, 1997). The reported front-variation series show a general trend of retreat without a common period of distinct re-advances. On Jan Mayen, Sorbreen shows a retreat starting in the late 19th century with a re-advance period in the mid-20th century.

Glaciological mass-balance measurements indicate continued ice loss at a rate of a few hundred mm w.e. per year over the second half of the 20th century, well supported by results from geodetic survey of a few dozen glaciers. Mass loss increased to –490 mm w.e. a^{-1} in the 2000s. Seasonal balances show a relatively low mass turnover. The average mass balance of 2019/20 was –1,719 mm w.e. and –610 mm w.e. in 2020/21. Regional glacier change assessments were recently published by Morris et al. (2020), Schuler et al. (2020), Sobota et al. (2016) and Sobota (2013, 2021).

Estimated total glacier area (km²):	34,000
Front variations	
- # of series*:	27/1
- # of obs. from stat. or adv. glaciers*:	36/0
- # of obs. from retreating glaciers*:	165/2
Glaciological balances	
- # of series*:	23/10
- # of observations*:	377/17
Geodetic balances	
- # of series°:	1,637/1,614
- # of observations°:	16,487/13,046

* (total/2020 & 2021), ° (total/>2009)

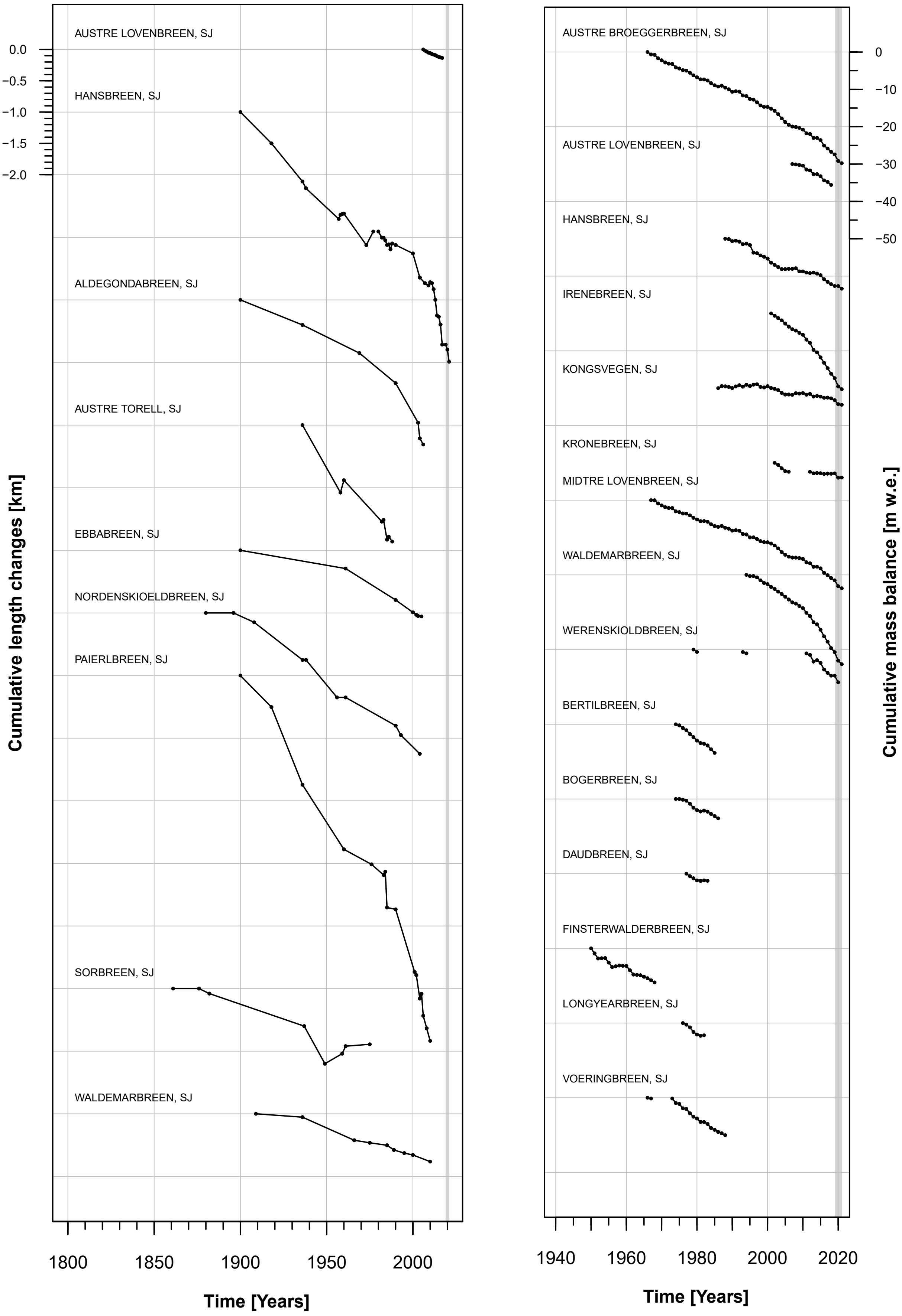

Figure 3.6.2 Cumulative length changes (left) and cumulative mass balances (right) of selected glaciers in Svalbard and Jan Mayen over the entire observation period.

3.7 SCANDINAVIA

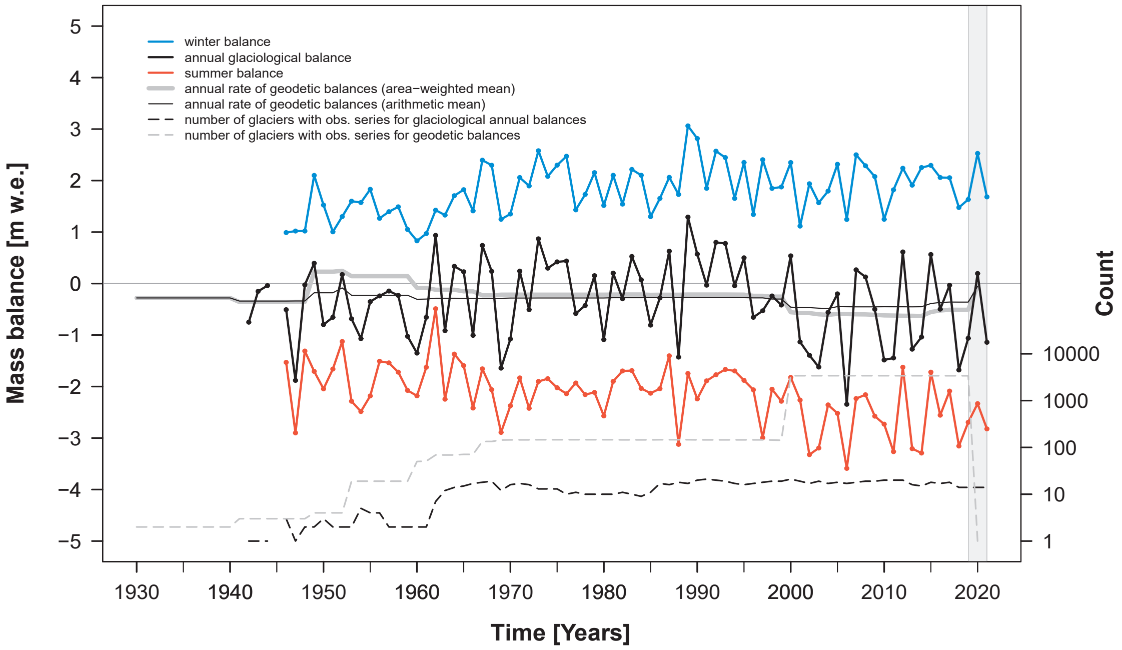

Figure 3.7.1 Regional mass balances: Annual glaciological balances (m w.e.) and annual rates of geodetic balances (m w.e. a^{-1}) are shown together with the corresponding number of glaciers with observations. Geodetic balances were calculated assuming a glacier-wide average density of 850 kg m^{-3}.

In Scandinavia, the greater part of the ice cover is concentrated in southern Norway, namely in Folgefonna, Hardangerjøkulen, Breheimen, Jotunheimen, and Jostedalsbreen, which is the largest ice cap of mainland Europe. In northern Norway there are the Okstindan and Svartisen ice caps, glaciers in Lyngen and Skjomen as well as in the adjacent Kebnekaise region in Sweden. Together, these glaciers cover about 3,000 km^2. Glaciers are situated in different climatic regimes, ranging from maritime along the Norwegian west coast, humid continental in the central part, to subarctic further north.

Scandinavia is one of the regions with the most and longest reported observation series. From the approx. 60 mass balance series, eight have continuously reported series since 1970; those in Norway have recently been reanalysed by Andreassen et al. (2016). Front-variations series are available from almost 90 glaciers extending back to the 19th century, with some reconstructions even back to the 17th century.

After having disappeared most likely during the early/mid-Holocene (Nesje et al., 2008), most of the Scandinavian glaciers reached their LIA maximum extent in the mid-18th century (Grove, 2004). Following a minor retreat trend with small frontal oscillations up until the late 19th century, the glaciers experienced a general recession during the 20th century with intermittent periods of re-advances around 1910 and 1930, in the 1970s, and around 1990; the last advance stopped at the beginning of the 21st century. On average, the observed mass balances were slightly positive from the 1970s to the 1990s. This was because coastal glaciers were able to gain mass while the glaciers further inland continued to lose mass. Geodetic results are well centred within the variability of the glaciological results with slightly negative average balances. After 2000, glaciers in both the coastal and the inland region lost mass resulting in an average balance of –790 mm w.e. a^{-1}. Seasonal balances show a large mass turnover. The regional average of reported balances was positive with 195 mm w.e. in 2019/20 and –1,140 mm w.e. in 2020/21. Regional glacier change assessments were recently published by Andreassen et al. (2020), Jiao et al. (2020), and NVE (2019, and earlier issues).

Estimated total glacier area (km^2):	3,000
Front variations	
- # of series*:	94/38
- # of obs. from stat. or adv. glaciers*:	945/7
- # of obs. from retreating glaciers*:	2,962/59
Glaciological balances	
- # of series*:	58/14
- # of observations*:	996/28
Geodetic balances	
- # of series°:	3,406/3,403
- # of observations°:	29,223/22,172

* (total/2020 & 2021), ° (total/>2009)

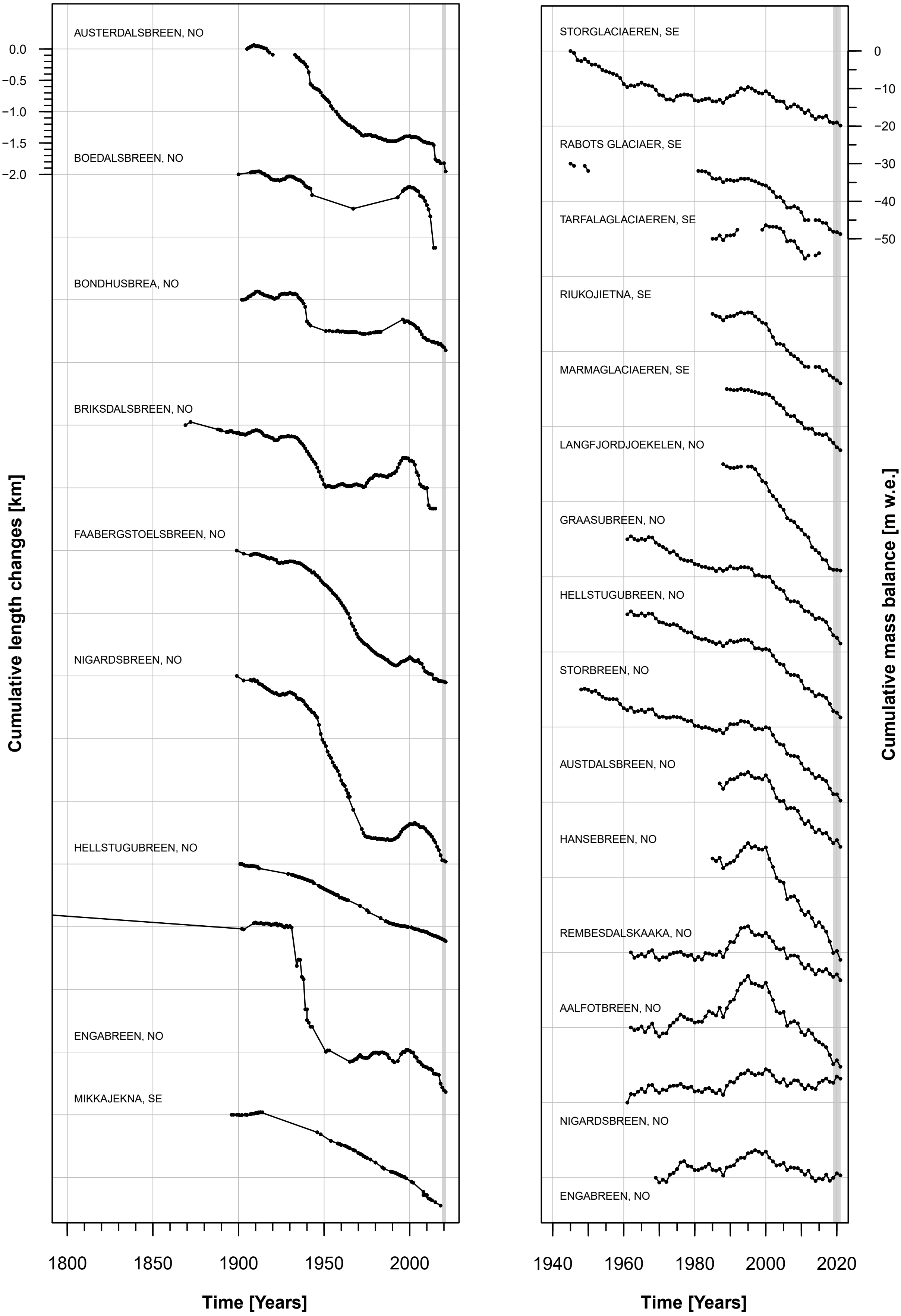

Figure 3.7.2 Cumulative length changes (left) and cumulative mass balances (right) of selected glaciers in Scandinavia over the entire observation period.

3.8 CENTRAL EUROPE

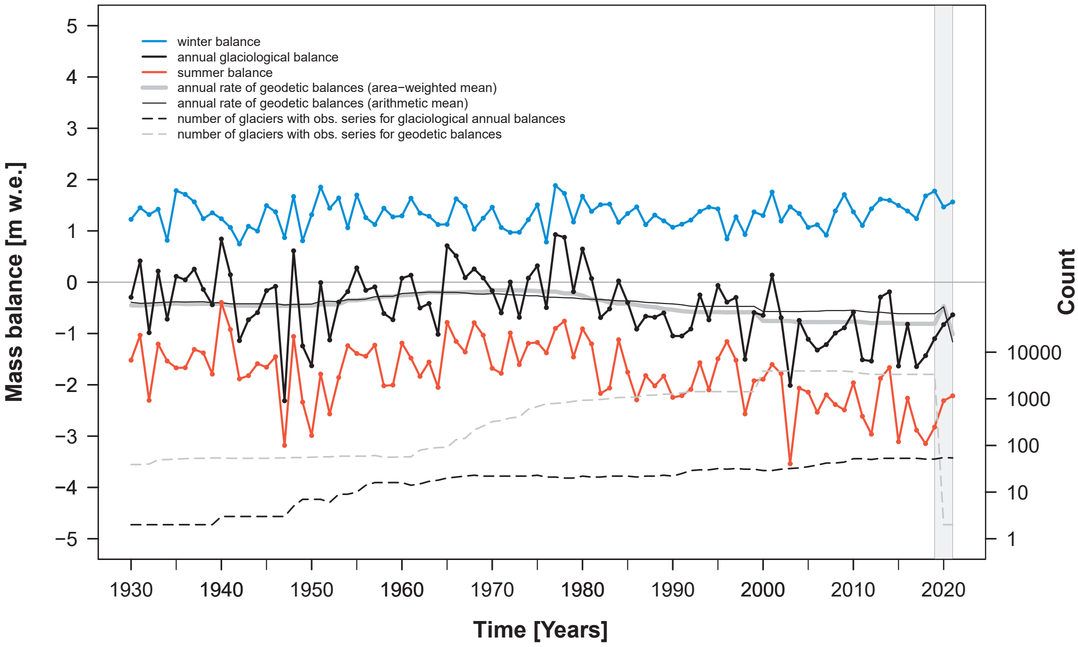

Figure 3.8.1 Regional mass balances: Annual glaciological balances (m w.e.) and annual rates of geodetic balances (m w.e. a^{-1}) are shown together with the corresponding number of glaciers with observations. Geodetic balances were calculated assuming a glacier-wide average density of 850 kg m^{-3}.

Central Europe has about 2,000 km^2 of glacier ice. The major part of it is located in the Alps with Grosser Aletschgletscher as its largest valley glacier. The Alps represent the 'water tower' of Europe and form the watershed of the Mediterranean Sea, the North Sea/North Atlantic Ocean, and the Black Sea. Some smaller glaciers are found in the Pyrenees – a mountain range in southwest Europe which extends from the Bay of Biscay to the Mediterranean Sea. The glaciers are situated in the Maladeta massif in Spain and around the Vignemale peak in France. A few more perennial icefields exist e.g., in the Apennine, Italy, as well as in Slovenia and Poland.

Central Europe has the greatest number of available front-variation and mass-balance measurements, with many long-term series. From the over 60 mass-balance series, ten have been maintained for more than 30 years. Over 700 front-variation series cover the entire Alps, many with more than 100 observation years. In addition, reconstructed front variations are available for a dozen glaciers extending back to the 16th century. About three dozen front-variation series are available from the Pyrenees range, some of them extending back to the 19th century. Mass-balance measurements have been carried out at Maladeta (ES) and Ossoue (FR) glaciers. In the Apennine, long-term measurements are available from Calderone (IT).

Front-variation observations give good documentation of the subsequent retreat with intermittent periods of re-advances in the 1890s, 1920s, and 1970–80s.

Glacier-mass loss accelerated from close to zero balances in the 1960s and 1970s, to –560/–720/–1,030 mm w.e. a^{-1} in the 1980s/1990s/2000s. Glaciological results are well supported by results from geodetic surveys from air-borne (Fischer et al. 2015) and space-borne (Sommer et al. 2020) surveys.

Seasonal balances show a relatively large mass turnover and a tendency towards more negative summer balances over the past decades. Regional mean balances were negative with –826 mm w.e. in 2019/20 and –636 mm w.e. in 2020/21. Regional glacier change assessments were recently published by Davaze et al. (2020), GLAMOS (2020), Haeberli et al. (2019), Huss et al. (2015), Lieb & Kellerer-Pirklbauer (2019, and earlier issues), and Žebre et al. (2021).

Estimated total glacier area (km^2):	2,000
Front variations	
- # of series*:	740/281
- # of obs. from stat. or adv. glaciers*:	7,473/32
- # of obs. from retreating glaciers*:	24,451/377
Glaciological balances	
- # of series*:	82/56
- # of observations*:	2,150/109
Geodetic balances	
- # of series°:	3,960/3,781
- # of observations°:	20,530/11,374

* (total/2020 & 2021), ° (total/>2009)

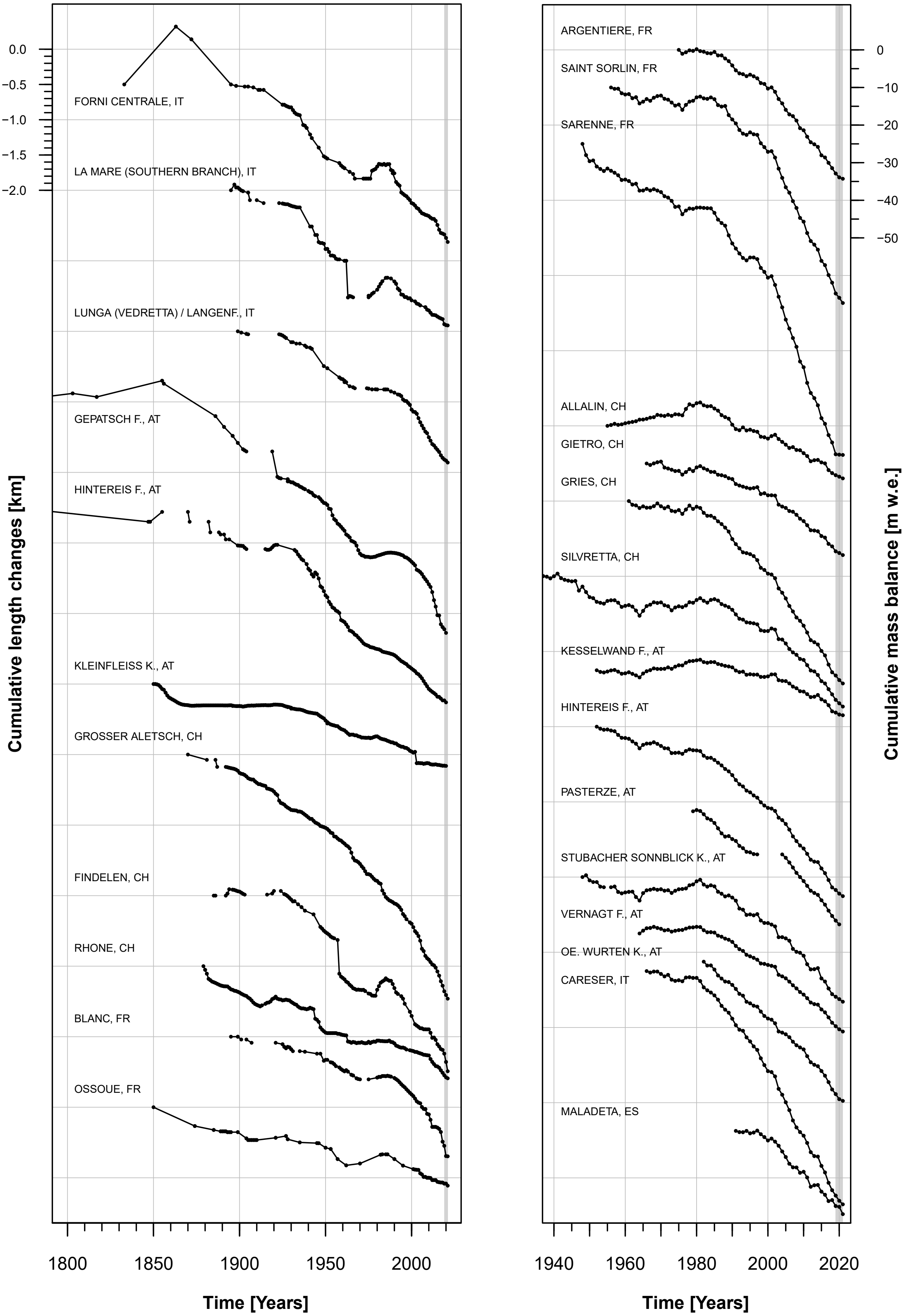

Figure 3.8.2 Cumulative length changes (left) and cumulative mass balances (right) of selected glaciers in Central Europe over the entire observation period.

3.9 CAUCASUS & MIDDLE EAST

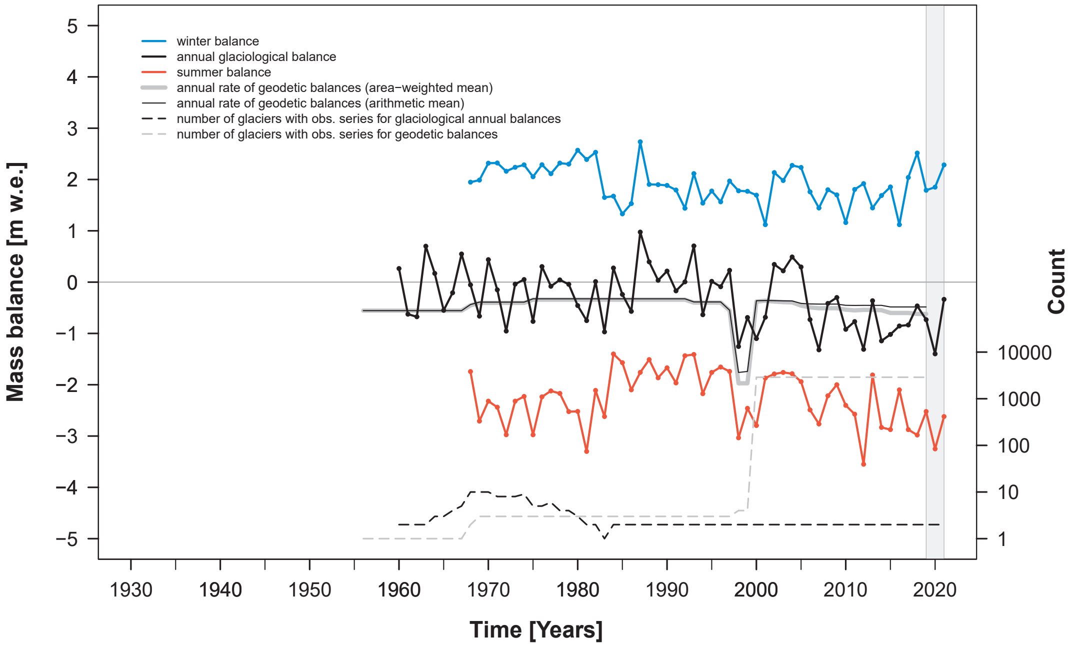

Figure 3.9.1 Regional mass balances: Annual glaciological balances (m w.e.) and annual rates of geodetic balances (m w.e. a^{-1}) are shown together with the corresponding number of glaciers with observations. Geodetic balances were calculated assuming a glacier-wide average density of 850 kg m^{-3}.

The Greater Caucasus mountain range contains over 2000 glaciers (Tielidze & Wheate, 2018), with total area of about 1500 km^2. This is about 96% of the contemporary glacier area of the Caucasus and Middle East glacier region. Most of the glaciers are located in the northern Caucasus, with Mount Elbrus (5,642 m a.s.l.) considered the highest peak in Europe. The climate of the Caucasus varies with elevation and latitude. The northern slopes are a few degrees colder than the southern slopes and precipitation increases from east to west in most regions. In the Middle East, small glaciers are found on Mount Erciyes in Central Anatolia, Turkey, as well as in the higher elevations of the Sabalan, Takhte-Soleiman, Damavand, Oshtorankuh, and Zardkuh regions in Iran.

Mass-balance measurements are reported from a dozen glaciers located in the Caucasus with ongoing long-term series at Djankuat and Garabashi (RU). Frontal variations of glaciers in the Caucasus as well as of Erciyes Glacier (TR) are well-documented throughout the 20th century. Geodetic measurements are available for only Djankuat (Rets et al., 2019) and Alamkouh glaciers located in the Russian Caucasus and in the Takhte–Soleiman of Iran, respectively. In the Caucasus, glaciers reached their LIA maximum extents around 1850 (Grove, 2004). Glacier-front variations show a general trend of glacier retreat with intermittent re-advances around the 1980s. Few further length-change measurements have been reported since 2010.

The few mass-balance measurement series indicate negative mean balances around –250 mm w.e. a^{-1} over the past decades, with a relatively large mass turnover (Tielidze et al. 2022). The negative peak in the geodetic results before 2000 is caused by the very small geodetic sample size, and an unfortunate mixture of the moderately negative values from the Caucasus glaciers with the strongly negative values from Alamkouh Glacier, Iran. The mean balances of Djankuat and Garabashi glaciers were –1,398 mm w.e. and –336 mm w.e. in 2019/20 and 2020/21, respectively.

Regional glacier change assessments were recently published by Kutuzov et al. (2019), and Tielidze et al. (2018, 2020).

Estimated total glacier area (km^2):	1,500
Front variations	
- # of series*:	76/2
- # of obs. from stat. or adv. glaciers*:	243/0
- # of obs. from retreating glaciers*:	805/4
Glaciological balances	
- # of series*:	13/2
- # of observations*:	196/4
Geodetic balances	
- # of series°:	2,895/2,895
- # of observations°:	18,079/12,207

* (total/2020 & 2021), ° (total/>2009)

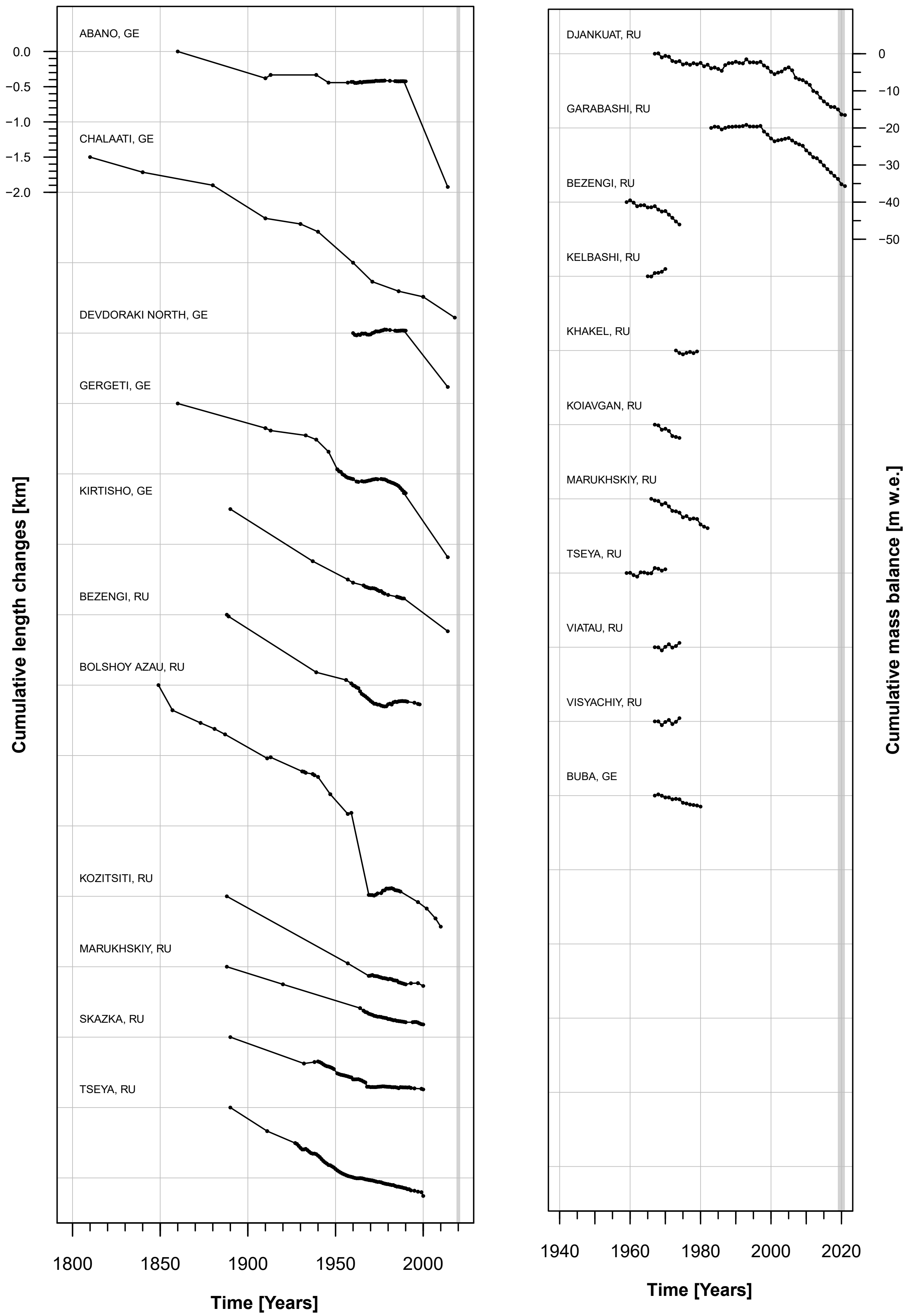

Figure 3.9.2 Cumulative length changes (left) and cumulative mass balances (right) of selected glaciers in Caucasus and Middle East over the entire observation period.

3.10 RUSSIAN ARCTIC

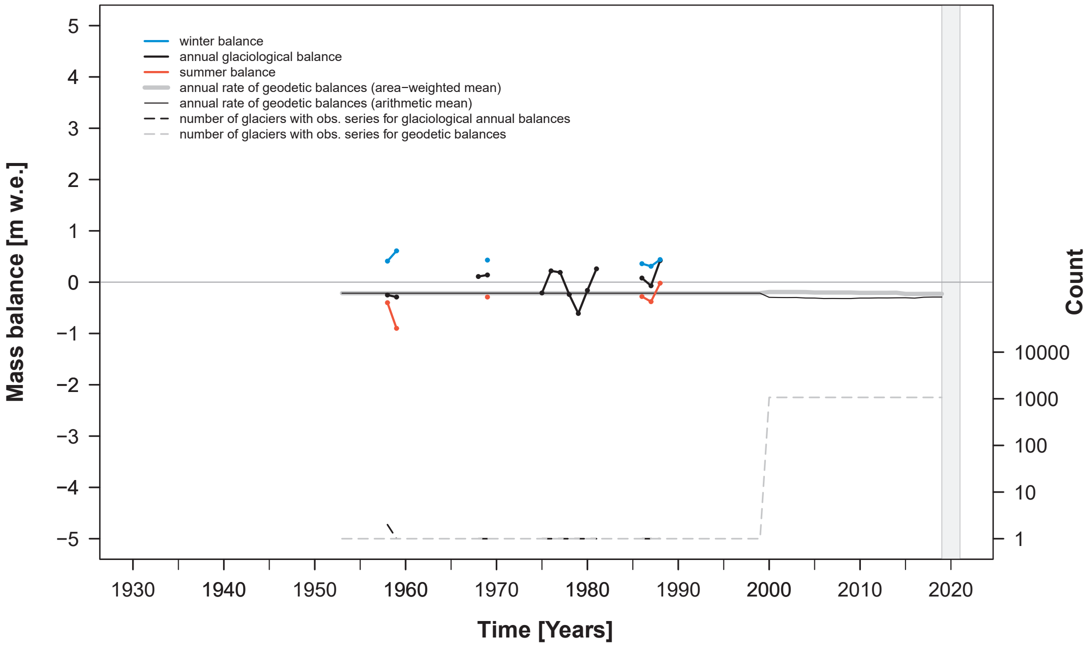

Figure 3.10.1 Regional mass balances: Annual glaciological balances (m w.e.) and annual rates of geodetic balances (m w.e. a^{-1}) are shown together with the corresponding number of glaciers with observations. Geodetic balances were calculated assuming a glacier-wide average density of 850 kg m^{-3}.

Large ice caps are located on the Russian high Arctic archipelagos such as Novaya Zemlya, Severnaya Zemlya and Franz Josef Land totalling an area of 51,500 km^2. These glaciers are very much influenced by the North Atlantic Oscillation and sea-ice conditions in the Barents and Kara Seas.

The glaciers in this region are not well investigated due to their remote locations. Front variations have been reported from about 40 outlet glaciers on Novaya Zemlya based on expeditions, topographic maps and remote sensing data (e.g., Carr et al., 2014).

Mass-balance measurements are limited to a few observation years from Sedov Glacier on Hooker Island, Franz Josef Land, and Glacier No. 104, which is part of Vavilov Ice Cap on October Revolution Island, Severnaya Zemlya.

Dated moraines suggest LIA maxima around or after 1300 for some glaciers, and the late 19th century for others on Novaya Zemlya (Zeeberg & Forman, 2001). In the Russian Arctic islands, a slight reduction was found in the glacierized area of little more than one per cent over the past 50 years (Kotlyakov, 2006). Front-variation observations document a rapid retreat of tidewater glaciers on Novaya Zemlya over the 20th century, with a more stable period during the 1950s and 1960s.

The geodetic observations indicate a mass-change rate between 200 and 350 mm w.e. a^{-1}.

Regional glacier change assessments were recently published by Carr et al. (2014), Melkonian et al. (2016), Sommer et al. (2020), and Zheng et al. (2018).

Estimated total glacier area (km^2):	51,500
Front variations	
- # of series*:	44/0
- # of obs. from stat. or adv. glaciers*:	151/0
- # of obs. from retreating glaciers*:	382/0
Glaciological balances	
- # of series*:	3/0
- # of observations*:	15/0
Geodetic balances	
- # of series°:	1,070/1,070
- # of observations°:	9,025/6,875

* (total/2020 & 2021), ° (total/>2009)

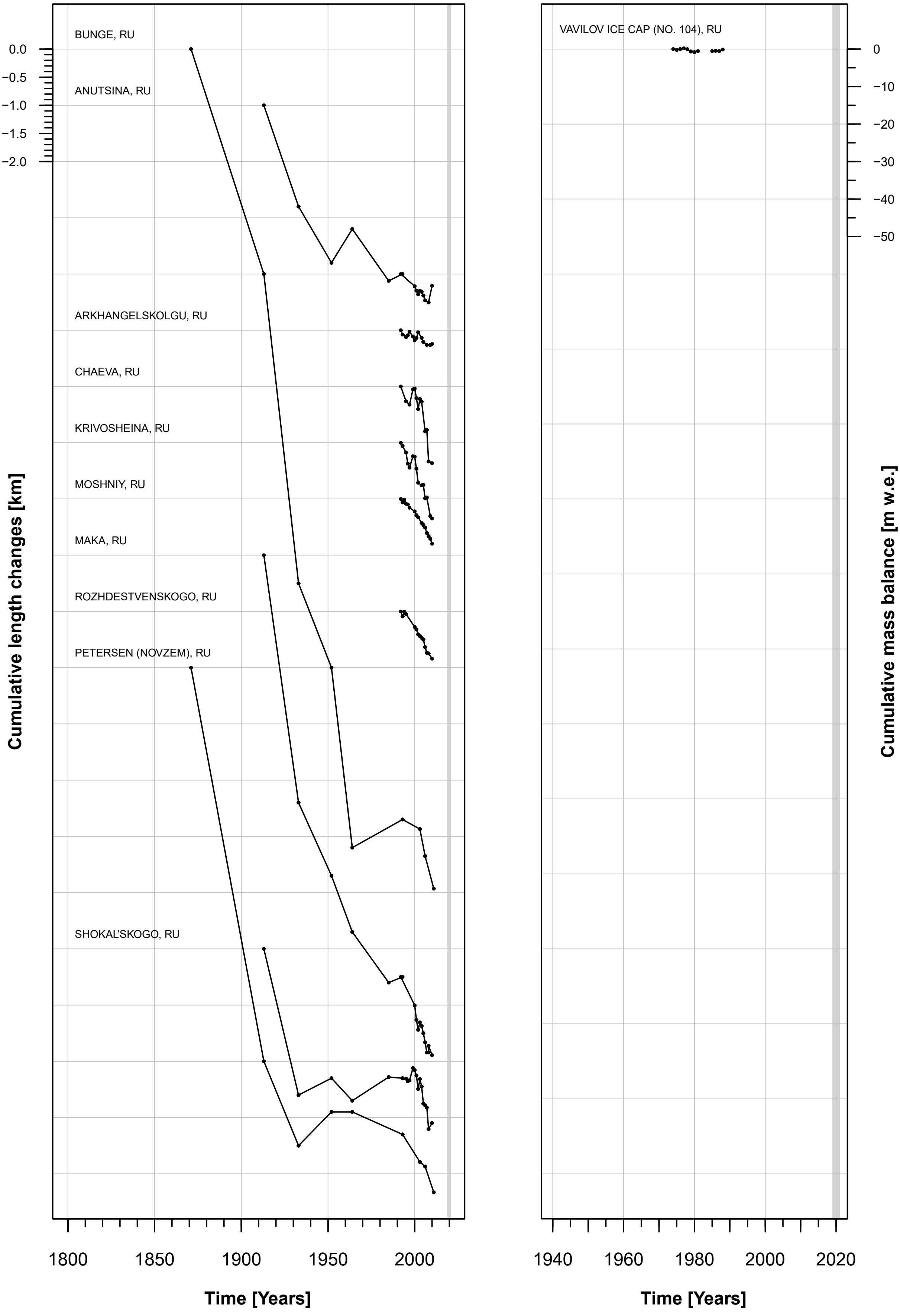

Figure 3.10.2 Cumulative length changes (left) and cumulative mass balances (right) of selected glaciers in the Russian Arctic over the entire observation period.

3.11 ASIA NORTH

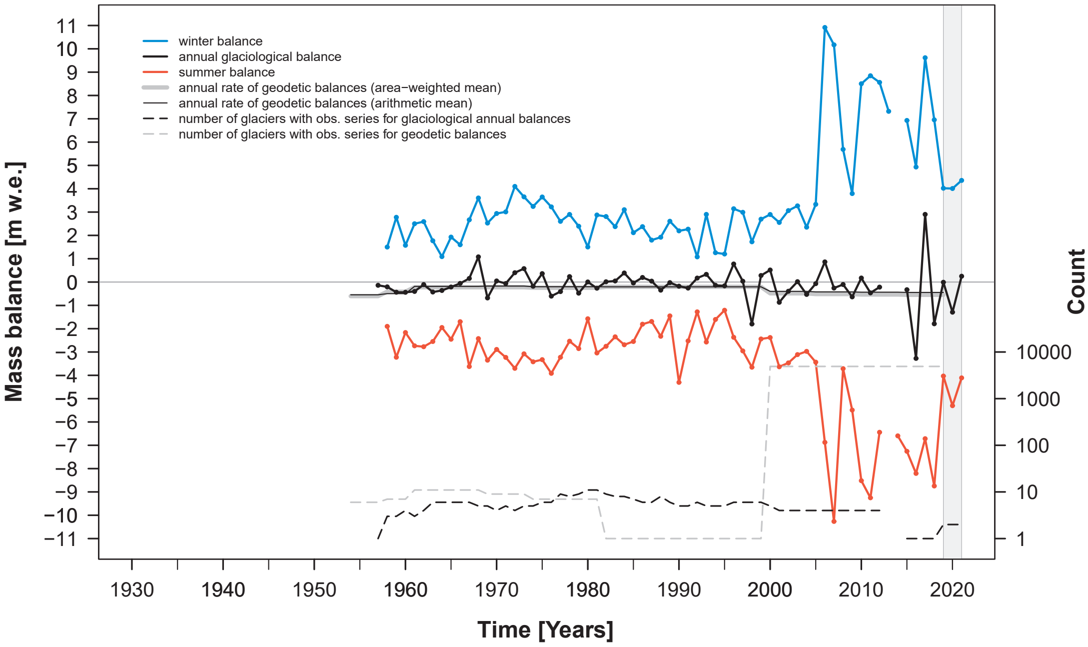

Figure 3.11.1 Regional mass balances: Annual glaciological balances (m w.e.) and annual rates of geodetic balances (m w.e. a^{-1}) are shown together with the corresponding number of glaciers with observations. Geodetic balances were calculated assuming a glacier-wide average density of 850 kg m^{-3}.

In Northern Asia, glaciers with a total area of about 2,500 km^2 are located in the mountain ranges from the Ural to the Altai, in the east Siberian Mountains, and Kamchatka. The Ural Mountains form a north-south running mountain chain that extends about 2,500 km. Its mountain peaks reach 900 to 1,400 m a.s.l. hosting about 140 small glaciers in a continental climate. The Altai extends over about 2,100 km from Kazakhstan, China, and Russia to Mongolia, and hosts the greatest number of glaciers in this region. The east Siberian Mountains such as Cherskiy Range, Suntar-Khayata, and Kodar Mountains, have only small amounts of glacier ice. The topography of Kamchatka is characterized by numerous volcanoes with heights up to almost 5,000 m a.s.l. Here, many glaciers are strongly influenced by volcanic activities.

The available data series are sparse and most of them were discontinued in the latter decades of the 20^{th} century. The few mass-balance programmes were reported from Maliy Aktru, Leviy Aktru, and Vodopadniy (No. 125) glaciers in the Russian Altai, but got interrupted after 2012. In 2018/19, the mass-balance programme at Leviy Aktru was resumed. In Japan, long-term observations are carried out on Hamagury Yuki, a perennial snow patch which is located in the northern Alps of Central Japan.

Until some years ago, investigations in the Altay failed to reveal evidence of early LIA advances (Kotlyakov et al., 1991). New studies based on lichenometry indicate extended glacier states in the late 14^{th} and mid-19^{th} centuries (Solomina, 2000). In the Cherskiy Range, the LIA maxima extents have been dated as 1550–1850 (Gurney et al., 2008). On Kamchatka, the maximum stage of the LIA was reached in the 19^{th} century (Grove, 2004), with advances of similar magnitude in the 17^{th} and 18^{th} centuries (Solomina, 2000). The few front-variation series show a centennial retreat with no distinct re-advance periods. Kozelskiy Glacier on Kamchaka advanced during the 1950s to the mid-1980s.

Available mass-balance measurements reveal slightly negative balances since the 1960s. The regional average balance (i.e. Leviy Aktru) was negative with –1,292 and –249 mm w.e. for 2019/20 and 2020/21, respectively.

Estimated total glacier area (km^2):	2,500
Front variations	
- # of series*:	23/0
- # of obs. from stat. or adv. glaciers*:	43/0
- # of obs. from retreating glaciers*:	322/0
Glaciological balances	
- # of series*:	19/2
- # of observations*:	319/4
Geodetic balances	
- # of series°:	4,917/4,908
- # of observations°:	24,558/14,724
* (total/2020 & 2021), ° (total/>2009)	

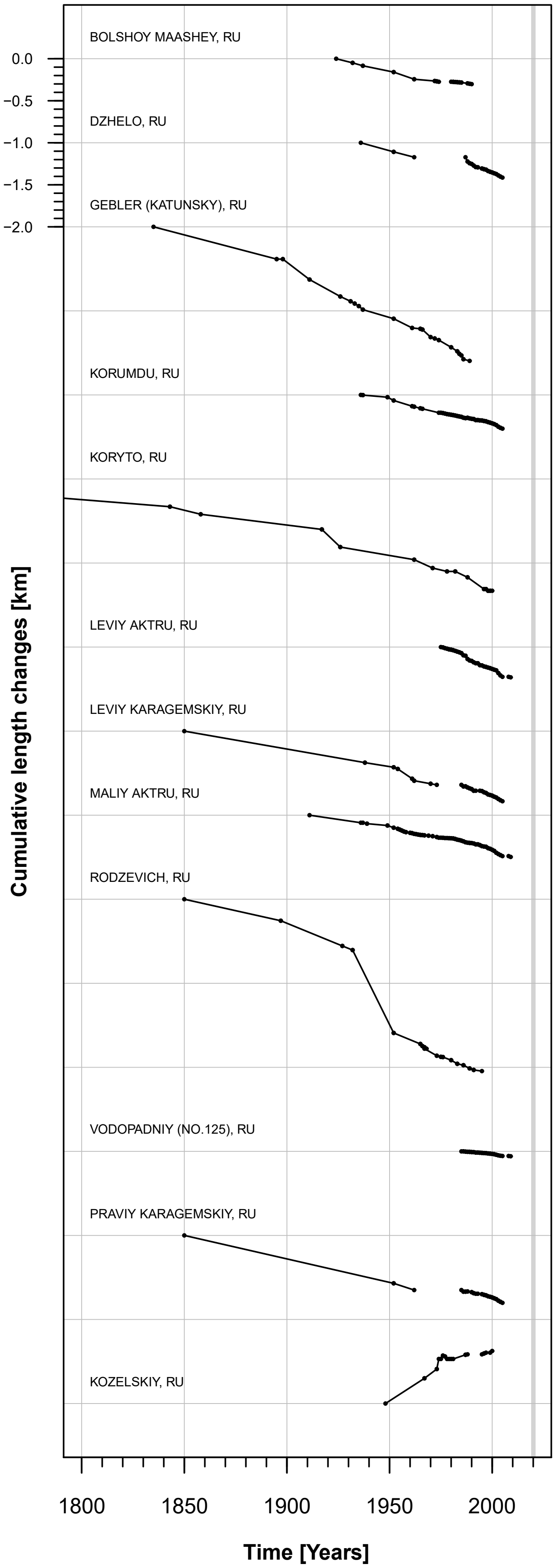

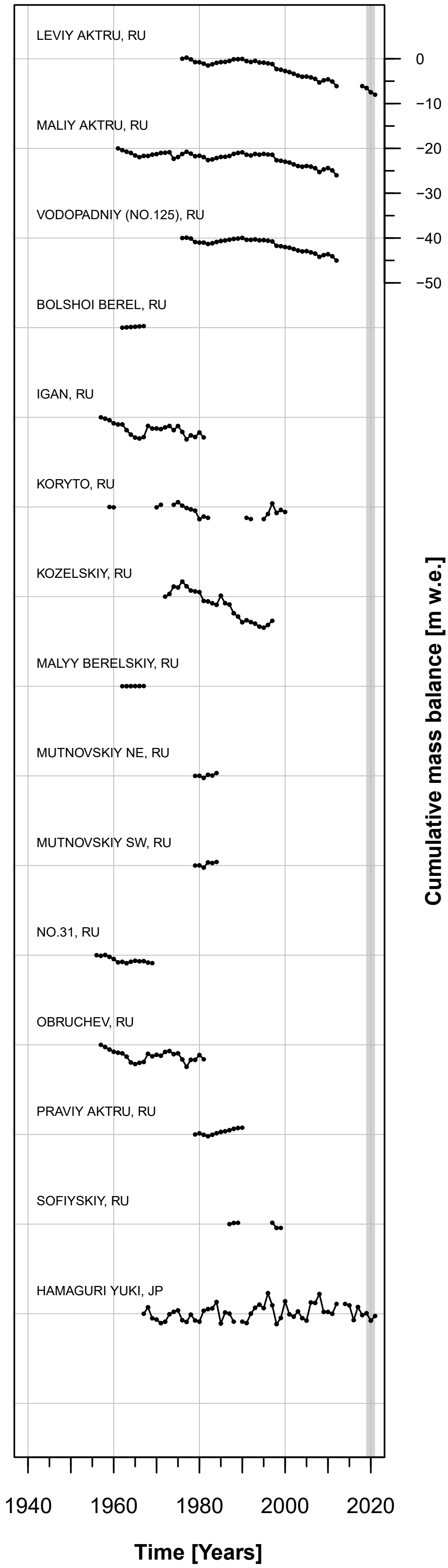

Figure 3.11.2 Cumulative length changes (left) and cumulative mass balances (right) of selected glaciers in Asia North over the entire observation period.

3.12 ASIA CENTRAL

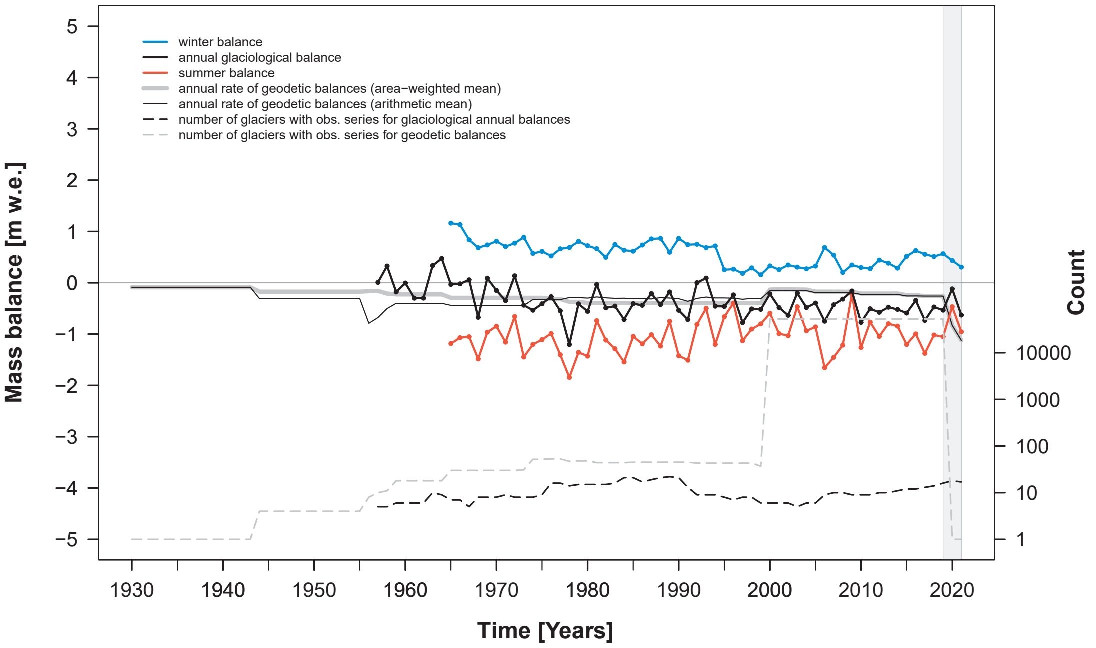

Figure 3.12.1 Regional mass balances: Annual glaciological balances (m w.e.) and annual rates of geodetic balances (m w.e. a^{-1}) are shown together with the corresponding number of glaciers with observations. Geodetic balances were calculated assuming a glacier-wide average density of 850 kg m^{-3}.

Central Asia stretches from the Caspian Sea in the west to China in the east and from Russia in the north to Afghanistan in the south. It is characterised by a continental climate. Glaciers cover a total area of about 49,500 km^2 and are located in the Hissar Alay, Pamir, Tien Shan, Kunlun, and Qilian Mountains.

There is a large number of glacier fluctuation series available, distributed evenly over the region. However, continuous long-term measurements are sparse. Most of the observation series were discontinued after the demise of the Soviet Union. Only two of the long-term mass-balance programmes have been continued: Ts. Tuyuksuyskiy and Urumqi Glacier No. 1 in the Kazakh and Chinese Tien Shan, respectively. In recent years, interrupted long-term mass-balance measurements have been resumed at Abramov, Golubin, Glacier No. 354 (Akshiyrak), Batysh Sook/Syek Zapadniy, and Kara-Batkak in Kyrgyzstan.

The LIA is considered to have lasted until the mid or late 19th century in most regions (Grove, 2004) with glacier maximum extents occurring between the 17th and mid 19th centuries (Solomina, 1996; Su & Shi, 2002; Kutuzov, 2005). Front-variation observations show a general retreat over the 20th century with some re-advances around the 1970s.

The available mass-balance measurements indicate slightly negative balances in the 1950s and 1960s with increased ice loss of about –500 mm w.e. a^{-1} between the 1970s and 2000s. Seasonal balances show a relatively small mass turnover. The glaciological results are supported by the available geodetic surveys. Regional average balances for 2019/20 and 2020/21 were –119 and –629 mm w.e., respectively.

Geodetic assessments were made available from various studies (Brun et al., 2017; Gardelle et al. 2013; Holzer et al., 2015; Piedzonka & Bolch, 2015) and show a mass-change rate of about –250 mm a^{-1} since 2000.

Regional glacier change assessments were recently published by Barandun et al. (2020, 2021), Sorg et al. (2012), Unger-Shayesteh et al. (2013), Farinotti et al. (2015), and Hoelzle et al. (2017).

Estimated total glacier area (km^2):	49,500
Front variations	
- # of series*:	302/9
- # of obs. from stat. or adv. glaciers*:	396/6
- # of obs. from retreating glaciers*:	1,205/12
Glaciological balances	
- # of series*:	52/19
- # of observations*:	720/35
Geodetic balances	
- # of series°:	52,973/52,962
- # of observations°:	276,453/169,646
* (total/2020 & 2021), ° (total/>2009)	

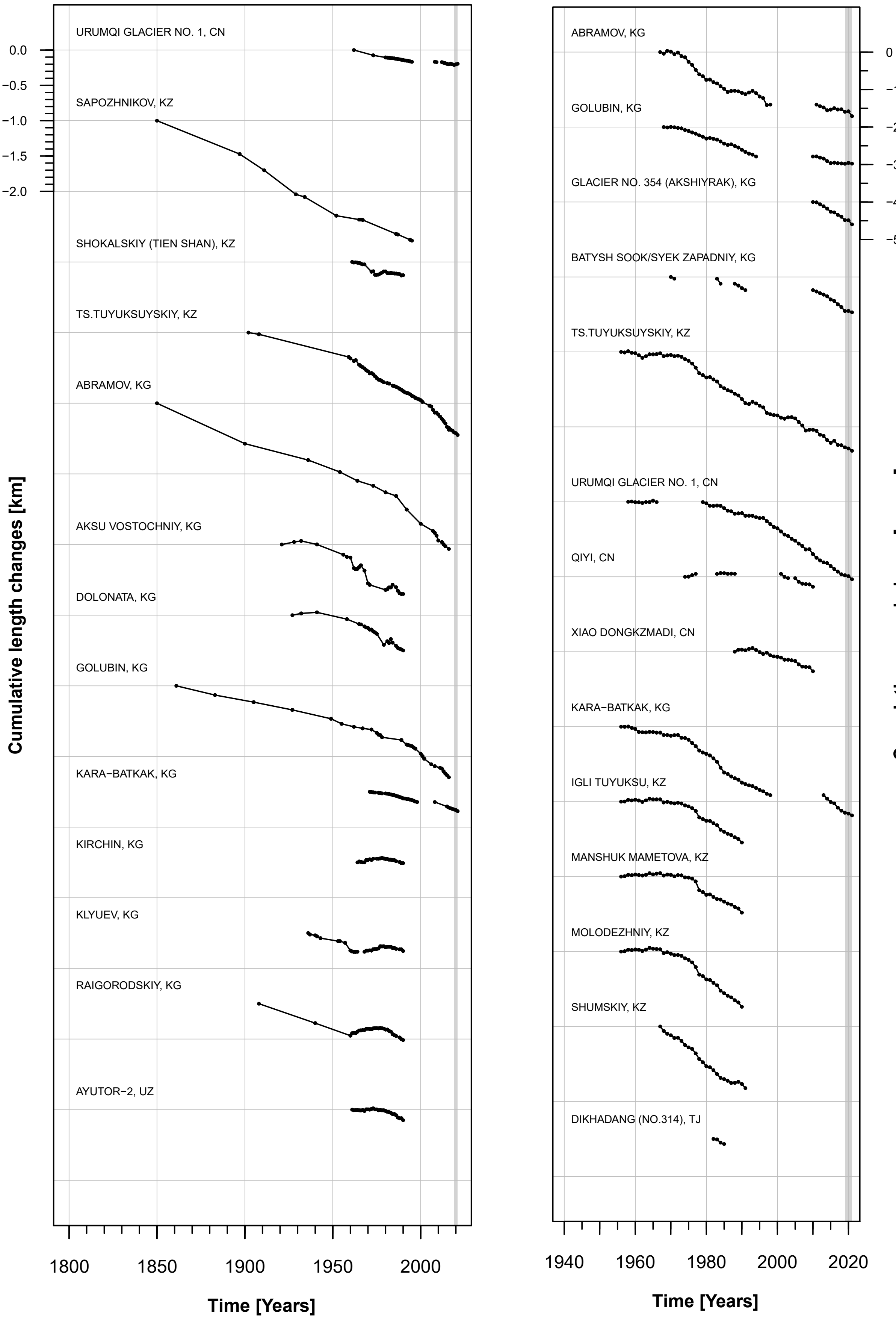

Figure 3.12.2 Cumulative length changes (left) and cumulative mass balances (right) of selected glaciers in Asia Central over the entire observation period.

3.13 ASIA SOUTH WEST & SOUTH EAST

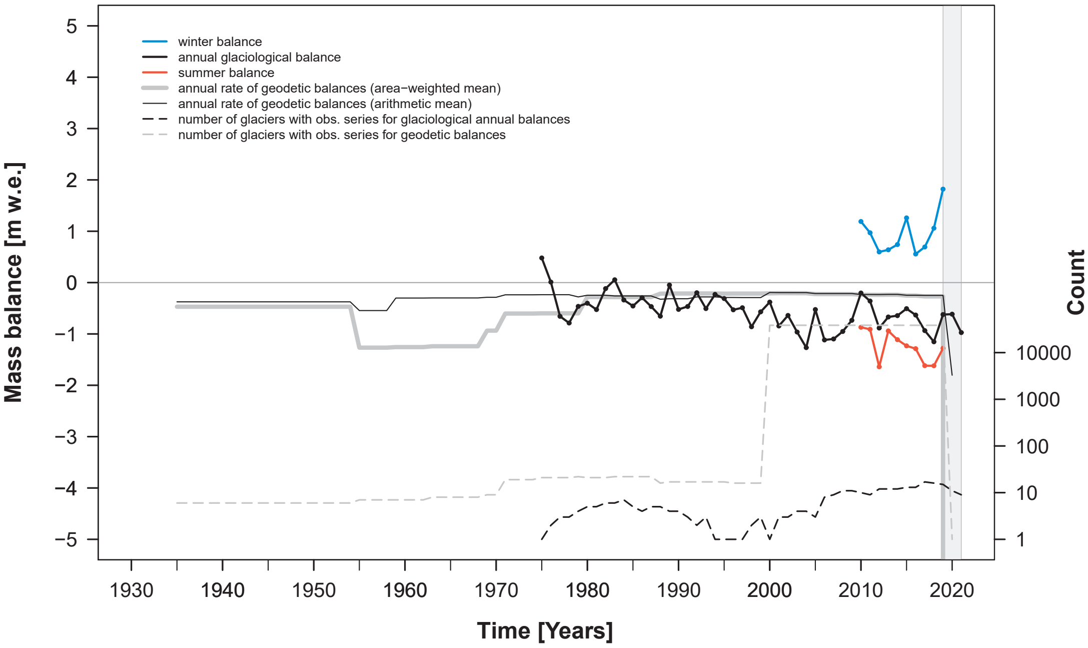

Figure 3.13.1 Regional mass balances: Annual glaciological balances (m w.e.) and annual rates of geodetic balances (m w.e. a^{-1}) are shown together with the corresponding number of glaciers with observations. Geodetic balances were calculated assuming a glacier-wide average density of 850 kg m^{-3}.

Adjacent to Central Asia, the regions Asia South West and Asia South East comprise the Karakoram, Hindu Kush, Himalaya, and Hengduan Shan mountain ranges. The Himalaya is the largest mountain range in the world and extends from the Nanga Parbat (8,126 m a.s.l.) in the NW over 2,500 km to the Mancha Barwa (7,782 m a.s.l.) in the SE. The climate, and the precipitation in particular, is characterized by the influence of the South Asian monsoon in summer and the mid-latitude westerlies in winter. The glacier area in this region totals about 48,500 km^2.

The data coverage of Asia South West is very sparse. The only reported mass-balance series of more than ten years is from Chhota Shigri located in the Himachal Pradesh, India. Also Asia South East lacks long-term glacier observation series. Recent mass-balance results are reported from Parlung Glacier No. 94, located in the south-eastern Tibetan Plateau, and from Yala, Rikha Samba, Pokalde, West Changri Nup and Mera glaciers in Nepal.

The LIA is considered to have lasted until the mid or late 19th century in most regions (Grove, 2004) with glacier maximum extents occurring between the 17th and mid-19th century (Solomina, 1996; Su & Shi, 2002; Kutuzov, 2005). Front-variation observations show a general retreat over the 20th century with no marked period of glacier re-advances.

Glaciological and geodetic surveys reported from a variable glacier sample indicate an ice loss at the rate of a few hundred millimetres w.e. a^{-1} over the past decades. For 2019/20 and 2020/21, reported balances were –1,092 and –531 mm w.e., respectively, in Asia South East and –138 and –1,415 mm w.e., respectively, in Asia South West. From the Karakoram, information about positive mass balances and re-advances of (mainly surge-type) glaciers has been reported for the beginning of the 21st century.

Regional glacier change assessments were recently made available by Azam et al. (2018), Bolch et al. (2011), Brun et al. (2015), Dehecq et al. (2019), Gardelle et al. (2013), Rankl et al. (2014), Shean et al. (2020), and Vijay & Braun (2016).

Estimated total glacier area (km^2):	48,500
Front variations	
- # of series*:	114/4
- # of obs. from stat. or adv. glaciers*:	69/0
- # of obs. from retreating glaciers*:	337/05
Glaciological balances	
- # of series*:	43/11
- # of observations*:	299/20
Geodetic balances	
- # of series°:	38,572/38,568
- # of observations°:	198,867/121,477

* (total/2020 & 2021), ° (total/>2009)

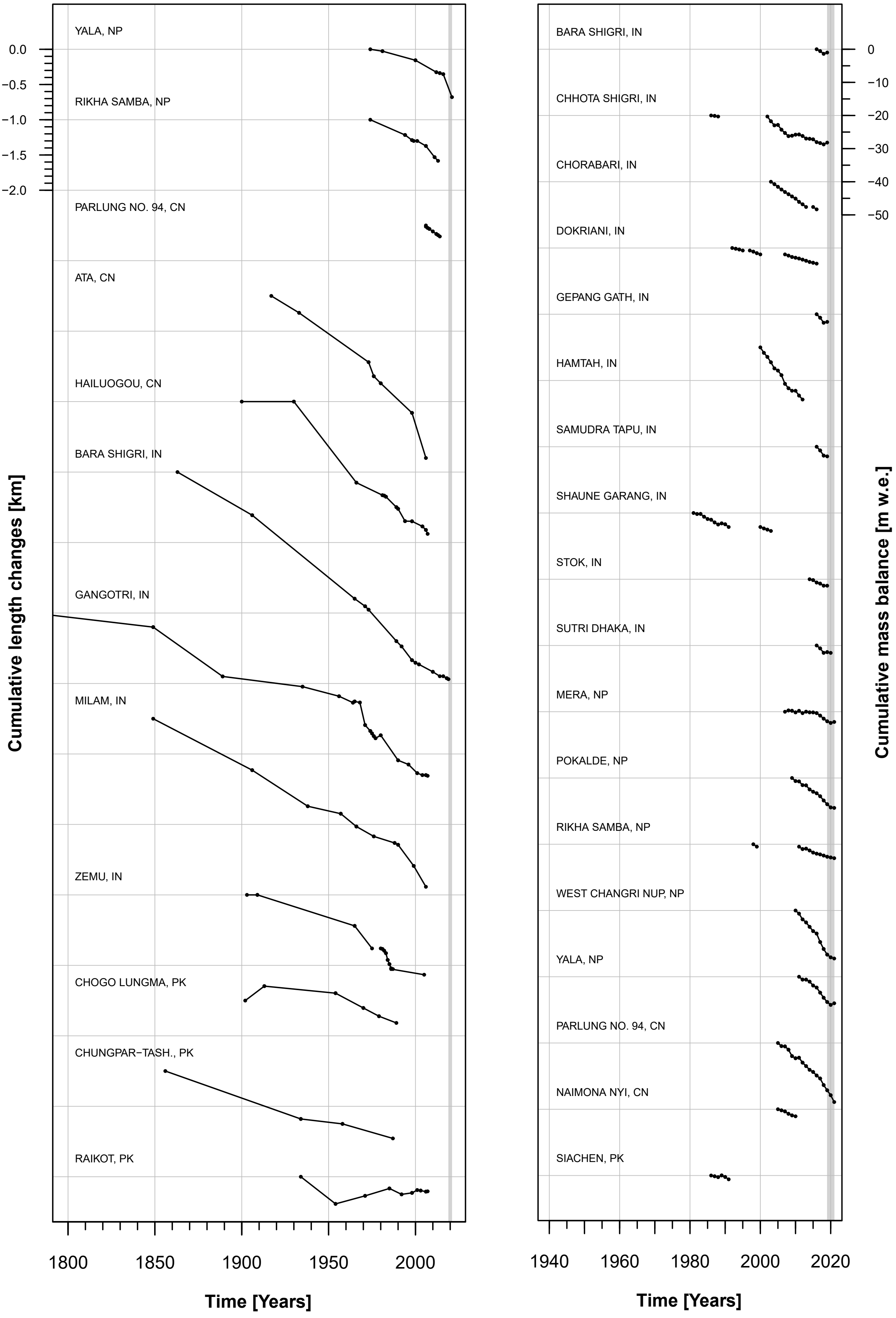

Figure 3.13.2 Cumulative length changes (left) and cumulative mass balances (right) of selected glaciers in Asia South East and South West over the entire observation period.

3.14 LOW LATITUDES (incl. Africa & New Guinea)

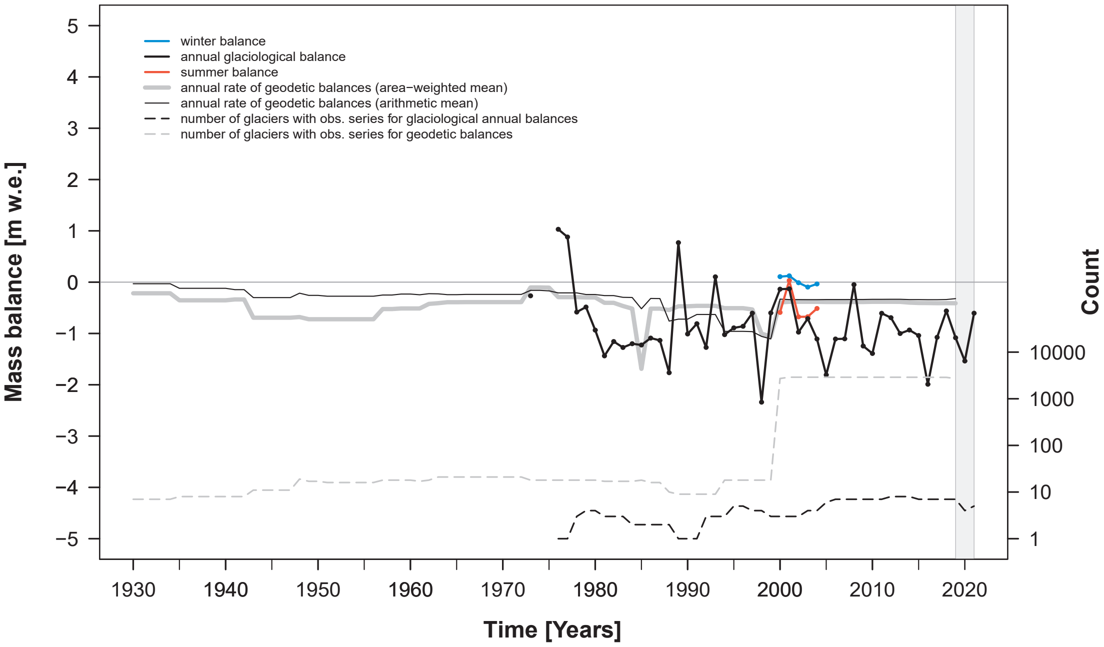

Figure 3.14.1 Regional mass balances: Annual glaciological balances (m w.e.) and annual rates of geodetic balances (m w.e. a^{-1}) are shown together with the corresponding number of glaciers with observations. Geodetic balances were calculated assuming a glacier-wide average density of 850 kg m^{-3}.

Glaciers in the low latitudes are situated on the highest mountain peaks of Mexico and in the tropical Andes. In addition, a few ice bodies are located in East Africa on Ruwenzori, Mount Kenya and Kilimanjaro, as well as in Papua (formerly Irian Jaya, Indonesia) and Papua New Guinea. The glacier area of the Low Latitudes totals about 2,500 km² of which the largest parts are located in Peru and Bolivia. In the tropical Andes, long-term monthly mass-balance measurements are carried out at Zongo and Charquini Sur glaciers (BO), Antizana 15 Alpha (EC), and Conejeras (CO). Several dozen front-variation series document glacier retreat over the past half-century. Front variations of glaciers in Africa and New Guinea are well documented with a few observation series back to the 19th century. From Lewis Glacier on Mount Kenya, mass-balance measurements have been reported between 1978/79 and 1995/96 and again between 2010/11 and 2013/14.

In the tropical Andes, glaciers reached their latest LIA maximum extensions between the mid-17th and early 18th centuries (Rabatel et al., 2013). Glaciers in Peru and Ecuador were in advanced positions until the 1860s, followed by a rapid retreat (Grove, 2004). Front-variation observations document a general retreat over the 20th century, with increase retreat rates since the late 1970s. In Africa, glaciers reached their LIA maximum extents towards the late 19th century (Hastenrath, 2001) followed by a continuous retreat until present. In New Guinea, glaciers reached their LIA maxima in the mid-19th century. Here the glacier changes have been traced from information on glacier extents derived from historical records, dated cairns erected during several expeditions, and remote sensing data. All ice masses except some on Punkcak Java seem to have now disappeared.

The regional mass balance shows a strong interannual variability with an average mass balance around –800 mm w.e. a^{-1} since between the 1970s and the 2000s. The reported balances for 2019/20 and 2020/21 were –1,537 and –605 mm w.e., respectively. Geodetic observations show a smaller ice loss than indicated by glaciological observations. Regional glacier change assessments were recently published by Braun et al. (2019), Dussaillant et al. (2019), Prinz et al. (2011), and Rabatel et al. (2013).

Estimated total glacier area (km²):	2,500
Front variations	
- # of series*:	95/3
- # of obs. from stat. or adv. glaciers*:	58/0
- # of obs. from retreating glaciers*:	646/5
Glaciological balances	
- # of series*:	14/5
- # of observations*:	200/9
Geodetic balances	
- # of series°:	2,922/2,895
- # of observations°:	18,419/12,865

* (total/2020 & 2021), ° (total/>2009)

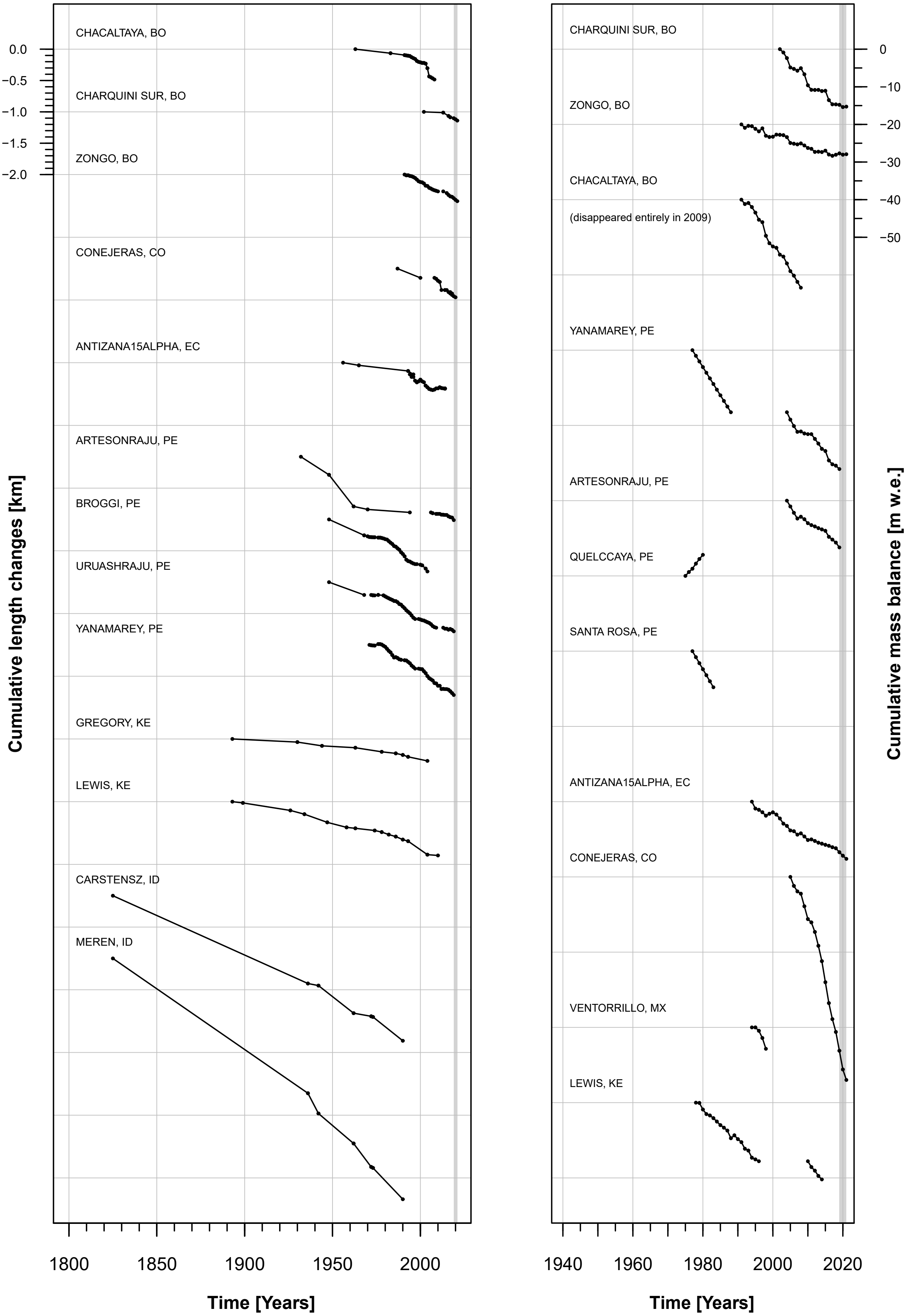

Figure 3.14.2 Cumulative length changes (left) and cumulative mass balances (right) of selected glaciers in the Low Latitudes over the entire observation period.

3.15 SOUTHERN ANDES

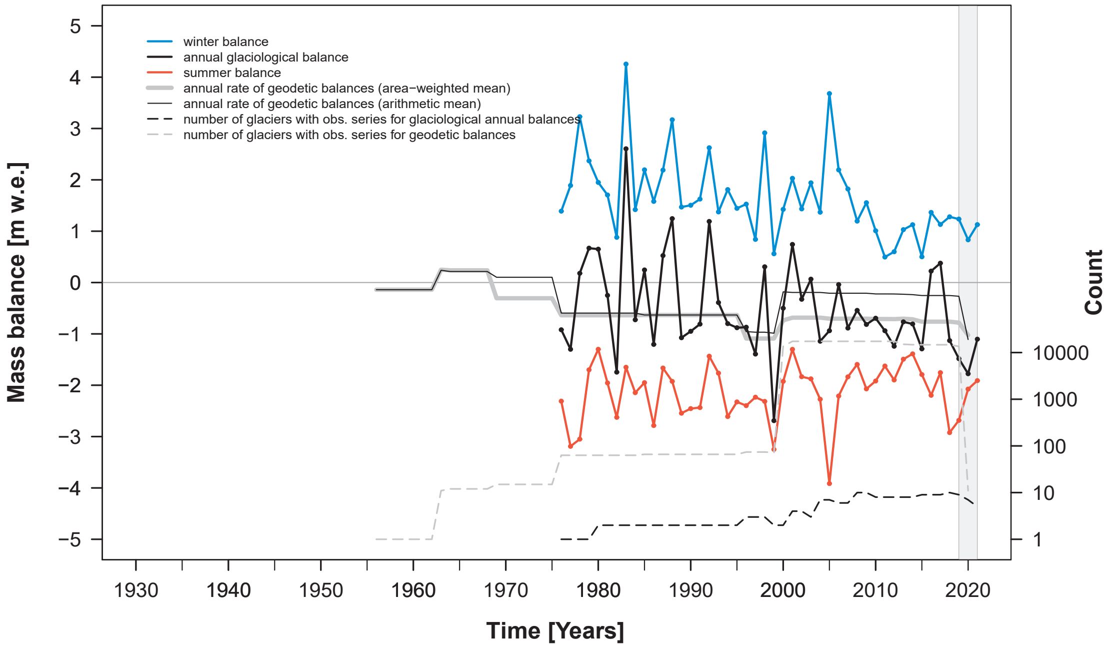

Figure 3.15.1 Regional mass balances: Annual glaciological balances (m w.e.) and annual rates of geodetic balances (m w.e. a^{-1}) are shown together with the corresponding number of glaciers with observations. Geodetic balances were calculated assuming a glacier-wide average density of 850 kg m^{-3}.

The Southern Andes contain the glaciers of Argentina and Chile, with a total glacier area of about 29,500 km² (cf., Barcaza et al., 2017; Zalazar et al., 2017). The climate and topography vary along the Andes with an important transition around 35° S, between the Dry Andes to the north and the Wet Andes to the south. Most of the glacier area is located in the Wet Andes, including the large Northern and Southern Patagonian Icefields and Cordillera Darwin in Tierra del Fuego. However, the importance of glaciers as a freshwater storage is much higher in the Dry Andes where major cities with large irrigation areas, like Santiago and Mendoza, are located.

The longest mass-balance series of the entire Andes is reported from Echaurren Norte (CL) with continuous measurements since 1975/76. The available mass-balance measurements indicate a strong interannual variability with decadal mean balances slightly negative in the 1970s, 1980s, and 2000s; and –680 mm w.e. a^{-1} in the 1990s. In the last 10 years, several new monitored series were initiated on glaciers in different regions. Regional mean balances were negative with –1,776 mm w.e. in 2019/20 and –1,103 mm w.e. in 2020/21.

Geodetic thickness changes for most glaciers in the Southern Andes were comprehensively assessed and show widespread loss since 2000, with larger rates in the Wet Andes (Braun et al., 2019; Dussaillant et al., 2019; Falaschi et al. 2019; Ferri et al. 2020). The icefields of Patagonia have the highest down-wasting rates, contributing significantly to sea-level rise (Rignot et al., 2003; Malz et al., 2018).

In the Southern Andes, most glaciers reached their LIA maximum between the late 17th and early 19th century (Masiokas et al., 2009). Most front-variation measurements document a general retreat since the LIA maximum extent with some re-advances in the 1980s and a general retreat trend in recent decades (Espizua & Maldonado, 2007; Espizua & Pitte, 2009; Lopez et al., 2010; Meier et al., 2018). In the Dry Andes, 21 glaciers with surge-type behavior were found (Falaschi et al., 2018); the most recent being Horcones Inferior and Nevado del Plomo in Argentina (Harrison et al., 2015; Pitte et al., 2016).

Estimated total glacier area (km²):	29,500
Front variations	
- # of series*:	220/0
- # of obs. from stat. or adv. glaciers*:	200/0
- # of obs. from retreating glaciers*:	623/0
Glaciological balances	
- # of series*:	16/7
- # of observations*:	208/12
Geodetic balances	
- # of series°:	17,418/17,404
- # of observations°:	89,934/62,681

* (total/2020 & 2021), ° (total/>2009)

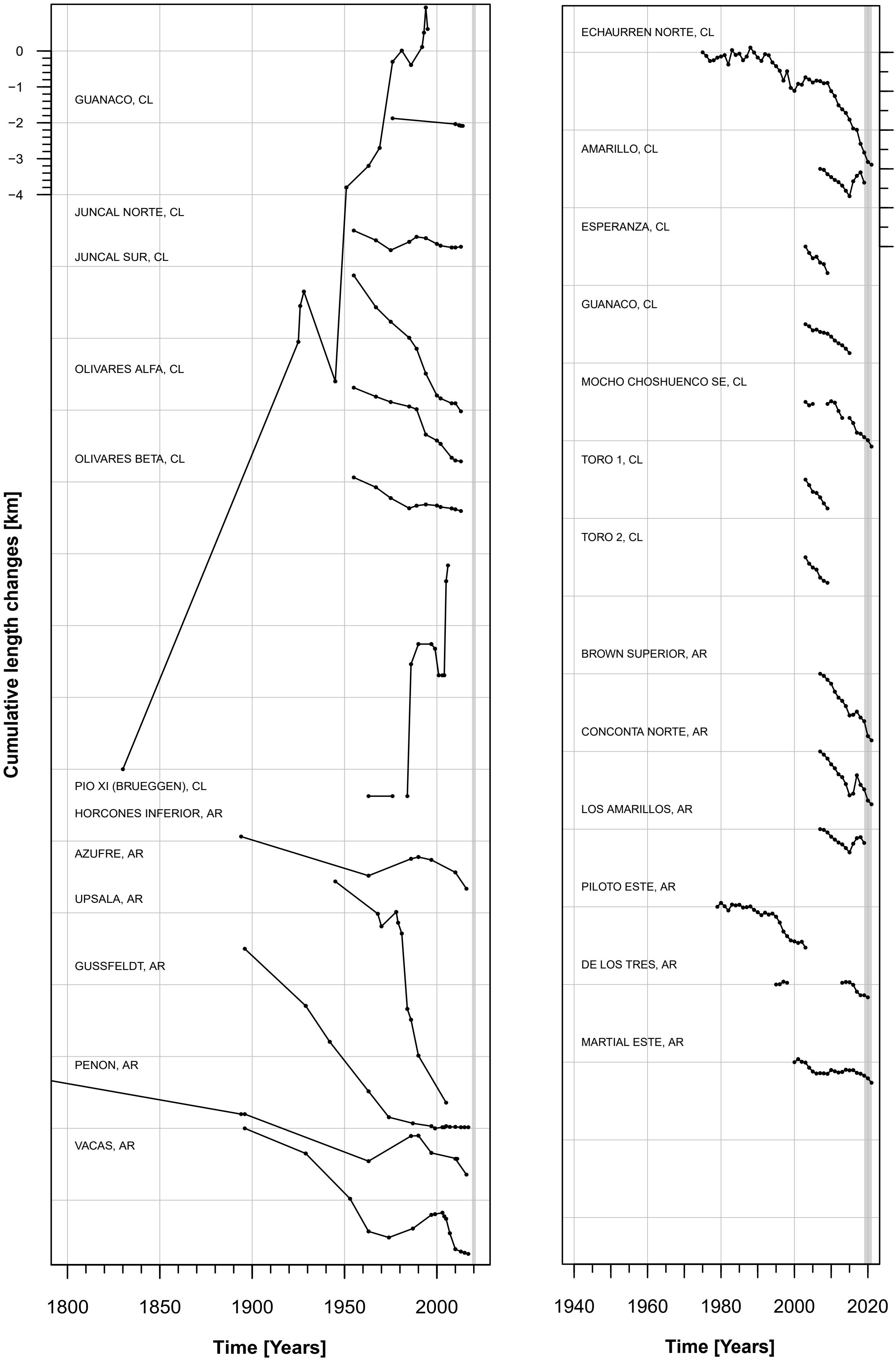

Figure 3.15.2 Cumulative length changes (left) and cumulative mass balances (right) of selected glaciers in the Southern Andes over the entire observation period.

3.16 NEW ZEALAND

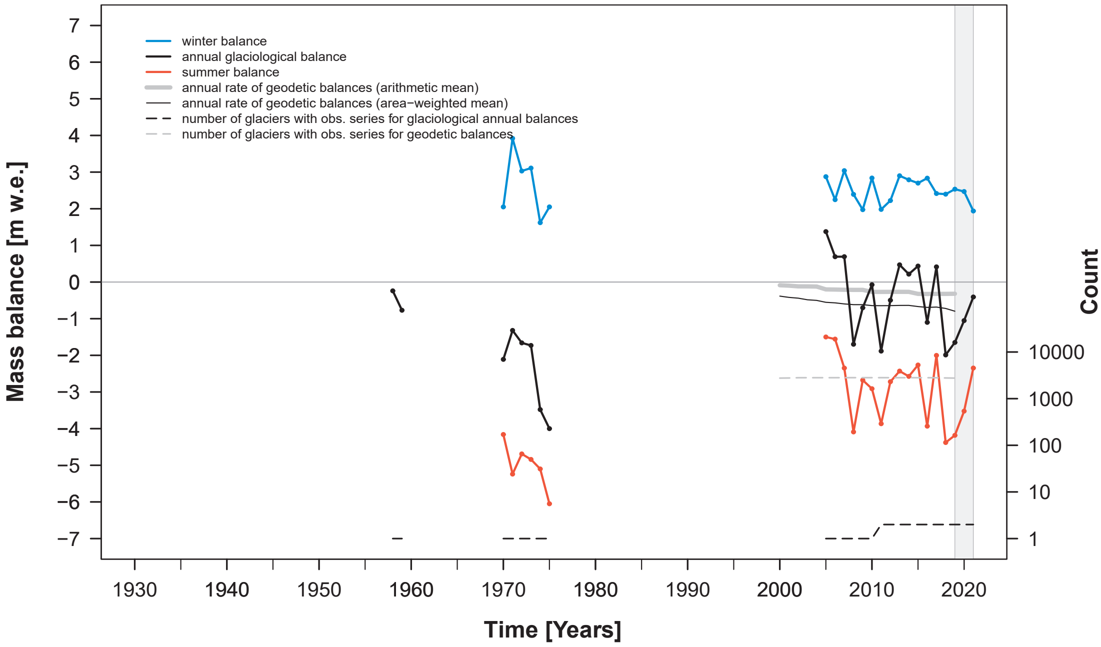

Figure 3.16.1 Regional mass balances: Annual glaciological balances (m w.e.) and annual rates of geodetic balances (m w.e. a^{-1}) are shown together with the corresponding number of glaciers with observations. Geodetic balances were calculated assuming a glacier-wide average density of 850 kg m^{-3}.

The majority of glaciers in New Zealand are located along the Southern Alps spanning the length of the South Island between 42° and 46° south. Their climatic regime is characterized by high precipitation with extreme gradients. Mean annual precipitation amounts to 4,500 mm on the west side (Whataroa) of the Alps and maximum values of up to 15,000 mm (cf. WGMS, 2008). Aoraki/Mount Cook is the highest peak at 3,724 m a.s.l. The Haupapa/Tasman Glacier, the largest glacier in New Zealand, is located below its flank. In total, the inventory of 1978 reported 3,144 glaciers covering an area of about 1,000 km^2 with an estimated total ice volume of about 53 km^3 at that time (Chinn, 2001).

New Zealand has a long history of glacier observation; however, most of the available front variation series are of qualitative character, i.e., indicating whether glacier fronts are advancing, retreating or stationary. Long-term quantitative front-variation series are reported for Franz Josef Glacier/Kā Roimata o Hine Hukatere, Fox Glacier/Te Moeka o Tuāwe, and Stocking/Te Wae Wae Glacier. Mass-balance observations are available for only a few glaciers; recent measurements have been reported for Brewster and Rolleston.

Since 1977, the end-of-summer-snow-line has been surveyed on fifty index glaciers distributed over the Southern Alps. The surveys are carried out by hand-held oblique photography taken from a light aircraft. Methods, data and more details are given in Chinn et al. (2005).

The few mass-balance measurements indicate a large interannual variability with an average mean balance of a few hundred millimetres w.e. a^{-1}. Seasonal balances indicate very large mass turnover. Average annual balances (of Rolleston and Brewster) were negative in 2019/20 and 2020/21 with –1,052 and –408 mm w.e., respectively.

Geodetic assessments show a mass-change rate between –300 and –500 mm w.e. a^{-1} since 2000. Regional glacier change assessments were recently published by Carrivick et al. (2020), Mackintosh et al. (2017), and Salinger et al. (2021).

Estimated total glacier area (km^2):	1,000
Front variations	
- # of series*:	95/3
- # of obs. from stat. or adv. glaciers*:	504/0
- # of obs. from retreating glaciers*:	677/4
Glaciological balances	
- # of series*:	5/2
- # of observations*:	38/4
Geodetic balances	
- # of series°:	2,816/2,816
- # of observations°:	45,643/40,032

* (total/2020 & 2021), ° (total/>2009)

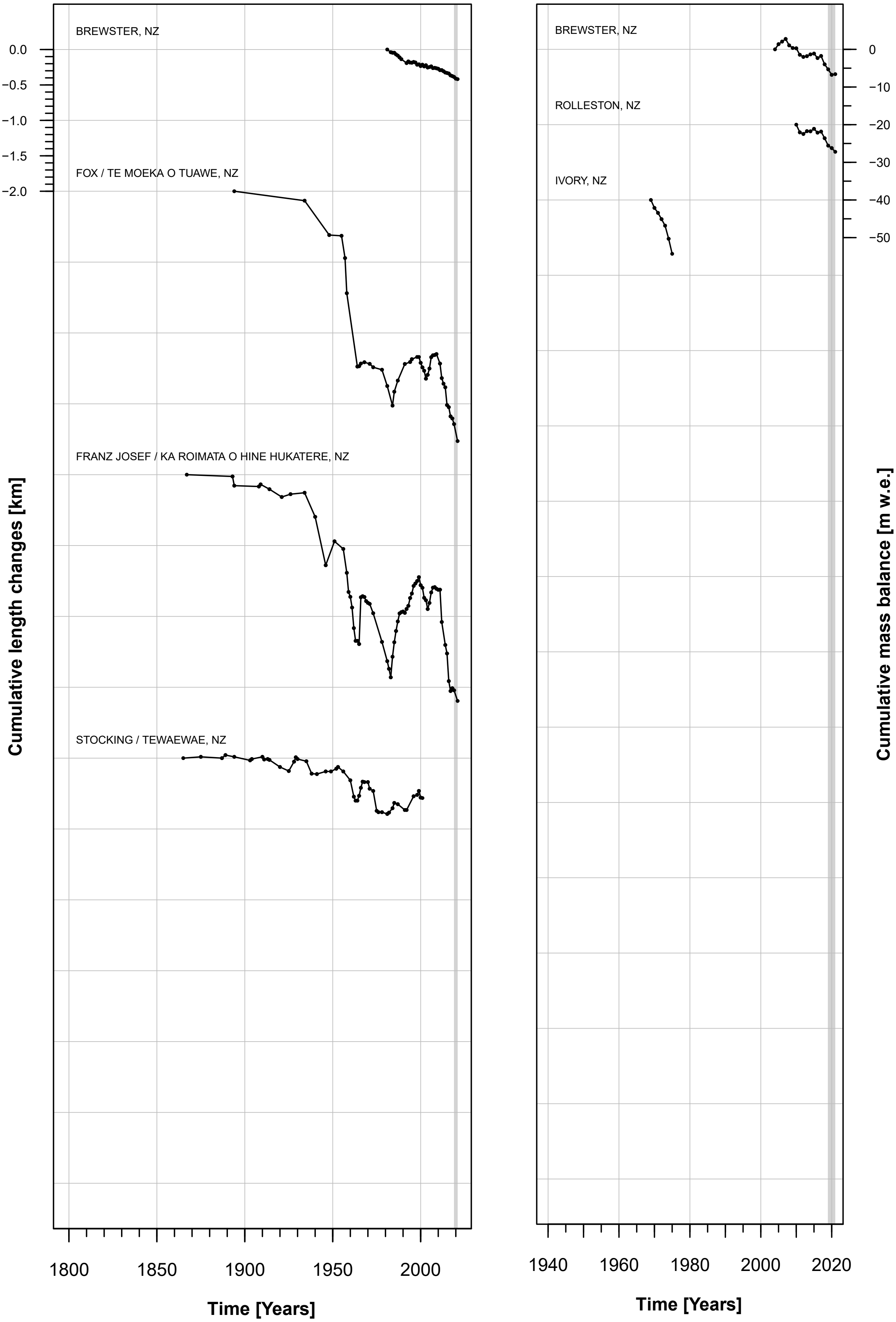

Figure 3.16.2 Cumulative length changes (left) and cumulative mass balances (right) of selected glaciers in New Zealand over the entire observation period.

3.17 ANTARCTICA & SUBANTARCTIC ISLANDS

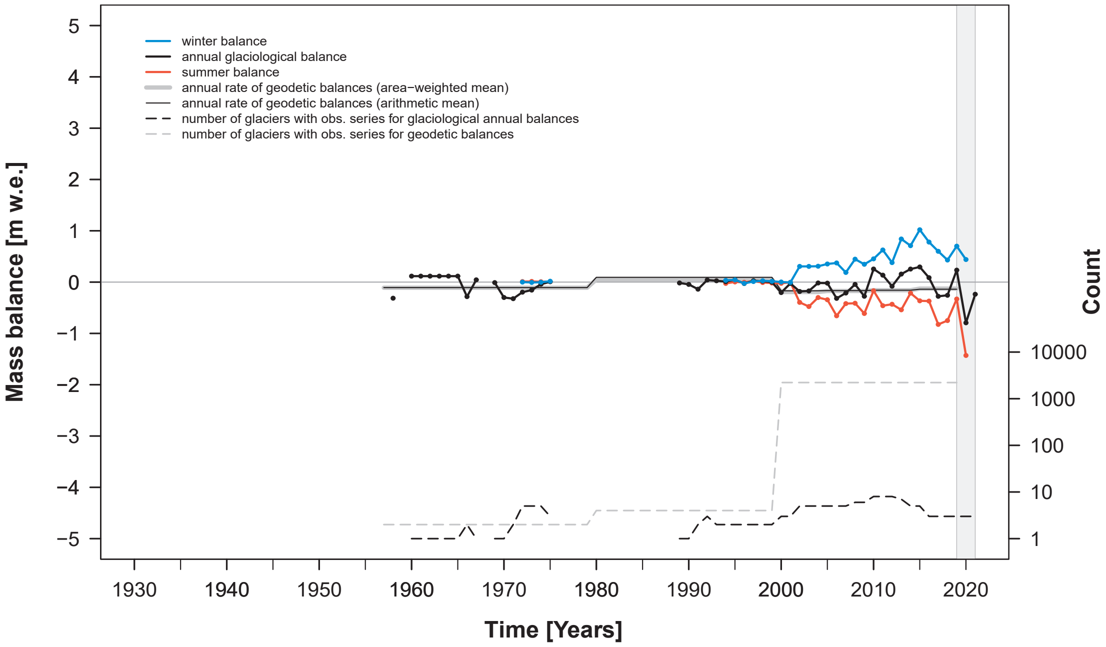

Figure 3.17.1 Regional mass balances: Annual glaciological balances (m w.e.) and annual rates of geodetic balances (m w.e. a^{-1}) are shown together with the corresponding number of glaciers with observations. Geodetic balances were calculated assuming a glacier-wide average density of 850 kg m^{-3}.

The total area of local glaciers in and around Antarctica is estimated to be about 133,000 km^2. Mainly due to the remoteness and the immense size of the ice masses, little is known about these glaciers. There are three categories of local glaciers outside the ice sheet: coastal glaciers, ice streams which are discrete dynamic units attached to the ice sheet, and isolated ice caps. In addition, glaciers are situated on Subantarctic Islands such as the South Shetland Islands, South Georgia, Heard Islands, and Kerguelen with a total estimated ice cover of roughly 7,000 km^2. Mass-balance measurements are available from only a dozens of glaciers. Series of more than ten years are reported from Bahía del Diablo on Vega Island as well as from Hurd and Johnsons glaciers on Livingston Island located east and west of the northern tip of the Antarctic Peninsula.

Evidence of the timing of LIA glacier maxima south of the Antarctic Circle (66° 30’ S) is sparse due to the lack of organic material for dating (Grove, 2004). For South Georgia, LIA maximum extends are reported for the 18th, 19th, and 20th centuries (Clapperton et al., 1989a, b) and LIA end is suggested to be 1870s from lichenometry (Roberts et al., 2010).

Front variations, derived from aerial photographs and satellite images, of glaciers on the Antarctic Peninsula show a vast majority of glaciers retreating over the past six decades (e.g., Cook et al. 2005). Glaciers on South Georgia receded overall by varying amounts from their more advanced positions in the 19th century, with large tidewater glaciers showing a more variable behaviour and remaining in relatively advanced positions until the 1980s. According to expedition records, little or no change occurred on glaciers at Heard Island during the first decades of the 20th century (Grove, 2004). However, in the second half, glacier recession has been widespread, interrupted by a period of some re-advancing glaciers in the 1960s. The very few glaciological surveys indicate negative mass balances since the 1960s, supported by geodetic observations, and some positive years recently. Reported balances for 2019/20 and 2020/21 averaged at –793 and –237 mm w.e., respectively.

Regional glacier change assessments were recently published by Farías-Barahona et al. (2020).

Estimated total glacier area (km^2):	133,000
Front variations	
- # of series*:	309/1
- # of obs. from stat. or adv. glaciers*:	139/1
- # of obs. from retreating glaciers*:	366/0
Glaciological balances	
- # of series*:	21/3
- # of observations*:	163/6
Geodetic balances	
- # of series°:	2,221/2,219
- # of observations°:	11,096/6,655

* (total/2020 & 2021), ° (total/>2009)

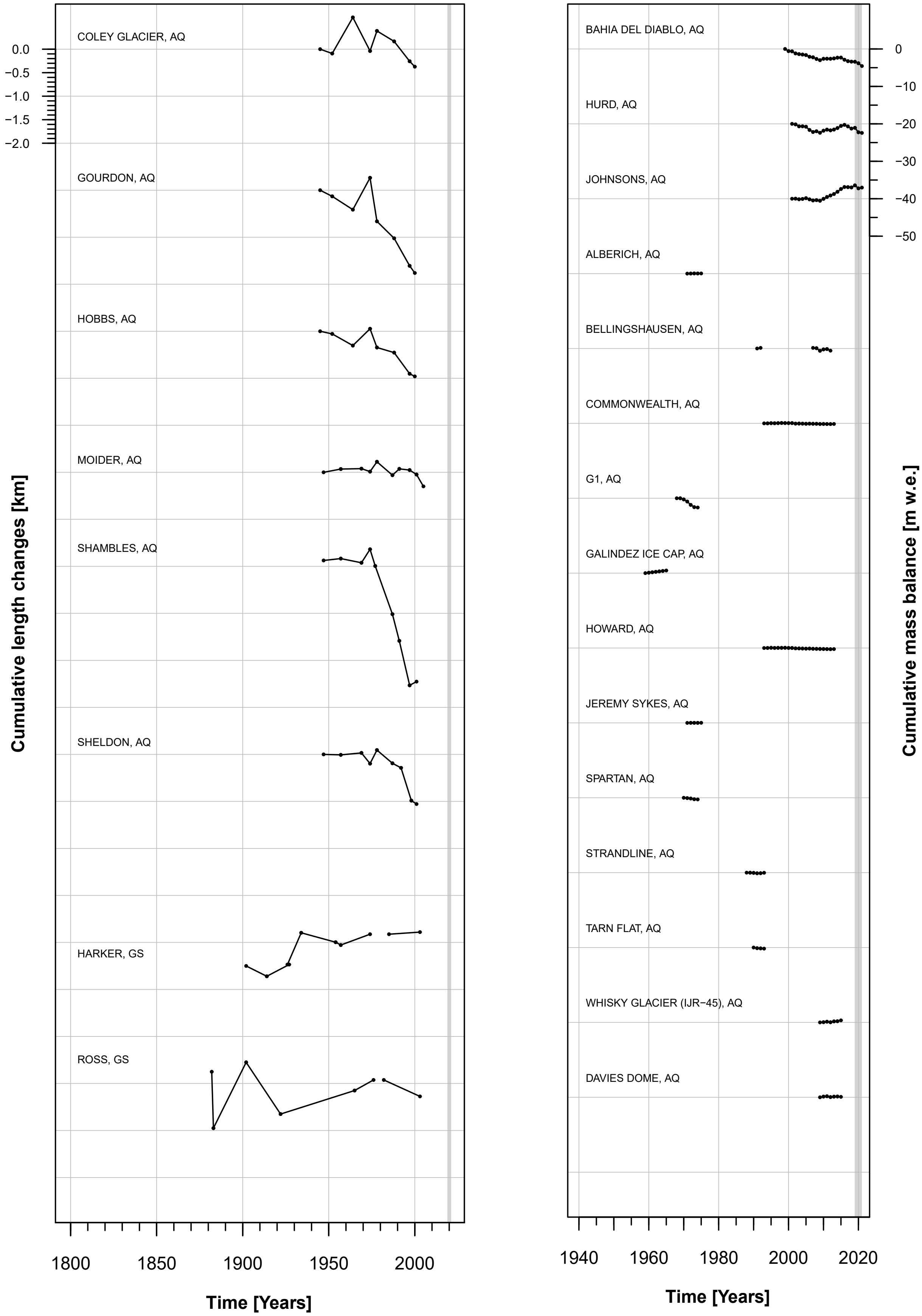

Figure 3.17.2 Cumulative length changes (left) and cumulative mass balances (right) of of selected glaciers in Antarctica and the Subantarctic Islands over the entire observation period.

4 DETAILED INFORMATION

Detailed information on selected glaciers with ongoing direct glaciological mass-balance measurements in various mountain ranges is presented here, in addition to the global and regional information contained in the previous chapters. In order to facilitate comparison between the individual glaciers, the submitted material (text, maps, graphs and tables) was standardized, and in some cases generalized.

The text provides general information on the glacier followed by characteristics of the two reported balance years. General information concerns basic geographic, topographic, climatic and glaciological characteristics of the observed glacier which may help with the interpretation of climate/glacier relationships. A recent photograph showing the glacier is included.

Three maps are presented for each glacier: the first one, a topographic map, shows the stakes, snow pits and snow probing network. This network is basically the same from one year to the next on most glaciers. In cases of differences between the two reported years, the second was chosen, i.e., the network from the year 2020/21. The second and third maps are mass-balance maps from the reported years, illustrating the pattern of ablation and accumulation. The accuracy of such mass-balance maps depends on the density of the observation network, the complexity of the mass-balance distribution, the applied technique for spatial extrapolation, and the experience of the local investigators.

A graph of glacier mass balance versus elevation is given for both reported years, overlaid with the corresponding glacier hypsography and point measurements (if available). The relationship between mass balance and elevation – the mass-balance gradient – is an important parameter in climate/glacier relationships and represents the climatic sensitivity of a glacier. It constitutes the main forcing function of glacier flow over long time intervals. Therefore, the mass-balance gradient near the balanced-budget equilibrium line altitude (ELA_0) is often called the ‘activity index’ of a glacier. The glacier hypsography reveals the glacier elevation bands that are most influential for the specific mass balance, and indicates how the specific mass balance might change with a shift in the ELA. An additional graph compares the mean annual glaciological and the geodetic balances (if available) for the whole observation period. For the comparison, the geodetic values were converted with a density factor of 850 kg m^{-3}.

The last two graphs show the relationship between the specific mass balance and the accumulation area ratio (AAR) and the ELA for the whole observation period. The linear regression equation is given at the top of both diagrams. The AAR regression equation is calculated using integer values only (in percent). AAR values of 0 or 100% as well as corresponding ELA values outside the elevation range of the observed glaciers were excluded from the regression analysis. The regressions were used to determine the AAR_0 and ELA_0 values for each glacier. The points from the two reported balance years (2019/20 and 2020/21) are marked in black. Minimum sample size for regression was defined as six ELA or AAR values.

4.1 BAHÍA DEL DIABLO (ANTARCTICA/A. PENINSULA)

COORDINATES: 63.82° S / 57.43° W

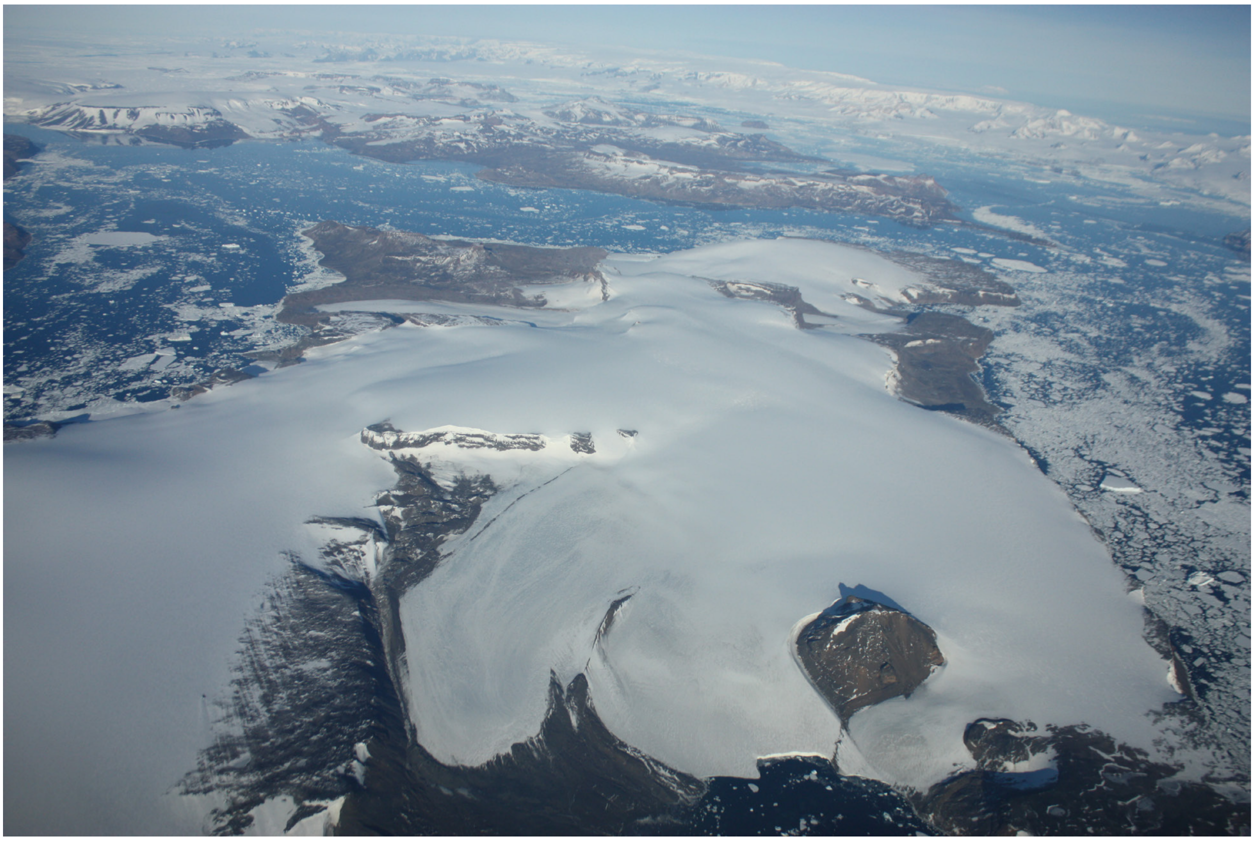

Photograph taken by S. Marinsek, 2 March 2019.

This polythermal-type outlet glacier is located on Vega Island, on the northeastern side of the Antarctic Peninsula. The glacier is exposed to the northeast, covers an area of ~12.9 km², and extends from an altitude of 630 m to 50 m a.s.l. The mean annual air temperature at the equilibrium line around the 400 m a.s.l. ranges between –7 and –8 °C. The glacier snout overrides an ice-cored moraine over a periglacial plain of continuous permafrost. The mass balance measurements on this glacier began in austral summer 1999/2000, using a simplified version of the combined stratigraphic annual mass balance method because the glacier can be visited only once a year.

The mass balance for the year 2019/20 was –400 mm w.e. and the mass balance for the year 2020/21 was –740 mm w. e., both very negative. The values obtained for the ELA were 450 and 500 m a.s.l., respectively, both above the ELA_0.The AAR values of the reporting period were 25% and 27%, also both below the AAR_0.

Precipitation in the region, recorded annually at 650 m a.s.l and at sea level, continues to be lower than the average recorded since the beginning of the mass balance program. For 2019/20 precipitation at 650 m a.s.l. was ~410 mm and ~195 mm at sea level. For 2020/21 precipitation at 650 m a.s.l was ~430 mm and ~135 mm at sea level. Warm summers, with average temperatures of 0.8 °C in 2019/20 and 1.5 °C in 2020/21, with continuing low annual precipitation are main responsible for mass loss during the last years.

Figure 4.1.1 Topography and observation network and mass-balance maps 2019/20 and 2020/21.

Topography and observational network

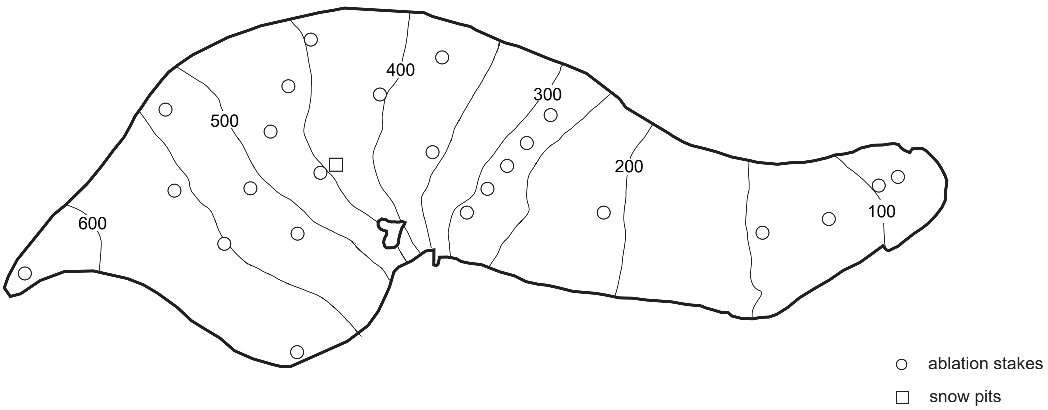

Mass-balance maps 2019/20 and 2020/21

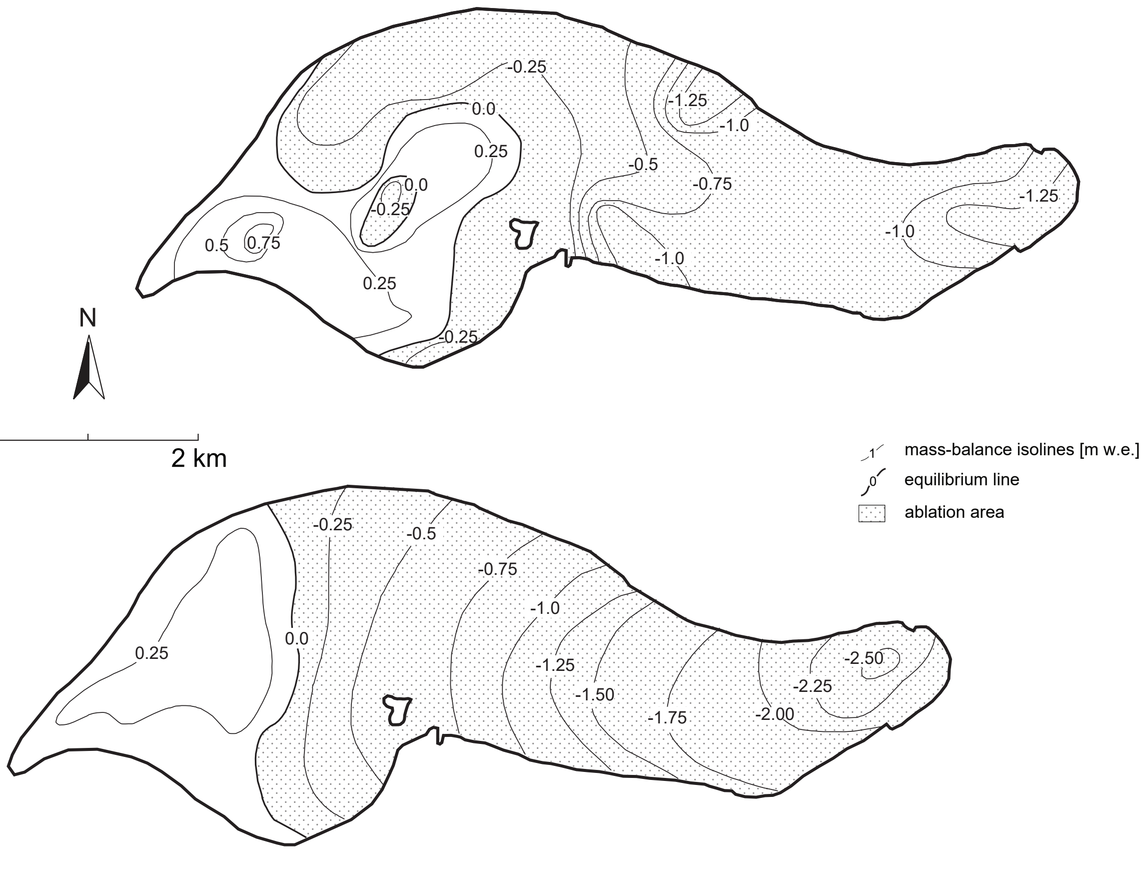

Bahía del Diablo (ANTARCTICA)

Figure 4.1.2 Mass balance versus elevation for 2019/20 and 2020/21.

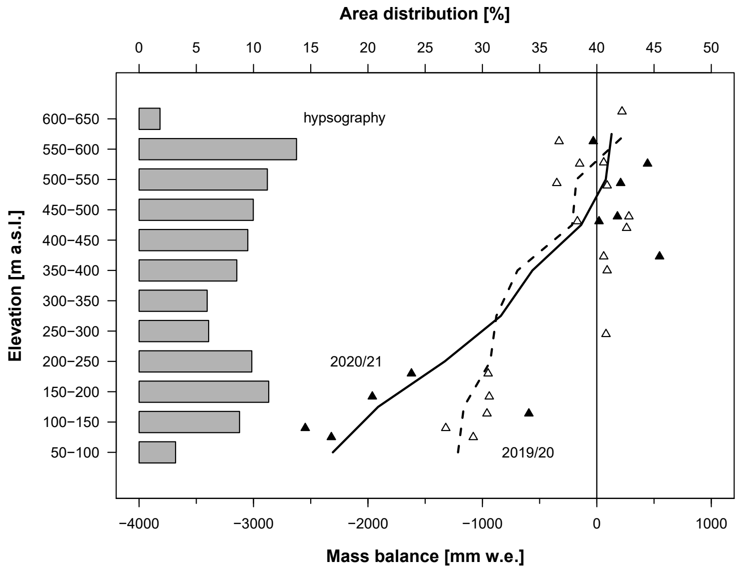

Figure 4.1.3 Glaciological balance versus geodetic balance for the whole observation period.

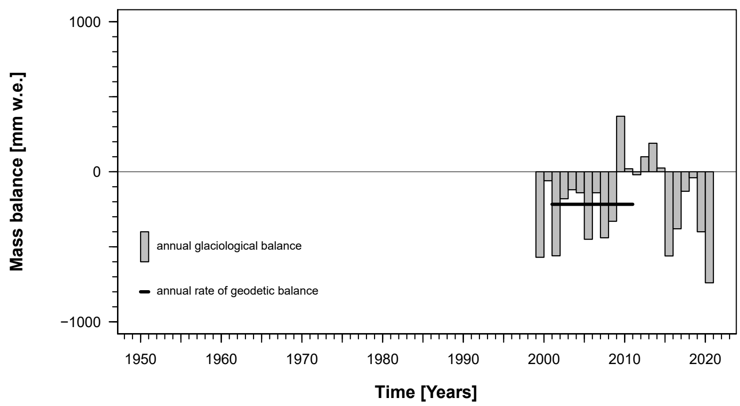

Figure 4.1.4 Accumulation area ratio (AAR) and equilibrium line altitude (ELA) versus specific mass balance for the whole observation period.

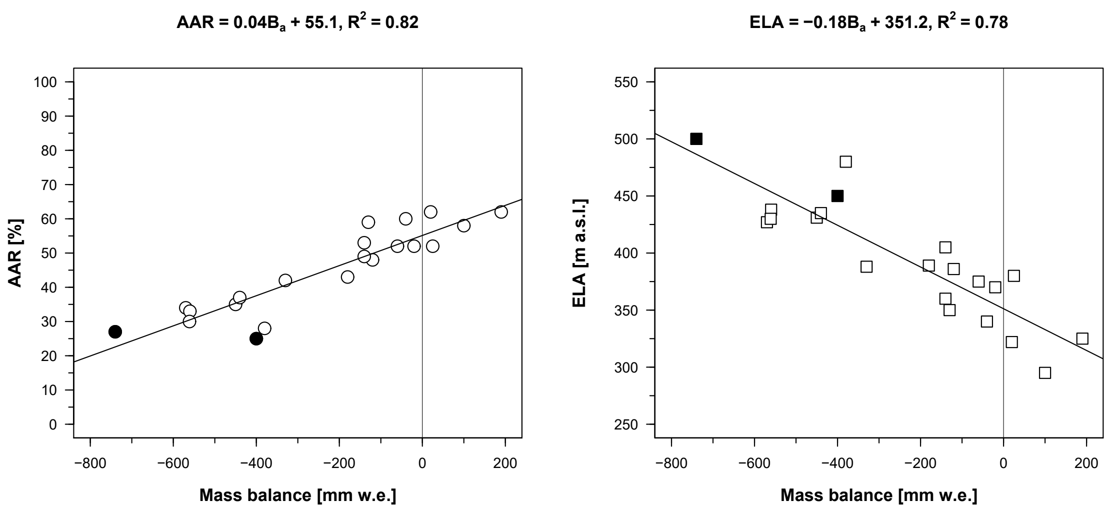

Bahía del Diablo (ANTARCTICA)

4.2 MARTIAL ESTE (ARGENTINA/ANDES FUEGUINOS)

COORDINATES: 54.78° S / 68.40° W

Photograph of Martial Este taken by R. Iturraspe, 3 February 2021.

On the southern shore of the Tierra del Fuego Island, facing the Beagle Channel, the Martial Glacier dominates the headwaters of the Buena Esperanza basin, whose main river is one of the water sources of Ushuaia city. This glacier has lost 75% of its area since the Little Ice Age. The Martial Este is one of the main ice bodies that compose the whole Martial Glacier. The hydrological cycle starts in April and the maximum accumulation on the glacier usually succeeds in October/November. The mean annual air temperature at the ELA level (1,080 m a.s.l.) is –1.5 °C and the annual precipitation, well distributed over the whole year, reaches 1300 mm (530 mm at the sea level).

The glacier lost mass in 2019/20 and 2020/21 with balances of –692 and –1,133mm w.e., respectively. The annual balances of the reporting period were negative in all elevation bins for the first time in the previous 17 years. These results confirm the end of the relatively stable conditions that were observed in the period from 2006 to 2016 period, as well as the continuity of the historical trend in glacier retreat. The behavior of the Martial Glacier is representative of the small cirque glaciers of the Argentinean side of Tierra del Fuego with fronts higher than 950 m a.s.l. (Strelin & Iturraspe, 2007). Glaciers reaching into lower elevations present higher mass loss. On 7 April 2020, a large rock fall event covered about one quarter of Martial East's surface, as visible in the photograph taken one year after the incident. This event led to significant morphological changes in the glacier's surface, and it is likely that related changes in albedo will affect the glacier's behaviour in the years to come.

This glacier monitoring is a collaborative research of the Water Agency of the Province of Tierra del Fuego and the National University of Tierra del Fuego.

Figure 4.2.1 Topography and observation network and mass-balance maps 2019/20 and 2020/21.

Topography and observational network

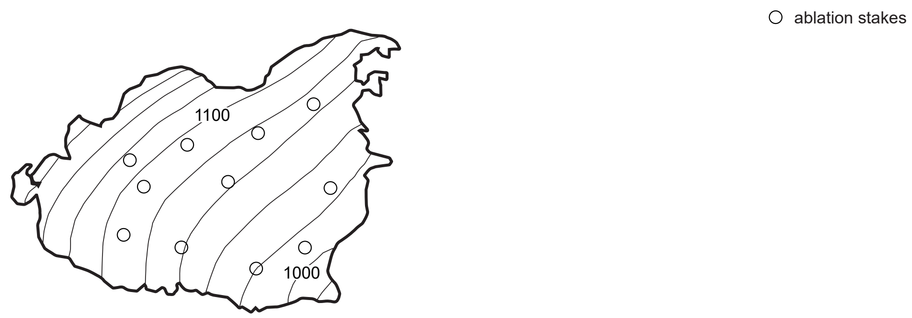

Mass-balance maps 2019/20 and 2020/21

Martial Este (ARGENTINA)

Figure 4.2.2 Mass balance versus elevation for 2019/20 and 2020/21.

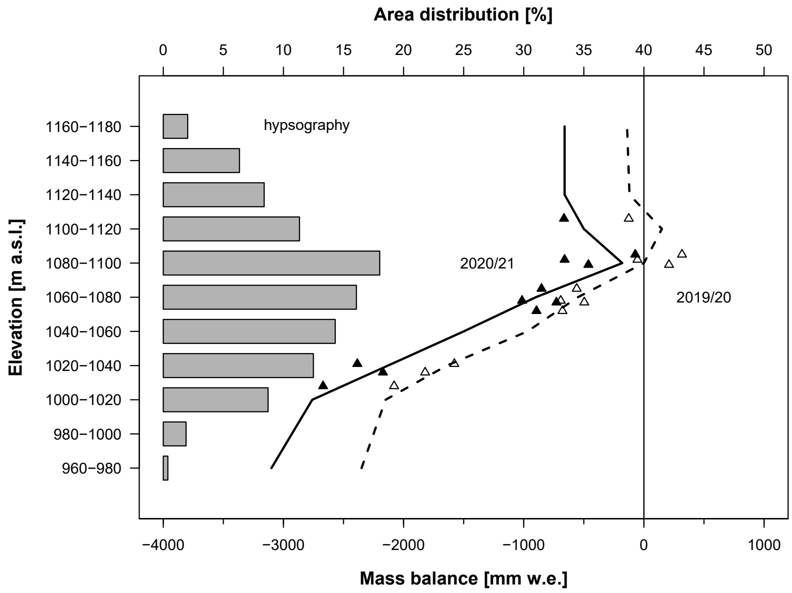

Figure 4.2.3 Glaciological balance versus geodetic balance for the whole observation period.

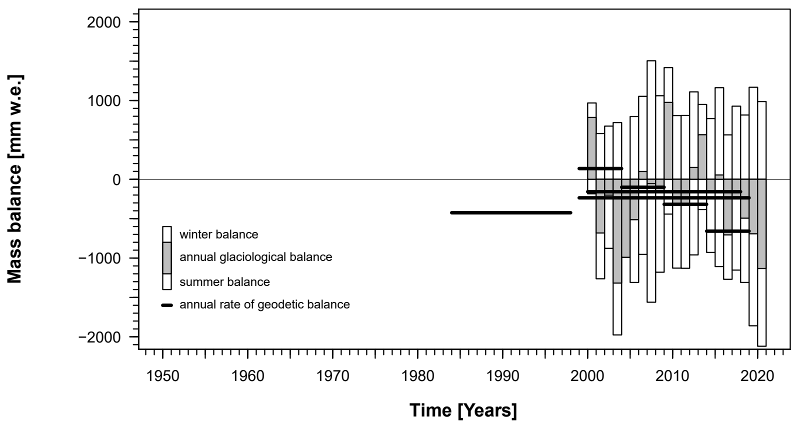

Figure 4.2.4 Accumulation area ratio (AAR) and equilibrium line altitude (ELA) versus specific mass balance for the whole observation period.

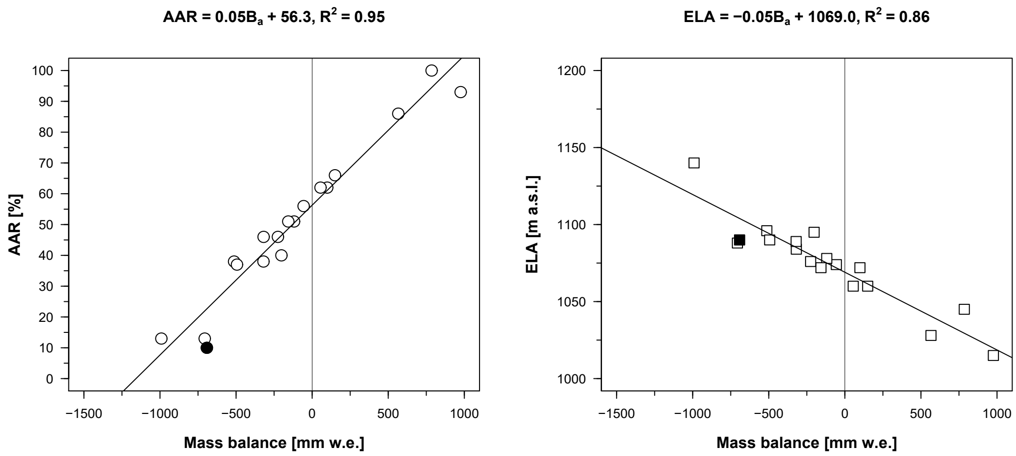

Martial Este (ARGENTINA)

4.3 GOLDBERGKEES (AUSTRIA/ALPS)

COORDINATES: 47.04° N / 12.97° E

Photograph of Goldbergkees taken by A. Neureiter on 27 August 2020.

Goldbergkees, also known as Vogelmeier-Ochsenkarkees, is a small mountain glacier in the Eastern Alps, situated very close to the Observatory on top of Sonnblick (3,105 m a.s.l.) directly at the main Alpine ridge. The glacier covers an area of 0.96 km² (2021), ranges from 3,060 m a.s.l. to 2,380 m a.s.l., and has separated into three parts. The upper part (0.25 km²) shares a drainage divide with Kleinfleißkees and is oriented to south-east. Both the middle part (0.62 km²) and the lower part (0.09 km²) of the glacier are mainly oriented to north-east and exhibit proglacial lakes.

The glacier mass balance of 2019/20 was –1,093 mm w.e., with an ELA at 3,050 m a.s.l. and an AAR of 10%. The balance of 2020/21 was –504 mm w.e., with an ELA at 2,850 m a.s.l. and an AAR of 35%.

Annual (winter) mass-balance observations date back to 1988/89 (1986/87). Average annual air temperature at 3,100 m a.s.l., which corresponds to the average ELA, is –4.5 °C (1991–2020). Measured average annual precipitation at Sonnblick is 2,560 mm (1991–2020). Average (1991–2020) winter (annual) mass balance of the glacier is 1,710 mm (–780 mm). Detailed analysis of the glacier monitoring program are found in Schöner et al. (1999, 2009). Since a few years, the actual and former state of the glacier can be followed via two high quality webcams: CAM 1 and CAM 2.

Figure 4.3.1 Topography and observation network and mass-balance maps 2019/20 and 2020/21.

Topography and observational network

Mass-balance maps 2019/20 and 2020/21

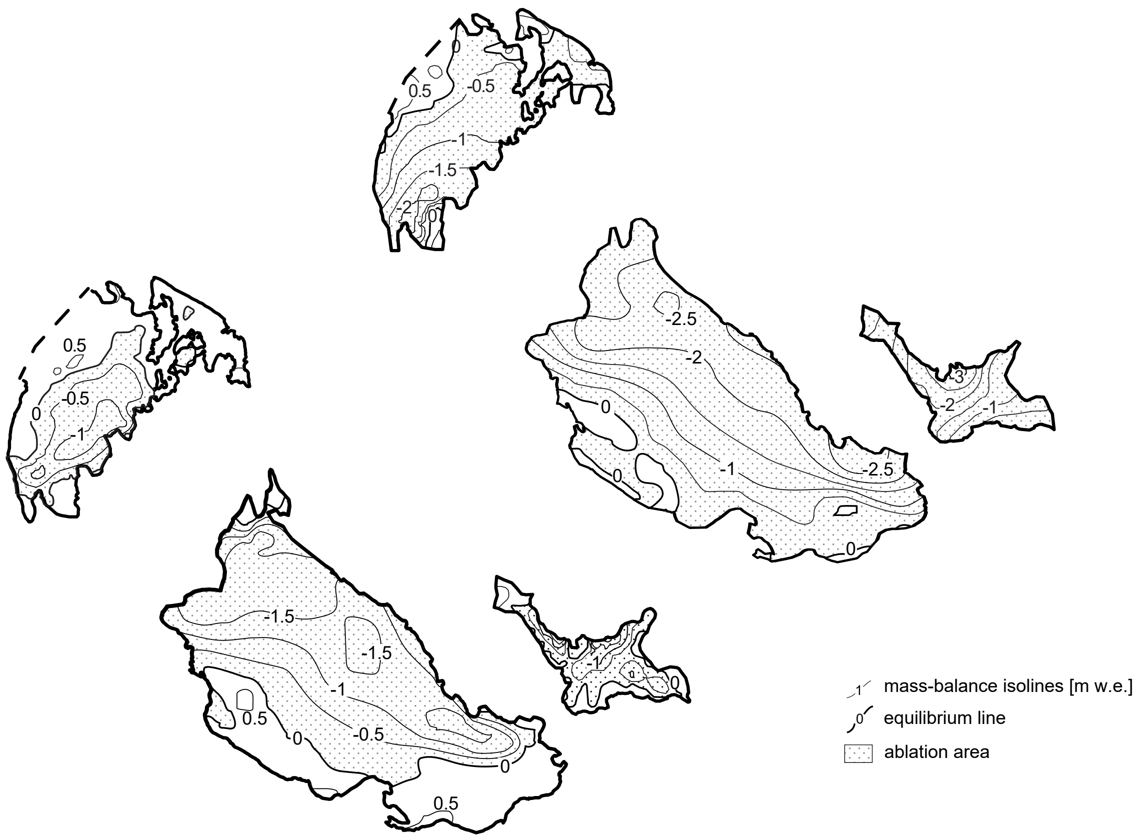

Goldbergkees (AUSTRIA)

Figure 4.3.2 Mass balance versus elevation for 2019/20 and 2020/21.

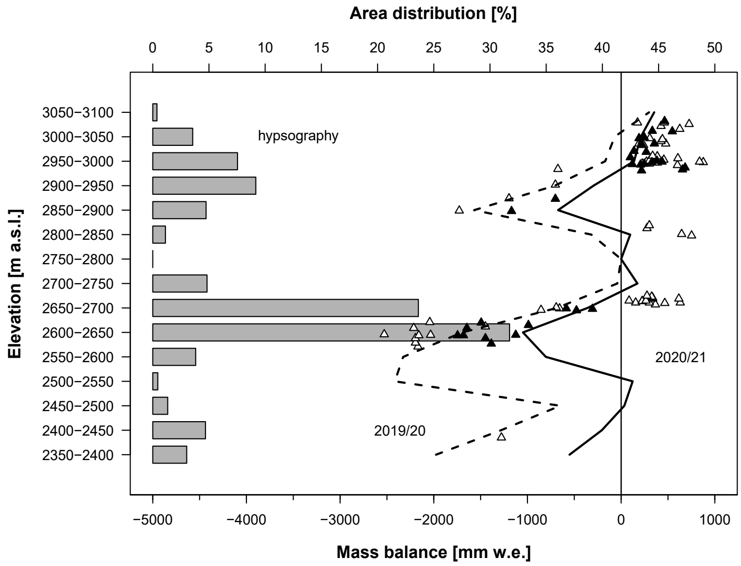

Figure 4.3.3 Glaciological balance versus geodetic balance for the whole observation period.

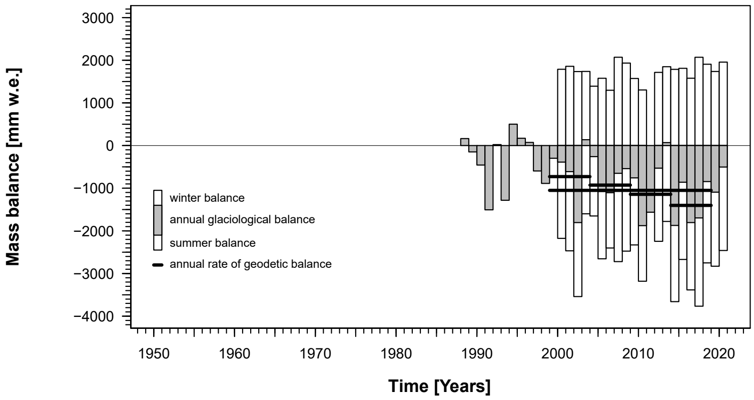

Figure 4.3.4 Accumulation area ratio (AAR) and equilibrium line altitude (ELA) versus specific mass balance for the whole observation period.

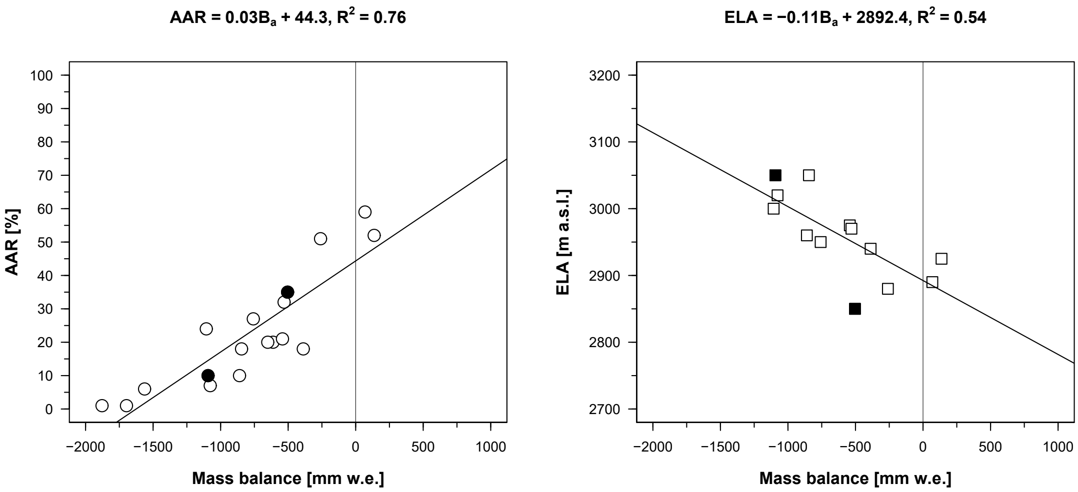

Goldbergkees (AUSTRIA)

4.4 JAMTALFERNER (AUSTRIA/ALPS)

COORDINATES: 46.86° N / 10.16° E

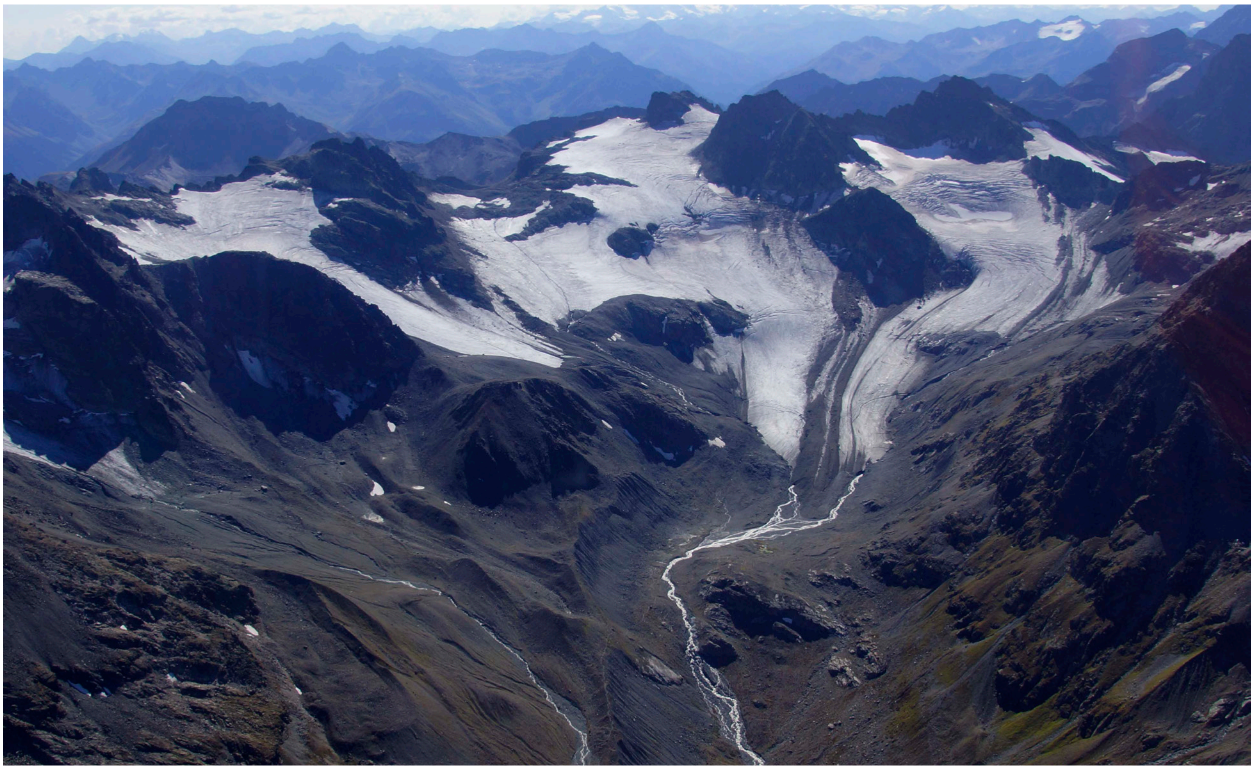

Photograph of Jamtalferner by A. Fischer, taken on 20 September 2018.

Jamtalferner is a temperate valley glacier located in the Austrian part of the Silvretta region close to the border to Switzerland. The glacier covers an area of 2.52 km² (2020) and has three tributaries (exposed to NW, N, and NE) joining into one glacier tongue. In 2018, the highest point of the glacier was at an altitude of 3,116 m a.s.l. near Hintere Jamspitze. The terminus reached down to 2,428 m a.s.l., with a length of the main tributary between Hintere Jamspitze and the terminus of 2.2 km. The ice thickness was measured by GPR in 2015 and returned a maximum ice thickness of 58 m. In 18 out of 33 years of the total record length, the ELA was above the summit. From 2002/03 onwards, the ELA was above summit in 14 out of 19 years, with four years featuring an AAR of 0%. The average summer air temperature, measured at the closest weather station in Galtür (1,587 m a.s.l.), is 12.9 °C (June, July, August, 1951–2000), 10.9 °C for the summer half year (i.e., May to September), and 3.9 °C for the hydrological year. Presuming a lapse rate of 0.65 °C per 100 m, the summer air temperature at the glacier tongue is 7.4 °C. The mean annual precipitation measured at Galtür is 1,013 mm. Jamtalferner has been surveyed regularly since 1891 (Fischer et al. 2016a, Fischer et al., 2018), with detailed winter and annual mass-balance measurements since 1988/89 (Fischer et al., 2016b). The network includes around 4–9 snow pits and 10–20 ablation stakes. The number of snow pits has decreased and the number of stakes increased over the measurement period due to the reduction of the accumulation area. Surface topography has been documented in a number of maps and DEMs from the early 19th century onwards (Fischer et al., 2019).

If we take the glacier area of 1988/89 as reference, Jamtalferner has lost 34% of this area over the total length of mass balance records. The downwasting of Jamtalferner is rapid, with the glacier tongue going to lose the connection to the higher areas in the next couple of years. The glacier mass balances in 2019/20 and 2020/21 were negative with –1,675 mm w.e. and –1,000 mm w.e., respectively. These are more negative balances than the average of –960 mm w.e., but much less negative than the minimum balance of –2,277 mm w.e. recorded in 2017/18. ELA was above summit in in both years, AAR was 9% in 2018/19 and 0% in 2019/20.

Figure 4.4.1 Topography and observation network and mass-balance maps 2019/20 and 2020/21.

Topography and observational network

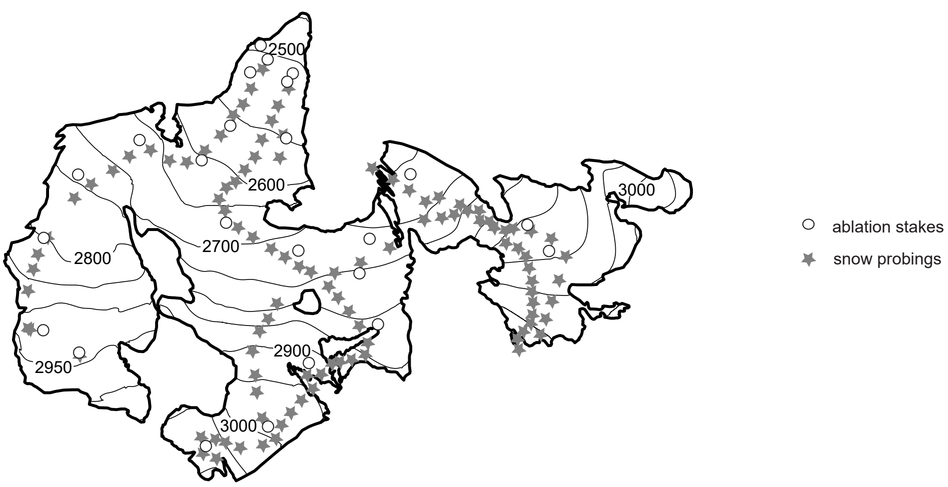

Mass-balance maps 2019/20 and 2020/21

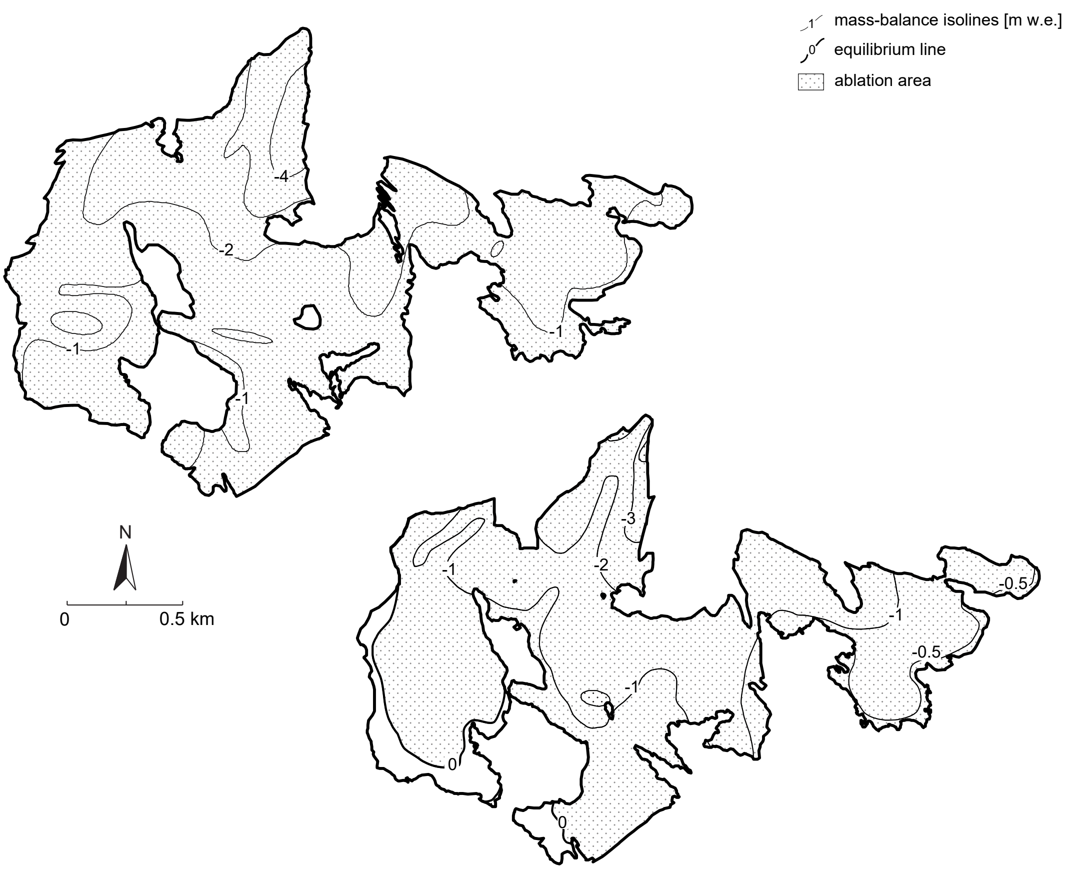

Jamtalferner (AUSTRIA)

Figure 4.4.2 Mass balance versus elevation for 2019/20 and 2020/21.

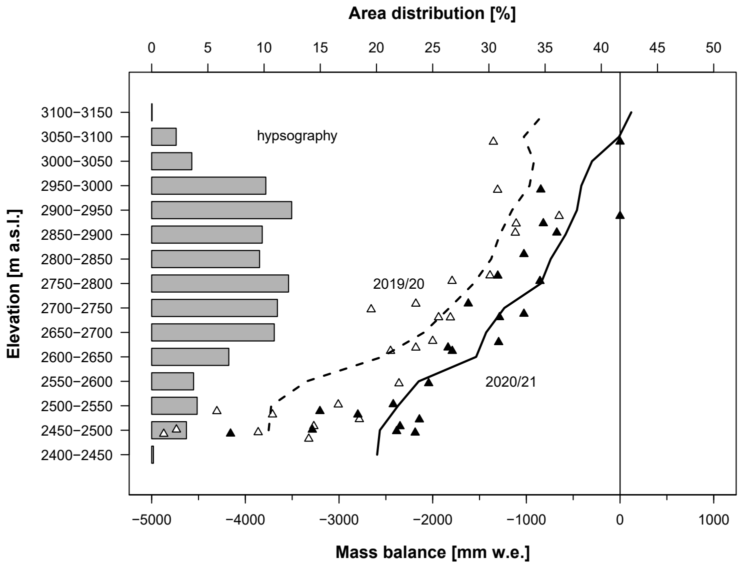

Figure 4.4.3 Glaciological balance versus geodetic balance for the whole observation period.

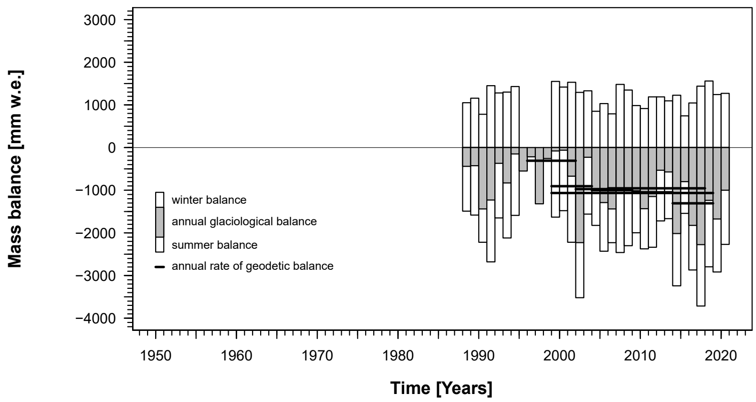

Figure 4.4.4 Accumulation area ratio (AAR) and equilibrium line altitude (ELA) versus specific mass balance for the whole observation period.

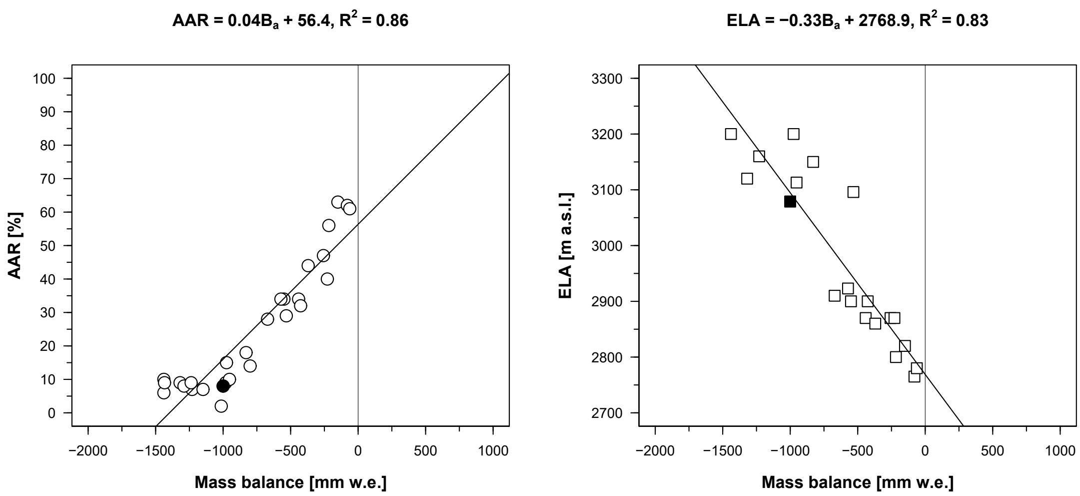

Jamtalferner (AUSTRIA)

4.5 ZONGO (BOLIVIA/TROPICAL ANDES)

COORDINATES: 16.25° S / 68.17° W

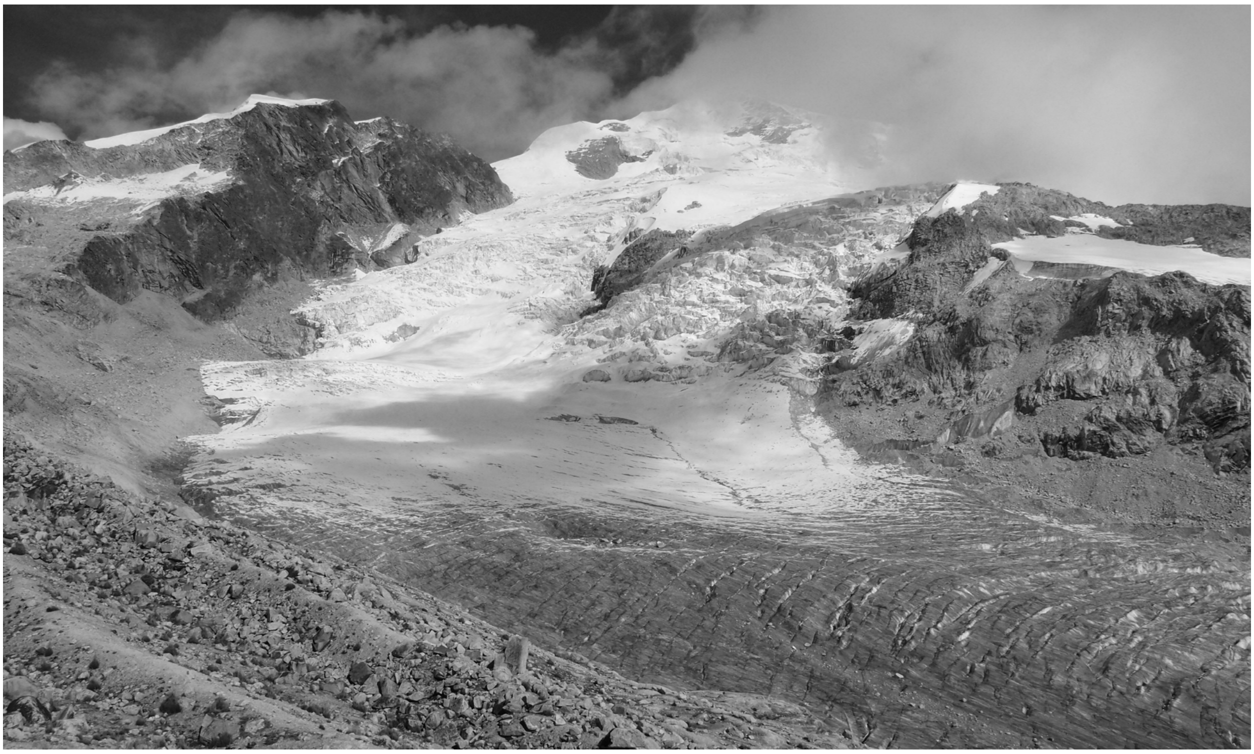

Photograph taken by Alvaro Soruco on 2 June 2017.

Zongo Glacier is a small temperate valley glacier located at 30 km northeast of La Paz city. Its length is around 3 km and its width is around 0.75 km, flowing from 6,100 to 5,000 m a.s.l. ELA_0 is estimated at 5,274 m a.s.l. with a corresponding AAR_0 of 67%. The valley has a southern exposure in its upper part and a south-eastern exposure in the lower one. Climate is characterized by one dry and one wet season, the latter occurring during the austral summer. Melting takes place mainly during the summer, reaching a peak in November, before the peak of precipitation, which take place between January and March. As all glaciers in the region, Zongo shows a long-term trend of mass loss, with positive and negative mass-balance periods coinciding with La Niña and El Niño events, respectively. The biggest loss (–2,173 mm w.e.) took place during the El Niño event of 1997/98.

The reporting period was characterized by a transition from El Niño to La Niña conditions. The mass balance of Zongo glacier was –334 mm w.e. in 2019/20 and 119 mm w.e. in 2020/21. ELA values were 5,260 m a.s.l. and 5,359 m a.s.l. with corresponding AAR values of 72% and 68%, respectively. With these, Zongo experienced four consecutive years of positive balances. However, the glacier front continues to retreat by around 19 m per year.

Glaciological and geodetic measurements of Zongo and other tropical glaciers are carried out within GREAT ICE (Sicart et al. 2015) and were analyzed by Rabatel et al. (2013). Soruco et al. (2009) compared the glaciological series with geodetic and hydrological methods.

Figure 4.5.1 Topography and observation network and mass-balance maps 2019/20 and 2020/21.

Topography and observational network

Mass-balance maps 2019/20 and 2020/21

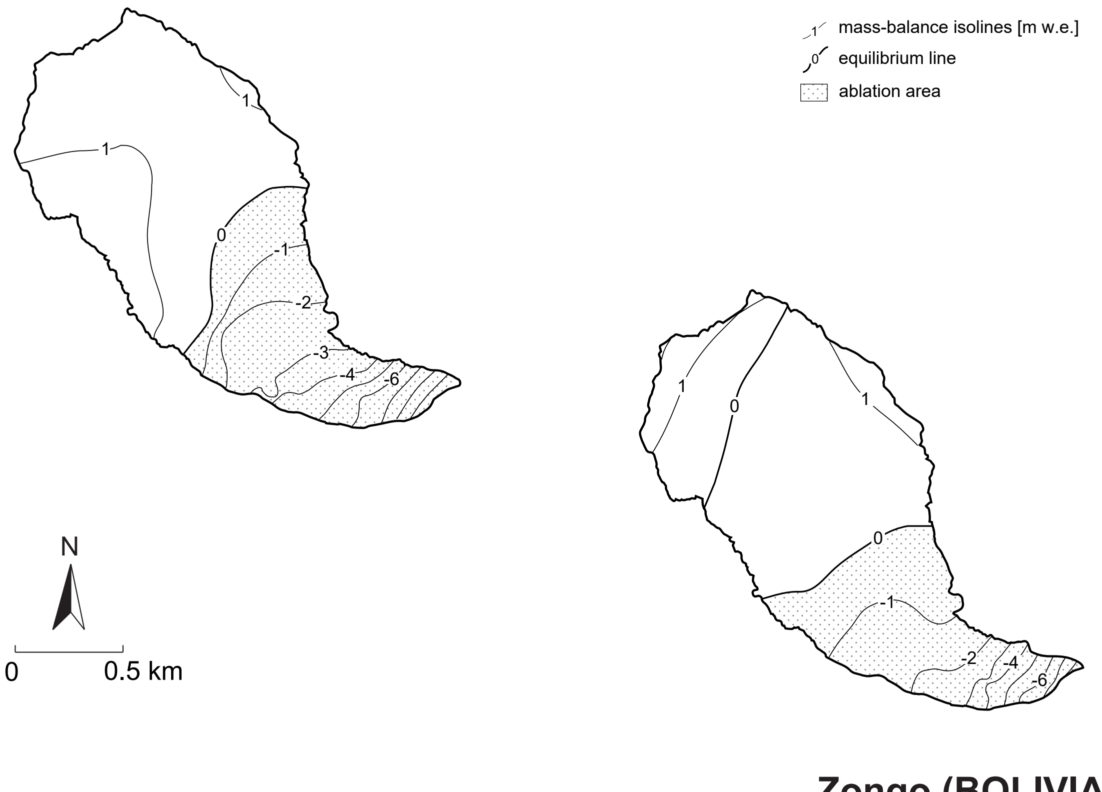

Zongo (BOLIVIA)

Figure 4.5.2 Mass balance versus elevation for 2019/20 and 2020/21.

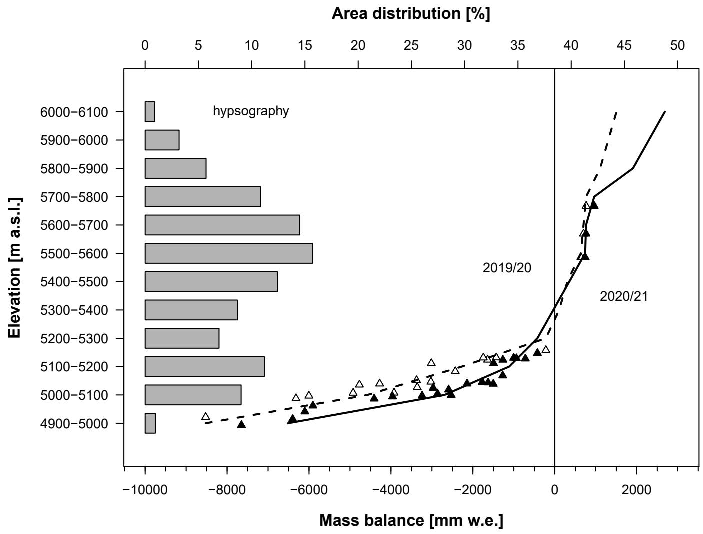

Figure 4.5.3 Glaciological balance versus geodetic balance for the whole observation period.

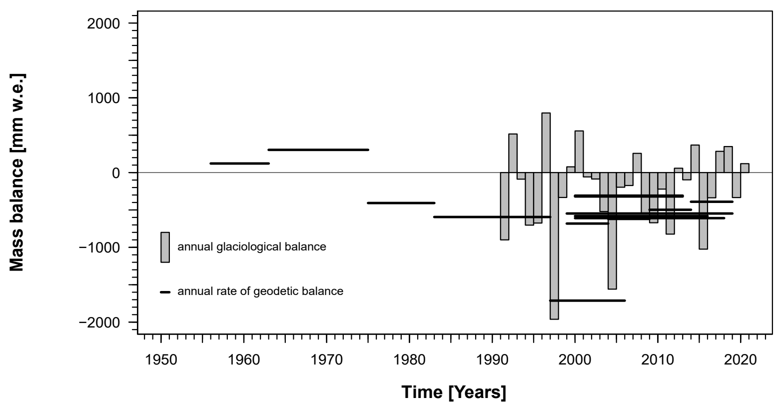

Figure 4.5.4 Accumulation area ratio (AAR) and equilibrium line altitude (ELA) versus specific mass balance for the whole observation period.

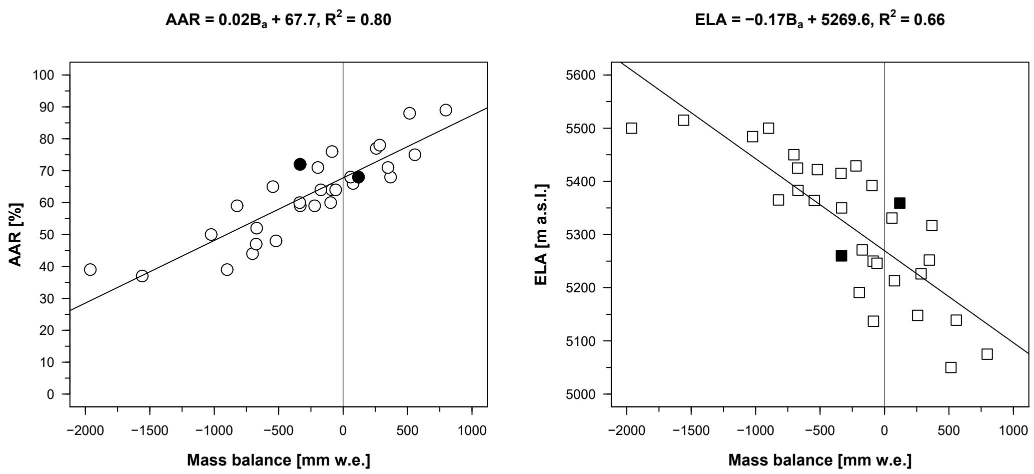

Zongo (BOLIVIA)

4.6 URUMQI GLACIER NO. 1 (CHINA/TIEN SHAN)

COORDINATES: 43.08° N / 86.82° E

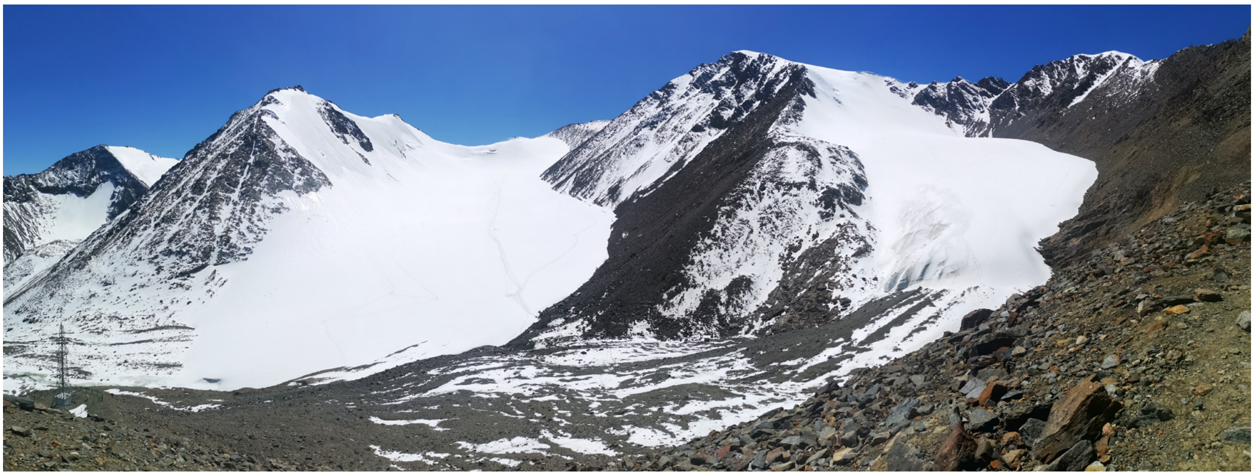

Photograph of Urumqi Glacier No. 1 taken by Chunhai Xu in April 2021.

Urumqi Glacier No. 1 is a valley glacier located 100 km south of Urumqi City, northwest China. As in 1959, the starting date of observation on Urumqi Glacier No. 1, it was composed by two branches. After decades of constant recession, the two branches separated into two small glaciers in 1993, which are now referred to as the east and west branches of Urumqi Glacier No. 1. ELA_0 and AAR_0 are 4,051 m a.s.l. and 61%, respectively, for the west branch; and 3,948 m a.s.l. and 64%, respectively, for the east branch. The area of the glacier was determined by a survey in 2019 as being 0.972 km^2 for east branch and 0.551 km^2 for the west branch. The latest radar echo-sounding measurements were conducted on the glacier in August 2012, which indicated its maximum thickness as 124 ± 5 m.

The mass balance of Urumqi Glacier No. 1 was –230 mm w.e. in 2019/20 and –829 mm w.e.in 2020/21. To obtain the glacier-wide mean mass balance, the specific values observed at each stake was used for interpolation, together with simulated values obtained using a simple energy-balance model (Oerlemans, 2011) in area without measurements.

Figure 4.6.1 Topography and observation network and mass-balance maps of 2019/20 and 2020/21.

Topography and observational network

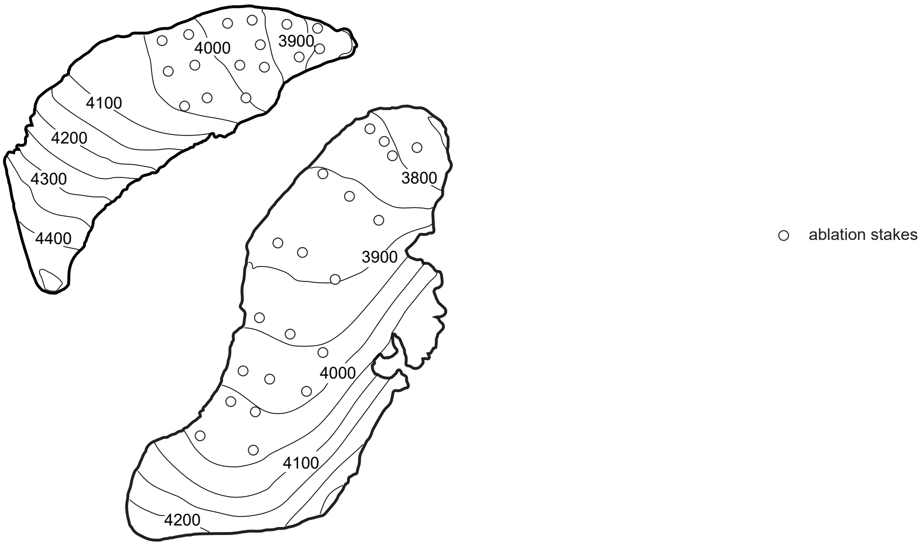

Mass-balance map 2019/20 and 2020/21

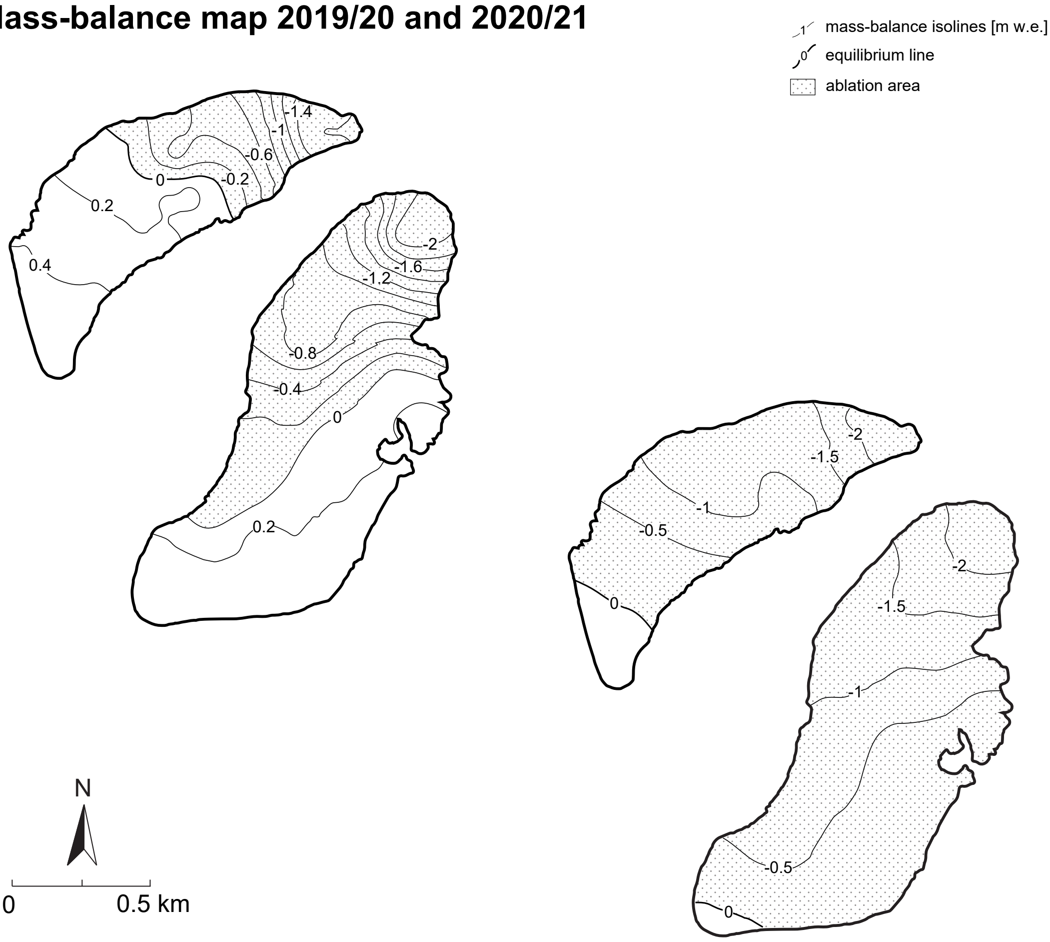

Urumqi Glacier No. 1 (CHINA)

Figure 4.6.2 Mass balance versus elevation for 2019/20 and 2020/21, West Branch on the left and East Branch on the right.

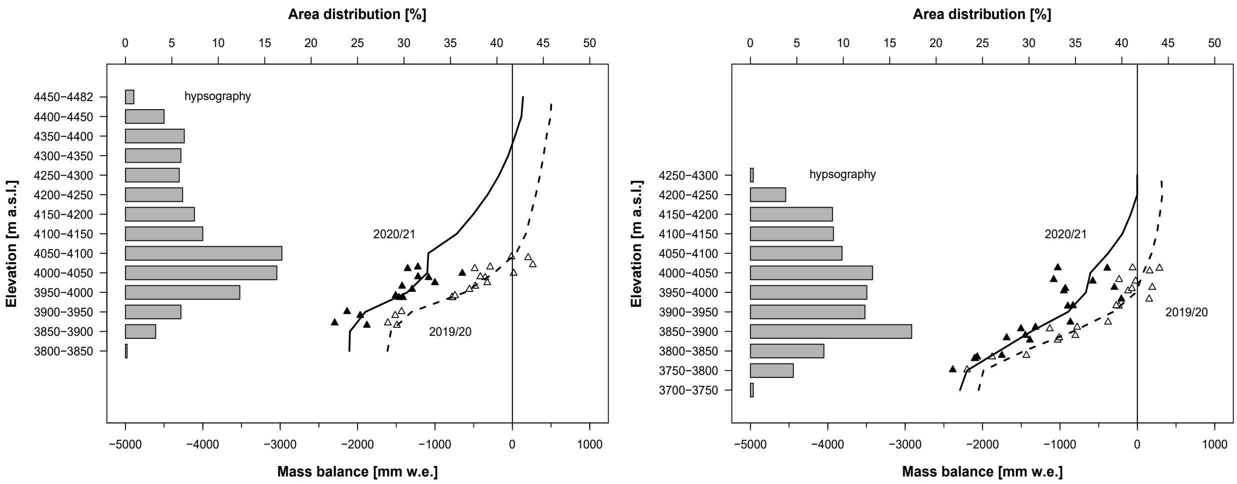

Figure 4.6.3 Glaciological balance versus geodetic balance for the whole observation period.

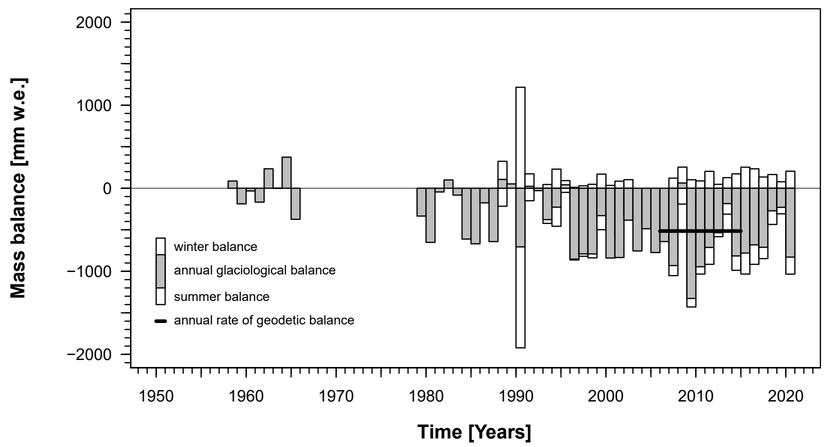

Figure 4.6.4 Accumulation area ratio (AAR) and equilibrium line altitude (ELA) versus specific mass balance for the whole observation period.

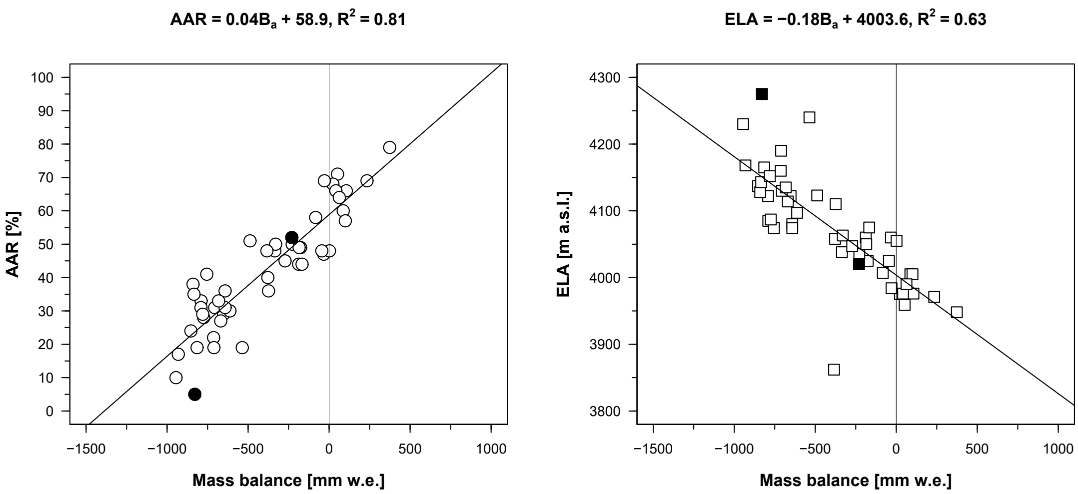

Urumqi Glacier No. 1 (CHINA)

4.7 CONEJERAS (COLOMBIA/CORDILLERA CENTRAL)

COORDINATES: 4.82° N / 75.37° W

Photograph of Conejeras taken by J.L. Ceballos on 4 December 2020.

Conejeras Glacier is a small glacier (0.062 km², 2021) and part of the (former) ice cap (0,35 km², 2021) located at the top of Santa Isabel glacier-volcano in the northern Andes. Along with the glacierized volcanoes Nevado del Ruiz and Nevado del Tolima, it is surrounded by the "Páramo" ecosystem and Andean forests. Conejeras, which has a minimum elevation of 4,686 m a.s.l. and maximum of 4,876 m a.s.l. is located at Santa Isabel's northwest side. In the period 2010–2021 Santa Isabel glacier reduced its area by 82%.

Conejeras' mass balance has been calculated monthly with the direct glaciological method since April 2006, starting with 14 stakes and meanwhile reduced to 9 due to the strong glacier retreat. Since 2006, Conejeras Glacier has shown a permanent negative annual mass balance with a cumulative mass balance of –53.97 m w.e. In 2019/20, the mass balance was –4,986 mm w.e. and –2,786 mm w.e. in 2021. The (theoretical) ELA was located at 4,913 m a.s.l. (AAR 0%) in 2019/20 and at 4,871 m a.s.l. (AAR < 1%) in 2020/21. In 2021, weather patterns in these mountains lead to an annual average precipitation of 1,166 mm and mean annual air temperature of 0.3 °C.

The glacier reacts swiftly to atmospheric changes and is strongly influenced by climatic variability generated by the Intertropical Convergence Zone (ITCZ) and the El Niño-Southern Oscillation (ENSO). In 2021, "La Niña" limited the annual mass loss due to increased snowfall. The recent appearance of volcanic ash on its surface is another important factor that influences its melting. The remaining ice thickness is estimated to be 8 m (2021), located in the middle part of the glacier.

Figure 4.7.1 Topography and observation network and mass-balance maps of 2019/20 and 2020/21.

Topography and observational network

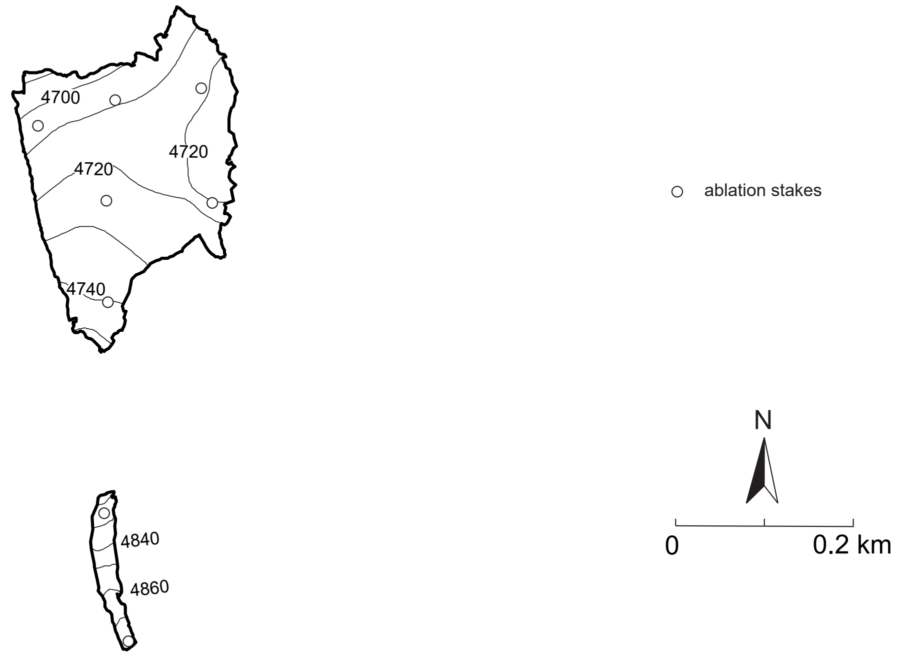

Mass-balance maps 2019/20 and 2020/21

Conejeras (COLOMBIA)

Figure 4.7.2 Mass balance versus elevation for 2019/20 and 2020/21.

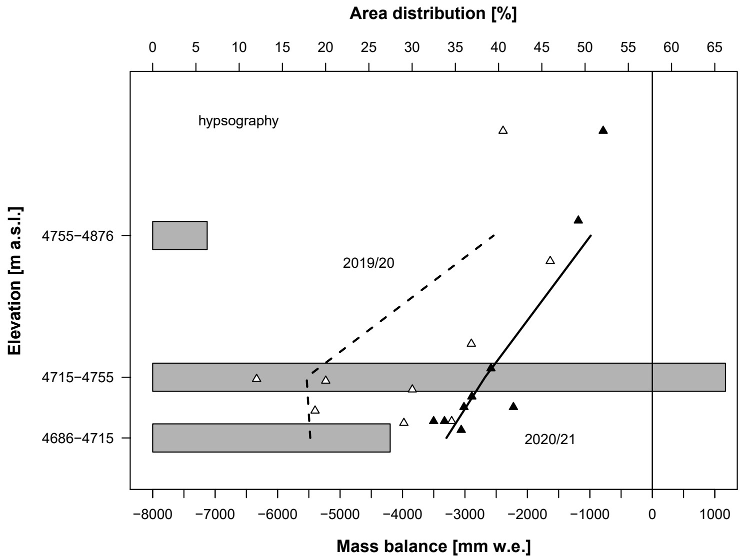

Figure 4.7.3 Glaciological balance versus geodetic balance for the whole observation period.

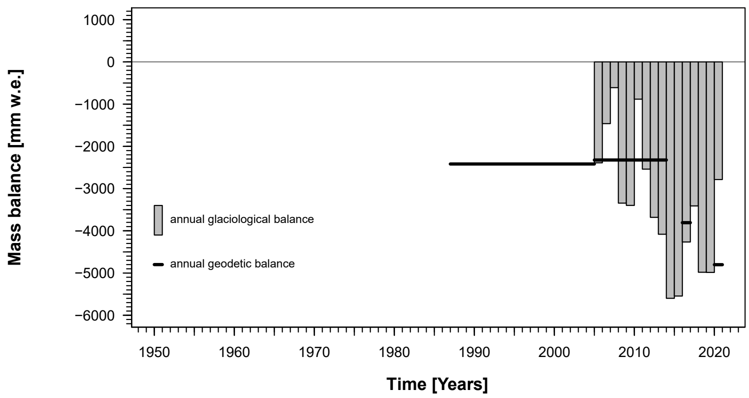

Figure 4.7.4 Accumulation area ratio (AAR) and equilibrium line altitude (ELA) versus specific mass balance for the whole observation period.

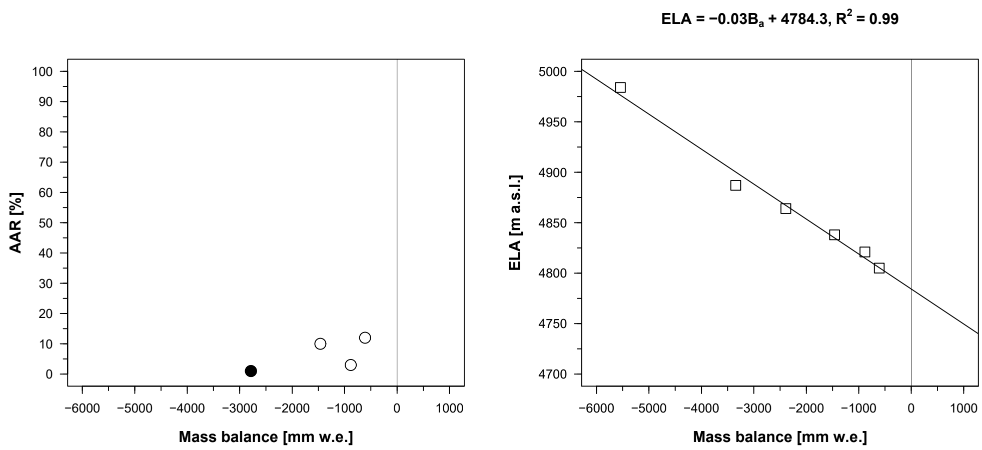

Conejeras (COLOMBIA)

4.8 HOFSJÖKULL (ICELAND)

COORDINATES: 64.81° N / 18.82° W

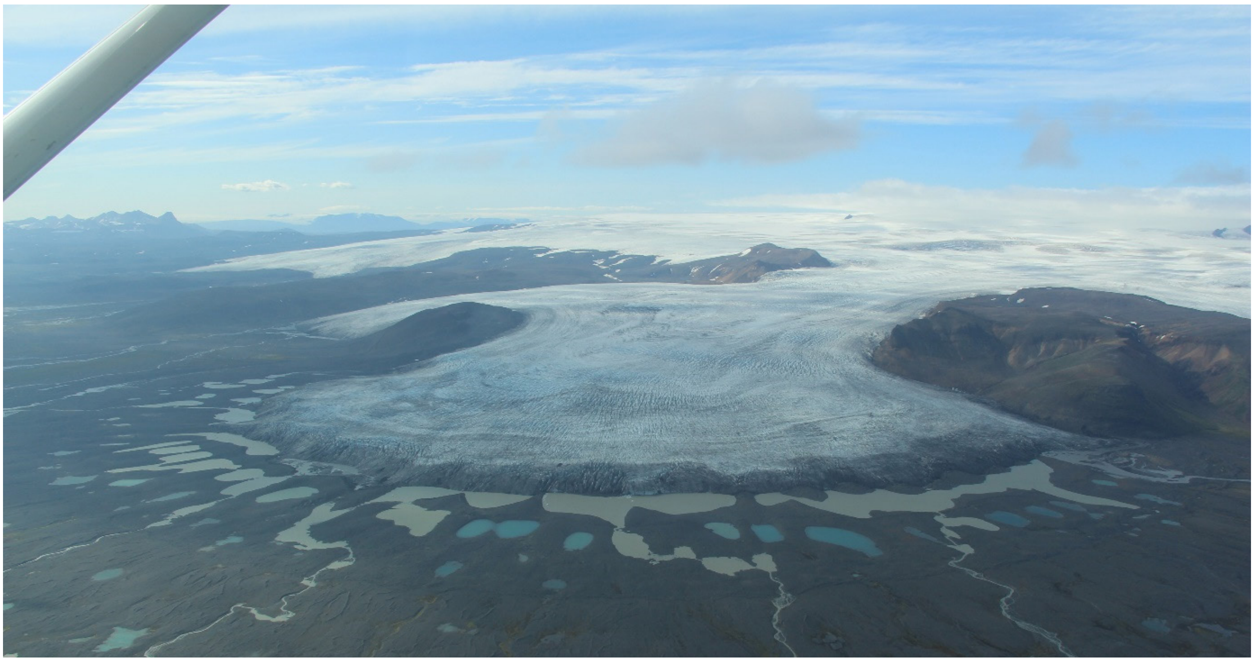

Aerial view from the south towards Hofsjökull. Photograph taken by Thorsteinn Thorsteinsson, 20 August 2020.

Hofsjökull is an ice cap with an area of about 800 km² (Hannesdóttir et al. 2020), located in Central Iceland, about 100 km from the north coast and 130 km from the south coast. The climate in Iceland is maritime and the precipitation regime of Hofsjökull is dominated both by low pressure systems moving eastward across the North Atlantic Ocean and by atmospheric transport from a northerly direction. The mean annual temperature at the Hveravellir weather station, located 20 km west of Hofsjökull, was –1.0 °C in the period 1961–1990 and 0.0 °C in the period 1991–2020. The ice cap spans an elevation range from 600 m a.s.l. to 1,790 m a.s.l. and the maximum ice thickness is 750 m according to radio-echo soundings carried out in 1983 (Björnsson 1988).

Mass-balance studies using standard glaciological methods of core drilling and stake readings were started on Hofsjökull N in 1988 and have been operated annually since 1989 on three transects within the ice-flow basins of Sátujökull (Hofsjökull N), Þjórsárjökull (Hofsjökull E), and Blágnípujökull (Hofsjökull SW). Together, these three basins comprise 40% of the total area of the ice cap. Measurements of winter balance have in most years been made by the end of April or beginning of May and summer balance has been recorded by end of September or beginning of October. Mass balances are calculated in the floating date system and using the profile method, which explains the lack of distributed mass-balance maps. In addition, results from airborne and spaceborne surveys have been used to estimate the geodetic mass balance and to correct biases in the glaciological mass-balance series (Jóhannesson et al. 2013, Aðalgeirsdóttir et al. 2020). Also, non-surface mass-balance components were estimated (Jóhannesson et al. 2020). During the entire 33-year period from 1989–2021 the (bias-corrected) mass balance has been negative in 28 years and positive in 5 years. The average mass balance was –0.90 ± 0.15 m w.e.

In 2019/20 the mass balances of Hofsjökull E, N, and SW were –680, –390, and –80 mm w.e., respectively. In 2020/21, corresponding balances were –800, –1,410, and –480 mm w.e., respectively.

The Icelandic Meteorological Office produces annual reports in Icelandic on the mass balance of Hofsjökull. For additional information on the status of the ice cap and on data relating to annual mass balance and other measurements, visit: https://icelandicglaciers.is (Thorsteinsson et al. 2017).

Figure 4.8.1 Topography and observation network on Hofsjökull 2019/20 and 2020/21.

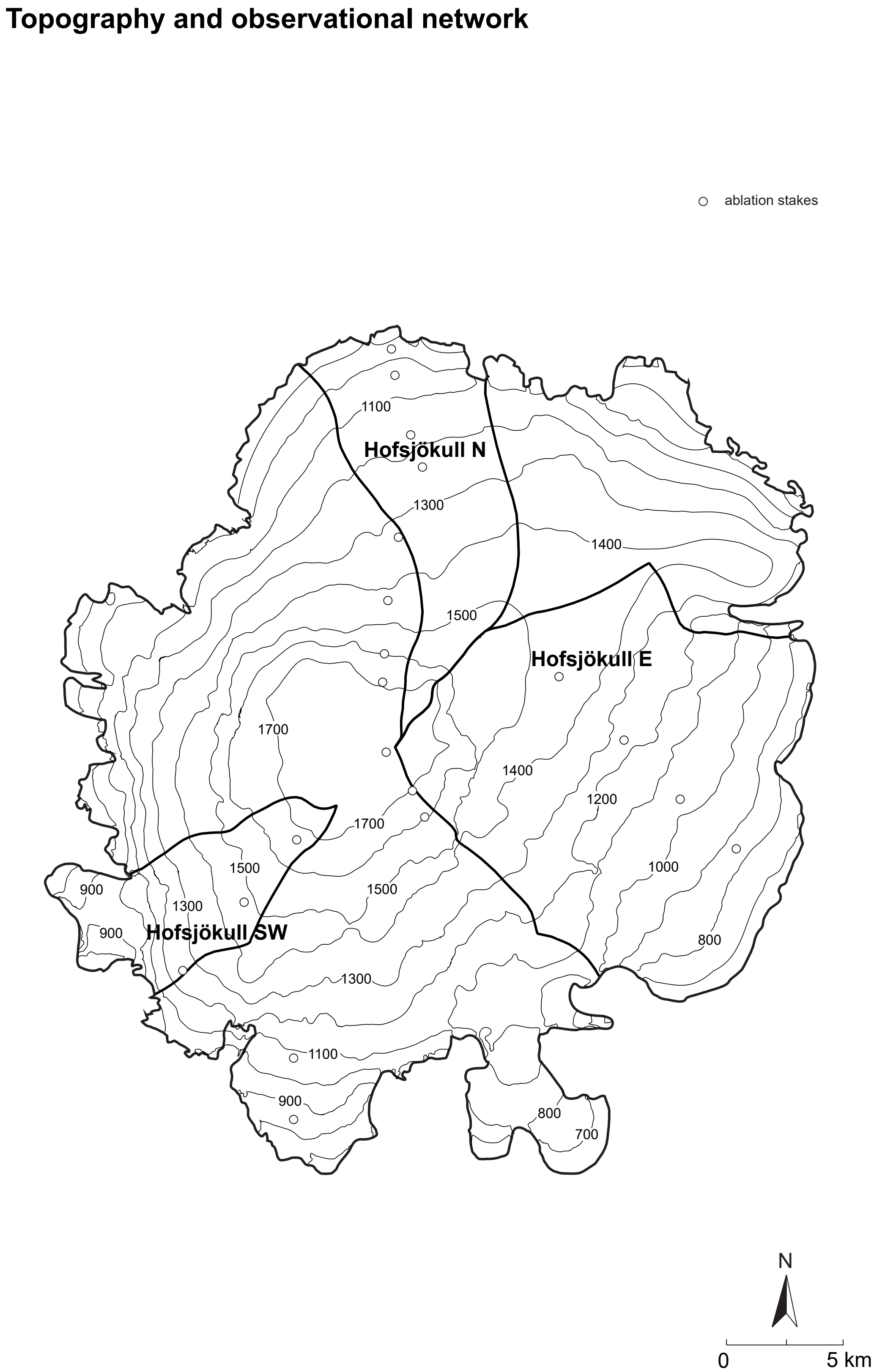

Hofsjökull (ICELAND)

Figure 4.8.2 Mass balance versus elevation for 2019/20 and 2020/21, shown for the entire ice cap (upper graph) and for the single branches (lower graph).

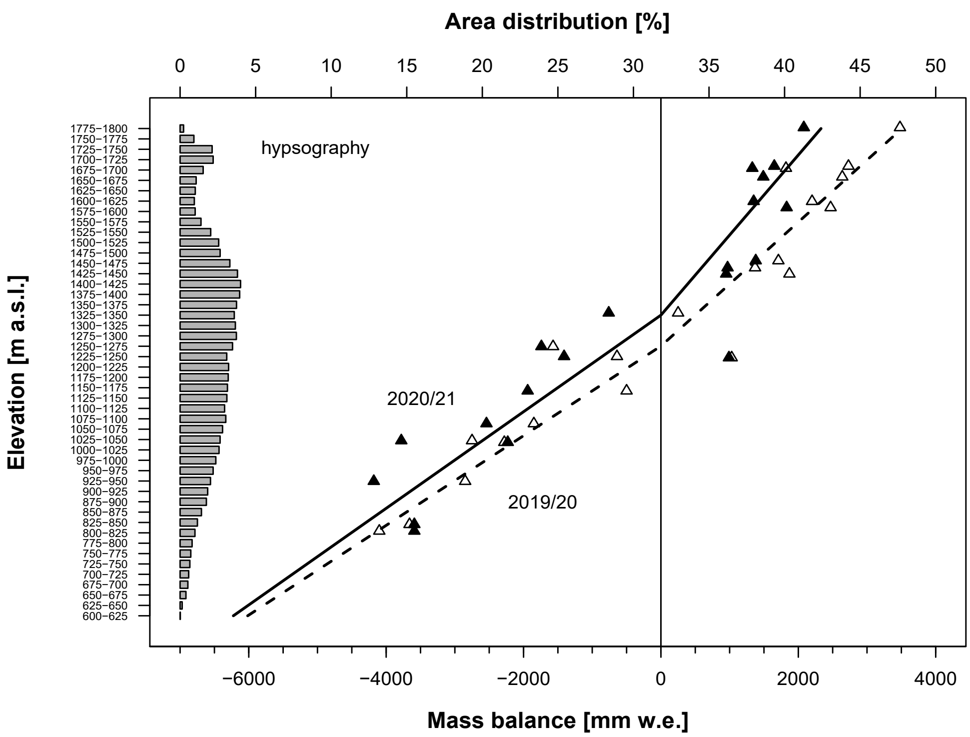

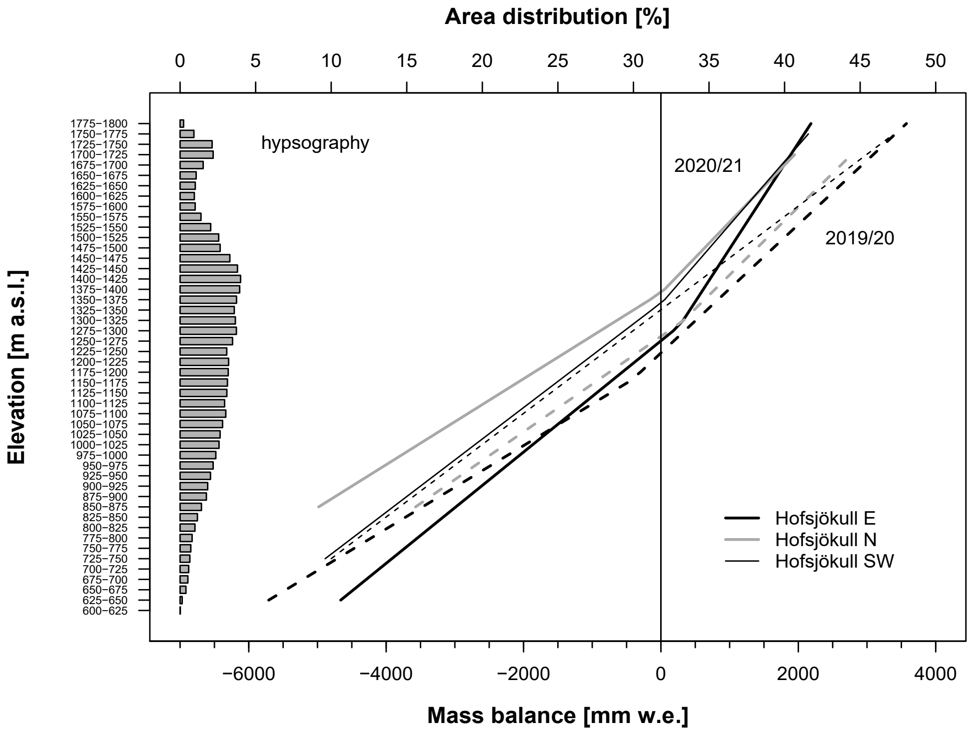

Figure 4.8.3 Glaciological balance versus geodetic balance for the whole observation period, shown for the eastern branch (upper graph), the northern branch (middle graph) and the southwest branch of Hofsjökull (lower graph).

Hofsjökull E

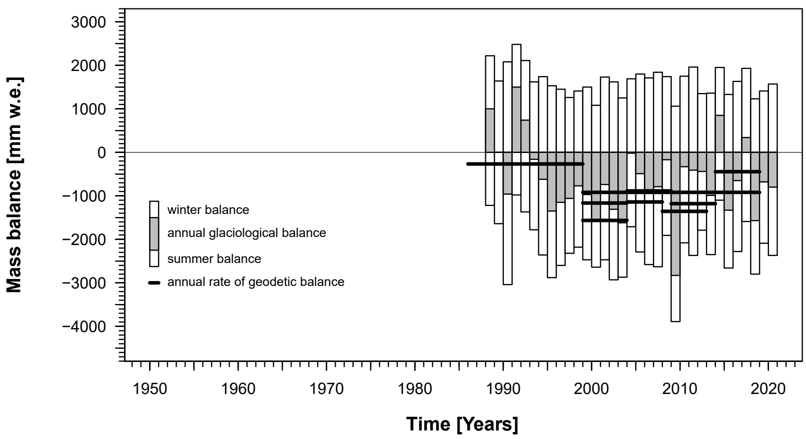

Hofsjökull N

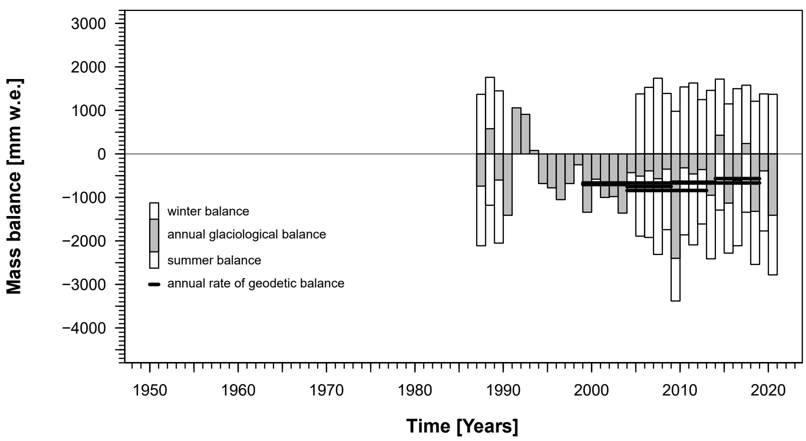

Hofsjökull SW

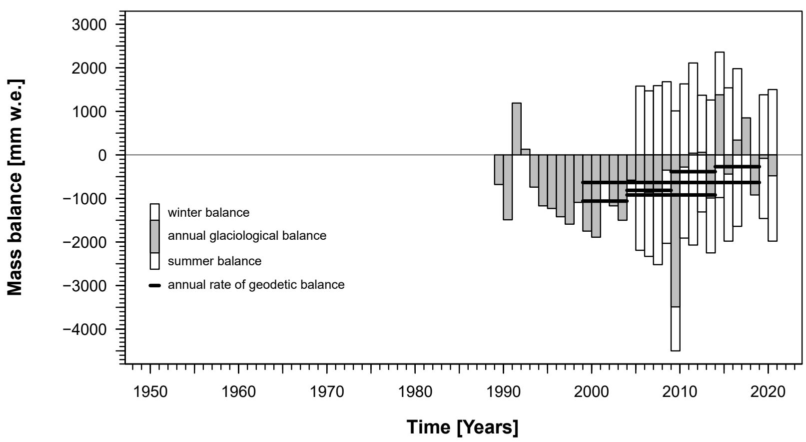

Figure 4.8.4 Accumulation area ratio (AAR) and equilibrium line altitude (ELA) versus specific mass balance for the whole observation period, shown for the eastern branch (upper graph), the northern branch (middle graph) and the southwest branch of Hofsjökull (lower graph).

Hofsjökull E

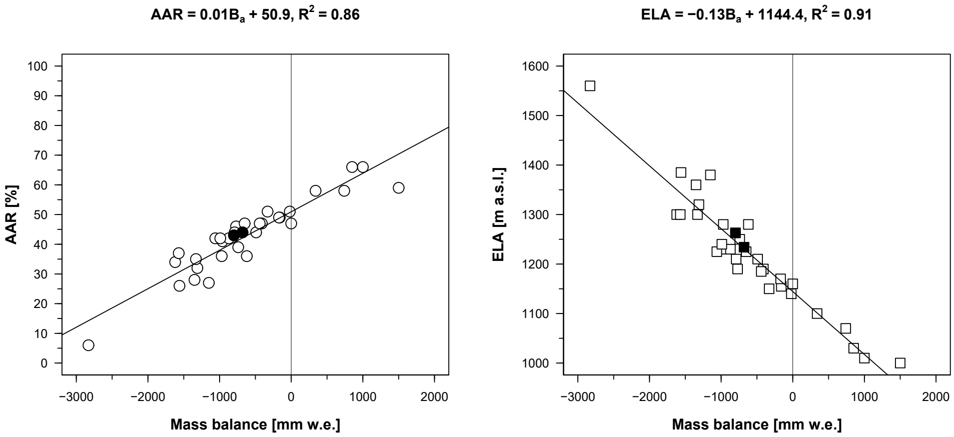

Hofsjökull N

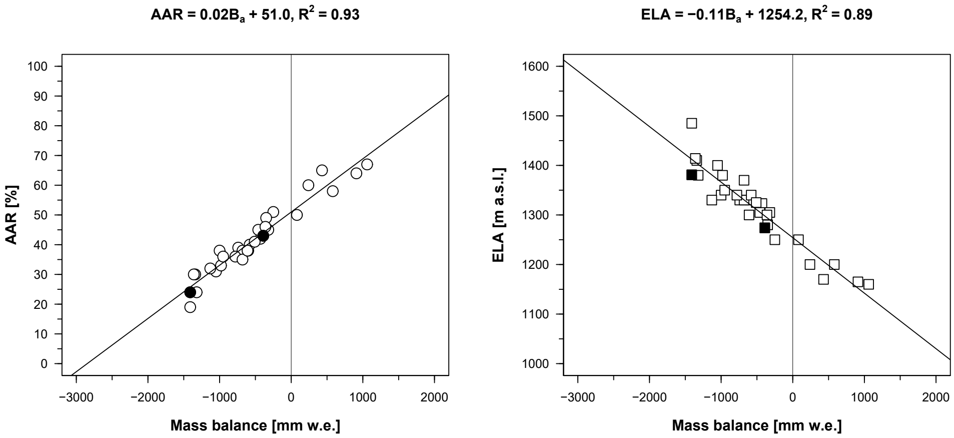

Hofsjökull SW

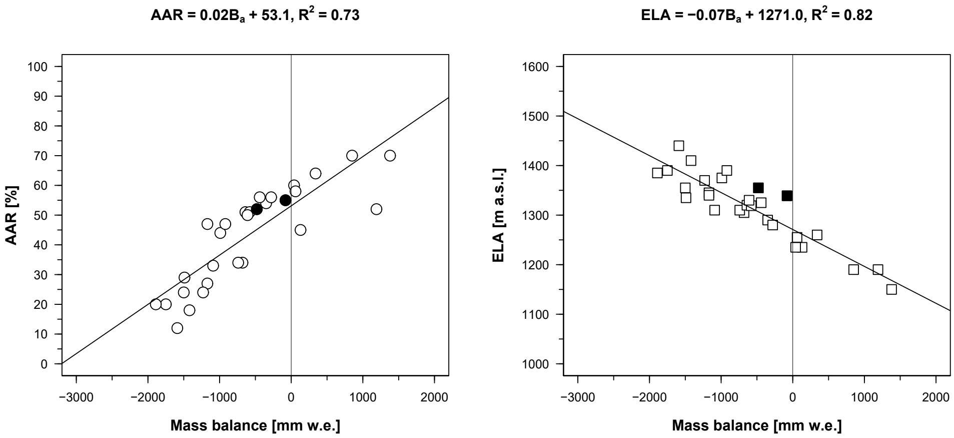

4.9 CARESÈR (ITALY/ALPS)

COORDINATES: 46.45° N / 10.70° E

Photograph of Caresèr Glacier taken by L. Carturan on 13 September 2021.

Caresèr Glacier is located in the Ortles-Cevedale group (Eastern European Alps, Italy). It occupies an area of 0.77 km² (in 2020) and its elevation ranges from 2,969 to 3,133 m a.s.l. The remnant of the former glacier is exposed mainly to the west, is rather flat, and comprised in a narrow elevation range of less than 100 m. The median altitude is 3,064 m a.s.l. and it is progressively decreasing. The mean annual air temperature at this elevation is about –3 to –4 °C and annual precipitation averages 1,450 mm.

Glaciological mass-balance investigations on Caresèr Glacier started in 1967, and until 1980 the mass balance was close to equilibrium. Imbalanced conditions and steadily negative mass balances followed, and in the last three decades the ELA was mostly above the maximum elevation of the glacier. The mean value of the annual mass balance was –1,200 mm w.e. from 1981 to 2001, and decreased to about –1,800 mm w.e. in the last two decades. Starting in 2006, the glacier separated into several ice patches vanishing over the years, with the exception of the eastern ice body (maximum thickness of 88 m in 2006), which is the only one still surviving.

In 2019/20, both winter snow accumulation and summer ablation were 14% below the average of the last 30 years. The melt season started late, in the third week of June, but was warm afterwards. The annual balance was –1,371 mm w.e., which is less negative than the last 30-year mean value of –1,588 mm w.e. The ELA was at 3,114 m a.s.l., and the AAR was 1%. The hydrological year 2020/21 was characterized by abundant winter snow accumulation (40% above the average of the last 30 years). As in 2020, the onset of the melt season was late, in the second week of June, but the summer was once again warm, leading to an annual balance of –950 mm w.e., even though significantly less negative than the long term mean. The ELA was at 3,106 m a.s.l. and the AAR was 3%.

An overview and detailed analysis of the long-term monitoring programme at Caresèr Glacier was published by Carturan et al. (2013).

Figure 4.9.1 Topography and observation network and mass-balance maps of 2019/20 and 2020/21.

Topography and observational network

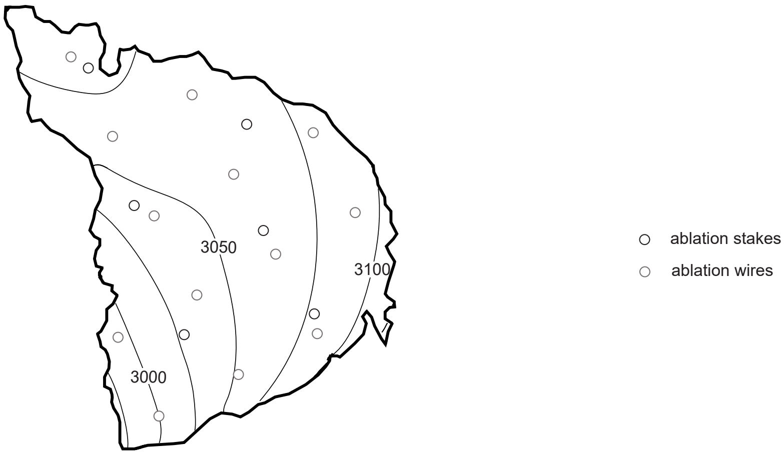

Mass-balance maps 2019/20 and 2020/21

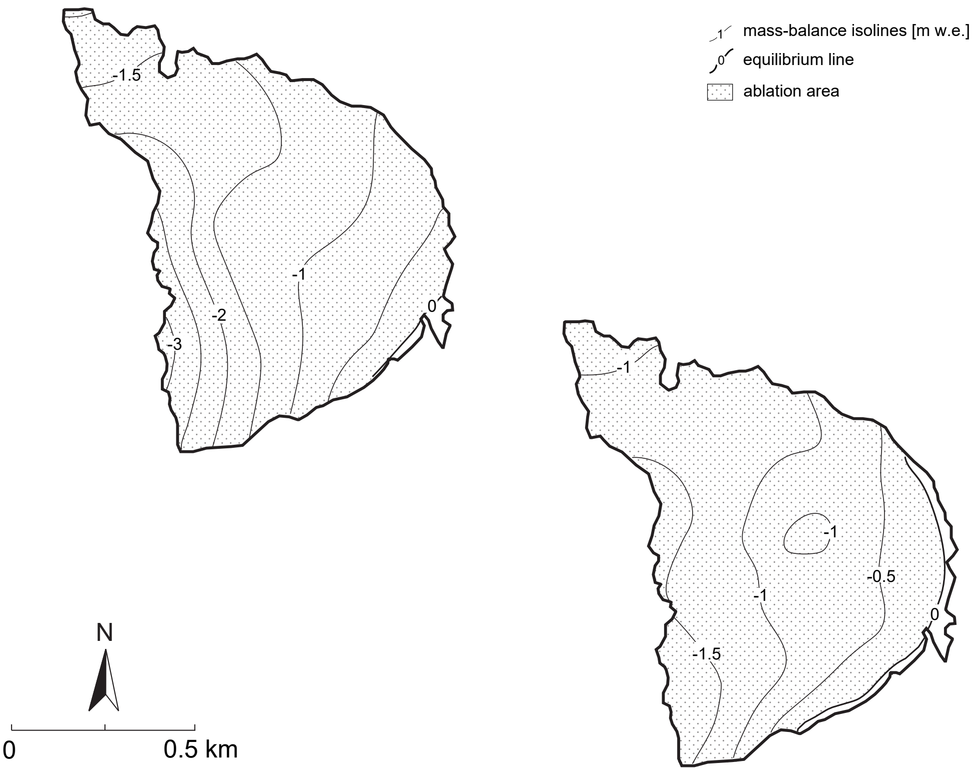

Caresèr (ITALY)

Figure 4.9.2 Mass balance versus elevation for 2019/20 and 2020/21.

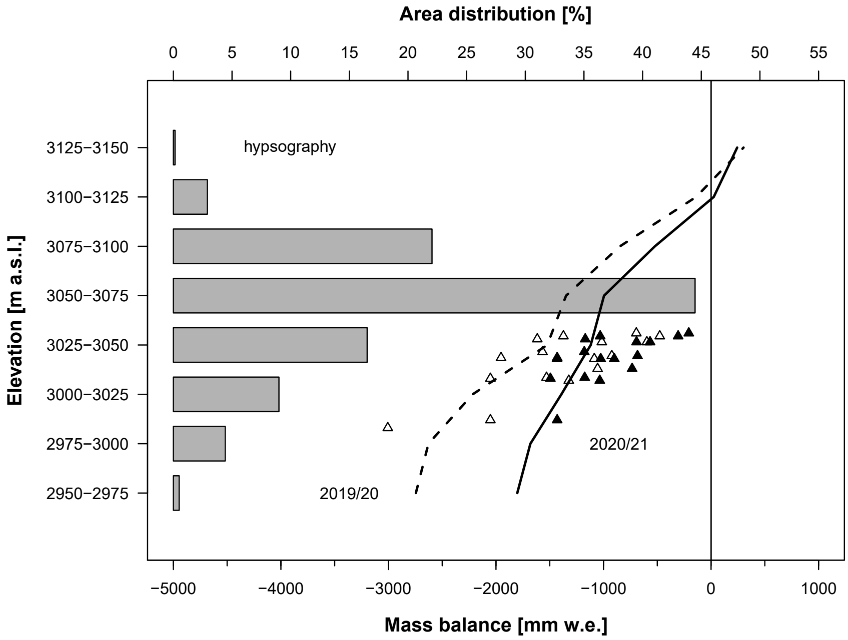

Figure 4.9.3 Glaciological balance versus geodetic balance for the whole observation period.

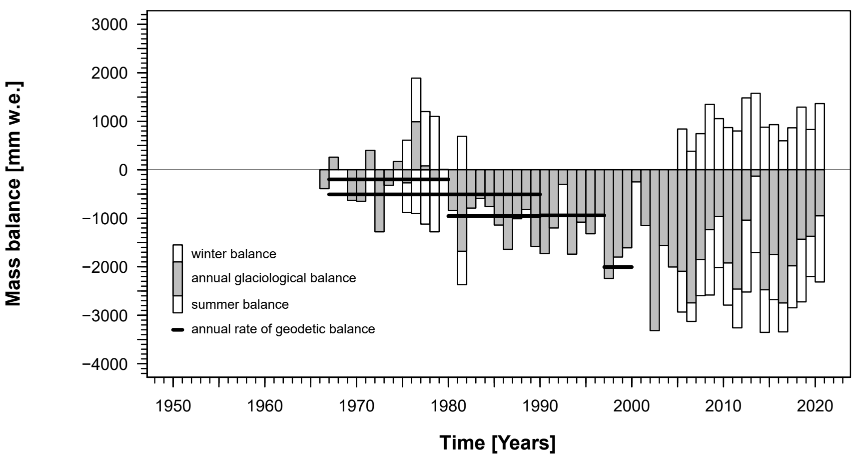

Figure 4.9.4 Accumulation area ratio (AAR) and equilibrium line altitude (ELA) versus specific mass balance for the whole observation period.

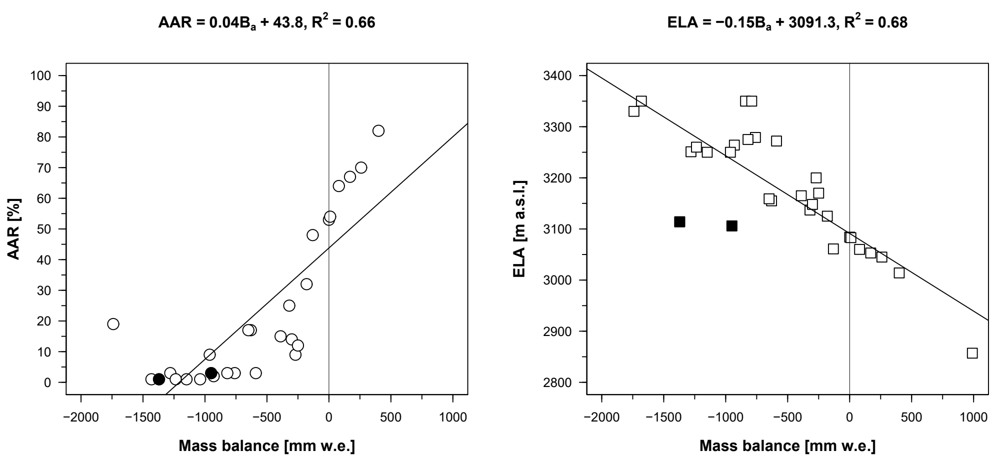

Caresèr (ITALY)

4.10 TSENTRALNIY TUYUKSUYSKIY (KAZAKHSTAN/TIEN SHAN)

COORDINATES: 43.05° N / 77.08° E

Ts. Tuyuksuyskiy Glacier on 23 July 2021. Photograph by N. E. Kassatkin.

Tsentralniy Tuyuksuyskiy is a valley glacier located on the northern slope of the Zailiyskiy Alatau ridge. The glacier ranges from about 3,500 to 4,200 m a.s.l. and is considered to be cold to polythermal and is surrounded by continuous permafrost. Its debris-free surface area amounted to 2.21 km^2 in 2022.

The mean annual air temperature at the ELA (3,980 m a.s.l. in 2021/22) was –7.5 °C and the annual precipitation at the Tuyuksu meteorological station was 941 mm, of which 41% were measured during the summer period. The ELA_0 is at 3,752 m a.s.l. with a corresponding AAR_0 of 52%

The mean air temperature during the warm season (June to September) at the Tuyuksu meteorological station was 5.4 ºC, which was 0.9 ºC above the average for 1972–2022, while the annual precipitation for the warm season was 33 mm less than the average for a specified period.

Glacier mass balances for 2019/20 and 2020/21 were –287 and –609 mm w.e., respectively. Corresponding ELA (AAR) values were 3,800 (46%) and 3,870 m a.s.l. (36%). The mean annual mass balance for the period 1972–2022 was –529 mm w.e.

Comparisons of glaciological and geodetic mass balances were carried out by Hagg et al. (2004) and Kapitsa et al. (2020) finding a systematic bias in the glaciological observations, which was attributed to the lack of observations in the accumulation zone of the glacier.

Figure 4.10.1 Topography and observation network and mass-balance maps of 2019/20 and 2020/21.

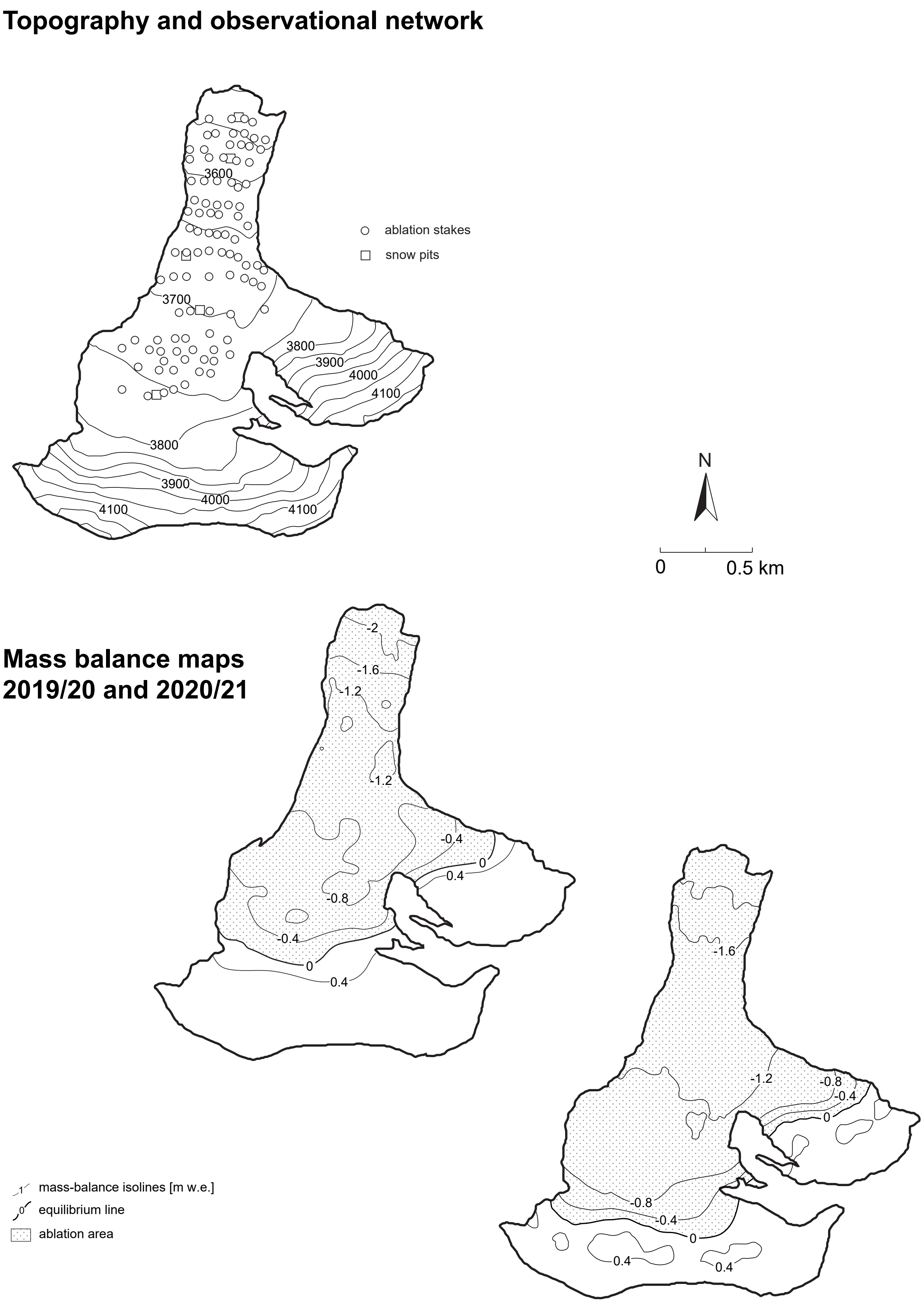

Tsentralniy Tuyuksuyskiy (KAZAKHSTAN)

Figure 4.10.2 Mass balance versus elevation for 2019/20 and 2020/21.

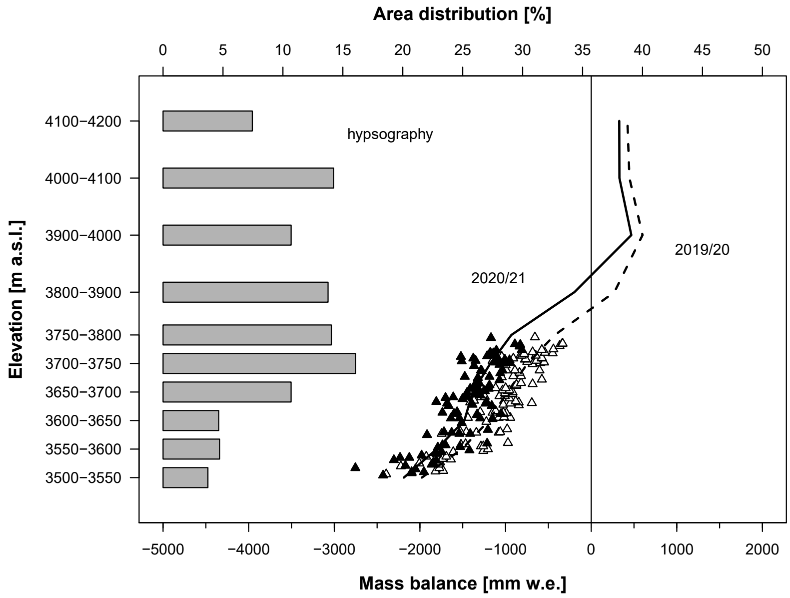

Figure 4.10.3 Glaciological balance versus geodetic balance for the whole observation period.

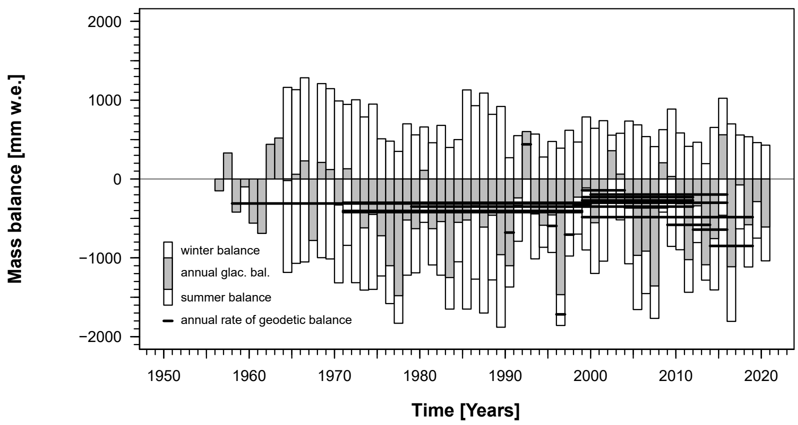

Figure 4.10.4 Accumulation area ratio (AAR) and equilibrium line altitude (ELA) versus specific mass balance for the whole observation period.

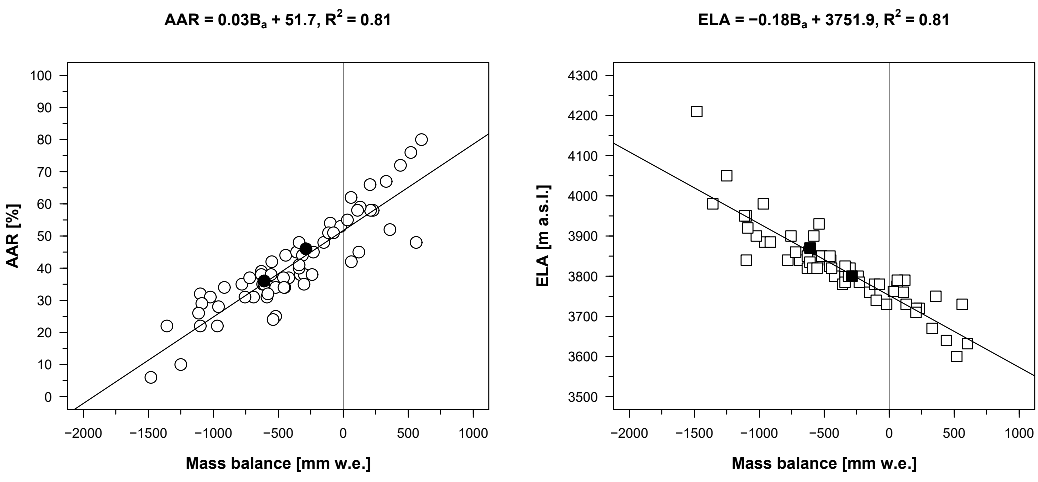

Tsentralniy Tuyuksuyskiy (KAZAKHSTAN)

4.11 ABRAMOV (KYRGYZSTAN/TIEN SHAN)

COORDINATES: 39.63° N / 71.60° E

Photograph of Abramov Glacier taken on 26 July 2022 by Sultanbek Belekov.

Abramov Glacier is a valley glacier located on the northern slope of the Pamir-Alai in the Kok-Suu River basin in Kyrgyzstan. The glacier has an area of 23 km² (in 2022) and spans an altitudinal range between about 3,650 and almost 5,000 m a.s.l. The average annual air temperature (1968–1998), measured at 3,837 m a.s.l. near the glacier tongue, was –4.1 °C and the annual precipitation for the same period was 750 mm. The ELA_0 is 4,156 m a.s.l. and the corresponding AAR_0 is 65%.

Intensive glaciological investigations started in the late 1960s with the installation of a glaciological station next to the glacier. A detailed and intense programme to monitor the glacier mass change was launched in 1968 and continued until 1998. Due to political instability the mass balance programme was stopped abruptly in the late 1990s, terminating a mass balance series after 31 years of investigation. In 2011, the mass-balance monitoring program was re-established thanks to the joint efforts of the Central Asian Institute of Applied Geosciences (CAIAG, Kyrgyzstan), the Geoforschungszentrum Potsdam (GFZ, Germany), and the University of Fribourg (UNIFR, Switzerland).

In 2019/20 the mass balance of Abramov Glacier was slightly positive with 124 mm w.e., with an ELA at 4,115 m a.s.l., and an AAR of 71%. In 2020/21, the glacier experience a negative balance of –1,296 mm w.e. with an ELA at 4,310 m a.s.l., and an AAR of 48%.

The old and new mass-balance observations of Abramov Glacier were homogenized and reanalysed with the use of geodetic surveys by Barandun et al. (2015) and Denzinger et al. (2021).

Figure 4.11.1 Topography and observation network and mass-balance maps of 2019/20 and 2020/21.

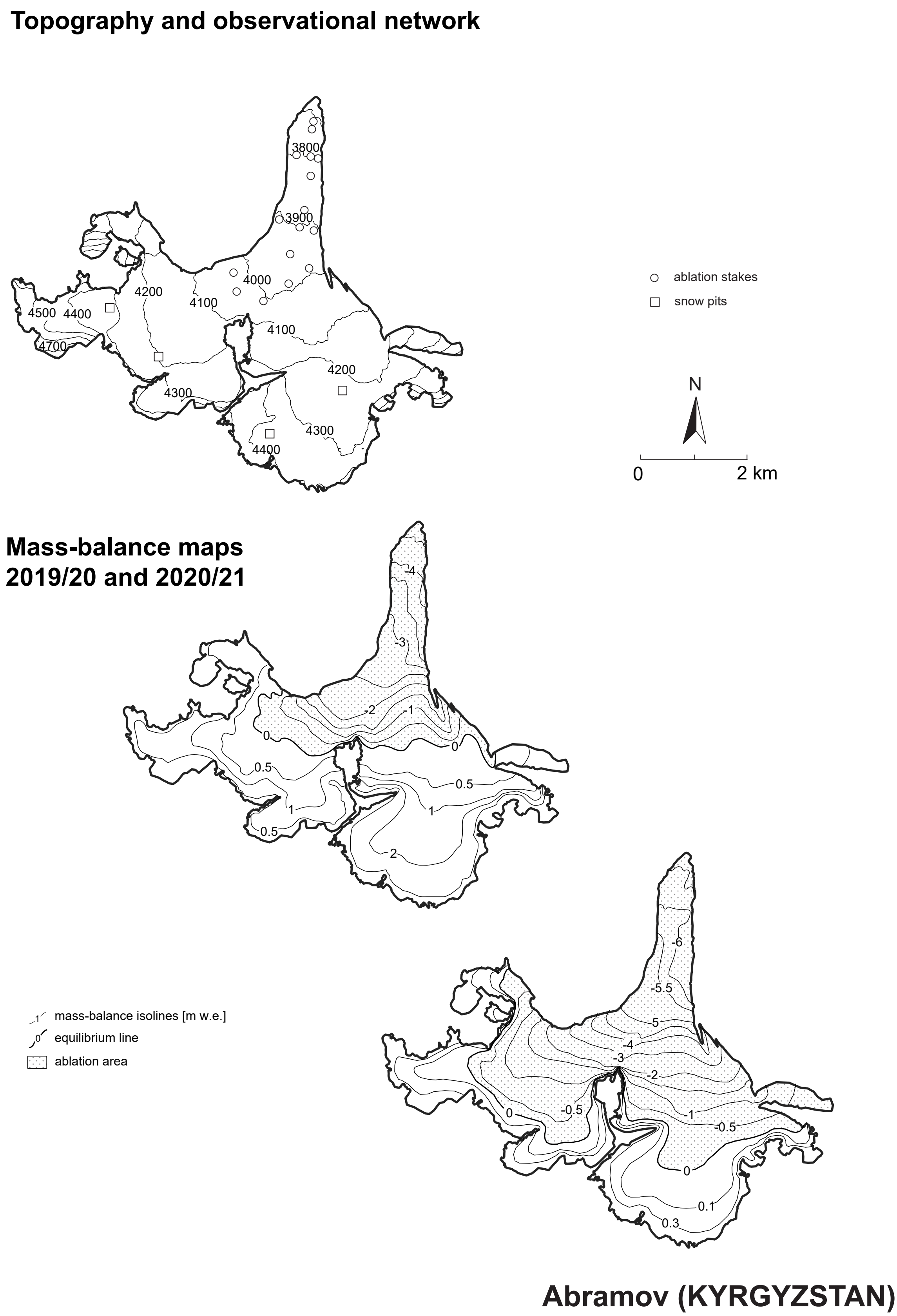

Figure 4.11.2 Mass balance versus elevation for 2019/20 and 2020/21.

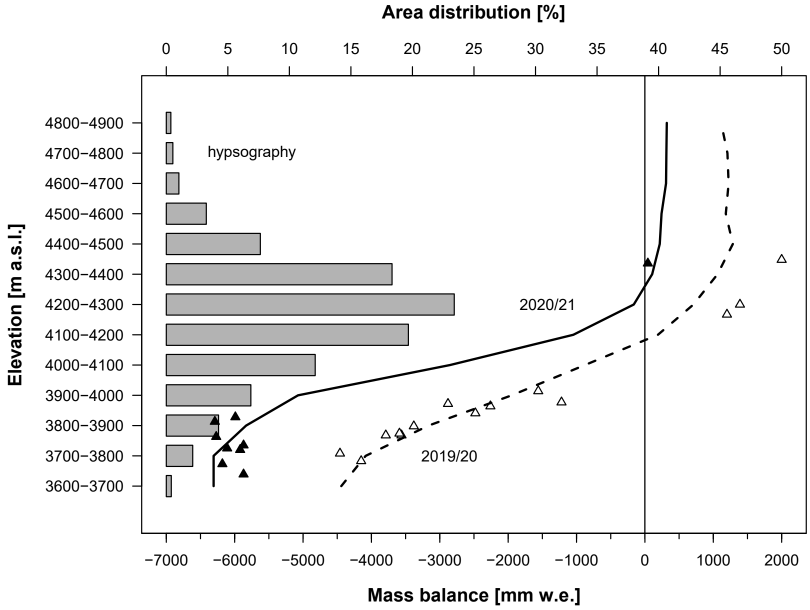

Figure 4.11.3 Glaciological balance versus geodetic balance for the whole observation period.

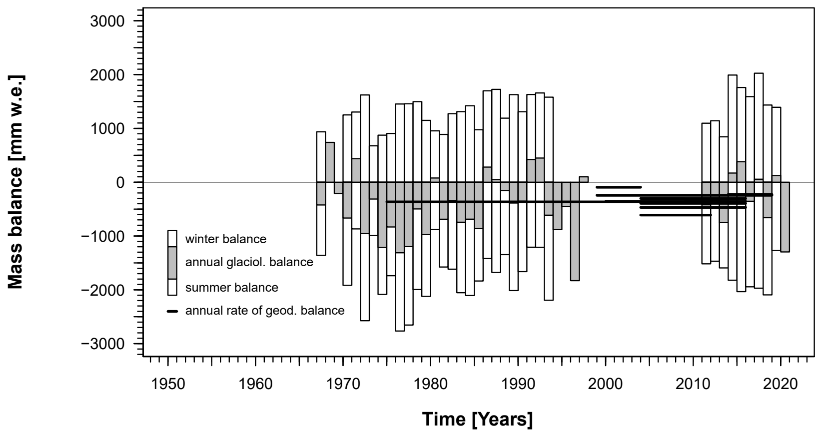

Figure 4.11.4 Accumulation area ratio (AAR) and equilibrium line altitude (ELA) versus specific mass balance for the whole observation period.

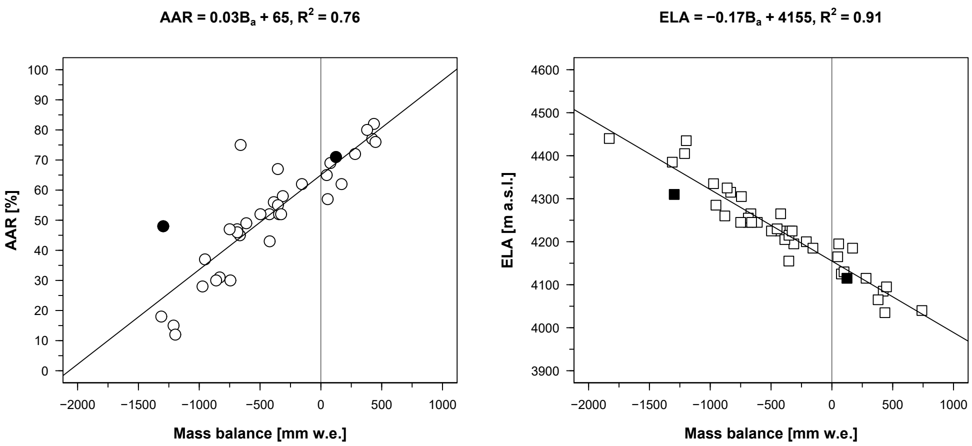

Abramov (KYRGYZSTAN)

4.12 DJANKUAT (RUSSIA/CAUCASUS)

COORDINATES: 43.20° N / 42.77° E

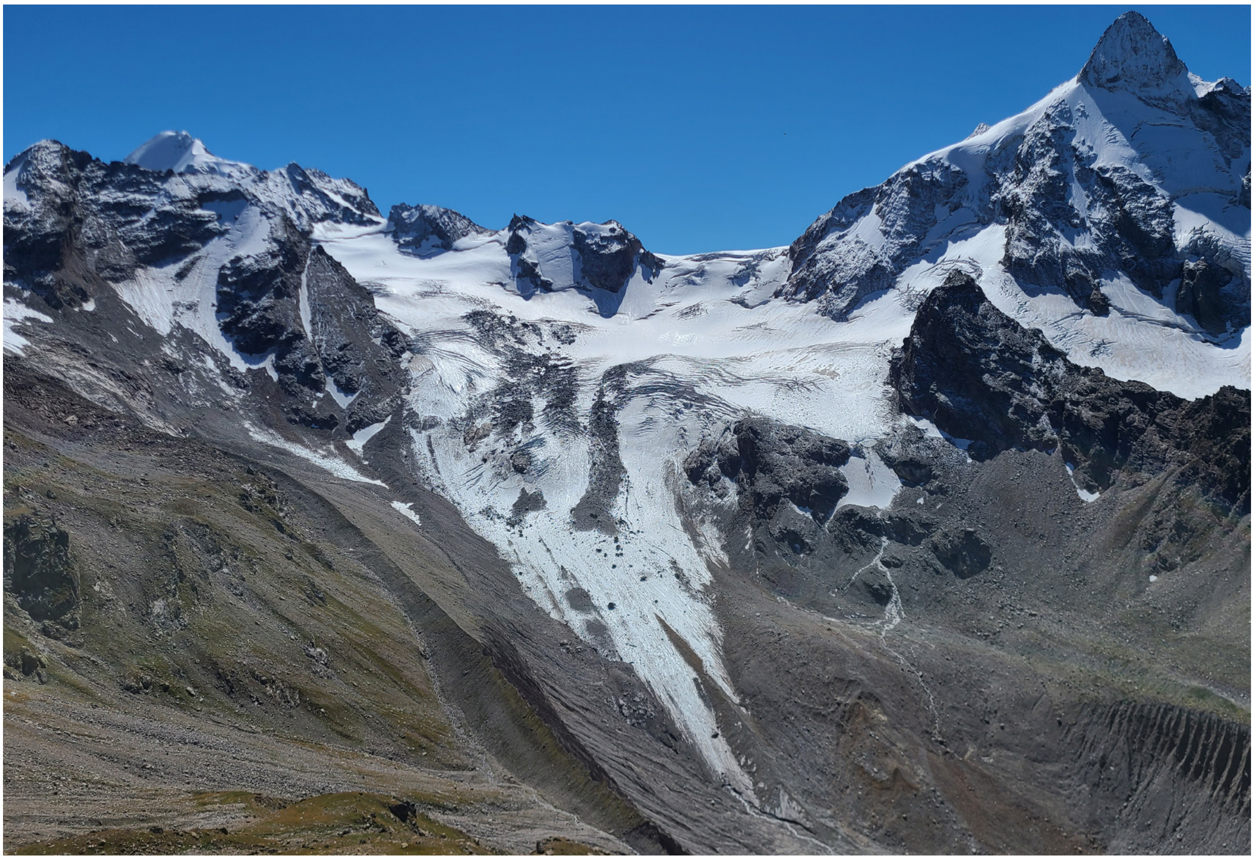

Photograph of Djankuat glacier taken on 9 September 2022.

The valley-type glacier is located on the northern slope of the central section of the Main Caucasus Ridge and extends at present from 3,670 to 2,738 m a.s.l. Its surface area is 2.3 km² and the exposure is to the north-west. Mean annual air temperature at the ELA, at about 3,200 m a.s.l., is –3 to –4.5 °C, and the glacier is temperate. Average annual precipitation as measured near the snout is between 1,100 and 1,200 mm, but roughly three times that amount at the ELA. The peculiarity of the glacier is the migration of the ice divide on the divergent firn plateau south of the crest zone (on the territory of Georgia), redistributing mass flux between adjacent slopes of the main ridge. Another characteristic feature of Djankuat Glacier, which tends to influence progressively mass-balance patterns, is the dynamic expansion of debris cover during the recent period; in 2022 it occupied 20% of the glacier area. The debris originates from a series of tremendous rock falls into the firn basin between 2001 and 2003, and is now been melting out melt middle section of the glacier. Four complete debris thickness surveys over the entire glacier area have been undertaken in 1983, 1994, 2010 and 2022. The latter revealed an average thickness value of 0.6 m. The increase of total debris volume between 1983 and 2022 is fourfold.
Mass balance over the reporting period was negative as usual (–1,370 mm w.e. in 2019/20, –170 mm w.e. in 2020/21), with moduli of both income and discharge items higher than their long-term means. Nevertheless, the two balance years differed greatly. 2019/20 was particularly unfavorable for the glacier state – mainly owing to the absolute record of ablation (i.e. summer balance of –4,360 mm w.e.) since the beginning of direct monitoring in 1968. On the contrary, the next year was characterized by one of the least negative balances over the last decades – it was predetermined by high winter snow accumulation that exceeded its multi-year norm by 31% (the third value in the 55-year-long series). Thus, the duration of period with continuous negative mass balance values reached 16 years that is unprecedented since late 19th century, judging by reconstructed series.

Figure 4.12.1 Topography and observation network and mass-balance maps of 2019/20 and 2020/21.

Topography and observational network

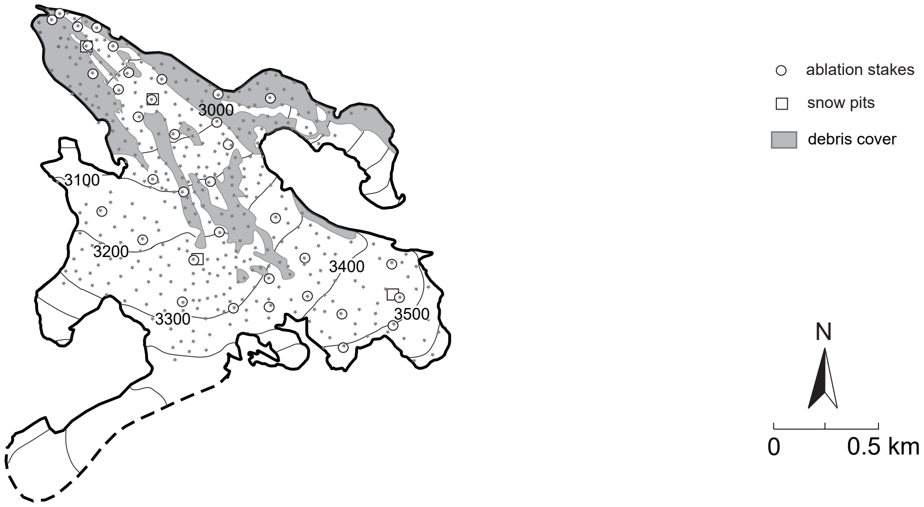

Mass-balance maps 2019/20 and 2020/21

Djankuat (RUSSIA)

Figure 4.12.2 Mass balance versus elevation for 2019/20 and 2020/21.

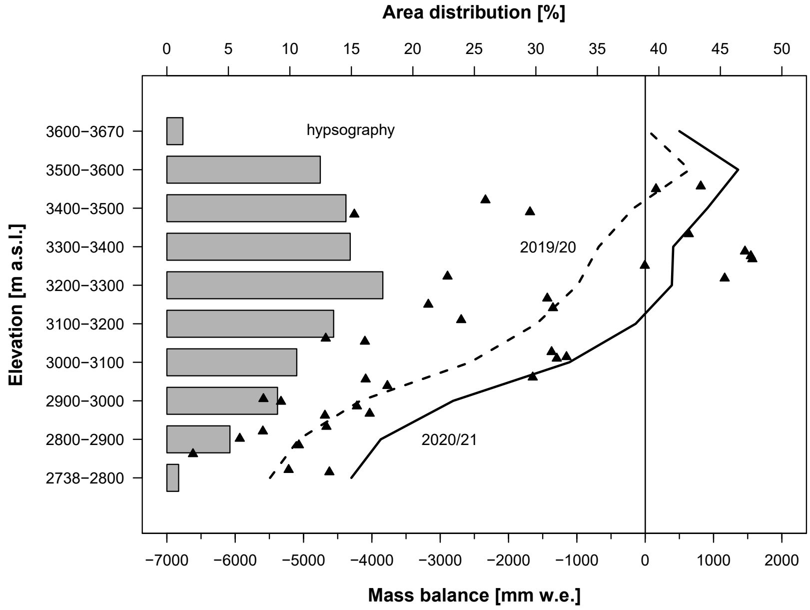

Figure 4.12.3 Glaciological balance versus geodetic balance for the whole observation period.

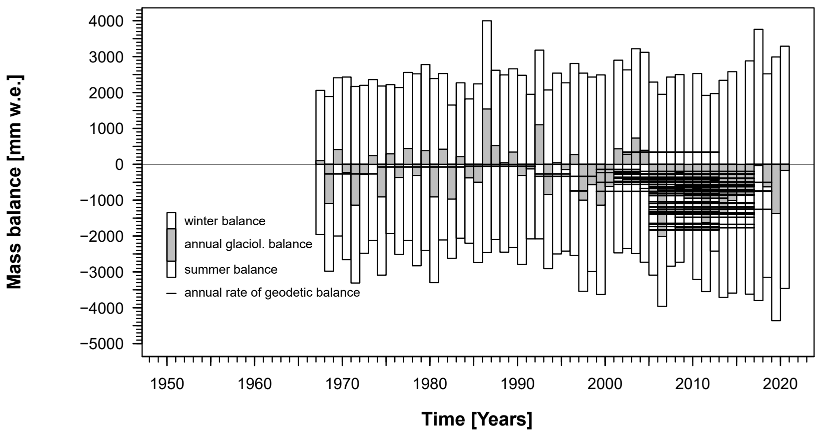

Figure 4.12.4 Accumulation area ratio (AAR) and equilibrium line altitude (ELA) versus specific mass balance for the whole observation period.

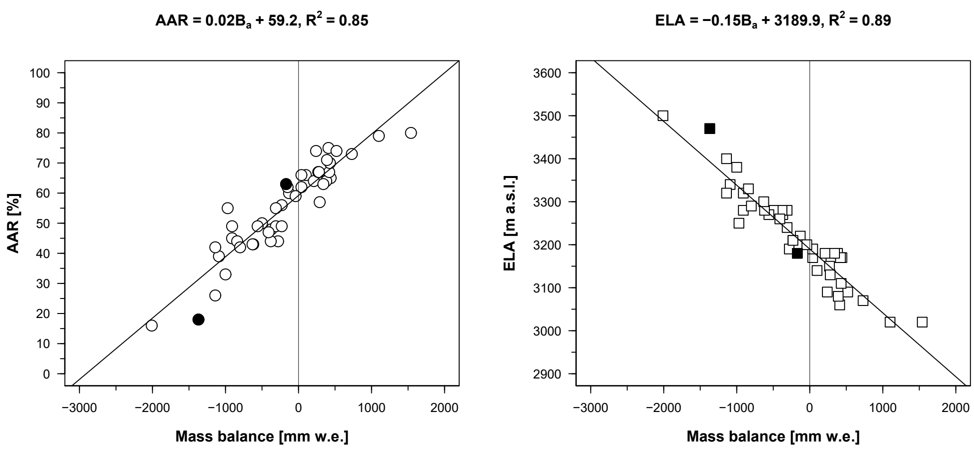

4.13 WALDEMARBREEN (NORWAY/SPITSBERGEN)

COORDINATES: 78.67° N / 12.00° E

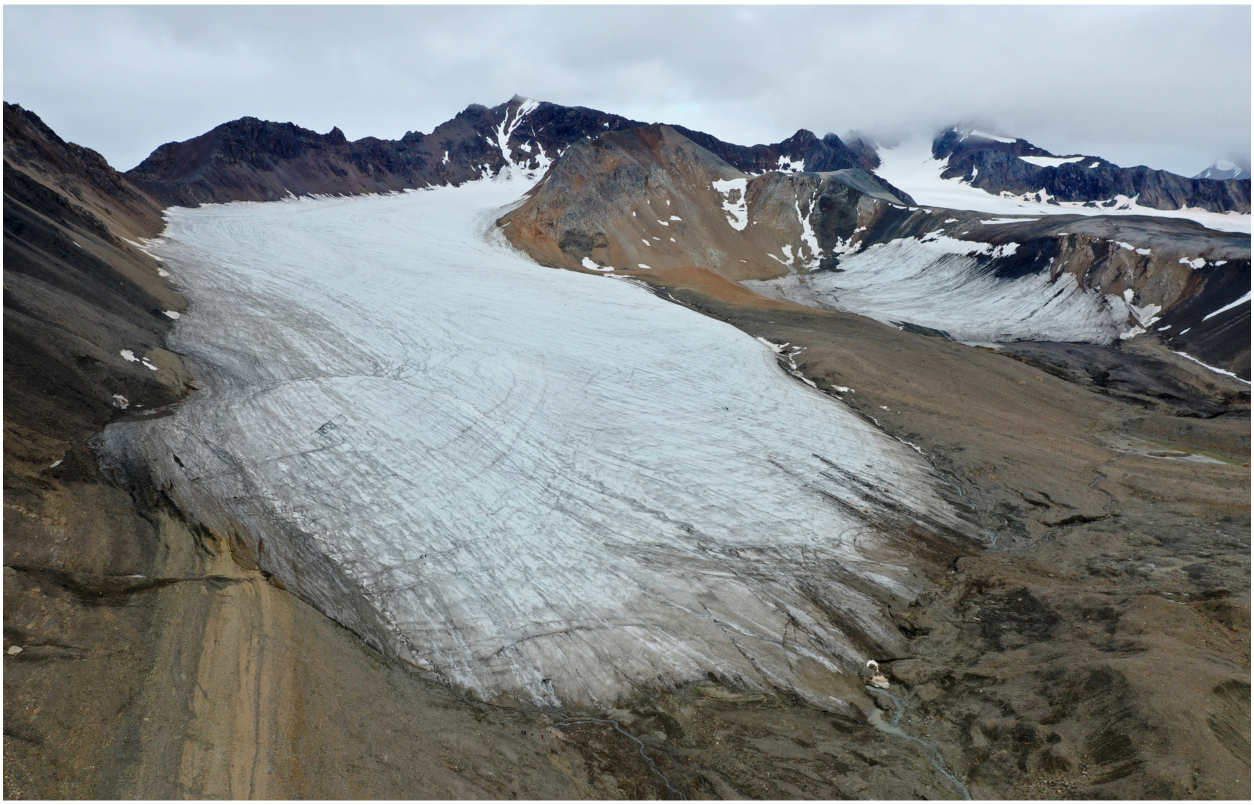

Waldemarbreen in the summer of 2021 (photograph taken by I. Sobota).

Waldemarbreen is located in the northern part of the Oscar II Land, north-western Spitsbergen, and flows down valley to the Kaffiøyra plain. Kaffiøyra is a coastal lowland situated on the Forlandsundet. The glacier is composed of two parts separated by a 1,600 m long medial moraine. It occupies an area of about 2 km² and extends from 500 m to 150 m a.s.l. with a general exposure to the west. Mean annual air temperature in this area is about –4 to –5 °C and annual precipitation is generally 300–400 mm. In the years 1997 to 2021, the mean air temperature during the summer season in this region was 5.5 °C. Since the 19th century, the surface area of the Kaffiøyra region glaciers has decreased by about 50%. Recently, Waldemarbreen has been retreating.

Mass-balance investigations have been conducted since 1996. Detailed glaciological research methods and geodetic surveys are described by Sobota et al. (2016) and Sobota (2013, 2017, 2021).

The balance in 2019/20 showed a mass loss of –2,276 mm w.e. The corresponding ELA was 642 m a.s.l., with an AAR of 0%. In 2020/21 the mass balance was –947 mm w.e. The ELA was at 493 m a.s.l., with an AAR of 1%. The mean value of the mass balance for the period 1996–2021 was –907 mm w.e.

Figure 4.13.1 Topography and observation network and mass-balance maps of 2019/20 and 2020/21.

Topography and observational network

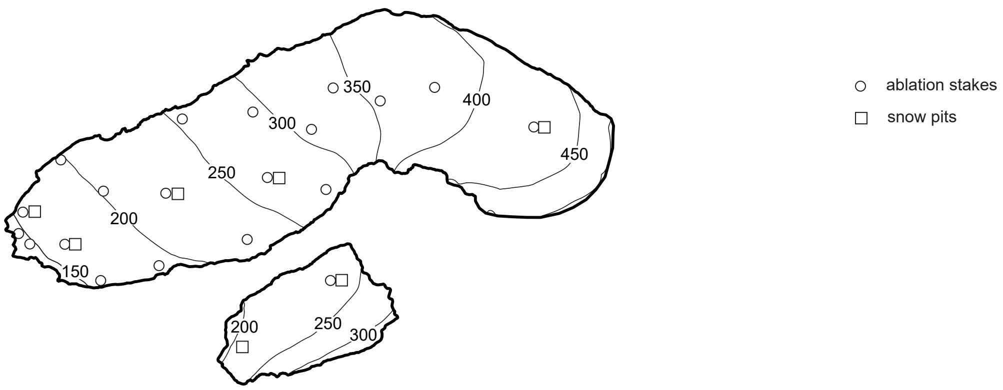

Mass-balance maps 2019/20 and 2020/21

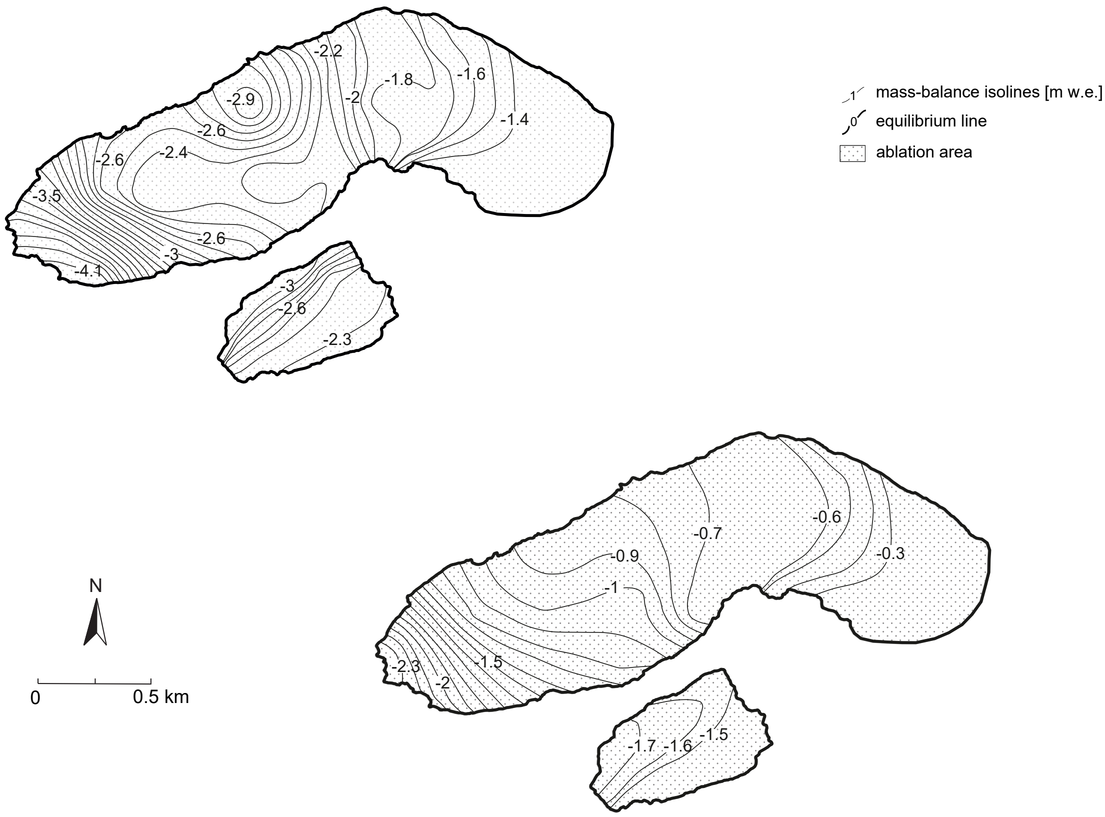

Waldemarbreen (NORWAY)

Figure 4.13.2 Mass balance versus elevation for 2019/20 and 2020/21.

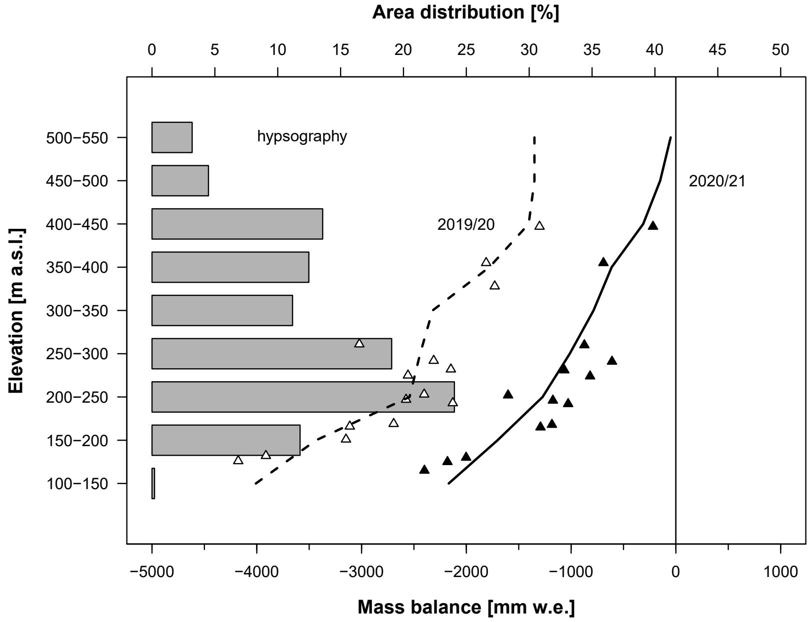

Figure 4.13.3 Glaciological balance versus geodetic balance for the whole observation period.

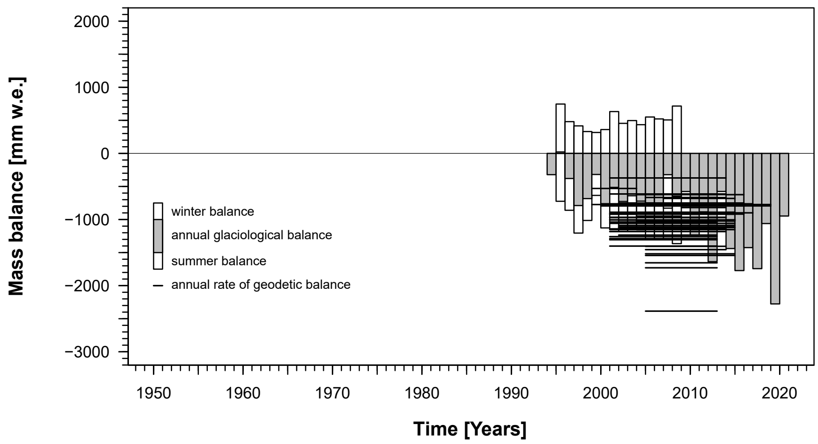

Figure 4.13.4 Accumulation area ratio (AAR) and equilibrium line altitude (ELA) versus specific mass balance for the whole observation period.

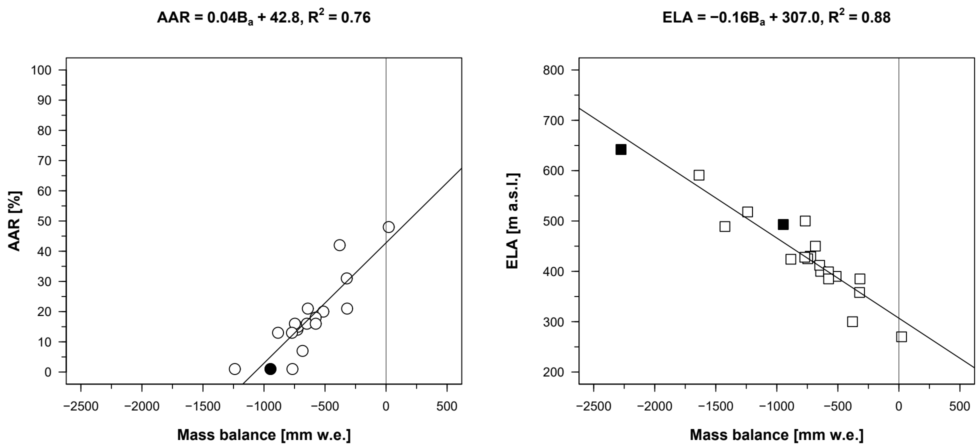

Waldemarbreen (NORWAY)

4.14 STORGLACIÄREN (SWEDEN/SCANDINAVIA)

COORDINATES: 67.90° N / 18.57° E

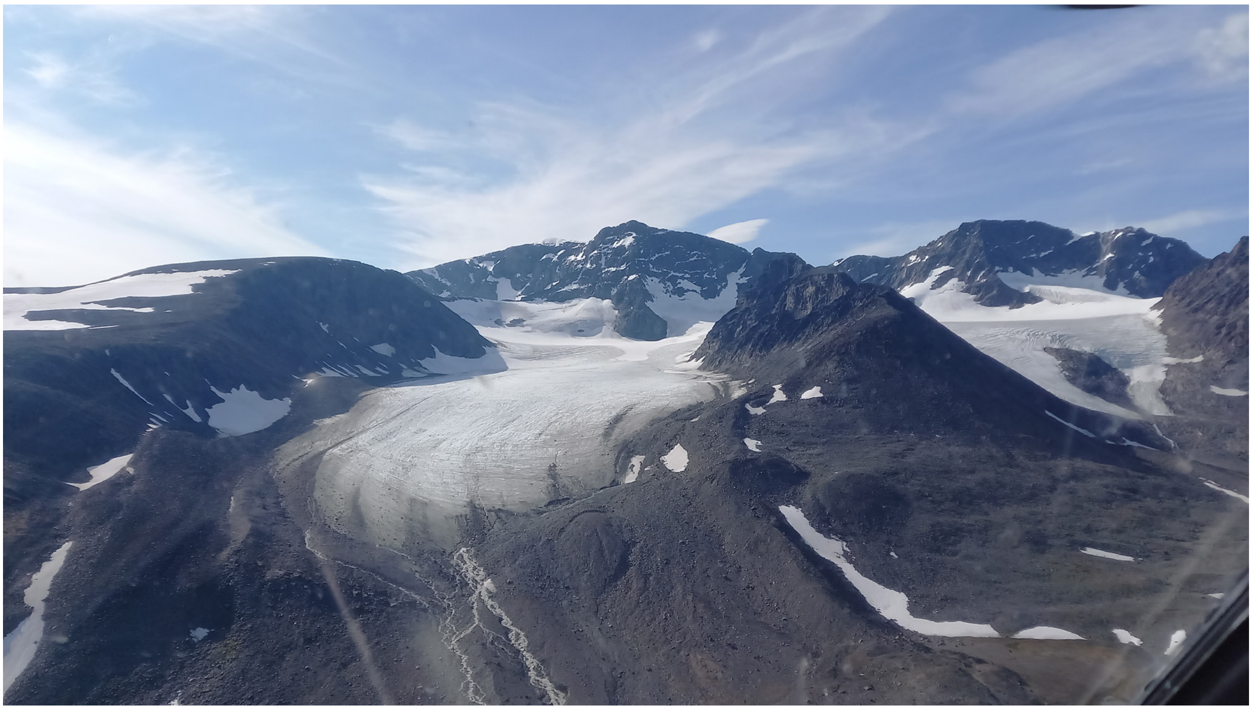

Storglaciären on August 7, 2021, with Kebnekaise's Southern Peak in the distance and Isfallsglaciären to the right (N. Kirchner).

Storglaciären is a small polythermal valley glacier located in the alpine Kebnekaise mountains, Arctic Sweden. The glacier stretches about 3 km from West (~1,720 m a.s.l.) towards East (~1,150 m a.s.l.) and has an area of 2.9 km². The glacier is made up of a large, primarily flat (2° to 15°) ablation area and a small primarily steep (2° to 80°) accumulation area. The average thickness is estimated to be near 100 m with a maximum thickness of over 200 m at overdeepenings. The regional climate is continental with a prevailing westerly wind. Temperature usually peaks in July and is at its lowest in January, but extreme events may occur in any season. Climate records from Tarfala Research Station (1,130 m a.s.l.), situated about one kilometre from the glacier, exist from 1965. Additional melt season weather observations from the glacier (1,350 m a.s.l.) exist from 2013. At the location of the glacial automatic weather station, the mean annual air temperature is approximately −3.3 °C and the annual precipitation is around 1,500 mm where two thirds of the precipitation fall as snow. The latest high-resolution geodetic data from the Tarfala Valley is from 2015 and was compiled by the Swedish national land survey agency Lantmäteriet. Since the start of the surface mass-balance measurements of Storglaciären in year 1945/46, the cumulative mass change has been c. −20 m w.e. Today, the mass balance is measured with an extensive network of almost 300 snow-depth probe points, 73 ablation stakes and several density pits and is calculated using universal kriging with a Gaussian model.

The mass-balance year 2019/20 was a positive year with an annual mass balance of 136 mm w.e. (winter balance, 1,776 mm w.e.; summer balance, −1,640 mm w.e.). The mass-balance year 2020/21 was a negative year with a surface mass balance of −823 mm w.e. (winter balance, 1,099 mm w.e.; summer balance, −1,922 mm w.e.). Similarly, the elevation of the ice covered Kebnekaise Southern Peak was 400 mm higher in September 2020 (2,096.0 m a.s.l.) as compared to 2019 (2,095.6 m a.s.l.), but was measured to only 2,094.6 m a.s.l. in September 2021.

The glaciological mass-balance series was reanalyzed with geodetic surveys (Koblet et al. 2010, Zemp et al. 2010) and reconstructed from historical images back to 1910 (Holmlund & Holmlund 2018).

Figure 4.14.1 Topography and observation network and mass-balance maps of 2019/20 and 2020/21.

Topography and observational network

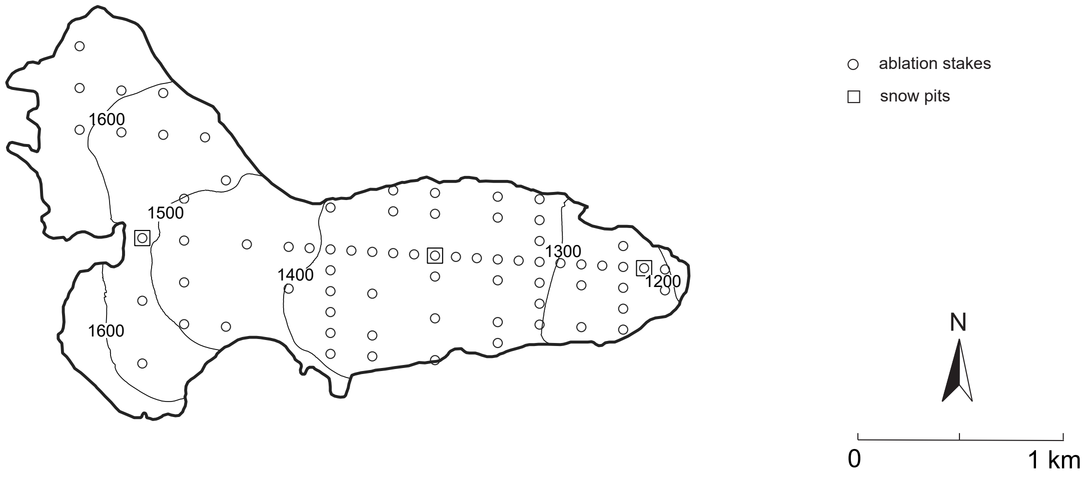

Mass-balance maps 2019/20 and 2020/21

Storglaciären (SWEDEN)

Figure 4.14.2 Mass balance versus elevation for 2019/20 and 2020/21.

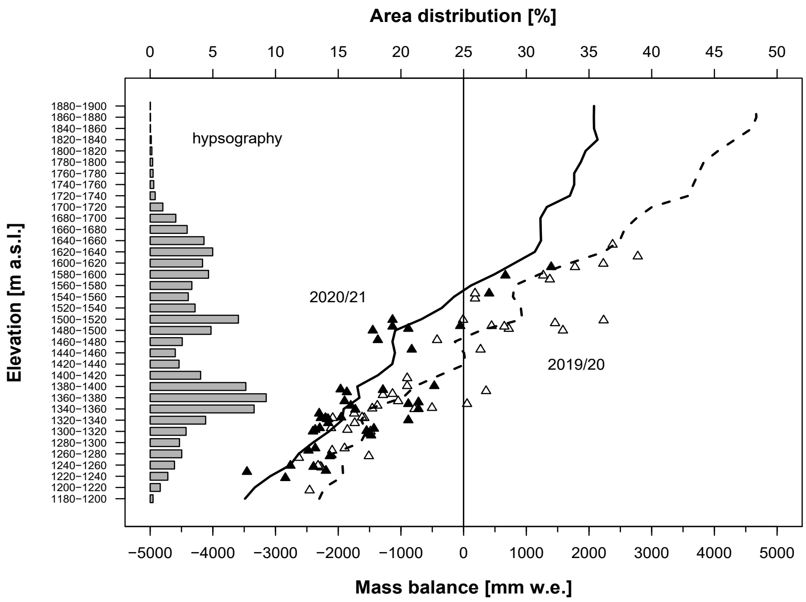

Figure 4.14.3 Glaciological balance versus geodetic balance for the whole observation period.

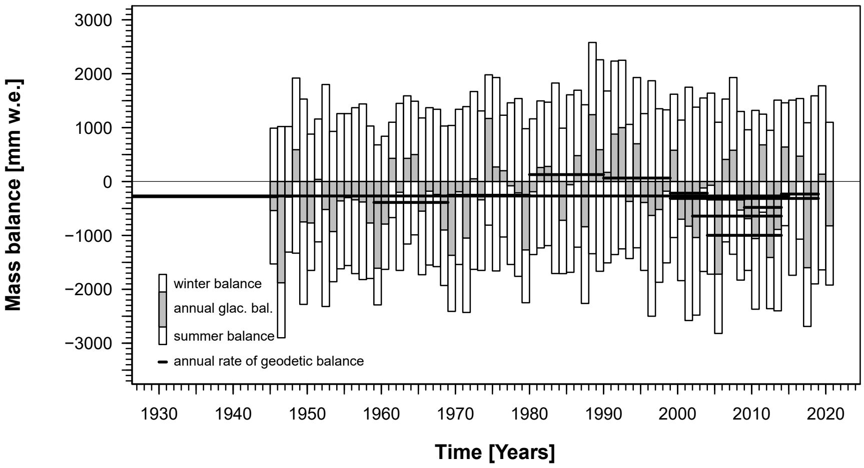

Figure 4.14.4 Accumulation area ratio (AAR) and equilibrium line altitude (ELA) versus specific mass balance for the whole observation period.

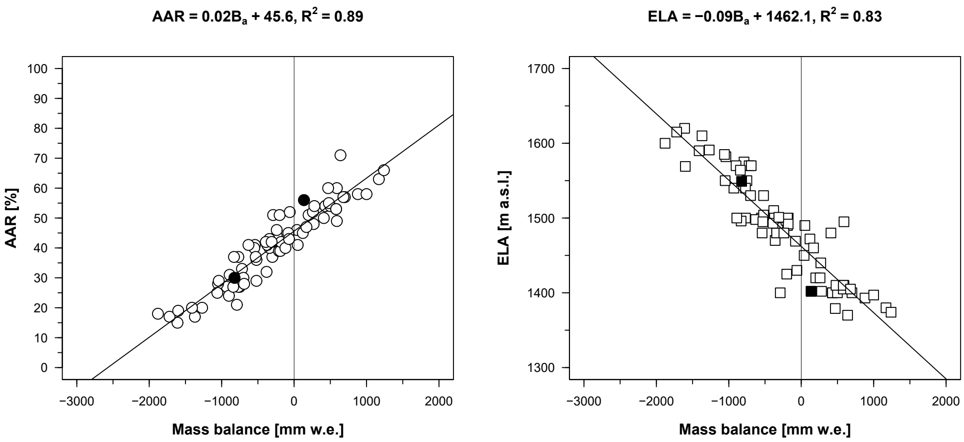

Storglaciären (SWEDEN)

4.15 BASÒDINO (SWITZERLAND/ALPS)

COORDINATES: 46.42° N / 8.48° E

Photograph of Ghiacciaio del Basòdino and its proglacial area, taken by G. Kappenberger in July 2022.

Ghiacciaio del Basòdino is a small north-east facing mountain glacier in the Southern Swiss Alps. The glacier covers an area of 1.64 km² (2018) and extends from 3,181 to 2,588 m a.s.l. It currently has a length of 1.3 km and ice thickness measurements indicate an ice volume of 0.022 km³ in 2018 corresponding to a mean ice thickness of 14 m, and a maximum thickness of 26 m (Grab et al., 2021). The average annual and summer air temperatures (1991–2020) at the median glacier elevation (2,908 m a.s.l.) is around –3 °C and +5 °C, respectively, and mean annual precipitation at the station Robièi (1,898 m a.s.l., 3 km from the glacier terminus) is 2,400 mm.

Detailed seasonal mass balance investigations have been carried out continuously since 1991. The network of initially six stakes has been gradually extended to 13 stakes that are observed both in spring and fall. The evolution of surface topography is documented by 10 digital elevation models at decadal intervals and volumetric changes have been determined over the period from 1929 to 2018 (Bauder et al., 2007). This data indicates that over the last roughly 90 years, Ghiacciaio del Basòdino has lost 85% of its ice volume. Nevertheless, Ghiacciaio del Basòdino is still the biggest glacier in the Ticino, the southernmost part of Switzerland, and thus is considered as representative for this region.

The glacier-wide annual surface mass balance 2019/20 was only moderately negative with –539 mm w.e., which is attributed to relatively high winter balance. The ELA was at 3,055 m a.s.l. and AAR was 10%. Even though summer melting was less pronounced than in previous years, mass loss also occurred in 2020/21 with a glacier-wide mass balance of –439 mm w.e. The ELA was at 3,065 m a.s.l. and AAR was 9%.

Figure 4.15.1 Topography and observation network and mass-balance maps of 2019/20 and 2020/21.

Topography and observational network

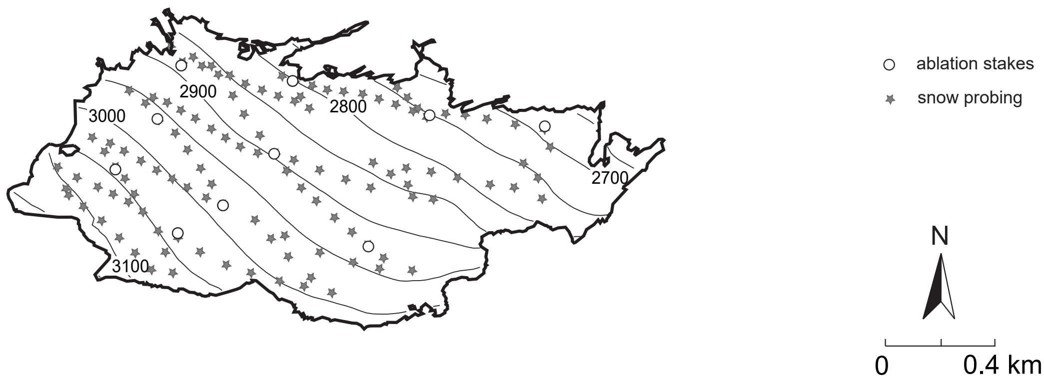

Mass-balance maps 2019/20 and 2020/21

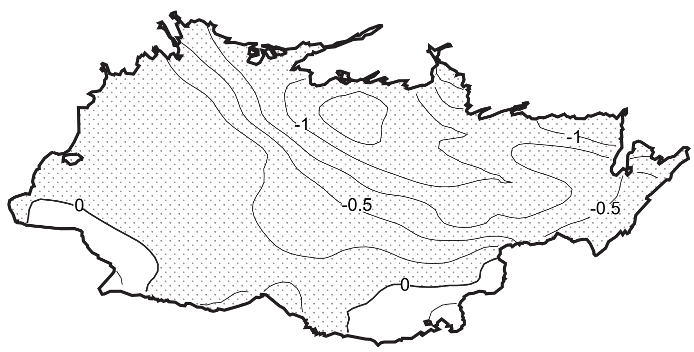

Basòdino (SWITZERLAND)

Figure 4.15.2 Mass balance versus elevation for 2019/20 and 2020/21.

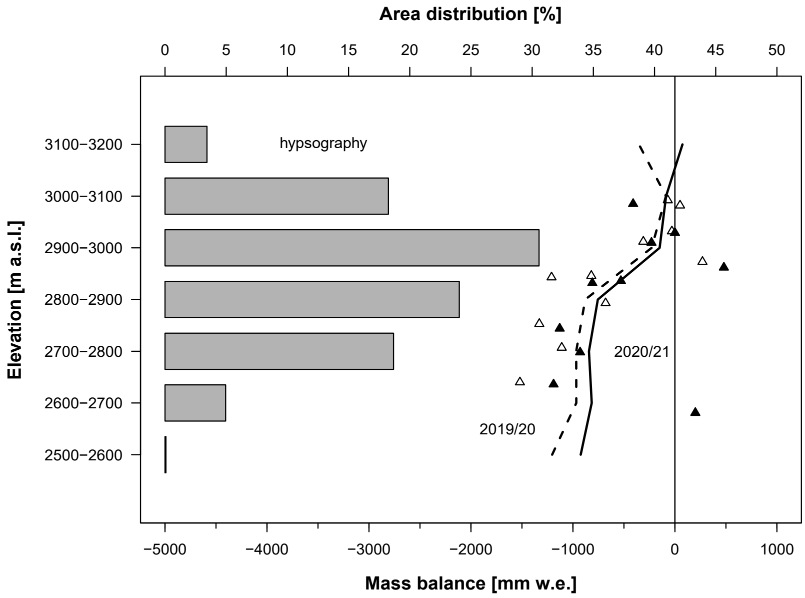

Figure 4.15.3 Glaciological balance versus geodetic balance for the whole observation period.

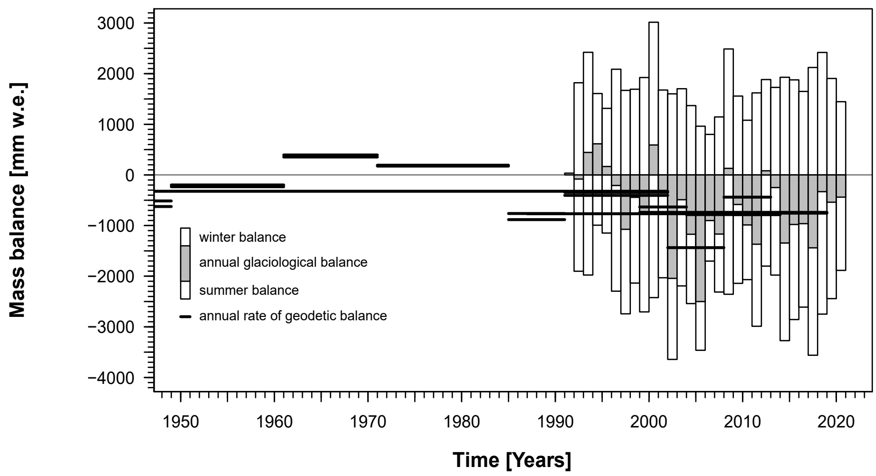

Figure 4.15.4 Accumulation area ratio (AAR) and equilibrium line altitude (ELA) versus specific mass balance for the whole observation period.

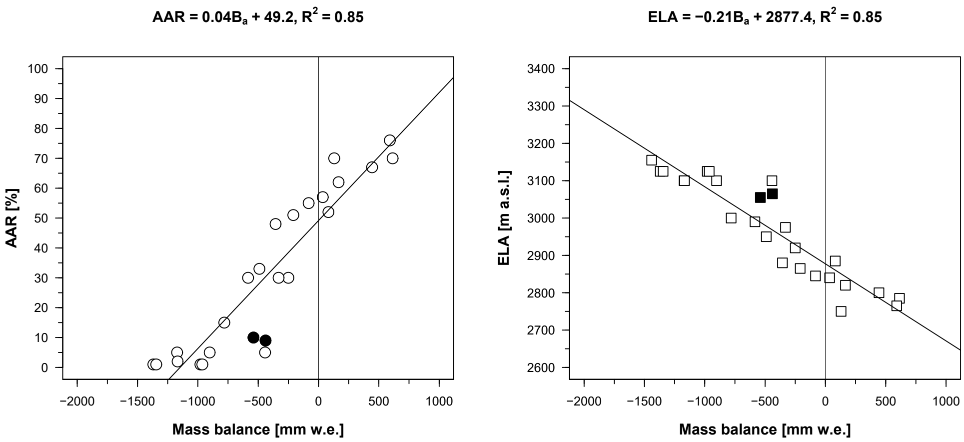

Basòdino (SWITZERLAND)

5 CONCLUDING REMARKS

Glacier monitoring has been coordinated internationally since 1894. This long-term effort has resulted in the compilation of an unprecedented dataset of changes in glacier length, area, volume, and mass. The dataset has been made freely available by the WGMS and its predecessor organizations and is widely used in scientific studies and assessment reports. The worldwide retreat of glaciers has become one of the most prominent icons of global climate change. Moreover, glacier decline has impacts on the local hazard situation, regional water availability, and global sea-level rise.

The retreat of glaciers from their Little Ice Age (LIA) moraines and trimlines can be observed in the field as well as on aerial and satellite images for tens of thousands of glaciers around the world. Large collections of historical and modern photographs (e.g., NSIDC, 2002, updated 2015) document this change in a qualitative manner. The dataset presented here allows these changes to be quantified at samples ranging from a few hundred to a few thousands of glaciers with data series from in situ and remotely sensed observations, respectively. There is a global trend to centennial glacier retreat from LIA maximum positions, with typical cumulative values of several hundred to a few thousand metres.

In various mountain ranges, glaciers with decadal response times have shown intermittent re-advances which, however, were short and thus much less extensive when compared to the overall frontal retreat. The most recent re-advance phases were reported from Scandinavia and New Zealand in the 1990s or from (mainly surge-type glaciers in) the Karakoram at the beginning of the 21st century. Early (geodetic) mass-balance measurements indicate moderate decadal ice losses of a few decimetre w.e. a^{-1} in the second half of the 19th and at the beginning of the 20th centuries, followed by increased ice losses around 0.4 m w.e. a^{-1} in the 1940s and 1950s. Larger data samples (from both glaciological and geodetic methods) with better global coverage adequately document the period of moderate ice loss which followed between the mid-1960s and mid-1980s, as well as the subsequent acceleration in ice loss to > 0.5 m w.e. a^{-1} in the early 21st century. Spaceborne geodetic observations with global coverage for the period from 2000 to 2020 indicate a negative bias of the glaciological sample of a few decimetre, which might apply for earlier periods too.

In the time period covered by the present bulletin, glaciers observed by the glaciological method lost about 0.75 m w.e. a^{-1}. This continues the historically unprecedented ice loss observed since the turn of the century and is amounting to double the ice loss rates of the 1990s. Recent global assessments estimate and correct for the bias in the glaciological sample (Zemp et al., 2020) and suggest that glaciers are currently contributing more than 1 mm to mean global sea-level rise, which corresponds to more than a quarter of the observed rise.

With their dynamic response to changes in climatic conditions – growth/reduction in area mainly through the advance/retreat of glacier tongues – glaciers re-adjust their extent to equilibrium conditions of ice geometry with a zero mass balance. Recorded mass balances document the degree of imbalance between glaciers and climate due to the delay in dynamic response caused by the characteristics of ice flow (deformation and sliding); over lengthy time intervals they depend on the rate of climatic forcing. With constant climatic conditions (no forcing), balances would tend towards and finally become zero. Long-term non-zero balances are, therefore, an expression of ongoing climate change and sustained forcing. Trends towards increasing nonzero balances are triggered by accelerated forcing. In the same way, comparison between present-day and past values of mass balance must take the changes in glacier area into account (Elsberg et al., 2001). Many of the relatively small glaciers, measured within the framework of the present mass balance observation network, have lost large percentages of their area during the past decades. The recent increase in the rates of ice loss over diminishing glacier surface areas, as compared with earlier losses related to larger surface areas, becomes even more pronounced and leaves no doubt about the accelerating change in climatic conditions, even if a part of the observed acceleration trend is likely to be caused by positive feedback processes.

Rising snowlines and cumulative mass losses lead to changes in the average albedo and to a continued surface lowering. Such effects cause pronounced positive feedbacks with respect to radiative and sensible heat fluxes. Albedo changes are especially effective in enhancing melt rates and can also be caused by the input of dust (Oerlemans et al., 2009). The cumulative length change of glaciers is the result of all effects combined, and constitutes the key to a global intercomparison of decadal with secular mass losses. Surface lowering, thickness loss and the resulting reduction in driving stress and flow, however, increasingly replace processes of tongue retreat with processes of downwasting, disintegration or even the collapse of entire glaciers. Moreover, the thickness of most glaciers regularly observed for their mass balance is measured in (a few) tens of metres (Gärtner-Roer et al. 2014, Welty et al. 2020). From the measured mass losses and thickness reductions, it is evident that several network glaciers with important long-term observations may not survive for many more decades. A special challenge therefore consists in developing a strategy for ensuring the continuity of adequate mass-balance observations under such extreme conditions.

Key tasks for the future of glacier mass-balance monitoring include the continuation of (long-term) measurement series, the extension of the presently available dataset, especially in under-represented regions (Nussbaumer et al., 2017; Hoelzle et al., 2017; Gärtner-Roer et al., 2019), the quantitative assessment of uncertainties relating to available measurements (e.g., Magnússon et al., 2016), and their representativeness for changes in corresponding mountain ranges. The latter requires a well-considered integration of in-situ measurements, remotely sensed observations (e.g., Gardner et al., 2013; Wouters et al., 2019, Hugonnet et al. 2021), and numerical modelling (e.g., Huss & Hock, 2018; Hock et al., 2019; Rounce et al. 2023) taking into account the related spatial and temporal scales.

6 ACKNOWLEDGEMENTS AND REFERENCES

We thank our National Correspondents (cf. Chapter 9) for coordinating the annual calls-for-data and the numerous Principal Investigators, as well as their sponsoring agencies (cf. Chapters 7 and 8) from around the world for their long-term collaboration and willingness to share glacier observations.

Special thanks are extended to Dilara Kim for assistance with editing the maps, and to Susan Braun-Clarke for carefully editing the English. We thank Isabelle Wüest, Frank Hitzemann, Lukas Japp, and Ruth Hunkeler-Wittleder for their support with administrative matters.

We thank Martin Hoelzle (University of Fribourg) and Frank Paul (University of Zurich) as well as the members of the GTN-G Advisory Board chaired by IUGG/IACS for constructive discussions and valuable feedback on WGMS matters. Gwenn Flowers (CA), Fanny Brun (FR), Stephen Briggs (IT), Alex Gardner (US), Ben Marzeion (DE), and Pierre Pitte (AR). Gwenn Flowers, Lauren Vargo, Liss Andreassen, and Regine Hock (IUGG/IACS), Pascal Peduzzi (UNEP), Anil Mishra (UNESCO), and Anthony Rea (GCOS) assisted in ensuring proper international administration and coordination. Continued data stewardship was supported by ISC/WDS.

Funding is mainly through the Swiss GCOS Office at the Federal Office of Meteorology and Climatology MeteoSwiss and the Department of Geography of the University of Zurich, Switzerland, with contributions from the Cryospheric Commission of the Swiss Academy of Sciences for the production of the present bulletin.

REFERENCES

Aðalgeirsdóttir, G., Magnússon, E., Pálsson, F., Thorsteinsson, T., Belart, J., Jóhannesson, T., Hannesdóttir, H., Sigurðsson, O., Gunnarsson, A., Einarsson, B., Berthier, E., Steffensen Schmidt, L., Haraldsson, H.H. & H. Björnsson (2020): Glacier Changes in Iceland From ~ 1890 to 2019. Frontiers in Earth Science, 8, 520. https://doi.org/10.3389/feart.2020.523646

Ageta,Y. & K. Fujita (1996): Characteristics of mass balance of summer-accumulation type glaciers in the Himalayas and Tibetan Plateau. Zeitschrift für Gletscherkunde und Glazialgeologie, 32, Part 2: 61–65.

Allison, I., Fierz, C., Hock, R., Mackintosh, A., Kaser, G. & S.U. Nussbaumer (2019): IACS: past, present, and future of the International Association of Cryospheric Sciences. History of Geo- and Space Sciences, 10 (1): 97–107.

Andreassen, L.M., Elvehøy, H., Kjøllmoen, B. & R. V. Engeset (2016): Reanalysis of long-term series of glaciological and geodetic mass balance for 10 Norwegian glaciers. The Cryosphere, 10 (2): 535–552.

Andreassen, L.M., Elvehøy, H.,Kjøllmoen, B. & J.M.C. Belart (2020): Glacier change in Norway since the 1960s – an overview of mass balance, area, length and surface elevation changes. Journal of Glaciology 66 (256): 313–328.

Azam, M.F., Wagnon, P., Berthier, E., Vincent, C., Fujita, K., & J.S. Kargel (2018): Review of the status and mass changes of Himalayan-Karakoram glaciers. Journal of Glaciology, 64(243), 61-74.

Barandun, M., Huss, M., Sold, L., Farinotti, D., Azisov, E., Salzmann, N.,Usuabliev, R., Merkushkin, A. & M. Hoelzle (2015): Re-analysis of seasonal mass balance at Abramov glacier 1968-2014. Journal of Glaciology, 61(230), 1103-1117. https://doi.org/10.3189/2015JoG14J239

Barandun, M., Fiddes, J., Scherler, M., Mathys, T., Saks, T., Petrakov, D., & M. Hoelzle (2020): The state and future of the cryosphere in Central Asia. Water Security, 11, 100072

Barandun, M., Pohl, E., Naegeli, K., McNabb, R., Huss, M., Berthier, E., Saks, T. & M. Hoelzle (2021): Hot spots of glacier mass balance variability in Central Asia. Geophysical Research Letters, e2020GL092084. https://doi.org/10.1029/2020GL092084

Barcaza, G., Nussbaumer, S.U., Tapia, G., Valdés, J., García, J.-L., Videla, Y., Albornoz, A. & V. Arias (2017): Glacier inventory and recent glacier variations in the Andes of Chile, South America. Ann. Glaciol.: 1–15.

Bauder, A., Funk, M. & M. Huss (2007): Ice volume changes of selected glaciers in the Swiss Alps since the end of the 19th century. Annals of Glaciology, 46: 145–150.

Belart J.M.C., Magnússon E., Berthier E., Gunnlaugsson Á.Þ., Pálsson F., Aðalgeirsdóttir G., Jóhannesson T., Thorsteinsson T. H. Björnsson (2020): Mass Balance of 14 Icelandic Glaciers, 1945–2017: Spatial Variations and Links With Climate. Front. Earth Sci. 8:163. doi: 10.3389/feart.2020.00163

Berthier, E., Larsen, C., Durkin, W.J., Willis, M.J., & M.E.Pritchard (2018): Brief communication: Unabated wastage of the Juneau and Stikine icefields (southeast Alaska) in the early 21st century. The Cryosphere, 12(4), 1523-1530.

Bjørk, A.A., Kjær, K.H., Korsgaard, N.J., Khan, S.A., Kjeldsen, K.K., Andresen, C.S. & S. Funder (2012): An aerial view of 80 years of climate-related glacier fluctuations in southeast Greenland. Nature Geoscience, 5 (6): 427–432.
Björnsson, H. (1988): Hydrology of ice caps in volcanic regions. Societas Scientarium Islandica, Vol. 45, 139 pp. Reykjavík, Iceland.
Björnsson, H., Pálsson, F., Gudmundsson, S., Magnússon, E., Adalgeirsdóttir, G., Jóhannesson, T., Berthier, E., Sigurdsson, O. & Th. Thorsteinsson (2013): Contribution of Icelandic ice caps to sea level rise: trends and variability since the Little Ice Age. Geophysical Research Letters, 40 (8): 1546–1550.
Bolch, T., Pieczonka, T. & D.I. Benn (2011): Multi-decadal mass loss of glaciers in the Everest area (Nepal Himalaya) derived from stereo imagery. The Cryosphere, 5 (2): 349–358.
Bolch, T., Sandberg Sørensen, L., Simonsen, S.B., Mölg, N., Machguth, H., Rastner, P. & F. Paul (2013): Mass loss of Greenland‘s glaciers and ice caps 2003–2008 revealed from ICESat laser altimetry data. Geophysical Research Letters, 40 (5): 875–881.
Braun, M.H., Malz, P., Sommer, C., Farías-Barahona, D., Sauter, T., Casassa, G., Soruco, A., Skvarca, P. & T.C. Seehaus (2019): Constraining glacier elevation and mass changes in South America. Nat. Clim. Change, 9: 130–136.
Brun, F., Dumont, M., Wagnon, P., Berthier, E., Azam, M.F., Shea, J.M., Sirguey, P., Rabatel, A. & Al. Ramanathan (2015): Seasonal changes in surface albedo of Himalayan glaciers from MODIS data and links with the annual mass balance. The Cryosphere 9: 341-355. https://doi.org/10.5194/tc-9-341-2015
Brun, F., Berthier, E., Wagnon, P., Kääb, A. & D. Treichler (2017): A spatially resolved estimate of High Mountain Asia glacier mass balances from 2000 to 2016. Nature Geoscience, 10: 668–673.
Burgess, D. & B. Danielson (2022): Meighen Ice Cap: Changes in geometry, mass, and climatic response since 1959. Canadian Journal of Earth Sciences. doi: 10.1139/cjes-2021-0126.
Carr, J.R., Stokes, C. & A. Vieli (2014): Recent retreat of major outlet glaciers on Novaya Zemlya, Russian Arctic, influenced by fjord geometry and sea-ice conditions. Journal of Glaciology, 60 (219): 155–170.
Carrivick, J.L., James, W.H.M., Grimes, M., Sutherland J.L. & A.M. Lorrey (2020): Ice thickness and volume changes across the Southern Alps, New Zealand, from the little ice age to present. Sci Rep 10, 13392. https://doi.org/10.1038/s41598-020-70276-8
Carturan, L., Baroni, C., Becker, M., Bellin, A., Cainelli, O., Carton, A., Casarotto, C., Dalla Fontana, G., Godio, A., Martinelli, T., Salvatore, M.C. & R. Seppi (2013): Decay of a long-term monitored glacier: Careser Glacier (Ortles-Cevedale, European Alps). The Cryosphere 7: 1819-1838. https://doi.org/10.5194/tc-7-1819-2013
Chinn, T.J. (1985): Structure and equilibrium of the dry valley glaciers. New Zealand Antarctica Records, 6: 73–88.
Chinn, T.J. (2001): Distribution of the glacial water resources of New Zealand. Journal of Hydrology New Zealand, 40 (2): 139–187.
Chinn, T.J., Heydenrych, C. & M.J. Salinger (2005): Use of the ELA as a practical method of monitoring glacier response to climate in New Zealand‘s Southern Alps. Journal of Glaciology, 51 (172): 85–95.
Citterio, M., Mottram, R., Larsen, S.H. & A. Ahlstrøm (2009): Glaciological investigations at the Malmbjerg mining prospect, central East Greenland. Geological Survey of Denmark and Greenland Bulletin, 17.
Clapperton, C.M., Sugden, D.E., Birnie, J. & M.J. Wilson (1989a): Late-glacial and Holocene glacier fluctuations and environmental change on South Georgia, Southern Ocean. Quaternary Research, 31 (2): 210–228.
Clapperton, C.M., Sugden, D.E. & M. Pelto (1989b): The relationship of land terminating and fjord glaciers to Holocene climatic change, South Georgia, Antarctica. In: Oerlemans, J. (ed.): Glacier fluctuations and climatic change. Dordrecht, Kluwer Academic Publishers, 57–75.
Cogley, J.G. (2009): Geodetic and direct mass-balance measurements: comparison and joint analysis. Annals of Glaciology 50 (50): 96-100.
Cogley, J.G. & W.P. Adams (1998): Mass balance of glaciers other than the ice sheets. Journal of Glaciology, 44 (147): 315–325.
Cogley, J.G., Hock, R., Rasmussen, L.A., Arendt, A.A., Bauder, A., Braithwaite, R.J., Jansson, P., Kaser, G., Möller, M., Nicholson, L. & M. Zemp (2011): Glossary of glacier mass balance and related terms. IHP-VII Technical Documents in Hydrology No. 86, IACS Contribution No. 2, UNESCO-IHP, Paris, 114 pp.
Cook, A.J., Fox, A.J., Vaughan, D.G. & J.G. Ferrigno (2005): Retreating glacier fronts on the Antarctic Peninsula over the past half-century. Science, 308 (5721): 541–544.
Copernicus Climate Change Service (C3S), 2023: European State of the Climate 2022, Full report: climate.copernicus.eu/ESOTC/2022
Davaze, L., Rabatel, A., Dufour, A., Hugonnet, R., & Y. Arnaud (2020): Region-wide annual glacier surface mass balance for the European Alps from 2000 to 2016. Frontiers in Earth Science, 8. https://doi.org/10.3389/feart.2020.00149
Dehecq, A., Gourmelen, N., Gardner, A.S., Brun, F., Goldberg, D., Nienow, P.W., Berthier, E., Vincent, C., Wagnon, P. & E. Trouvé (2019): Twenty-first century glacier slowdown driven by mass loss in High Mountain Asia. Nature Geoscience 12, 22–27. https://doi.org/10.1038/s41561-018-0271-9
Denzinger, F., Machguth, H., Barandun, M., Berthier, E., Girod, L, Kronenberg, M, Usubaliev, R. & M. Hoelzle (2021): Geodetic mass balance of Abramov Glacier from 1975 to 2015. Journal of Glaciology 67: 331-341. https://doi.org/10.1017/jog.2020.108
Dorigo, W. et al. (2021): The International Soil Moisture Network: serving Earth system science for over a decade. Hydrology and Earth System Science 25: 5749-5804.https://doi.org/10.5194/hess-25-5749-2021
Dussaillant, I., Berthier, E., Brun, F., Masiokas, M.H., Hugonnet, R., Rabatel, A., Pitte, P. & L. Ruiz (2019): Two decades of glacier mass loss along the Andes. Nature Geoscience, 12: 802–808.
Dussaillant, I., Bannwart, J., Paul, F., Zemp, M. (2023): Glacier mass change global gridded data from 1976 to present derived from the Fluctuations of Glaciers Database. World Glacier Monitoring Service. Copernicus Climate Change Service (C3S) Climate Data Store (CDS).
Dyurgerov, M.D. & M.F. Meier (2005): Glaciers and the changing earth system: A 2004 snapshot. Occasional paper 58. Institute of Arctic and Alpine Research, University of Colorado, Boulder.
Elsberg, D.H., Harrison, W.D., Echelmeyer, K.A. & R.M. Krimmel (2001): Quantifying the effects of climate and surface change on glacier mass balance. Journal of Glaciology, 47: 649–658.
Espizua, L.E. & G.I. Maldonado (2007): Glacier variations in the Central Andes (Mendoza province, Argentina), from 1896 to 2005. In Environmental change and rational water use. pp 353-366. Olga E. Scarpati and J.A.A. Jones, Eds.

Espizua, L.E. & P. Pitte (2009): The Little Ice Age Glacier advance in the Central Andes (35ºS), Argentina. Palaeogeography, Palaeoclimatology, Palaeogeography. 281 (3): 345-350. Elsevier, DOI: 10.1016/j.palaeo.2008.10.032.

Falaschi, D., Bolch, T., Lenzano, M.G., Tadono, T., Lo Vecchio, A. & L. Lenzano (2018): New evidence of glacier surges in the Central Andes of Argentina and Chile. Prog. Phys. Geogr. Earth Environ., 030913331880301.

Falaschi D., Lenzano M.G., Villalba R., Bolch T., Rivera A. & A. Lo Vecchio (2019): Six Decades (1958–2018) of Geodetic Glacier Mass Balance in Monte San Lorenzo, Patagonian Andes. Front. Earth Sci. 7:326. doi: 10.3389/feart.2019.00326

Farías-Barahona, D., Sommer, C., Sauter, T., Bannister, D., Seehaus, T.C., Malz, P., Casassa, G., Mayewski, P.A., Turton, J.V., & M.H. Braun (2020): Detailed quantification of glacier elevation and mass changes in South Georgia. Environmental Research Letters, 15(3), 034036. https://doi.org/10.1088/1748-9326/ab6b32

Farinotti, D., Longuevergne, L., Moholdt, G., Duethmann, D., Mölg, T., Bolch, T., Vorogushyn, S. & A. Güntner (2015): Substantial glacier mass loss in the Tien Shan over the past 50 years. Nature Geoscience, 8 (9): 716–722.

Ferri L., Dussaillant I., Zalazar L., Masiokas M.H., Ruiz L., Pitte P., Gargantini H., Castro M., Berthier E. & R. Villalba (2020): Ice Mass Loss in the Central Andes of Argentina Between 2000 and 2018 Derived From a New Glacier Inventory and Satellite Stereo-Imagery. Front. Earth Sci. 8:530997. doi: 10.3389/feart.2020.530997

Fischer, M., Huss, M. & M. Hoelzle (2015): Surface elevation and mass changes of all Swiss glaciers 1980–2010, The Cryosphere, 9 (2): 525–540.

Fischer, A., K. Helfricht, H. Wiesenegger, L. Hartl, B. Seiser & M. Stocker-Waldhuber (2016a): Chapter 9 - What Future for Mountain Glaciers? Insights and Implications From Long-Term Monitoring in the Austrian Alps, In: Gregory B. Greenwood and J.F. Shroder, Editor(s), Developments in Earth Surface Processes, Elsevier, 21, 325-382. http://dx.doi.org/10.1016/B978-0-444-63787-1.00009-3.

Fischer, A., Hartl, L., Markl, G. & M. Kuhn (2016b): Glacier mass balances and elevation zones of Jamtalferner, Silvretta, Austria, 1988/1989 et seq. Institut für Interdisziplinäre Gebirgsforschung der Österreichischen Akademie der Wissenschaften, Innsbruck, PANGAEA, https://doi.org/10.1594/PANGAEA.818772

Fischer, A., G. Patzelt, M. Achrainer, G. Groß, G. K. Lieb, A. Kellerer-Pirklbauer & G. Bendler (2018): Gletscher im Wandel: 125 Jahre Gletschermessdienst des Alpenvereins. Springer Spektrum, 140 S. doi:10.1007/978-3-662-55540-8. http://www.springer.com/de/book/9783662555392.

Fischer, A., Fickert, T., Schwaizer, G. et al. (2019): Vegetation dynamics in Alpine glacier forelands tackled from space. Sci Rep 9, 13918, https://doi.org/10.1038/s41598-019-50273-2

Foresta, L., Gourmelen, N., Pálsson, F., Nienow, P., Björnsson, H. & A. Shepherd (2016): Surface elevation change and mass balance of Icelandic ice caps derived from swath mode CryoSat-2 altimetry. Geophysical Research Letters , 43, 23: 12,138–12,145.

Forel, F.A. (1895): Les variations périodiques des glaciers. Discours préliminaire. Extrait des Archives des Sciences physiques et naturelles, XXXIV: 209–229.

Fujita, K. & Y. Ageta (2000): Effect of summer accumulation on glacier mass balance on the Tibetan Plateau revealed by mass-balance model. Journal of Glaciology, 46 (153): 244–252.

Gardelle, J., Berthier, E. & Y. Arnaud (2013): Slight mass gain of Karakoram glaciers in the early twenty-first century. Nature Geoscience, 5 (5): 322–325.

Gardner, A.S., Moholdt, G., Cogley, J.G., Wouter, B., Arendt, A.A., Wahr, J., Berthier, E.,Hock, R., Pfeffer W.T., Kaser, G., Ligtenberg, S.R.M., Bolch, T., Sharp, M.J., Hagen, J.O., van den Broeke, M.R. & F. Paul (2013): A Reconciled Estimate of Glacier Contributions to Sea Level Rise: 2003 to 2009. Science 340 (6134): 852–857.

Gärtner-Roer, I., Naegeli, K., Huss, M., Knecht, T., Machguth, H. & M. Zemp (2014): A database of worldwide glacier thickness observations. Global and Planetary Change. DOI: 10.1016/j.gloplacha.2014.09.003

Gärtner-Roer, I., Nussbaumer, S.U., Hüsler, F. & M. Zemp (2019): Worldwide assessment of national glacier monitoring and future perspectives. Mountain Research and Development, 39 (2): A1–A11.

GCOS (2010): Implementation Plan for the Global Observing System for Climate in Support of the UNFCCC (2010 Update), 180 pp.

Geoestudios (2014): Estimación de volúmenes de hielo mediante sondajes de radar en zonas norte, central y sur. Technical Report, DGA S.I.T. No 338.

GLAMOS (2020): The Swiss Glaciers 2017/18 and 2018/19, Bauder, A., Huss, M. & A. Linsbauer (edd.), Glaciological Report No. 139/140 of the Cryospheric Commission (EKK) of the Swiss Academy of Sciences (SCNAT) published by VAW / ETH Zürich, doi: 10.18752/glrep_139-140.

Grab, M., Mattea, E., Bauder, B., Huss, M., Rabenstein, L., Hodel, E., Linsbauer, A., Hellmann, S., Church, G., Langhammer, L., Schmid, L., Deleze, K, Schaer, P., Lathion, P., Farinotti, D. & H. Maurer (2021): Ice thickness distribution of all Swiss glaciers based on extended ground-penetrating radar data and glaciological modeling. Journal of Glaciology 1–19. https://doi.org/10.1017/jog.2021.55

Grove, J.M. (2004): Little Ice Ages: ancient and modern. Vol. I + II, 2nd edition. Routledge, London and New York.

GTOS (2009): Assessment of the status of the development of the standards for the terrestrial Essential Climate Variables: T06 – Glaciers and Ice Caps. Zemp, M., I. Gärtner-Roer, W. Haeberli, M. Hoelzle, F. Paul, R. Armstrong, R. Barry, J. Cihlar, A. Kääb, J. Kargel, S. J. Khalsa, M. Monteduro, B. Raup, G. Seiz, and R. Sessa (eds.), Global Terrestrial Observing System, 61, 17 pp.

GTN-G (2017): GTN-G Glacier Regions. Global Terrestrial Network for Glaciers. Doi:10.5904/gtng-glacreg-2017-07

Gurney, S.D., Popovnin, V.V., Shahgedanova, M. & C.R. Stokes (2008): A glacier inventory for the Buordakh Massif, Cherskiy Range, Northeast Siberia, and evidence for recent glacier recession. Arctic, Antarctic and Alpine Research, 40 (1): 81–88.

Haeberli, W. (1998): Historical evolution and operational aspects of worldwide glacier monitoring. In: W. Haeberli, M. Hoelzle and S. Suter (eds.), Into the second century of world glacier monitoring: prospects and strategies. Studies and reports in hydrology. UNESCO, Paris, 35–51.

Haeberli, W., Cihlar, J. & R.G. Barry (2000): Glacier monitoring within the Global Climate Observing System. Annals of Glac., 31: 241–246.

Haeberli, W., Oerlemans, J., and M. Zemp (2019): The future of Alpine glaciers and beyond. In: Oxford Research Encyclopedia of Climate Science. Oxford University Press. http://dx.doi.org/10.1093/acrefore/9780190228620.013.769

Hagg, W., Braun, L., Uvarov, V.N. & K.G. Makarevich (2004): A comparison of three methods of mass-balance determination in the Tuyuksu glacier region, Tien Shan, Central Asia. Journal of Glaciology 50 (171): 505-510. https://doi.org/10.3189/172756504781829783

Hannesdóttir, H., Björnsson, H., Pálsson, F., Aðalgeirsdóttir, G. & S. Guðmundsson (2015): Variations of southeast vatnajökull ice cap (Iceland) 1650–1900 and reconstruction of the glacier surface geometry at the little ice age maximum. Geografiska Annaler: Series A, Physical Geography, 97, 2: 237–264.

Hannesdóttir H., Sigurðsson, O., Þrastarson, R.H., Guðmundsson, S., Belart, J.M.C., Pálsson, F., Magnússon, E., Víkingsson, S., Kaldal, I. & T. Jóhannesson (2020): A national glacier inventory and variations in glacier extent in Iceland from the Little Ice Age maximum to 2019. JÖKULL, 70, 1-34.

Hastenrath, S. (2001): Variations of East African climate during the past two centuries. Climatic Change, 50 (1–2): 209–217.

Hock, R., Marzeion, B., Bliss, A., Giesen, R., Hirabayashi, Y., Huss, M., Radic, V. & A. Slangen (2019): GlacierMIP - A model intercomparison of global-scale glacier mass-balance models and projections. Journal of Glaciology, 65 (251), 453-467, doi:10.1017/jog.2019.22.

Hoelzle, M. & M. Trindler (1998): Data management and application. In: W. Haeberli, M. Hoelzle and S. Suter (eds.), Into the second century of world glacier monitoring: prospects and strategies. Studies and reports in hydrology. UNESCO, Paris, 53–72.

Hoelzle, M., Azisov, E., Barandun, M., Huss, M., Farinotti, D., Gafurov, A., Hagg, W., Kenzhebaev, R., Kronenberg, M., Machguth, H., Merkushkin, A., Moldobekov, B., Petrov, M., Saks, T., Salzmann, N., Schöne, T., Tarasov, Y., Usubaliev, R., Vorogushyn, S., Yakovlev, A. & M. Zemp (2017): Re-establishing glacier monitoring in Kyrgyzstan and Uzbekistan, Central Asia. Geoscientific Instrumentation, Methods and Data Systems, 6 (2): 397–418.

Holmlund, P. & E.S. Holmlund (2018): Recent climate-induced shape changes of the ice summit of Kebnekaise, Northern Sweden. Geografiska Annaler: Series A, Physical Geography 101,1: 68-78. https://doi.org/10.1080/04353676.2018.1542130

Holzer, N., Vijay, S., Yao, T., Xu, B., Buchroithner, M. & T. Bolch (2015): Four decades of glacier variations at Muztagh Ata (eastern Pamir):a multi-sensor study including Hexagon KH-9 and Pléiades data. The Cryosphere, 9: 2071–2088.

Huber, J., McNabb, R. & M. Zemp (2020): Elevation changes of west-central Greenland glaciers from 1985 to 2012 from remote sensing. Frontiers in Earth Science 8 (35). doi: https://doi.org/10.3389/feart.2020.00035

Hugonnet, R., McNabb, R., Berthier, E., Menounos, B., Nuth, C., Girod, L., Farinotti, D., Huss, M., Dussaillant, I., Brun, F. & A. Kääb (2021): Accelerated global glacier mass loss in the early twenty-first century. Nature, 592(7856), 726-731. doi: 10.1038/s41586-021-03436-z

Huss, M. (2013): Density assumptions for converting geodetic glacier volume change to mass change. The Cryosphere, 7 (3): 877–887.

Huss, M. & R. Hock (2018): Global-scale hydrological response to future glacier mass loss. Nature Climate Change, 8: 135–140.

Huss, M., Dhulst, L. & A. Bauder (2015): New long-term mass-balance series for the Swiss Alps. Journal of Glaciology, 61 (227): 551–562.

IPCC, 2021: Climate Change 2021: The Physical Science Basis. Contribution of Working Group I to the Sixth Assessment Report of the Intergovernmental Panel on Climate Change [Masson-Delmotte, V., P. Zhai, A. Pirani, S.L. Connors, C. Péan, S. Berger, N. Caud, Y. Chen, L. Goldfarb, M.I. Gomis, M. Huang, K. Leitzell, E. Lonnoy, J.B.R. Matthews, T.K. Maycock, T. Waterfield, O. Yelekçi, R. Yu, and B. Zhou (eds.)]. Cambridge University Press, Cambridge, United Kingdom and New York, NY, USA.

Jakob, L., Gourmelen, N., Ewart, M. & S. Plummer (2020): Ice loss in High Mountain Asia and the Gulf of Alaska observed by CryoSat-2 swath altimetry between 2010 and 2019. The Cryosphere, Copernicus Publications. https://doi.org/10.5194/tc-2020-176

Jiao, J., Zhang, Y., Bilker-Koivula, M., Poutanen, M., Yin, P. & Y. Zhang (2020): Interannual glacier and lake mass changes over Scandinavia from GRACE. Geophysical Journal International 221,3: 2126–2141, https://doi.org/10.1093/gji/ggaa146

Jóhannesson T., Björnsson, H., Magnússon, E., Guðmundsson, S., Pálsson, F., Sigurðsson, O., Thorsteinsson, Th. & E. Berthier (2013): Ice-volume changes, bias estimation of mass-balance measurements and changes in subglacial lakes derived by lidar-mapping of the surface of Icelandic glaciers. Annals of Glaciology 2013, 54 (63), 63–74. doi:10.3189/2013AoG63A422

Jóhannesson, T., Pálmason, B., Hjartarson, Á, Jarosch, A., Magnússon, E., Belart, J., & M. Gudmundsson (2020): Non-surface mass balance of glaciers in Iceland. Journal of Glaciology, 66(258), 685-697. doi:10.1017/jog.2020.37

Kapitsa, V., Shahgedanova, M., Severskiy, I., Kasatkin, N., White, K. & Z. Usmanova (2020): Assessment of changes in mass balance of the Tuyuksu group of glaciers, Northern Tien Shan, between 1958 and 2016 using ground-based observations and Pléiades satellite imagery. Frontiers in Earth Sciences 8, https://doi.org/10.3389/feart.2020.00259

Kaser, G. & H. Osmaston (2002): Tropical glaciers. Cambridge University Press, Cambridge.

Kaser, G., Cogley, J.G., Dyurgerov, M.B., Meier, M.F. & A. Ohmura (2006): Mass balance of glaciers and ice caps: consensus estimates for 1961–2004. Geophysical Research Letters, 33(19), L19501, doi:10.1029/2006GL027511.

Kaufmann, D.S., Porter, S.C. & A.R. Gillespie (2004): Quaternary alpine glaciation in Alaska, the Pacific Northwest, Sierra Nevada, and Hawaii. In: Gillespie, A.R., Porter, S.C. & B.F. Atwater (eds.): The Quaternary period in the United States. Elsevier, Amsterdam.

Koblet, T., Gärtner-Roer, I., Zemp, M., Jansson, P., Thee, P., Haeberli, W. & P. Holmlund (2010): Reanalysis of multi-temporal aerial images of Storglaciären, Sweden (1959–99) – Part 1: Determination of length, area, and volume changes. The Cryosphere 4: 333–343, doi:10.5194/tc-4-333-2010

Kotlyakov, V.M. (2006): Glaciation in North and Central Eurasia at present time. Nauka, Moscow (in Russian with abstract in English), 1–481.

Kotlyakov, V.M., Grosswald, M.G., Dyurgerov, M.B. & V.L. Mazo (1991): The reaction of glaciers to impending climate change. Polar Geography and Ecology, 15 (3): 203–217.

Kuhn, M., Markl, G., Kaser, G., Nickus, U., Obleitner, F., & H. Schneider (1985): Fluctuations of climate and mass balance: Different responses of two adjacent glaciers. Zeitschrift für Gletscherkunde und Glazialgeologie, 21: 409–416.

Kuhn, M., Dreiseitl, E., Hofinger, S., Markl, G., Span, N. & G. Kaser (1999): Measurements and models of the mass balance of Hintereisferner. Geografiska Annaler, A81 (4): 659–670.

Kutuzov, S. (2005): The retreat of Tien Shan glaciers since the Little Ice Age obtained from the moraine positions, aerial photographs and satellite images. In: PAGES Second Open Science Meeting 10–12 August 2005, Beijing, China.

Kutuzov, S., Lavrentiev, I., Smirnov, A., Nosenko, G., & D. Petrakov (2019): Volume changes of Elbrus Glaciers from 1997 to 2017. Frontiers in Earth Science, 7, 153. https://doi.org/10.3389/feart.2019.00153

Larsen, C.F., Burgess, E., Arendt, A.A., O'Neel, S., Johnson, A.J. & C. Kienholz (2015): Surface melt dominates Alaska glacier mass balance. Geophysical Research Letters, 42 (14): 5902–5908.

Lieb, G.K. & A. Kellerer-Pirklbauer (2019): Sammelbericht über die Gletschermessungen des Österreichischen Alpenvereins im Jahre 2019. Bergauf 02/2019, 74 (144): 20–29.

Le Bris, R. & F. Paul (2015): Glacier-specific elevation changes in parts of western Alaska. Annals of Glaciology, 56 (70): 184–192.

Letreguilly, A. & L. Reynaud (1990): Space and time distribution of glacier mass-malance in the Northern Hemisphere. Arctic and Alpine Research, 22 (1): 43–50.

Lopez, P., Chevallier, P., Favier, V., Pouyaud, B., Ordenes, F. & J. Oerlemans (2010): A regional view of fluctuations in glacier length in southern South America. Glob. Planet. Change, 71 (1–2): 85–108.

Machguth, H., Thomsen, H.H., Weidick, A., Abermann, J., Ahlstrøm, A.P., Andersen, M.L., Andersen, S.B., Bjørk, A.A., Box, J.E., Braithwaite, R.J., Bøggild, C.E., Citterio, M., Clement, P., Colgan, W., Fausto, R.S., Gleie, K., Hasholt, B., Hynek, B., Knudsen, N.T., Larsen, S.H., Mernild, S., Oerlemans, J., Oerter, H., Olesen, O.B., Smeets, C.J.P.P., Steffen, K., Stober, M., Sugiyama, S., van As, D., van den Broeke, M.R & R.S. van de Wal (2016): Greenland surface mass balance observations from the ice sheet ablation area and local glaciers. Journal of Glaciology, 62 (235): 861–887.

Mackintosh, A.N., Anderson, B.M., Lorrey, A.M., Renwick, J.A., Frei, P. & S.M. Dean (2017): Regional cooling caused recent New Zealand glacier advances in a period of global warming. Nature Communications, 8, 14202, doi:10.1038/ncomms14202.

Magnússon, E., Muñoz-Cobo Belart, J., Pálsson, F., Ágústsson, H. & P. Crochet (2016): Geodetic mass balance record with rigorous uncertainty estimates deduced from aerial photographs and lidar data – case study from Drangajökull ice cap, NW Iceland. The Cryosphere, 10 (1): 159–177.

Malz, P., Meier, W., Casassa, G., Jaña, R., Skvarca, P. & M. Braun (2018): Elevation and mass changes of the Southern Patagonia Icefield derived from TanDEM-X and SRTM data. Remote Sens. 10 (2): 188.

Masiokas, M.H., Rivera, A., Espizua, L.E., Villalba, R., Delgado, S. & J.C. Aravena (2009): Glacier fluctuations in extratropical South America during the past 1000 years. Palaeogeography, Palaeoclimatology, Palaeoecology, 281 (3–4): 242–268.

McNabb, R.W. & R. Hock (2014): Alaska tidewater glacier terminus positions, 1948–2012. Journal of Geophysical Research: Earth Surface, 119 (2): 153–167.

McNeil, C., O'Neel, S., Loso, M., Pelto, M., Sass, L., Baker, E. H., & S. Campbell (2020): Explaining mass balance and retreat dichotomies at Taku and Lemon Creek Glaciers, Alaska. Journal of Glaciology, 66(258), 530-542.

Meier, W.J.-H., Grießinger, J., Hochreuther, P. & M.H. Braun (2018): An updated multi-temporal glacier inventory for the Patagonian Andes with changes between the Little Ice Age and 2016. Front. Earth Sci. 6.

Melkonian, A.K., Willis, M.J., Pritchard, M.E. & A.J. Stewart (2016): Recent changes in glacier velocities and thinning at Novaya Zemlya. Remote Sensing of Environment, 174: 244–257.

Menounos, B., Hugonnet, R., Shean, D., Gardner, A., Howat, I., Berthier, E., Pelto, B., Tennant, C., Shea, J., Myoung-Jong, N., Brun, F. & A. Dehecq (2019): Heterogeneous changes in western North American glaciers linked to decadal variability in zonal wind strength. Geophysical Research Letters, 46(1), 200-209. https://doi.org/10.1029/2018GL080942

Mercanton, P.-L. (1916): Vermessungen am Rhonegletscher 1874–1915. Neue Denkschriften der Schweizerischen Naturforschenden Gesellschaft (SNG), Band 52. Kommissions-Verlag von Georg & Co., Basel, 190 pp.

Mernild, S.H., Lipscomb, W.H., Bahr, D.B., Radić, V. & M. Zemp (2013): Global glacier changes: a revised assessment of committed mass losses and sampling uncertainties. The Cryosphere, 7 (5): 1565–1577.

Milana, J.P. & A. Maturano (1999): Application of radio echo sounding at the arid Andes of Argentina: the Agua Negra Glacier. Global and Planetary Change 22: 179-191.

Molnia, B.F. (2007): Late nineteenth to early twenty-first century behaviour of Alaskan glaciers as indicators of changing regional climate. Global and Planetary Change, 56 (1–2): 23–56.

Morris, A., Moholdt, G., & L. Gray (2020): Spread of Svalbard Glacier Mass Loss to Barents Sea Margins Revealed by CryoSat-2. Journal of Geophysical Research: Earth Surface, 125(8), e2019JF005357. https://doi.org/10.1029/2019JF005357

Nesje, A., Bakke, J., Dahl, S.O., Lie, O. & J.A. Matthews (2008): Norwegian mountain glaciers in the past, present and future. Global and Planetary Change, 60 (1–2): 10–27.

Noël, B., van de Berg, W.J., Lhermitte, S., Wouters, B., Schaffer, N., & M.R. van den Broeke (2018): Six decades of glacial mass loss in the Canadian Arctic Archipelago. Journal of Geophysical Research: Earth Surface, 123(6), 1430-1449.

Nussbaumer, S.U., Hoelzle, M., Hüsler, F., Huggel, C., Salzmann, N., & M. Zemp (2017): Glacier monitoring and capacity building: important ingredients for sustainable mountain development. Mountain Research and Development, 37 (1): 141–152.

NSIDC (2002, updated 2015): Glacier Photograph Collection. U.S. National Snow and Ice Data Center, Boulder, Colorado, USA. Digital media. Online available from: http://nsidc.org/data/glacier_photo/

NVE (2019): Glaciological investigations in Norway 2018. B. Kjøllmoen, L.M. Andreassen, H. Elvehøy & M. Jackson (eds.), NVE Rapport 46-2019, 84 pp +app.

Oerlemans, J. (2011): Minimal Glacier Models. Second edition. Igitur, Utrecht University: 103 pp.

Oerlemans, J., Giesen, R.H. & M.R. van den Broeke (2009): Retreating alpine glaciers: increased melt rates due to accumulation of dust (Vadret da Morteratsch, Switzerland). Journal of Glaciology 55 (192): 729–736.

O'Neel, S., McNeil, C., Sass, L., Florentine, C., Baker, E., Peitzsch, E., McGrath, D., Fountain, A. & D. Fagre (2019): Reanalysis of the US Geological Survey Benchmark Glaciers: Long-term insight into climate forcing of glacier mass balance. J. of Glac., 65 (253): 850–866.

Østrem, G. & M. Brugman (1991): Glacier mass-balance measurements: a manual for field and office work. National Hydrology Research Institute, NHRI Science Report No. 4.

Pelto, M.S. (2018): How unusual was 2015 in the 1984-2015 period of the North Cascade glacier annual mass balance? Water 10, 543.

Pelto, M.S. & C. Brown (2012): Mass balance loss of Mount Baker, Washington glaciers 1990–2010. Hydrological Processes, 26 (17): 2601–2607.

Pieczonka, T. & T. Bolch (2015): Region-wide glacier mass budgets and area changes for the Central Tien Shan between ~1975 and 1999 using Hexagon KH-9 imagery. Global and Planetary Change, 128: 1–13.

Pitte, P., Berthier, E., Masiokas, M.H., Cabot, V., Ruiz, L., Ferri Hidalgo, L., Gargantini, H. & L. Zalazar (2016): Geometric evolution of the Horcones Inferior Glacier (Mount Aconcagua, Central Andes) during the 2002-2006 surge: Horcones Inferior Glacier Surge. J. Geophys. Res. Earth Surf. 121 (1): 111–127.

Pope E.L., Willis, I.C., Pope, A., Miles, E.S., Arnold, N.S. & W.G. Rees (2016): Contrasting snow and ice albedos derived from MODIS, Landsat ETM+ and airborne data from Langjökull, Iceland. Remote Sensing of Environment, 175: 183–195.

Prinz, R., Fischer, A., Nicholson, L. & G. Kaser (2011): Seventy-six years of mean mass balance rates derived from recent and re-evaluated ice volume measurements on tropical Lewis Glacier, Mount Kenya. Geophysical Research Letters, 38 (20), L20502, doi:10.1029/2011GL049208.
PSFG (1967): Fluctuations of Glaciers 1959–1965 (Vol. I). P. Kasser (ed.), IASH (ICSI) / UNESCO, Permanent Service on Fluctuations on Glaciers, Zurich, Switzerland, 52 pp.
Rabatel, A., Francou, B., Soruco, A., Gomez, J., Cáceres, B., Ceballos, J. L., Basantes, R., Vuille, M., Sicart, J.-E., Huggel, C., Scheel, M., Lejeune, Y., Arnaud, Y., Collet, M., Condom, T., Consoli, G., Favier, V., Jomelli, V., Galarraga, R., Ginot, P., Maisincho, L., Mendoza, J., Ménégoz, M., Ramirez, E., Ribstein, P., Suarez, W., Villacis, M. & P. Wagnon (2013): Current state of glaciers in the tropical Andes: a multi-century perspective on glacier evolution and climate change. The Cryosphere, 7 (1): 81–102.
Rankl M., Kienholz C. & M. Braun (2014): Glacier changes in the Karakoram region mapped by multimission satellite imagery. The Cryosphere, 8 (3): 977–989.
Rastner, P., Bolch, T., Mölg, N., Machguth, H., Le Bris, R. & F. Paul (2012): The first complete inventory of the local glaciers and ice caps on Greenland. The Cryosphere, 6 (6): 1483–1495.
Rets, E.P., Popovnin, V.V., Toropov, P.A., Smirnov, A.M., Tokarev, I.V., Chizhova, J.N., Budantseva, N.A., Vasil'chuk, Y.K., Kireeva, M.B., Ekaykin, A.A., Veres, A.N., Aleynikov, A.A., Frolova, N.L., Tsyplenkov, A.S., Poliukhov, A.A., Chalov, S.R., Aleshina, M.A., and E.D. Kornilova (2019): Djankuat glacier station in the North Caucasus, Russia: a database of glaciological, hydrological, and meteorological observations and stable isotope sampling results during 2007–2017, Earth Syst. Sci. Data, 11, 1463–1481, https://doi.org/10.5194/essd-11-1463-2019.
RGI Consortium (2017): Randolph Glacier Inventory (RGI) – a dataset of global glacier outlines: Version 6.0. Technical Report, Global Land Ice Measurements from Space, Boulder, Colorado, USA. Digital Media. Doi:10.7265/N5-RGI-60.
Rignot, E., Rivera, A. & G. Cassasa (2003): Contribution of the Patagonia Icefields to sealevel rise. Science, 302: 434–437.
Roberts, S.J., Hodgson, D.A., Shelley, S., Royles, J., Griffiths, H.J., Deen, T.J. & M.A. Thorne (2010): Establishing lichenometric ages for nineteenth and twentieth century glacier fluctuations on South Georgia (South Atlantic). Geografiska Annaler: Series A, Physical Geography, 92 (1): 125–139.
Rounce, D.R., Hock, R., Maussion, F., Hugonnet, R., Kochtitzky, W., Huss, M., Berthier, E., Brinkerhoff, D., Compagno, L., Copland, L., Farinotti, D., Menounos, B. & R.W. McNabb (2023): Global glacier change in the 21st century: Every increase in temperature matters. Science379,78-83(2023).DOI:10.1126/science.abo1324
Salinger, M.J., Fitzharris, B.B., & T. Chinn (2021): Extending End-of-Summer-Snowlines for the Southern Alps Glaciers of New Zealand back to 1949. International Journal of Climatology. https://doi.org/10.1002/joc.7177
Schöner, W., Hynek, B., Böhm, R., Binder, D., Koboltschnig, G. & H. Holzmann (2009): Glazialhydrologisches Monitoring im Bereich des Rauriser Sonnblicks (Hohe Tauern, Österreich), Österr Wasser- und Abfallw, 61, 1–8, https://doi.org/10.1007/s00506-008-0059-z.
Schöner, W., R. Böhm, I. Auer & M. Staudinger (1999): Gletschermonitoring im Sonnblickgebiet. In: Österr. Beiträge zu Meteorologie und Geophysik, Heft 21, Zentralanstalt für Meteorologie und Geophysik.
Schuler T.V., Kohler J., Elagina N., Hagen J.O.M., Hodson A.J., Jania J.A., Kääb A.M., Luks B., Małecki J., Moholdt G., Pohjola V.A., Sobota I. & W.J.J. Van Pelt (2020): Reconciling Svalbard Glacier Mass Balance. Front. Earth Sci. 8:156. doi: 10.3389/feart.2020.00156
Seehaus, T., Malz, P., Sommer, C., Lippl, S. Cochachin, A. & M. Braun (2019): Changes of the tropical glaciers throughout Peru between 2000 and 2016 - mass balance and area fluctuations. The Cryosphere, 13, 2537-2556, https://doi.org/10.5194/tc-13-2537-2019
Shea, J.M., Menounos, B., Moore, R.D. & C. Tennant (2013): An approach to derive regional snow lines and glacier mass change from MODIS imagery, western North America. The Cryosphere, 7 (2): 667–680.
Shean, D.E., Bhushan, S., Montesano, P., Rounce, D.R., Arendt, A., & B. Osmanoglu (2020): A systematic, regional assessment of high mountain Asia glacier mass balance. Frontiers in Earth Science, 7, 363. https://doi.org/10.3389/feart.2019.00363
Sicart, J.E., Villacís, M., Condom, T. & A. Rabatel (2015): GREAT ICE monitors glaciers in the tropical Andes, Eos, Volume 96. https://doi.org/10.1029/2015EO037993
Sigurðsson, O. (2005): Variations of termini of glaciers in Iceland in recent centuries and their connection with climate. In: Caseldine, C., Russell, A., Harðardóttir, J. & Ó. Knudsen (eds.): Iceland – modern processes and past environments. Developments in Quaternary Science, 5: 241–258.
Slater, T., Lawrence, I.R., Otosaka, I.N., Shepherd, A., Gourmelen, N., Jakob, L., Tepes, P., Gilbert, L. & P. Nienow (2021): Review article: Earth's ice imbalance. The Cryosphere, 15: 233-246. https://doi.org/10.5194/tc-15-233-2021
Sobota, I. (2013): Recent changes of cryosphere of north-western Spitsbergen based on Kaffiøyra region. Wydawnictwo UMK, Toruń, 449 pp [in polish].
Sobota, I. (2017): Selected problems of snow accumulation on glaciers during long-term studies in north-western Spitsbergen, Svalbard. Geografiska Annaler: Series A, Physical Geography, 1–16.
Sobota, I. (2021): Glaciers of Svalbard. In: Atlas of changes in the glaciers of Kaffioyra (Svalbard, the Arctic), Sobota, I. (ed). Wydawnictwo Naukowe Uniwersytetu Mikolaja Kopernika: 1-216.
Sobota I., Nowak, M. & P. Weckwerth (2016): Long-term changes of glaciers in north-western Spitsbergen. Global and Planetary Change, 144: 182–197.
Solomina, O. (1996): Glaciers recession in the mountains of the former USSR after the maximum of the Little Ice Age: Time and scale. In: The proceedings of Meeting of the Work Group on Geospatial Analysis of Glaciated Environments. IUQR, Dublin.
Solomina, O. (2000): Retreat of mountain glaciers of northern Eurasia since the Little Ice Age maximum. Annals of Glaciology, 31: 26–30.
Sommer, C., Malz, P., Seehaus, T.C., Lippl, S., Zemp, M., and M.H. Braun (2020): Rapid glacier retreat and downwasting throughout the European Alps in the early 21st century. Nature Communications, 11, 3209. https://doi.org/10.1038/s41467-020-16818-0.
Sommer, C., Seehaus, T., Glazovsky, A., and M.H. Braun (2020): Brief communication: Accelerated glacier mass loss in the Russian Arctic (2010–2017), The Cryosphere Discuss. [preprint], https://doi.org/10.5194/tc-2020-358, in review.
Sorg, A., Bolch, T., Stoffel, M., Solomina, O. & M. Beniston (2012): Climate change impacts on glaciers and runoff in Tien Shan (Central Asia). Nature Climate Change, 2 (10): 725–731.

Soruco, A., Vincent, C., Francou, B., Ribstein, P., Berger, T., Sicart, J.E., Wagnon, P., Arnaud, Y., Favier, V. & Y. Lejeune (2009): Mass balance of Glaciar Zongo, Bolivia, between 1956 and 2006, using glaciological, hydrological and geodetic methods. Annals of Glaciology 50 (50). DOI: https://doi.org/10.3189/172756409787769799

Strelin, J.A. & R. Iturraspe (2007): Recent evolution and mass balance of Cordón Martial glaciers, Cordillera Fueguina Oriental. Global and Planetary Change 59 (1-4): 17-26. https://doi.org/10.1016/j.gloplacha.2006.11.019

Stumm, D., Joshi, S.P., Salzmann, N. & S. MacDonell (2017): In situ monitoring of mountain glaciers. Experiences from mountain ranges around the world and recommendations for the Hindu Kush Himalaya. ICIMOD, Kathmandu, Nepal (http://lib.icimod.org/record/32696/files/icimodWP7-017.pdf)

Su, Z. & Y. Shi (2002): Response of monsoonal temperature glaciers to global warming since the Little Ice Age. Quaternary International, 97 (98): 123–131.

Svendsen, J.I. & J. Mangerud (1997): Holocene glacial and climatic variations on Spitsbergen, Svalbard. The Holocene, 7 (1): 45–57.

Tennant, C. & B. Menounos (2013): Glacier change of the Columbia Icefield, Canadian Rocky Mountains, 1919–2009. Journal of Glaciology, 59 (216): 671–686.

Tennant, C., Menounos, B., Wheate, R. & J.J. Clague (2012): Area change of glaciers in the Canadian Rocky Mountains, 1919 to 2006. The Cryosphere, 6 (6): 1541–1552.

Thomson, L., Zemp, M., Copland, L., Cogley, G. & M. Ecclestone (2017): Comparison of geodetic and glaciological mass budgets for White Glacier, Axel Heiberg Island, Canada. Journal of Glaciology, 63 (237): 55–66.

Thorarinsson, S. (1943): Vatnajökull. The scientific results of the Swedish-Icelandic investigations 1936-37-38. Chapter XI. Oscillations of the Icelandic glaciers in the last 250 years. Geografiska Annaler, 25 (1–2): 1–56.

Thorsteinsson, Th., Jóhannesson, T., Sigurðsson, O. & Einarsson, B. (2017). Afkomumælingar á Hofsjökli 1988-2017 (Mass balance measurements on Hofsjökull 1988-2017). Report VÍ 2017-016, Icelandic Meteorological Office (in Icelandic), ISSN 1670-8261. 84 pp.

Tielidze, L.G. & R.D. Wheate (2018): The Greater Caucasus Glacier Inventory (Russia, Georgia and Azerbaijan). The Cryosphere, 12: 81–94.

Tielidze, L.G., Bolch, T., Wheate, R.D., Kutuzov, S.S., Lavrentiev, I.I., and M. Zemp (2020): Supra-glacial debris cover changes in the Greater Caucasus from 1986 to 2014, The Cryosphere, 14, 585–598, https://doi.org/10.5194/tc-14-585-2020.

Tielidze, L.G., Nosenko, G.A., Khromova, T.E. & F. Paul (2022): Strong acceleration of glacier area loss in the Greater Caucasus between 2000 and 2020. The Cryosphere, 16, 489-504, https://doi.org/10.5194/tc-16-489-2022.

UNESCO (1970): Perennial ice and snow masses - a guide for compilation and assemblage of data for the World Glacier Inventory. Technical Papers in Hydrology No. 1.

UNESCO, IUCN (2022): World Heritage Glaciers: Sentinels of Climate Change, Paris, UNESCO; gland, IUCN. https://doi.org/10.3929/ethz-b-000578916

Unger-Shayesteh, K., Vorogushyn, S., Farinotti, D., Gafurov, A., Duethmann, D., Mandychev, A. & B. Merz (2013): What do we know about past changes in the water cycle of Central Asian headwaters? A review. Global and Planetary Change, 110: 4–25.

Vijay, S. & M. Braun (2016): Elevation change rates of glaciers in the Lahaul-Spiti (Western Himalaya, India) during 2000–2012 and 2012–2013. Remote Sensing, 8(12), 1038, doi:10.3390/rs8121038.

von Schuckmann, K., Minière, A., Gues, F., Cuesta-Valero, F. J., Kirchengast, G., Adusumilli, S., Straneo, F., Ablain, M., Allan, R. P., Barker, P. M., Beltrami, H., Blazquez, A., Boyer, T., Cheng, L., Church, J., Desbruyeres, D., Dolman, H., Domingues, C. M., García-García, A., Giglio, D., Gilson, J. E., Gorfer, M., Haimberger, L., Hakuba, M. Z., Hendricks, S., Hosoda, S., Johnson, G. C., Killick, R., King, B., Kolodziejczyk, N., Korosov, A., Krinner, G., Kuusela, M., Landerer, F. W., Langer, M., Lavergne, T., Lawrence, I., Li, Y., Lyman, J., Marti, F., Marzeion, B., Mayer, M., MacDougall, A. H., McDougall, T., Monselesan, D. P., Nitzbon, J., Otosaka, I., Peng, J., Purkey, S., Roemmich, D., Sato, K., Sato, K., Savita, A., Schweiger, A., Shepherd, A., Seneviratne, S. I., Simons, L., Slater, D. A., Slater, T., Steiner, A. K., Suga, T., Szekely, T., Thiery, W., Timmermans, M.-L., Vanderkelen, I., Wjiffels, S. E., Wu, T. & M. Zemp (2023): Heat stored in the Earth system 1960-2020: where does the energy go?, Earth Syst. Sci. Data, 15, 1675-1709, https://doi.org/10.5194/essd-15-1675-2023

Wagnon P., Ribstein P., Francou B. & J.E. Sicart (2001): Anomalous heat and mass budget of Glaciar Zongo, Bolivia, during the 1997/98 El Nĩno year. Journal of Glaciology, 47 (156): 21–28.

Welty, E., Zemp, M., Navarro, F., Huss, M., Fürst, J.J., Gärtner-Roer, I., Landmann, J., Machguth, H., Naegeli, K., Andreassen, L.M., Farinotti, D., Li, H. & GlaThiDa Contributors (2020): Worldwide version-controlled database of glacier thickness observations. Earth System Science Data 12, 3039-3055. doi: 10.5194/essd-12-3039-2020

WGMS (1991): Glacier Mass Balance Bulletin No. 1 (1988–1989). Haeberli, W. & E. Herren (eds.), IAHS (ICSI) / UNEP / UNESCO, World Glacier Monitoring Service, Zurich, Switzerland, 70 pp.

WGMS (2008): Global Glacier Changes: facts and figures. Zemp, M., Roer, I., Kääb, A., Hoelzle, M., Paul, F. & W. Haeberli (eds.), UNEP, World Glacier Monitoring Service, Zurich, Switzerland, 88 pp.

WGMS (2012): Fluctuations of Glaciers 2005–2010, Volume X. Zemp, M., Frey, H., Gärtner-Roer, I., Nussbaumer, S.U., Hoelzle, M., Paul, F. & W. Haeberli (eds.), ICSU(WDS)/IUGG(IACS)/UNEP/UNESCO/WMO, World Glacier Monitoring Service, Zurich, 336 pp.

WGMS (2013): Glacier Mass Balance Bulletin No. 12 (2010–2011). Zemp, M., Nussbaumer, S.U., Naegeli, K., Gärtner-Roer, I., Paul, F., Hoelzle, M. & W. Haeberli (eds.), ICSU (WDS) / IUGG (IACS) / UNEP / UNESCO / WMO, World Glacier Monitoring Service, Zurich, Switzerland, 106 pp.

Wouters, B. Gardner, A.S. & G. Moholdt (2019): Global glacier mass loss during the GRACE satellite mission (2002-2016). Frontiers in Earth Science, 7: 96.

Yang, R., Hock, R., Kang, S., Shangguan, D., & W. Guo (2020): Glacier mass and area changes on the Kenai Peninsula, Alaska, 1986–2016. Journal of Glaciology, 66(258), 603-617.

Zalazar, L., Ferri Hidalgo, L., Castro, M., Gargantini, H., Giménez, M., Pitte, P., Ruiz, L., Masiokas, M. & R. Villalba (2017): Glaciares de Argentina: resultados preliminares del Inventario Nacional de Glaciares. Rev. Glaciares Ecosistemas Mont., 2: 13–22.

Žebre, M., Colucci, R.R., Giorgi, F., Glasser, N.F., Racoviteanu, A.E., & C. Del Gobbo (2021): 200 years of equilibrium-line altitude variability across the European Alps (1901− 2100). Climate Dynamics, 56(3), 1183-1201.

Zeeberg, J.J. & S.L. Forman (2001): Changes in glacier extent on north Novaya Zemlya in the twentieth century. The Holocene, 11 (2): 161–175.

Zemp, M., Hoelzle, M. & W. Haeberli (2009): Six decades of glacier mass-balance observations: a review of the worldwide monitoring network. Annals of Glaciology, 50 (50): 101–111.

Zemp, M., Jansson, P., Holmlund, P., Gärtner-Roer, I., Koblet, T., Thee, P. and Haeberli, W. (2010): Reanalysis of multi-temporal aerial images of Storglaciären, Sweden (1959-99) - Part 2: Comparison of glaciological and volumetric mass balances. The Cryosphere, 4: 345-357.

Zemp, M., Thibert, E., Huss, M., Stumm, D., Rolstad Denby, C., Nuth, C., Nussbaumer, S.U., Moholdt, G., Mercer, A., Mayer, C., Joerg, P.C., Jansson, P., Hynek, B., Fischer, A., Escher-Vetter, H., Elvehøy, H. & L.M. Andreassen (2013): Reanalysing glacier mass balance measurement series. The Cryosphere, 7 (4): 1227–1245.

Zemp, M., Frey, H., Gärtner-Roer, I., Nussbaumer, S.U., Hoelzle, M., Paul, F., Haeberli, W., Denzinger, F., Ahlstroem, A.P., Anderson, B., Bajracharya, S., Baroni, C., Braun, L.N., Caceres, B.E., Casassa, G., Cobos, G., Davila, L.R., Delgado Granados, H., Demuth, M.N., Espizua, L., Fischer, A., Fujita, K., Gadek, B., Ghazanfar, A., Hagen, J.O., Holmlund, P., Karimi, N., Li, Z., Pelto, M., Pitte, P., Popovnin, V.V., Portocarrero, C.A., Prinz, R., Sangewar, C.V., Severskiy, I., Sigurdsson, O., Soruco, A., Usubaliev, R. & C. Vincent (2015): Historically unprecedented global glacier decline in the early 21st century. Journal of Glaciology, 61 (228): 745–762.

Zemp, M., Huss, M., Thibert, E., Eckert, N., McNabb, R., Huber, J., Barandun, M., Machguth, H., Nussbaumer, S.U., Gärtner-Roer, I., Thomson, L., Paul, F., Maussion, F., Kutuzov, S. & J.G. Cogley (2019): Global glacier mass changes and their contributions to sea-level rise from 1961 to 2016. Nature, 568, p. 382–386. https://doi.org/10.1038/s41586-019-1071-0

Zemp, M., Huss, M., Eckert, N., Thibert, E., Paul, F., Nussbaumer, S.U. & I. Gärtner-Roer (2020): Brief communication: Ad hoc estimation of glacier contributions to sea-level rise from latest glaciological observations. The Cryosphere, 14: 1043–1050.

Zheng, W., Pritchard, M.E., Willis, M.J., Tepes, P., Gourmelen, N., Benham, T.J., & J.A. Dowdeswell (2018): Accelerating glacier mass loss on Franz Josef Land, Russian Arctic. Remote Sensing of Environment, 211, 357-375. https://doi.org/10.1016/j.rse.2018.04.004

7 PRINCIPAL INVESTIGATORS

7.1 PRINCIPAL INVESTIGATORS MASS BALANCE

(in alphabetic order, for observation periods 2019/20, 2020/21, and 2021/22)

PU	GLACIER	Principal Investigator (sponsoring agency; contact)
AQ	BAHIA DEL DIABLO	Ermolin E. (IAA-DG; ivgen52@yahoo.com), Marinsek S. (IAA-DG; smarinsek@dna.gov.ar), Seco J. (IAA-DG; jlseco@dna.gov.ar)
AQ	HURD	Navarro F. (AEI; francisco.navarro@upm.es)
AQ	JOHNSONS	Navarro F. (AEI; francisco.navarro@upm.es)
AR	AGUA NERA	Gargantini H. (IANIGLA), Pitte P. (IANIGLA; pierrepitte@mendoza-conicet.gov.ar)
AR	BROWN SUPERIOR	Cabrera G. (IANIGLA; inggabrielcabrera@yahoo.com.ar)
AR	CONCONTA NORTE	Cabrera G. (IANIGLA; inggabrielcabrera@yahoo.com.ar)
AR	DE LOS TRES	Ferri Hidalgo L. (IANIGLA), Pitte P. (IANIGLA; pierrepitte@mendoza-conicet.gov.ar)
AR	LOS AMARILLOS	Cabrera G. (IANIGLA; inggabrielcabrera@yahoo.com.ar)
AR	MARTIAL ESTE	Camargo S. (GTF), Iturraspe R. (UNTDF; rodolfoiturraspe@yahoo.com), Strelin J. (IAA-UNC; jstrelin@yahoo.com.ar)
AT	GOLDBERG KEES	Hynek B. (GeoSphere Austria; bernhard.hynek@geosphere.at), Neureiter A. (GeoSphere Austria; anton.neureiter@geosphere.at)
AT	HALLSTAETTER GLETSCHER	Helfricht K. (FGUA, EnergieAG; kay.helfricht@oeaw.ac.at), Reingruber K. (FGUA, EnergieAG; office@blueskywetter.at)
AT	HINTEREIS FERNER	Prinz R. (ACINN; rainer.prinz@uibk.ac.at)
AT	JAMTAL FERNER	Fischer A. (HD/LT; andrea.fischer@oeaw.ac.at), Hartl L. (HD/LT)
AT	KESSELWAND FERNER	Prinz R. (ACINN; rainer.prinz@uibk.ac.at)
AT	KLEINFLEISS KEES	Hynek B. (GeoSphere Austria; bernhard.hynek@geosphere.at), Neureiter A. (GeoSphere Austria; anton.neureiter@geosphere.at)
AT	OE. WURTEN K.	Reisenhofer S. (GeoSphere Austria; stefan.reisenhofer@geosphere.at)
AT	PASTERZE	Neureiter A. (GeoSphere Austria; anton.neureiter@geosphere.at)
AT	SEEKARLES FERNER	Strudl M. (markus.strudl@gmail.com)
AT	STUBACHER SONNBLICK KEES	Slupetzky H. (HD/SB, HD; heinz.slupetzky@sbg.ac.at), Wiesenegger H. (HD/SB; hans.wiesenegger@salzburg.gv.at), Zagel B. (HD/SB)
AT	VENEDIGERKEES	Seiser B. (HD/SB, HD; bernd.seiser@oeaw.ac.at)
AT	VERNAGT FERNER	Mayer C. (GGBAS; christoph.mayer@badw.de)
AT	ZETTALUNITZ/ MULLWITZ KEES	Stocker-Waldhuber M. (HD/LT, NHT; martin.stocker-waldhuber@oeaw.ac.at)

PU	GLACIER	Principal Investigator (sponsoring agency; contact)
BO	CHARQINI SUR	(Great-Ice, IRD, UMSA)
BO	ZONGO	(Great-Ice, IRD, UMSA)
BT	THANA	Tshering T. (NCHM; tsheringtashi@nchm.gov.bt), Tsheten N. (NCHM; namgaytsheten95@gmail.com), Wangchuk N. (NCHM; wnamgay@nchm.gov.bt)
CA	ATHABASCA	Ednie M. (NRCan, JNP; mark.ednie@nrcan-rncan.gc.ca)
CA	BOLOGNA	Ednie M. (NRCan; mark.ednie@nrcan-rncan.gc.ca)
CA	DEVON ICE CAP NW	Burgess D. (NRCan; david.burgess@nrcan-rncan.gc.ca)
CA	HELM	Ednie M. (NRCan; mark.ednie@nrcan-rncan.gc.ca)
CA	KOKANEE	Pelto B. (BC-Parks, UNBC; peltoglacier@gmail.com)
CA	MEIGHEN ICE CAP	Burgess D. (NRCan; david.burgess@nrcan-rncan.gc.ca)
CA	MELVILLE SOUTH ICE CAP	Burgess D. (NRCan; david.burgess@nrcan-rncan.gc.ca)
CA	PEYTO	Ednie M. (NRCan; mark.ednie@nrcan-rncan.gc.ca)
CA	PLACE	Ednie M. (NRCan; mark.ednie@nrcan-rncan.gc.ca)
CA	WHITE	Thomson L. (ICELab; l.thomson@queensu.ca)
CH	ADLER	Huss M. (DGUF, UNIFR, GLAMOS; matthias.huss@unifr.ch), Linsbauer A. (GIUZ, UZH, GLAMOS; andreas.linsbauer@geo.uzh.ch)
CH	ALLALIN	Bauder A. (VAW, GLAMOS; bauder@vaw.baug.ethz.ch)
CH	BASODINO	Kappenberger G. (VAW, GLAMOS; glkappenberger@hotmail.com)
CH	CLARIDENFIRN	Steinegger U. (VAW, GLAMOS; steinegger@meteodat.ch)
CH	CORBASSIERE	Bauder A. (VAW, GLAMOS; bauder@vaw.baug.ethz.ch)
CH	CORVATSCH SOUTH (PART OF E23/18)	Huss M. (DGUF, UNIFR, GLAMOS; matthias.huss@unifr.ch)
CH	FINDELEN	Huss M. (DGUF, UNIFR, GLAMOS; matthias.huss@unifr.ch), Linsbauer A. (GIUZ, UZH, GLAMOS; andreas.linsbauer@geo.uzh.ch)
CH	GIETRO	Bauder A. (VAW, GLAMOS; bauder@vaw.baug.ethz.ch)
CH	GRIES	Huss M. (VAW, GLAMOS; matthias.huss@unifr.ch)
CH	GROSSER ALETSCH	Bauder A. (VAW, GLAMOS; bauder@vaw.baug.ethz.ch), Huss M. (VAW, GLAMOS; matthias.huss@unifr.ch)
CH	HOHLAUB	Bauder A. (VAW, GLAMOS; bauder@vaw.baug.ethz.ch), Hodel E. (VAW, GLAMOS; hodel@vaw.baug.ethz.ch)
CH	MURTEL VADRET DAL	Huss M. (UNIFR, GLAMOS; matthias.huss@unifr.ch)
CH	OBERAAR	Nussbaumer S. (UZH; samuel.nussbaumer@geo.uzh.ch)
CH	OTEMMA	Fischer M. (UniBe; mauro.fischer@unibe.ch)
CH	PERS, VADRET	(VUB), Huss M. (DGUF, UNIFR, GLAMOS; matthias.huss@unifr.ch), Huybrechts P. (VUB; phuybrec@vub.ac.be), Linsbauer A. (DGUF, UNIFR, GLAMOS; andreas.linsbauer@geo.uzh.ch)
CH	PIZOL	Huss M. (DGUF, VAW, UNIFR, GLAMOS; matthias.huss@unifr.ch)
CH	PLAINE MORTE, GLACIER DE LA	Huss M. (DGUF, UNIFR, GLAMOS; matthias.huss@unifr.ch)
CH	RHONE	Bauder A. (VAW, GLAMOS; bauder@vaw.baug.ethz.ch)
CH	SANKT ANNA	Huss M. (DGUF, UNIFR, GLAMOS; matthias.huss@unifr.ch)

PU	GLACIER	Principal Investigator (sponsoring agency; contact)
CH	SCHWARZBACH	Huss M. (DGUF, UNIFR, GLAMOS; matthias.huss@unifr.ch)
CH	SCHWARZBERG	Bauder A. (VAW, GLAMOS; bauder@vaw.baug.ethz.ch), Hodel E. (VAW, GLAMOS; hodel@vaw.baug.ethz.ch)
CH	SEX ROUGE	Fischer M. (UNIFR, GLAMOS; mauro.fischer@unibe.ch), Huss M. (DGUF; matthias.huss@unifr.ch)
CH	SILVRETTA	Bauder A. (VAW, GLAMOS; bauder@vaw.baug.ethz.ch)
CH	TSANFLEURON	Fischer M. (UNIFR, GLAMOS; mauro.fischer@unibe.ch), Huss M. (DGUF; matthias.huss@unifr.ch)
CL	ECHAURREN NORTE	Buglio F. (DGA), Carrión D. (DGA), Casassa G. (DGA; gino.casassa@mop.gov.cl), Espinoza A. (DGA), Hernández J. (DGA), Huenante J. (DGA), Puga P. (DGA), Segovia A. (DGA)
CL	MOCHO CHOSHUENCO SE	Berkhoff J. (UACH), Rodriguez J. (UACH), Schaefer M. (UACH; mschaefer@uach.cl)
CN	PARLUNG NO. 94	Li S. (CAS/ITPR; shenghaili1984@gmail.com), Yang W. (CAS/ITPR)
CN	URUMQI GLACIER NO. 1	Li H. (CAREERI, CAREERI-TGS; lihuilin@lzb.ac.cn), Li Z. (CAREERI-TGS; lizq@lzb.ac.cn)
CN	URUMQI GLACIER NO. 1 E-BRANCH	Li H. (CAREERI, CAREERI-TGS; lihuilin@lzb.ac.cn), Li Z. (CAREERI-TGS; lizq@lzb.ac.cn)
CN	URUMQI GLACIER NO. 1 W-BRANCH	Li H. (CAREERI, CAREERI-TGS; lihuilin@lzb.ac.cn), Li Z. (CAREERI-TGS; lizq@lzb.ac.cn)
CO	CONEJERAS	Ceballos Liévano J. (IDEAM; jceballos@ideam.gov.co), Ospina A. (IDEAM)
EC	ANTIZANA15 ALPHA	Cáceres Correa B. (INAMHI; ernestocaceres2002@yahoo.com.mx)
ES	MALADETA	Cobos Campos G. (UPV; gcobosc@trr.upv.es)
FR	ARGENTIERE	Six D. (CNRS-UGA, UGA, CNRS; delphine.six@univ-grenoble-alpes.fr), Vincent C. (CNRS-UGA; christian.vincent@univ-grenoble-alpes.fr)
FR	GEBROULAZ	Six D. (UGA, CNRS, IGE; delphine.six@univ-grenoble-alpes.fr), Vincent C. (IGE; christian.vincent@univ-grenoble-alpes.fr)
FR	OSSOUE	René P. (AM; asso.moraine@wanadoo.fr)
FR	SAINT SORLIN	Six D. (UGA, CNRS, IGE; delphine.six@univ-grenoble-alpes.fr), Vincent C. (IGE; christian.vincent@univ-grenoble-alpes.fr)
FR	SARENNES	Bonnefoy M. (INRAE), Thibert E. (INRAE; emmanuel.thibert@inrae.fr)
FR	TRE LA TETE	Moreau L. (EDYTEM; moreauluc@chx.fr)
GL	FREYA	Hynek B. (ZAMG, UG/GRS; bernhard.hynek@geosphere.at)
GL	MITTIVAKKAT	de Villiers S. (HVL; simon.de.villiers@hvl.no)
GL	QASIGIANNGUIT	Langley K. (ASIAQ, GEM, ASIAQ-GBN; kal@asiaq.gl)
IN	BATAL	Sharma P. (NCPOR; pnsharma@ncpor.res.in)
IN	CHHOTA SHIGRI	Azam M. (farooqaman@yahoo.co.in)
IN	HOKSAR	Romshoo S. (DST; shakilrom@uok.edu.in)
IN	KOLAHOI	Romshoo S. (DST; shakilrom@uok.edu.in)
IN	SUTRI DHAKA	Sharma P. (NCPOR; pnsharma@ncpor.res.in)
IS	BRUARJOKULL	Gunnarsson A. (NPC; andri.gunnarsson@landsvirkjun.is), Pálsson F. (IES; fp@hi.is)

PU	GLACIER	Principal Investigator (sponsoring agency; contact)
IS	DYNGJUJOKULL	Gunnarsson A. (NPC; andri.gunnarsson@landsvirkjun.is), Pálsson F. (IES; fp@hi.is)
IS	EYJABAKKA-JOKULL	Gunnarsson A. (NPC; andri.gunnarsson@landsvirkjun.is), Pálsson F. (IES; fp@hi.is)
IS	HOFSJOKULL E	Þorsteinsson Þ. (IMO; thor@vedur.is)
IS	HOFSJOKULL N	Þorsteinsson Þ. (IMO; thor@vedur.is)
IS	HOFSJOKULL SW	Þorsteinsson Þ. (IMO; thor@vedur.is)
IS	KOLDUKVISLAR-JOKULL	Gunnarsson A. (NPC; andri.gunnarsson@landsvirkjun.is), Pálsson F. (IES; fp@hi.is)
IS	LANGJOKULL ICE CAP	Gunnarsson A. (NPC; andri.gunnarsson@landsvirkjun.is), Pálsson F. (IES; fp@hi.is)
IS	TUNGNAAR-JOKULL	Gunnarsson A. (NPC; andri.gunnarsson@landsvirkjun.is), Pálsson F. (IES; fp@hi.is)
IS	VATNAJOKULL	Gunnarsson A. (NPC; andri.gunnarsson@landsvirkjun.is), Pálsson F. (IES; fp@hi.is)
IT	CALDERONE	Boccabella P. (CGI), Bruschi F. (UPe), Caira T. (CGI), Cappelletti D. (UPe, CGI, CAI), Cimini D. (IMAA), D'Aquila P. (Engeoneering), Esposito G. (IIA), Martinelli M. (Engeoneering), Marzano F. (CETEMPS), Montini M. (CGI), Pecci M. (CGI), Pecci M. (DARA, CGI; m.pecci@governo.it), Raparelli E. (CETEMPS), Tuccella P. (CETEMPS; paolo.tuccella@univaq.it), di Fiore T. (AQCF)
IT	CAMPO SETT.	Bera A. (SGL), Colombarolli D. (SGL; sgl@servizioglaciologicolombardo.it), Peri I. (SGL), Scotti R. (SGL; riccardo.scotti@meteonetwork.it)
IT	CARESER	Carturan L. (UNIPD/TeSAF; luca.carturan@unipd.it), Gaddo M. (MeteoTrentino)
IT	CIARDONEY	Cat Berro D. (SMI; redazione@nimbus.it), Mercalli L. (SMI; info@nimbus.it)
IT	GRAND ETRET	Cerise S. (PNGP/CGI; stefano.cerise@pngp.it), Massoni D. (PNGP/CGI), Peracino A. (PNGP/CGI), Rossotto A. (PNGP/CGI; alberto.rossotto@pngp.it)
IT	LA MARE (SOUTHERN BRANCH)	Carturan L. (UNIPD/TeSAF, UNIPD/Dgsci; luca.carturan@unipd.it)
IT	LUPO	Manni M. (SGL), Masserini M. (SGL), Oreggioni M. (SGL), Porta R. (SGL), Scotti R. (SGL; riccardo.scotti@meteonetwork.it)
IT	MALAVALLE (VEDR. DI) / UEBELTALF.	Franchi G. (ApPC/AfBS; giangi.franchi@gmail.com)
IT	PENDENTE (VEDR.) / HANGENDERF.	Franchi G. (ApPC/AfBS; giangi.franchi@gmail.com)
IT	RIES OCC. (VEDR. DI) / RIESERF. WESTL.	Di Lullo A. (ApPC/AfBS), Dinale R. (ApPC/AfBS; roberto.dinale@provincia.bz.it)
IT	SURETTA MERID.	Gallo P. (SGL), Prandi G. (SGL), Scotti R. (SGL; riccardo.scotti@meteonetwork.it), Villa F. (SGL; sgl@servizioglaciologicolombardo.it)
IT	TIMORION	Morra di Cella U. (ARPA; u.morradicella@arpa.vda.it)
KG	ABRAMOV	Ajikeev A. (KyrgyzHydromet), Azisov E. (CAIAG; e.azisov@caiag.kg), Barandun M. (DGUF; martina.barandun@eurac.edu), Belekov S. (KyrgyzHydromet; sultbelekov@gmail.com), Kenzhebaev R. (CAIAG; r.kenzhebaev@caiag.kg), Mattea E. (UNIFR)
KG	BATYSH SOOK/ SYEK ZAPADNIY	Azisov E. (CAIAG; e.azisov@caiag.kg), Barandun M. (DGUF; martina.barandun@eurac.edu), Hoelzle M. (UNIFR; martin.hoelzle@unifr.ch), Kenzhebaev R. (CAIAG; r.kenzhebaev@caiag.kg), Saks T. (UNIFR; tomassakss@gmail.com), Usubaliev R. (CAIAG; r.usubaliev@caiag.kg)

PU	GLACIER	Principal Investigator (sponsoring agency; contact)
KG	BORDU	Ermenbayev B. (TshMRC), Omurbekov S. (TSHMRC), Popovnin V. (MSU; begemotina@hotmail.com), Satylkanov R. (TshMRC, TSHMRC; r.satylkanov@gmail.com), Sayakpayev D. (TshMRC)
KG	GLACIER NO. 354 (AKSHIYRAK)	Azisov E. (CAIAG; e.azisov@caiag.kg), Barandun M. (DGUF; martina.barandun@eurac.edu), Hoelzle M. (DGUF, UNIFR; martin.hoelzle@unifr.ch), Kenzhebaev R. (CAIAG; r.kenzhebaev@caiag.kg), Usubaliev R. (CAIAG; r.usubaliev@caiag.kg)
KG	GLACIER NO. 599 (KJUNGEI ALA-TOO)	(UNIFR), Azisov E. (CAIAG; e.azisov@caiag.kg), Esenaman uulu M. (CAIAG), Kenzhebaev R. (CAIAG; r.kenzhebaev@caiag.kg), Usubaliev R. (CAIAG; r.usubaliev@caiag.kg)
KG	GOLUBIN	Azisov E. (CAIAG; e.azisov@caiag.kg), Barandun M. (DGUF; martina.barandun@eurac.edu), Esenamanov M. (CAIAG), Hoelzle M. (DGUF, UNIFR; martin.hoelzle@unifr.ch), Kenzhebaev R. (CAIAG; r.kenzhebaev@caiag.kg), Saks T. (DGUF, UNIFR; tomassakss@gmail.com), Usubaliev R. (CAIAG; r.usubaliev@caiag.kg)
KG	KARA-BATKAK	Ermenbayev B. (TshMRC), Makeshov A. (TSHMRC), Popovnin V. (MSU; begemotina@hotmail.com), Satylkanov R. (TshMRC, TSHMRC; r.satylkanov@gmail.com), Sayakpayev D. (TshMRC)
KG	SARY TOR (NO.356)	Ermenbayev B. (TshMRC, TSHMRC), Popovnin V. (MSU; begemotina@hotmail.com), Satylkanov R. (TshMRC, TSHMRC; r.satylkanov@gmail.com), Sayakpayev D. (TshMRC)
KG	TURGEN-AKSUU	Ajikeev A. (KyrgyzHydromet), Belekov S. (KyrgyzHydromet; sultbelekov@gmail.com), Musaev T. (KyrgyzHydromet), Musaevs T. (KyrgyzHydromet)
KZ	TS.TUYUKSUYS-KIY	Kasatkin N. (INGEO, IGNANKaz, CARGC; kasatkinne@mail.ru)
NO	AALFOTBREEN	Kjøllmoen B. (NVE; bkj@nve.no)
NO	AUSTDALS-BREEN	Elvehøy H. (NVE; hae@nve.no)
NO	ENGABREEN	Elvehøy H. (NVE; hae@nve.no)
NO	GRAASUBREEN	Andreassen L. (NVE; lma@nve.no)
NO	HANSEBREEN	Kjøllmoen B. (NVE; bkj@nve.no)
NO	HELLSTUGU-BREEN	Andreassen L. (NVE; lma@nve.no)
NO	LANGFJORD JOEKELEN	Kjøllmoen B. (NVE; bkj@nve.no)
NO	NIGARDSBREEN	Kjøllmoen B. (NVE; bkj@nve.no)
NO	REMBESDALS SKAAKA	Elvehøy H. (NVE; hae@nve.no)
NO	STORBREEN	Andreassen L. (NVE; lma@nve.no)
NP	MERA	Wagnon P. (UG/IRD, IRD; patrick.wagnon@univ-grenoble-alpes.fr)
NP	POKALDE	Wagnon P. (UG/IRD, IRD; patrick.wagnon@univ-grenoble-alpes.fr)
NP	RIKHA SAMBA	Gurung T. (ICIMOD), Joshi S. (ICIMOD; sharad.joshi@icimod.org)
NP	WEST CHANGRI NUP	Wagnon P. (UG/IRD, IRD; patrick.wagnon@univ-grenoble-alpes.fr)
NP	YALA	Gurung T. (ICIMOD), Joshi S. (ICIMOD; sharad.joshi@icimod.org), Stumm D. (stummd@gmail.com)
NZ	BREWSTER	Anderson B. (ARC; brian.anderson@vuw.ac.nz), Cullen N. (DGUO-NZ; njc@geography.otago.ac.nz), Sirguey P. (DGUO-NZ), Vargo L. (ARC; lauren.vargo@vuw.ac.nz)

PU	GLACIER	Principal Investigator (sponsoring agency; contact)
NZ	ROLLESTON	Kerr T. (Rainfall.NZ; tim.kerr@rainfall.nz), Purdie H. (UCant/DG, UCant)
RU	DJANKUAT	Gubanov A. (MSU, RFBR), Popovnin V. (MSU, RFBR; begemotina@hotmail.com)
RU	GARABASHI	GARABASHI Kutuzov S. (RAS/IG, IG RAS; s.kutuzov@gmail.com), Lavrentiev I. (RAS/IG, IG RAS), Nikitin S. (RAS/IG, IG RAS), Nosenko G. (RAS/IG, IG RAS; gnosenko@gmail.com), Rototayeva O. (RAS/IG, IG RAS), Smirnov A. (RAS/IG, IG RAS)
RU	LEVIY AKTRU	Erofeev A. (TSU/DG, TSU), Kutuzov S. (RAS/IG, IG RAS; s.kutuzov@gmail.com), Smirnov A. (RAS/IG, TSU)
SE	MARMA GLACIAEREN	Tarfala Research Station Staff (tarfala@natgeo.su.se, nina.kirchner@natgeo.su.se)
SE	RABOTS GLACIAER	Tarfala Research Station Staff (tarfala@natgeo.su.se, nina.kirchner@natgeo.su.se)
SE	RIUKOJIETNA	Tarfala Research Station Staff (tarfala@natgeo.su.se, nina.kirchner@natgeo.su.se)
SE	STORGLACIAER-EN	Tarfala Research Station Staff (tarfala@natgeo.su.se, nina.kirchner@natgeo.su.se)
SJ	AUSTRE BROEG-GERBREEN	Kohler J. (NPI; jack.kohler@npolar.no)
SJ	GROENFJORD E	Chernov R. (IG RAS), Elagina N. (IG RAS)
SJ	HANSBREEN	Luks B. (PAS; luks@igf.edu.pl)
SJ	IRENEBREEN	Sobota I. (PRC/FESSM; irso@umk.pl)
SJ	KONGSVEGEN	Kohler J. (NPI; jack.kohler@npolar.no)
SJ	KRONEBREEN	Kohler J. (NPI; jack.kohler@npolar.no)
SJ	MIDTRE LOVEN-BREEN	Kohler J. (NPI; jack.kohler@npolar.no)
SJ	WALDEMAR-BREEN	Sobota I. (PRC/FESSM; irso@umk.pl)
SJ	WERENSKIOLD-BREEN	Ignatiuk D. (US/IES; dariusz.ignatiuk@us.edu.pl), Laska M. (US/IES; michal.laska@us.edu.pl)
TJ	EAST ZULMART (GLACIER NO 139)	(CRG)
TJ	GLACIER NO. 71 (YAKARCHA)	Kayumov A. (CRG; criosfera2017@gmail.com), Vosidov F. (CRG; firdavs.vosidov@mail.ru)
TJ	NO. 457 (NHD)	Kayumov A. (CRG; criosfera2017@gmail.com), Navruzshoev H. (CRG; nhd140704@gmail.com)
TJ	NO. 676 (GGP)	(CRG)
US	COLUMBIA (2057)	Pelto M. (NCGCP; mspelto@nichols.edu)
US	DANIELS	Pelto M. (NCGCP; mspelto@nichols.edu)
US	EASTON	Pelto M. (NCGCP; mspelto@nichols.edu)
US	GULKANA	Florentine C. (USGS-F, USGS; cflorentine@usgs.gov), Sass L. (USGS-F, USGS)
US	ICE WORM	Pelto M. (NCGCP; mspelto@nichols.edu)
US	LEMON CREEK	Florentine C. (USGS-F, USGS; cflorentine@usgs.gov), Sass L. (USGS-F, USGS)
US	LOWER CURTIS	Pelto M. (NCGCP; mspelto@nichols.edu)
US	LYNCH	Pelto M. (NCGCP; mspelto@nichols.edu)
US	RAINBOW	Pelto M. (NCGCP; mspelto@nichols.edu)
US	SHOLES	Pelto M. (NCGCP; mspelto@nichols.edu)

PU	GLACIER	Principal Investigator (sponsoring agency; contact)
US	SOUTH CASCADE	Florentine C. (USGS-F, USGS; cflorentine@usgs.gov), Sass L. (USGS-F, USGS)
US	SPERRY	Florentine C. (USGS-F, USGS; cflorentine@usgs.gov), McNeil C. (USGS), Sass L. (USGS-F, USGS)
US	TAKU	Florentine C. (USGS; cflorentine@usgs.gov), McNeil C. (USGS-F, USGS)
US	WOLVERINE	Florentine C. (USGS-F, USGS; cflorentine@usgs.gov), Sass L. (USGS-F, USGS)
UZ	BARKRAK SREDNIY	Eshmiratov D. (CICADA, Mininnovation), Mamirov H. (CICADA, Mininnovation), Petrov M. (CICADA, Mininnovation), Umirzakov G. (CICADA, Mininnovation; g.umirzakov@nuu.uz), Yakovlev A. (CICADA, Mininnovation; andreyakovlev@mail.ru)
UZ	BARKRAK SREDNIY EAST BRANCH	Eshmiratov D. (CICADA, Mininnovation), Mamirov H. (CICADA, Mininnovation), Petrov M. (CICADA, Mininnovation), Umirzakov G. (CICADA, Mininnovation; g.umirzakov@nuu.uz), Yakovlev A. (CICADA, Mininnovation; andreyakovlev@mail.ru)

7.2 PRINCIPAL INVESTIGATORS FRONT VARIATION
(in alphabetic order, for observation periods 2019/20, 2020/21, and 2021/22)

PU	GLACIER: Principal Investigator (sponsoring agency)
AQ	BAHIA DEL DIABLO: Ermolin E. (IAA-DG; ivgen52@yahoo.com), Marinsek S. (IAA-DG; smarinsek@dna.gov.ar), Seco J. (IAA-DG; jlseco@dna.gov.ar)
AT	ALPEINER F.: Stocker-Waldhuber M. (ÖAV; martin.stocker-waldhuber@oeaw.ac.at); BACHFALLEN F.: Dünser F. (ÖAV), Janz B. (ÖAV); BAERENKOPF K.: Seitlinger G. (ÖAV); BERGLAS F.: Stocker-Waldhuber M. (ÖAV; martin.stocker-waldhuber@oeaw.ac.at); BIELTAL F.: Groß G. (ÖAV); BRENNKOGL K.: Seitlinger G. (ÖAV); DAUNKOGEL F.: Stocker-Waldhuber M. (ÖAV; martin.stocker-waldhuber@oeaw.ac.at); DIEM F.: Strudl M. (ÖAV; markus.strudl@gmail.com); EISKAR G.: Hohenwarter G. (ÖAV); FERNAU F.: Stocker-Waldhuber M. (ÖAV; martin.stocker-waldhuber@oeaw.ac.at); FIRMISAN F.: Strudl M. (ÖAV; markus.strudl@gmail.com); FREIWAND K.: Kellerer-Pirklbauer A. (ÖAV), Lieb G. (ÖAV); FROSNITZ K.: Lang J. (ÖAV); FURTSCHAGL K.: Friedrich C. (ÖAV), Friedrich M. (ÖAV), Friedrich R. (ÖAV); GAISKAR F.: Dünser F. (ÖAV), Janz B. (ÖAV); GAISSBERG F.: Fischer A. (ÖAV; andrea.fischer@oeaw.ac.at); GEPATSCH F.: Noggler B. (ÖAV); GOESSNITZ K.: Krobath M. (ÖAV); GOLDBERG K.: Binder D. (ÖAV); GR. GOSAU G.: Reingruber K. (ÖAV; office@blueskywetter.at); GROSSELEND K.: Färber J. (ÖAV), Knittel A. (ÖAV); GRUENAU F.: Stocker-Waldhuber M. (ÖAV; martin.stocker-waldhuber@oeaw.ac.at); GURGLER F.: Fischer A. (ÖAV; andrea.fischer@oeaw.ac.at); GUSLAR F.: Stocker-Waldhuber M. (ÖAV; martin.stocker-waldhuber@oeaw.ac.at); HALLSTAETTER G.: Reingruber K. (ÖAV; office@blueskywetter.at); HINTEREIS F.: Stocker-Waldhuber M. (ÖAV; martin.stocker-waldhuber@oeaw.ac.at); HOCHALM K.: Färber J. (ÖAV), Knittel A. (ÖAV); HOCHJOCH F.: Stocker-Waldhuber M. (ÖAV; martin.stocker-waldhuber@oeaw.ac.at); HORN K. (SCHOB.): Krobath M. (ÖAV); HORN K. (ZILLER): Friedrich C. (ÖAV), Friedrich M. (ÖAV), Friedrich R. (ÖAV); JAMTAL F.: Groß G. (ÖAV); KAELBERSPITZ K.: Färber J. (ÖAV), Knittel A. (ÖAV); KALSER BAERENKOPF K.: Seitlinger G. (ÖAV); KARLINGER K.: Seitlinger G. (ÖAV); KESSELWAND F.: Stocker-Waldhuber M. (ÖAV; martin.stocker-waldhuber@oeaw.ac.at); KLEINEISER K.: Seitlinger G. (ÖAV); KLEINELEND K.: Färber J. (ÖAV), Knittel A. (ÖAV); KLEINFLEISS K.: Binder D. (ÖAV); KLOSTERTALER M: Groß G. (ÖAV); KRIMMLER K.: Luzian R. (ÖAV); LANDECK K.: Seitlinger G. (ÖAV); LANGTALER F.: Fischer A. (ÖAV; andrea.fischer@oeaw.ac.at); LATSCH F.: Strudl M. (ÖAV; markus.strudl@gmail.com); MARZELL F.: Plörer M. (ÖAV); MAURER K. (GLO.): Seitlinger G. (ÖAV); MUTMAL F.: Plörer M. (ÖAV); NIEDERJOCH F.: Plörer M. (ÖAV); OBERSULZBACH K.: Luzian R. (ÖAV); OCHSENTALER G.: Groß G. (ÖAV); OE. WURTEN K.: Binder D. (ÖAV, ZAMG), Galaoz M. (ZAMG), Hynek B. (ZAMG; bernhard.hynek@geosphere.at), Neureiter A. (ZAMG; anton.neureiter@zamg.ac.at), Weyss G. (ZAMG); OEDENWINKEL K.: Zagel B. (ÖAV); PASTERZE: Kellerer-Pirklbauer A. (ÖAV), Lieb G. (ÖAV); PFAFFEN F.: Dünser F. (ÖAV), Janz B. (ÖAV); RETTENBACH F.: Plörer M. (ÖAV); ROFENKAR F.: Plörer M. (ÖAV); ROTER KNOPF K.: Krobath M. (ÖAV); ROTMOOS F.: Fischer A. (ÖAV; andrea.fischer@oeaw.ac.at); SCHALF F.: Plörer M. (ÖAV); SCHLADMINGER G.: Reingruber K. (ÖAV; office@blueskywetter.at); SCHLATEN K.: Luzian R. (ÖAV); SCHLEGEIS K.: Friedrich C. (ÖAV), Friedrich M. (ÖAV), Friedrich R. (ÖAV); SCHMIEDINGER K.: Seitlinger G. (ÖAV); SCHNEEGLOCKEN: Groß G. (ÖAV); SCHNEELOCH G.: Reingruber K. (ÖAV; office@blueskywetter.at); SCHWARZENBERG F.: Dünser F. (ÖAV), Janz B. (ÖAV); SCHWARZENSTEIN: Friedrich C. (ÖAV), Friedrich M. (ÖAV), Friedrich R. (ÖAV); SCHWARZKARL K.: Seitlinger G. (ÖAV); SCHWEIKERT F.: Strudl M. (ÖAV; markus.strudl@gmail.com); SEEKARLES F.: Strudl M. (ÖAV; markus.strudl@gmail.com); SEXEGERTEN F.: Noggler B. (ÖAV); SIMONY K.: Lang J. (ÖAV); SPIEGEL F.: Strudl M. (ÖAV; markus.strudl@gmail.com); STUBACHER SONNBLICK K.: Seitlinger G. (ÖAV); SULZTAL F.: Dünser F. (ÖAV), Janz B. (ÖAV); TASCHACH F.: Noggler B. (ÖAV); TOTENFELD: Groß G. (ÖAV); TOTENKOPF K.: Seitlinger G. (ÖAV); TRIEBENKARLAS F.: Dünser F. (ÖAV), Janz B. (ÖAV); UMBAL K.: Lang J. (ÖAV); UNT. RIFFL K.: Zagel B. (ÖAV); UNTERSULZBACH K.: Luzian R. (ÖAV); VERBORGENBERG F.: Stocker-Waldhuber M. (ÖAV; martin.stocker-waldhuber@oeaw.ac.at); VERMUNT G.: Groß G. (ÖAV); VERNAGT F.: Stocker-Waldhuber M. (ÖAV; martin.stocker-waldhuber@oeaw.ac.at); VILTRAGEN K.: Luzian R. (ÖAV); W. TRIPP K.: Färber J. (ÖAV), Knittel A. (ÖAV); WASSERFALLWINKL K.: Kellerer-Pirklbauer A. (ÖAV), Lieb G. (ÖAV)

PU	GLACIER: Principal Investigator (sponsoring agency)
AT	WAXEGG K.: Friedrich C. (ÖAV), Friedrich M. (ÖAV), Friedrich R. (ÖAV); WEISSEE F.: Noggler B. (ÖAV); WILDGERLOS: Nussbaumer S. (ÖAV); WINKL K.: Färber J. (ÖAV), Knittel A. (ÖAV); ZETTALUNITZ/MULLWITZ K.: Lang J. (ÖAV)
BO	CHARQUINI SUR: (Great-Ice, IRD, UMSA); ZONGO: (Great-Ice, IRD, UMSA)
BT	GANGJU LA: Karma (NCHM), Tshering D. (NCHM), Tshering P. (NCHM; ptshering@nchm.gov.bt); THANA: Tshering T. (NCHM; tsheringtashi@nchm.gov.bt), Tsheten N. (NCHM; namgaytsheten95@gmail.com), Wangchuk N. (NCHM; wnamgay@nchm.gov.bt)
CA	KOKANEE: Pelto B. (BCHydro, UBC; peltoglacier@gmail.com)
CH	ALBIGNA: (VAW, GLAMOS), Kühne R. (AWN), Soder N. (AWN); ALLALIN: Bauder A. (VAW, GLAMOS; bauder@vaw.baug.ethz.ch); ALPETLI (KANDER): (VAW, GLAMOS), Burgener U. (KAWA); AMMERTEN: (VAW, GLAMOS), Hodel W.; AROLLA (BAS): (VAW, GLAMOS), Fellay F. (DWFL); BASODINO: (VAW, GLAMOS), Soldati M. (SF); BIFERTEN: (VAW, GLAMOS), Klauser H.; BOVEYRE: (VAW, GLAMOS), Stoebener P. (DWFL); BRESCIANA: (VAW, GLAMOS), Soldati M. (SF); BRUNNI: (VAW, GLAMOS), Planzer M. (AFJ); CAMBRENA: (VAW, GLAMOS), Berchier G. (AWN); CAVAGNOLI: (VAW, GLAMOS), Soldati M. (SF); CHEILLON: (VAW, GLAMOS), Bourdin O. (DWFL); CHLI (NO. 91): (VAW, GLAMOS), Brandes T. (KFA); CORBASSIERE: Bauder A. (VAW, GLAMOS; bauder@vaw.baug.ethz.ch); CORNO: (VAW, GLAMOS), Soldati M. (SF); EIGER: (VAW, GLAMOS), Bauder A. (VAW, GLAMOS; bauder@vaw.baug.ethz.ch), Schai R. (KAWA); EN DARREY: (VAW, GLAMOS), Bourdin O. (DWFL); FINDELEN: (GLAMOS), Bauder A. (VAW, GLAMOS; bauder@vaw.baug.ethz.ch); FORNO: (VAW, GLAMOS), Nyfeler R. (AWN); GAMCHI: (VAW, GLAMOS), Schenk M. (KAWA); GIETRO: Bauder A. (VAW, GLAMOS; bauder@vaw.baug.ethz.ch); GLAERNISCH: (VAW, GLAMOS), Klauser H.; GORNER: Bauder A. (VAW, GLAMOS; bauder@vaw.baug.ethz.ch); GRAND DESERT: (VAW, GLAMOS), Bourban F. (DWFL); GRIES: (GLAMOS), Bauder A. (VAW, GLAMOS; bauder@vaw.baug.ethz.ch); GRIESS (KLAUSEN): (VAW, GLAMOS), Annen B. (AFJ); GROSSER ALETSCH: (GLAMOS), Bauder A. (VAW, GLAMOS; bauder@vaw.baug.ethz.ch); HINTERSULZFIRN: (VAW, GLAMOS), Philippi N. (WN); HOHLAUB: Bauder A. (VAW, GLAMOS; bauder@vaw.baug.ethz.ch); KALTWASSER: (VAW, GLAMOS), Schmidhalter M. (DWFL); KEHLEN: (VAW, GLAMOS), Planzer R. (AFJ); LAVAZ: (VAW, GLAMOS), Brunner L. (AWN); LIMMERN: (VAW, GLAMOS), Steinegger U. (steinegger@meteodat.ch); LISCHANA: (VAW, GLAMOS), Renz G. (AWN); MOIRY: (VAW, GLAMOS), Fellay F. (DWFL); MORTERATSCH, VADRET DA: (VAW, GLAMOS), Godly G. (AWN); MUTT: Bauder A. (VAW, GLAMOS; bauder@vaw.baug.ethz.ch); OBERAAR: Bauder A. (VAW, GLAMOS; bauder@vaw.baug.ethz.ch); OBERER GRINDELWALD: (GLAMOS), Bauder A. (VAW, GLAMOS; bauder@vaw.baug.ethz.ch); PALUE: (VAW, GLAMOS), Berchier G. (AWN); PANEYROSSE: (VAW, GLAMOS), Desarzens J. (FFN); PARADIES: (VAW, GLAMOS), Fisler C. (AWN); PARADISINO (CAMPO): (VAW, GLAMOS), Berchier G. (AWN); PIZOL: (VAW, GLAMOS), Brandes T. (KFA); PLATTALVA: (VAW, GLAMOS), Steinegger U. (steinegger@meteodat.ch); PORCHABELLA: (VAW, GLAMOS), Bieler C. (AWN), Castelberg I. (AWN); RAETZLI (PLAINE MORTE): (GLAMOS), Bauder A. (VAW, GLAMOS; bauder@vaw.baug.ethz.ch); RHONE: (GLAMOS), Bauder A. (VAW, GLAMOS; bauder@vaw.baug.ethz.ch); RIED: (VAW, GLAMOS), Rovina P. (DWFL); SALEINA: (VAW, GLAMOS), Stoebener P. (DWL, DWFL); SANKT ANNA: (VAW, GLAMOS), Eggimann L. (AFJ); SARDONA: (VAW, GLAMOS), Brandes T. (KFA); SCALETTA: (VAW, GLAMOS), Teufen B.; SCHWARZBERG: Bauder A. (VAW, GLAMOS; bauder@vaw.baug.ethz.ch); SEEWJINEN: Bauder A. (VAW, GLAMOS; bauder@vaw.baug.ethz.ch); SESVENNA: (VAW, GLAMOS), Renz G. (AWN); SEX ROUGE: (VAW, GLAMOS), Binggeli J.; SILVRETTA: (GLAMOS), Bauder A. (VAW, GLAMOS; bauder@vaw.baug.ethz.ch); STEIN: (VAW, GLAMOS), Rohrer D. (KAWA); TIATSCHA: (GLAMOS), Bauder A. (VAW, GLAMOS; bauder@vaw.baug.ethz.ch); TIEFEN: (VAW, GLAMOS), Eggimann L. (AFJ); TORTIN GLACIER DE (MONT FORT): (VAW, GLAMOS), Bourban F. (DWFL); TRIENT: (VAW, GLAMOS), Ehinger J.; TRIFT (GADMEN): (GLAMOS), Bauder A. (VAW, GLAMOS; bauder@vaw.baug.ethz.ch); TSANFLEURON: (VAW, GLAMOS), Fellay F. (DWFL); TSCHIERVA: (VAW, GLAMOS), Godly G. (AWN); TSEUDET: (VAW, GLAMOS), Stoebener P. (DWFL); TSIDJIORE NOUVE: (VAW, GLAMOS), Fellay F. (DWFL); UNTERAAR: Bauder A. (VAW, GLAMOS; bauder@vaw.baug.ethz.ch);

PU	GLACIER: Principal Investigator (sponsoring agency)
CH	UNTERER GRINDELWALD: (GLAMOS), Bauder A. (VAW, GLAMOS; bauder@vaw.baug.ethz.ch); VALLEGGIA: (VAW, GLAMOS), Soldati M. (SF); VALSOREY: (VAW, GLAMOS), Stoebener P. (DWFL); VORAB: (VAW, GLAMOS), Deflorin R. (AWN); WALLENBUR: (VAW, GLAMOS), Kläger P. (AFJ); ZINAL: (VAW, GLAMOS), Chevalier G. (DWL)
CN	PARLUNG NO. 94: Li S. (CAS/ITPR; shenghaili1984@gmail.com), Yang W. (CAS/ITPR); URUMQI GLACIER NO. 1: Mu J. (CAREERI-TGS); URUMQI GLACIER NO. 1 E-BRANCH: Mu J. (CAREERI-TGS); URUMQI GLACIER NO. 1 W-BRANCH: Mu J. (CAREERI-TGS)
CO	CONEJERAS: Ceballos Liévano J. (IDEAM; jceballos@ideam.gov.co), Nocua Ruge Y. (IDEAM), Ospina A. (IDEAM)
ES	MALADETA: Cobos Campos G. (UPV; gcobosc@trr.upv.es)
FR	ARGENTIERE: Six D. (IGE; delphine.six@univ-grenoble-alpes.fr), Vincent C. (IGE; christian.vincent@univ-grenoble-alpes.fr); BLANC: Bonnefoy M. (IGE), Thibert E. (IGE; emmanuel.thibert@inrae.fr); BOSSONS: Six D. (IGE; delphine.six@univ-grenoble-alpes.fr), Vincent C. (IGE; christian.vincent@univ-grenoble-alpes.fr); GEBROULAZ: Six D. (IGE; delphine.six@univ-grenoble-alpes.fr), Vincent C. (IGE; christian.vincent@univ-grenoble-alpes.fr); MER DE GLACE: Six D. (IGE; delphine.six@univ-grenoble-alpes.fr), Vincent C. (IGE; christian.vincent@univ-grenoble-alpes.fr); OSSOUE: René P. (AM; asso.moraine@wanadoo.fr); SAINT SORLIN: Six D. (IGE; delphine.six@univ-grenoble-alpes.fr), Vincent C. (IGE; christian.vincent@univ-grenoble-alpes.fr)
IS	BLAGNIPUJOKULL: Gíslason P. (IGS-IMO); BREIDAMJOKULL E. A.: Guðmundsson S. (IGS-IMO); BREIDAMJOKULL E. B.: Guðmundsson S. (IGS-IMO); BREIDAMJOKULL W. A.: Guðmundsson S. (IGS-IMO); BROKARJOKULL: Pálsson B. (IGS-IMO); DEILDARDALSJOKULL: Brynjólfsson S. (IGS-IMO); FALLJOKULL: Þorláksdóttir S. (IGS-IMO); FJALLSJOKULL BY BREIDAMERKURFJALL: Guðmundsson S. (IGS-IMO); FJALLSJOKULL BY GAMLASEL: Guðmundsson S. (IGS-IMO); FLAAJOKULL: Pálsson B. (IGS-IMO); FLAAJOKULL E 148: Pálsson B. (IGS-IMO); GEITLANDSJOKULL: Kristinsson B. (IGS-IMO); GLJUFURARJOKULL: Hjartarson Á. (IGS-IMO); HAGAFELLSJOKULL E: Sigurðsson E. (IGS-IMO); HAGAFELLSJOKULL W: Sigurðsson E. (IGS-IMO); HEINABERGSJOKULL H: Skírnisdóttir H. (IGS-IMO); HRUTARJOKULL: Guðmundsson S. (IGS-IMO); HYRNINGSJOKULL: Haraldsson H. (IGS-IMO); JOKULKROKUR: Eyþórsdóttir K. (IGS-IMO); KALDALONSJOKULL: Matthíasson V. (IGS-IMO); KIRKJUJOKULL: Gröndal B. (IGS-IMO); KVIARJOKULL: Guðmundsson S. (IGS-IMO); LAMBATUNGNAJOKULL: Pálsson B. (IGS-IMO); LEIRUFJARDARJOKULL: Sólbergsson Á. (IGS-IMO); MORSARJOKULL: Kristjánsson R. (IGS-IMO); MULAJOKULL S: Jónsson L. (IGS-IMO); MULAJOKULL W: Jónsson L. (IGS-IMO); NAUTHAGAJOKULL: Jónsson L. (IGS-IMO); REYKJAFJARDARJOKULL: Jóhannesson Þ. (IGS-IMO); SATUJOKULL E: Kárason V. (IGS-IMO); SIDUJOKULL E M 177: Pálsson H. (IGS-IMO); SKAFTAFELLSJOKULL: Þorláksdóttir S. (IGS-IMO); SKEIDARARJOKULL E1: Kristjánsson R. (IGS-IMO); SKEIDARARJOKULL E2: Kristjánsson R. (IGS-IMO); SKEIDARARJOKULL E3: Kristjánsson R. (IGS-IMO); SOLHEIMAJOKULL W: Gunnlaugsson E. (IGS-IMO); SVINAFELLSJOKULL: Þorláksdóttir S. (IGS-IMO); THORISJOKULL: Margeirsson G. (IGS-IMO); TINDFJALLAJOKULL: Þorbergsson A. (IGS-IMO); TORFAJOKULL N: Hálfdánsson Á. (IGS-IMO); TORFAJOKULL S: Hálfdánsson Á. (IGS-IMO); TUNGNAARJOKULL: Hilmarsson S. (IGS-IMO); TUNGNAHRYGGSJOKULL: Jónsdóttir Þ. (IGS-IMO)
IT	ALTA (VEDRETTA) / HOHENF.: Benetton G. (CGI, SGAA), Benetton S. (CGI, SGAA), Perini G. (CGI, SGAA); AMOLA: Ferrari C. (SAT), Gasperini N. (SAT), Travaglia E. (SAT); ANTELAO SUP.: Benetton G. (CGI, SGAA), Benetton S. (CGI, SGAA), Perini G. (CGI, SGAA); AOUILLE: Chevrere R. (PNGP), Nicolino M. (PNGP), Vallet R. (PNGP); ARGUEREY SETT.: Chiarle M. (CNR-IRPI, CGI; marta.chiarle@irpi.cnr.it), Nigrelli G. (CNR-IRPI, CGI); AROLLA: Borre P. (PNGP), Caminada C. (PNGP), Dellanoce M. (PNGP), Peracino A. (PNGP); BARBADORSO DI DENTRO / BAERENBARTF. INNERER: Scaltriti A. (SGAA); BASEI: Cat Berro D. (SMI, d.catberro@nimbus.it), Cullino P. (PNGP), Miravalle R. (PNGP); BELVEDERE (MACUGNAGA): Mortara G. (CGI; giovanni.mortara@irpi.cnr.it), Tamburini A. (IMAGEO, CGI), Versaci S. (CGI); BESSANESE: Rogliardo F. (CGI); BORS: Piccini P. (CGI), Princisvalle T. (CGI), Viani C. (CGI); BROGLIO: Miravalle R. (PNGP);

PU	GLACIER: Principal Investigator (sponsoring agency)
IT	CALDERONE: Boccabella P. (CGI), Bruschi F. (UPe), Caira T. (CGI), Cappelletti D. (UPe, CGI, CAI), Cimini D. (IMAA), D'Aquila P. (Engeoneering), Esposito G. (IIA), Martinelli M. (Engeoneering), Marzano F. (CETEMPS), Montini M. (CGI), Pecci M. (CGI), Pecci M. (DARA, CGI; m.pecci@governo.it), Raparelli E. (CETEMPS), Tuccella P. (CETEMPS; paolo.tuccella@univaq.it), di Fiore T. (AQCF); CAPRA: Bertoglio V. (PNGP, CGI; bervergnano@libero.it), Costanzo L. (PNGP); CARESER: Carturan L. (UNIPD/TeSAF; luca.carturan@unipd.it); CARRO OCCIDENT.: Cullino P. (PNGP), Miravalle R. (PNGP); CASPOGGIO: Fazzini F. (SGL), Porta R. (SGL); CEDEC: Bonetti L. (SGL), Colombarolli D. (SGL; sgl@servizioglaciologicolombardo.it), Fioletti M. (SGL); CEVEDALE FORCOLA / FUERKELEF.: Benetton G. (CGI, SGAA), Benetton S. (CGI, SGAA), Perini G. (CGI, SGAA); CEVEDALE PRINCIPALE / ZUFALLF.: Benetton G. (CGI, SGAA), Benetton S. (CGI, SGAA), Perini G. (CGI, SGAA); CHATEAU BLANC: Perona S. (CGI); CIAMARELLA: Rogliardo F. (CGI); CIARDONEY: Cat Berro D. (SMI; d.catberro@nimbus.it), Fornengo F. (SMI), Mercalli L. (SMI; info@nimbus.it); CORNISELLO MER.: Toro M. (SAT), Valcanover E. (SAT); COUPE DE MONEY: Bertoglio V. (PNGP, CGI; bervergnano@libero.it), Borre P. (PNGP), Caminada C. (PNGP), Dellanoce M. (PNGP); CRODA ROSSA / ROTWANDF.: Benetton G. (SGAA), Benetton S. (SGAA), Toro M. (SGAA); DOSDE OR.: Lojacono G. (SGL), Sosio V. (SGL), Toffaletti A. (SGL), Toffaletti A. (SGL); DOSEGU: Borghi A. (SGL), Cipriani V. (SGL); DZASSET: Borre P. (PNGP), Caminada C. PNGP), Dellanoce M. (PNGP); ENTRELOR SETT.: Rossotto A. (PNGP,; alberto.rossotto@pngp.it), Valfre D. (PNGP); FOND OCCID.: Jordaney J. (PNGP), Pollicini F. (CGI), Rossotto A. (PNGP; alberto.rossotto@pngp.it); FOND OR.: Jordaney J. (PNGP), Pollicini F. (CGI), Rossotto A. (PNGP; alberto.rossotto@pngp.it); FORNI CENTRALE: Colombarolli D. (SGL; sgl@servizioglaciologicolombardo.it), Grasso S. (SGL), Peri I. (SGL), Prandi G. (SGL), Sosio V. (SGL); FRANE (VEDR. DELLE) / STEINSCHLAGF.: Carbone V. (SGAA), Greco G. (SGAA), Tosi P. (SGAA); GLIAIRETTA VAUDET: Pollicini F. (CGI); GOLETTA: Jordaney J. (PNGP), Pollicini F. (CGI); GRAMES ORIENT. + CENTR. / GRAMSENF. OESTL. + ZENTR.: Benetton G. (SGAA), Benetton S. (SGAA); GRAN NEYRON: Vallet V. (PNGP); GRAN PARADISO: Massoni D. (PNGP), Valfre D. (PNGP); GRAN VEDRETTA OR. / GRIESSF.: Bertinotti I. (SGAA); GRAN ZEBRU (CENTRALE): Bonetti L. (SGL), Colombarolli D. (SGL; sgl@servizioglaciologicolombardo.it), Fioletti M. (SGL); GRAN ZEBRU (OCCID.): Colombarolli D. (SGL; sgl@servizioglaciologicolombardo.it), Fioletti M. (SGL); GRAND ETRET: Cerise S. (PNGP; stefano.cerise@pngp.it), Massoni D. (PNGP), Rossotto A. (PNGP; alberto.rossotto@pngp.it), Vallet R. (PNGP); GRUETTA ORIENT.: Gadin G. (CGI); INDREN: Piccini P. (CGI), Princisvalle T. (CGI); LA MARE (SOUTHERN BRANCH): Bertoni E. (CGI, SAT), Carturan L. (CGI, SAT; luca.carturan@unipd.it), Ferrari C. (CGI, SAT), Speri P. (CGI, SAT), Voltolini C. (CGI, SAT); LAGAUN (VEDRETTA DI) / LAGAUN FERNER: Barison G. (SGAA), Sartori G. (SGAA); LANA (VEDR. DI) / AEUSSERES LAHNER KEES: Covi S. (SGAA); LARES: Bertoni E. (SAT), Fellin A. (SAT), Ferrari C. (SAT), Santoni M. (SAT), Speri P. (SAT); LASA / LAASER F.: Saltriti A. (SGAA); LAUSON: Grosa M. (PNGP), Peracino A. (PNGP); LAVACCIU: Nicolussi S. (PNGP); LAVASSEY: Jordaney J. (PNGP), Pollicini F. (CGI), Rossotto A. (PNGP; alberto.rossotto@pngp.it); LOBBIA: Fellin A. (SAT), Ferrari C. (SAT), Gasperini N. (SAT), Pedrotti F. (SAT); LUNGA (VEDRETTA) / LANGENF.: Benetton G. (CGI, SGAA), Benetton S. (CGI, SGAA), Perini G. (CGI, SGAA); LUPO: Oreggioni M. (SGL), Porta R. (SGL), Scotti R. (SGL; riccardo.scotti@meteonetwork.it); MADACCIO (VEDR. DEL) / MADATSCHF.: Rosa S. (SGAA), Rosan R. (SGAA), Sartori G. (SGAA), Seppi R. (SGAA); MALAVALLE (VEDR. DI) / UEBELTALF.: Franchi G. (CGI; giangi.franchi@gmail.com); MANDRONE: Fellin A. (SAT), Ferrari C. (SAT), Gasperini N. (SAT), Pedrotti F. (SAT); MARMOLADA CENTR.: Benetton S. (CGI), Donadelli G. (CGI), Varotto M. (CGI); MAZIA (VEDR. DI) / MATSCHERF.: Bruschi P. (SGAA), Crespi C. (SGAA), Greco G. (SGAA), Le Pera L. (SGAA); MONCIAIR: Massoni D. (PNGP), Vallet R. (PNGP); MONCORVE: Bertoglio V. (PNGP; bervergnano@libero.it), Massoni D. (PNGP), Valfre D. (PNGP), Vallet R. (PNGP); MONEY: Bertoglio V. (PNGP; bervergnano@libero.it), Borre P. (PNGP), Caminada C. (PNGP), Dellanoce M. (PNGP); MONTANDEYNE: Nicolussi S. (PNGP); NARDIS OCC.: Bertoni E. (SAT), Ferrari C. (SAT), Gasperini N. (SAT), Groff M. (SAT), Luchetta D. (SAT), Maestri C. (SAT), Speri P. (SAT);

PU	GLACIER: Principal Investigator (sponsoring agency)
IT	NEL CENTRALE: Miravalle R. ((PNGP), Naudin A. (PNGP); NEVES OR. (GHIAC. DI) / NOEFESF. OESTL.: Franchi G. (CGI; giangi.franchi@gmail.com); NOASCHETTA OCCID.: Naudin A. (PNGP), Permunian R. (PNGP); PALON DELLA MARE LOBO CENTR.: Farinella L. (SGL), Izzo M. (SGL); PALON DELLA MARE LOBO OR.: Farinella L. (SGL), Izzo M. (SGL); PASSO DI BONDO: Barilli A. (SGL); PENDENTE (VEDR.) / HANGENDERF.: Franchi G. (CGI; giangi.franchi@gmail.com); PIODE: Piccini P. (CGI), Princisvalle T. (CGI), Viani C. (CGI); PIZZO FERRE: Congiu E. (SGL), Pironi L. (SGL), Pironi L. (SGL); PIZZO SCALINO: Leoni S. (SGL), Lietti E. (SGL), Monti A. (SGL); PLANOL (VEDR. DI) / PLANAILF.: Benetton G. (SGAA), Benetton S. (SGAA); PREDAROSSA: Urso M. (SGL); RIES OCC. (VEDR. DI) / RIESERF. WESTL.: Benetton G. (SGAA); RIES OR. CENTR. / RIESERF. OESTL. ZENTR.: Toro M. (SGAA), Valcanover E. (SGAA); ROCCIA VIVA: Naudin A. (PNGP), Permunian R. (PNGP); ROSIM (VEDR. DI) / ROSIMF.: Baraldo E. (SGAA), Barison G. (SGAA), Sampieri R. (SGAA); ROSSO DESTRO: Mattiato M. (SGAA), Perotti G. (SGAA); RUTOR: Garino R. (CGI); SALDURA MER. (VEDR. DI) / SALDUR F. SUEDL.: Greco G. (SGAA); SASSO LUNGO OCC. (VEDR. DI) / LENKSTEINF. WESTL.: Perini G. (SGAA, CGI), Saccon G. (SGAA, CGI); SCERSCEN INFERIORE: Salvetti A. (SGL); SERANA (VEDR.) / SCHRANF.: Benetton G. (SGAA), Benetton S. (SGAA); SESIA: Piccini P. (CGI), Princisvalle T. (CGI), Viani C. (CGI); SFORZELLINA: Fugazza D. (CGI, CAI-Valfurva), Smiraglia C. (CGI, CAI-Valfurva; claudio.smiraglia@unimi.it); SISSONE: Almasio A. (SGL); SOCHES TSANTELEINA: Jordaney J. (PNGP), Pollicini F. (CGI), Rossotto A. (PNGP; alberto.rossotto@pngp.it); SOLDA (VEDRETTA DI) / SULDENF.: Rosan R. (SGAA), Sartori G. (SGAA), Seppi R. (SGAA); SURETTA MERID.: Villa F. (SGL; sgl@servizioglaciologicolombardo.it); TIMORION: Favre D. (PNGP); TORRENT: Pollicini F. (CGI); TRAJO: Borre P. (PNGP), Caminada C. (PNGP), Frasca M. (CGI), Rossotto A. (PNGP; alberto.rossotto@pngp.it); TRIBOLAZIONE: Borre P. (PNGP), Caminada C. (PNGP), Dellanoce M. (PNGP); VAL VIOLA OCC.: Sosio V. (SGL); VALEILLE: Borre P. (PNGP), Caminada C. (PNGP), Dellanoce M. (PNGP), Peracino A. (PNGP), Rossotto A. (PNGP; alberto.rossotto@pngp.it); VALLELUNGA (VEDR. DI) / LANGTAUFERERF.: Scaltriti A. (SGAA); VALTOURNANCHE: Giorcelli M. (CGI); VENEROCOLO: Lendvai A. (SGL), Nardon C. (SGL), Pagliardi P. (SGL), Triglia E. (SGL); VENTINA: Gussoni M. (SGL), Regazzoni A. (SGL); ZAI DI DENTRO / ZAY F. INNERER: Benetton G. (SGAA), Benetton S. (SGAA)
KG	BORDU: Ermenbayev B. (TshMRC, TSHMRC), Popovnin V. (MSU; begemotina@hotmail.com), Satylkanov R. (TshMRC, TSHMRC; r.satylkanov@gmail.com), Sayakpayev D. (TSHMRC); KARA-BATKAK: Ermenbayev B. (TshMRC, TSHMRC), Popovnin V. (MSU; begemotina@hotmail.com), Satylkanov R. (TshMRC, TSHMRC; r.satylkanov@gmail.com), Sayakpayev D. (TSHMRC); SARY-TOR: Ermenbayev B. (TshMRC, TSHMRC), Popovnin V. (MSU; begemotina@hotmail.com), Satylkanov R. (TshMRC, TSHMRC; r.satylkanov@gmail.com), Sayakpayev D. (TSHMRC)
KZ	TS.TUYUKSUYSKIY: Kasatkin N. (INGEO, CARGC; kasatkinne@mail.ru)
NO	AUSTERDALSBREEN: Elvehøy H. (NVE; hae@nve.no), Solnes P. (NVE); AUSTRE OKSTINDBREEN: Elvehøy H. (NVE; hae@nve.no), Nesengmo K. (NVE); BLOMSTOELSKARDSBREEN: Elvehøy H. (NVE; hae@nve.no), Probert J. (NVE); BOEVERBREEN: Bakke D. (NVE), Elvehøy H. (NVE; hae@nve.no); BONDHUSBREA: Elvehøy H. (NVE; hae@nve.no), Knudsen G. (NVE); BOTNABREA: Elvehøy H. (NVE; hae@nve.no), Knudsen G. (NVE); BRENNDALSBREEN: Briksdal R. (NVE), Elvehøy H. (NVE; hae@nve.no); BUERBREEN: Buer M. (NVE), Elvehøy H. (NVE; hae@nve.no); CORNELIUSSENBREEN: Elvehøy H. (NVE; hae@nve.no), Nesengmo K. (NVE); ENGABREEN: Elvehøy H. (NVE; hae@nve.no); FAABERGSTOELSBREEN: Elvehøy H. (NVE; hae@nve.no), Åsen S. (NVE); GRAAFJELLSBREA: Elvehøy H. (NVE; hae@nve.no), Knudsen G. (NVE); HAUGABREEN: Kielland P. (NVE); HELLSTUGUBREEN: Andreassen L. (NVE; lma@nve.no); KOPPANGSBREEN: Elvehøy H. (NVE; hae@nve.no), Skirnisson D. (NVE); LANGFJORDJOEKELEN: Elvehøy H. (NVE; hae@nve.no), Kjøllmoen B. (NVE; bkj@nve.no); LEIRBREEN: Bakke D. (NVE), Elvehøy H. (NVE; hae@nve.no); MAARAADALSBREEN: Elvehøy H. (NVE; hae@nve.no); MIDTDALSBREEN: Nesje A. (NVE); MJOELKEDALSBREEN: Elvehøy H. (NVE; hae@nve.no), Kvalberg J. (NVE); NIGARDSBREEN: Elvehøy H. (NVE; hae@nve.no), Åsen S. (NVE); REMBESDALSKAAKA: Elvehøy H. (NVE; hae@nve.no); RUNDVASSBREEN: Elvehøy H. (NVE; hae@nve.no), Jackson M. (NVE); SKJELAATINDBREEN: Elvehøy H. (NVE; hae@nve.no), Karlsen J. (NVE);

PU	GLACIER: Principal Investigator (sponsoring agency)
NO	STEGHOLTBREEN: Aasen J. (NVE), Elvehøy H. (NVE; hae@nve.no); STEINDALSBREEN: Elvehøy H. (NVE; hae@nve.no), Skirnisson D. (NVE); STORBREEN: Andreassen L. (NVE; lma@nve.no); STORJUVBREEN: Bakke D. (NVE), Elvehøy H. (NVE; hae@nve.no); STORSTEINSFJELLBREEN: Elvehøy H. (NVE; hae@nve.no), Sommerseth J. (NVE); STYGGEBREAN: Bakke D. (NVE), Elvehøy H. (NVE; hae@nve.no); STYGGEDALSBREEN: Aasen J. (NVE), Elvehøy H. (NVE; hae@nve.no); SVELGJABREEN: Elvehøy H. (NVE; hae@nve.no), Probert J. (NVE); SYDBREEN: Berg H. (NVE), Elvehøy H. (NVE; hae@nve.no); TROLLBERGDALSBREEN: Elvehøy H. (NVE; hae@nve.no), Karlsen J. (NVE); TROLLKYRKJEBREEN: Elvehøy H. (NVE; hae@nve.no), Klokk T. (NVE); TUFTEBREEN: Elvehøy H. (NVE; hae@nve.no), Åsen S. (NVE); VETLE SUPPHELLEBREEN: Kielland P. (NVE); VINNUFONNA: Elvehøy H. (NVE; hae@nve.no), Malvik A. (NVE)
NP	YALA: Joshi S. (ICIMOD; sharad.joshi@icimod.org)
NZ	BREWSTER: Vargo L. (VUW; lauren.vargo@vuw.ac.nz); FOX / TE MOEKA O TUAWE: Anderson B. (VUW; brian.anderson@vuw.ac.nz), Purdie H. (UCant); FRANZ JOSEF / KA ROIMATA O HINE HUKATERE: Anderson B. (VUW; brian.anderson@vuw.ac.nz)
RU	DJANKUAT: Aleynikov A. (MSU, RFBR), Popovnin V. (MSU, RFBR; begemotina@hotmail.com); GARABASHI: Smirnov A. (RAS/IG, IG RAS); LEVIY AKTRU: Smirnov A. (IG RAS)
SJ	HANSBREEN: Blaszczyk M. (US/IES, malgorzata.blaszczyk@us.edu.pl)
US	COLEMAN: Pelto M. (NCGCP; mspelto@nichols.edu); COLUMBIA (2057): Pelto M. (NCGCP; mspelto@nichols.edu); DEMING: Pelto M. (NCGCP; mspelto@nichols.edu); EASTON: Pelto M. (NCGCP; mspelto@nichols.edu); LOWER CURTIS: Pelto M. (NCGCP; mspelto@nichols.edu); RAINBOW: Pelto M. (NCGCP; mspelto@nichols.edu); SHOLES: Pelto M. (NCGCP; mspelto@nichols.edu)
UZ	BARKRAK SREDNIY: Eshmiratov D. (CICADA, Mininnovation), Mamirov H. (CICADA, Mininnovation), Petrov M. (CICADA, Mininnovation), Umirzakov G. (CICADA, Mininnovation; g.umirzakov@nuu.uz), Yakovlev A. (CICADA, Mininnovation; andreyakovlev@mail.ru); BARKRAK SREDNIY EAST BRANCH: Eshmiratov D. (CICADA, Mininnovation), Mamirov H. (CICADA, Mininnovation), Petrov M. (CICADA, Mininnovation), Umirzakov G. (CICADA, Mininnovation; g.umirzakov@nuu.uz), Yakovlev A. (CICADA, Mininnovation; andreyakovlev@mail.ru)

8 SPONSORING AGENCIES

Abbreviation	Sponsoring Agency
ACINN:	Institute of Atmospheric and Cryospheric Sciences, University of Innsbruck (AT)
AEI:	Agencia Estatal de Investigación, Ministerio de Ciencia e Innovación (ES)
AFJ:	Amt für Forst und Jagd, Kanton Uri (UR) (CH)
AM:	Association Moraine (FR)
ApPC/AfBS:	Agenzia per la Protezione civile, Provincia autonoma di Bolzano - Alto Adige / Agentur für Bevölkerungsschutz, Autonome Provinz Bozen - Südtirol (IT)
AQCF:	L'Aquila Caput Frigoris (IT)
ARC:	Antarctic Research Centre, Victoria University of Wellington (NZ)
ARPA:	Agenzia Regionale per la Protezione dell'Ambiente della Valle d'Aosta (IT)
ASIAQ:	Greenland Ecosystem Monitoring - Climate Basis, Asiaq - Greenland Survey (GL)
ASIAQ-GBN:	GlacioBasis Nuuk, ASIAQ Greenland Survey (GL)
AWN:	Amt für Wald und Naturgefahren, Kanton Graubünden (GR) (CH)
BC-Parks:	BC Parks (CA)
BCHydro:	B.C. Hydro - Power Smart (CA)
CAI:	Italian Alpine Club (IT)
CAI-Valfurva:	Valfurva, Italian Alpine Club (IT)
CAIAG:	Central Asian Institute of Applied Geosciences (KG)
CAREERI:	Cold and Arid Regions Environment and Engineering Research Institute, Chinese Academy of Sciences (CN)
CAREERI-TGS:	Tianshan Glaciological Station, Cold and Arid Regions Environment and Engineering Research Institute (CN)
CARGC:	Central Asian Regional Glaciological Center (KZ)
CAS/ITPR:	Institute of Tibetan Plateau Research, Chinese Academy of Sciences (CN)
CETEMPS:	Center of Excellence Telesensing of Environment and Model Prediction of Severe events (IT)
CGI:	Comitato Glaciologico Italiano (IT)
CICADA:	Cryospheric Climate Services for Improved Adaptation (CH/KG/UZ)
CNRS:	Centre national de la recherche scientifique (FR)
CNRS-UGA:	Centre national de la recherche scientifique, Université Grenoble Alpes (FR)
CRG:	Center for Research of Glaciers, Academy of Sciences of the Republic of Tajikistan (TJ)
DARA:	Dipartimento per gli Affari Regionali e le Autonomie, Presidenza del Consiglio dei Ministri (PCM) (IT)
DGA:	Dirección General de Aguas, Ministerio de Obras Públicas, Gobierno de Chile (CL)
DGUF:	Department of Geosciences, University of Fribourg (CH)
DGUO-NZ:	Department of Geography/Te Ihowhenua, University of Otago (NZ)
DST	Department of Science and Technology (IN)
DWFL:	Dienststelle für Wald, Flussbau und Landschaft, Kanton Wallis (VS) (CH)
DWL:	Dienststelle für Wald und Landschaft, Kanton Wallis (VS) (CH)
EDYTEM:	Laboratoire EDYTEM (UMR 5204 CNRS), CISM Université de Savoie (FR)
EnergieAG:	Energie AG (AT)

Abbreviation	Sponsoring Agency
Engeoneering:	Engeoneering (IT)
FFN:	Service des forêts, de la faune et de la nature, Canton de Vaud (VD) (CH)
FGUA:	Federal Government of Upper Austria (AT)
GEM:	Greenland Ecosystem Monitoring (DK/GL)
GeoSphere Austria	GeoSphere Austria
GGBAS:	Geodesy and Glaciology, Bavarian Academy of Sciences (DE)
GIUZ:	Department of Geography, University of Zurich (CH)
GLAMOS:	Glacier Monitoring in Switzerland (CH)
GTF:	Gobierno de Tierra del Fuego (AR)
Great-Ice:	Great-Ice, Institut de recherche pour le développement (FR)
HD:	Hydrographischer Dienst, Land Salzburg (AT)
HD/LT:	Hydrologischer Dienst, Land Tirol (AT)
HD/SB:	Hydrografischer Dienst, Land Salzburg (AT)
HVL:	Western Norway University of Applied Sciences (NO)
IAA-DG:	Departamento de Glaciología, Instituto Antártico Argentino (AR)
IAA-UNC:	Instituto Antártico Argentino Convenio DNA, Facultad de Ciencias Exactas Físicas y Naturales, Universidad Nacional de Córdoba (AR)
IANIGLA:	Instituto Argentino de Nivología, Glaciología y Ciencias Ambientales, CCT CONICET Mendoza (AR)
ICELab:	Ice, Climate and Environment Laboratory, Queen's University (CA)
ICIMOD:	International Centre for Integrated Mountain Development (NP)
IDEAM:	Instituto de Hidrología, Meteorología y Estudios Ambientales, Subdirección de Ecosistemas e Información Ambiental (CO)
IES:	Institute of Earth Sciences, University of Iceland (IS)
IG RAS:	Institute of Geography, Russian Academy of Sciences (RU)
IGE:	Institut des Géosciences de l'Environnement, CNRS & Université Joseph Fourier Grenoble (FR)
IGNANKaz:	Institute of Geography, National Academy of Sciences of the Kazakh Republic (KZ)
IGS-IMO:	Iceland Glaciological Society, Icelandic Meteorological Office (IS)
IIA:	Istituto sull'Inquinamento Atmosferico, Consiglio Nazionale delle Ricerche (IT)
IMAA:	Istituto di Metodologie per l'Analisi Ambientale, Consiglio Nazionale delle Ricerche (IT)
IMO:	Icelandic Meteorological Office (IS)
INAMHI:	Programa Glaciares Ecuador, Instituto Nacional de Meteorología e Hidrología (EC)
INGEO:	Institute of Geography and Water Security, Ministry of Education and Science (KZ)
INRAE:	Institut national de recherche pour l'agriculture, l' alimentation et l' environnement (FR)
IRD:	Institut de recherche pour le développement (FR)
JNP:	Jasper National Park (CA)
KAWA:	Kantonale Verwaltung Amt für Wald, Kanton Bern (BE) (CH)
KFA:	Kantonsforstamt, Kanton St.Gallen (SG) (CH)
KyrgyzHydromet:	Agency for Hydrometeorology, Ministry of Emergency Situations (KG)
MSU:	Geographical Faculty, Moscow State University (RU)
MeteoTrentino:	Meteo Trentino (IT)
Mininnovation:	Agency for Innovative Development (UZ)
NCGCP:	North Cascade Glacier Climate Project, Nichols College (US)

Abbreviation	Sponsoring Agency
NCHM:	National Center for Hydrology and Meteorology, Royal Government of Bhutan (BT)
NCPOR:	National Center for Polar and Ocean Research, Ministry of Earth Sciences, Government of India (IN)
NHT:	Nationalpark Hohe Tauern (AT)
NPC:	National Power Company (IS)
NPI:	Norwegian Polar Institute, Polar Environmental Centre (NO)
NRCan:	Natural Resources Canada, Geological Survey of Canada (CA)
NU:	Nagoya University (JP)
NU-ENV:	Graduate School of Environmental Studies, Nagoya University (JP)
NVE:	Norwegian Water Resources and Energy Directorate (NO)
ÖAV:	Österreichischer Alpenverein (AT)
PAS:	Institute of Geophysics, Polish Academy of Sciences (PL)
PNGP:	Parco Nazionale Gran Paradiso (IT)
PRC/FESSM:	Polar Research Center, Faculty of Earth Sciences and Spatial Management (PL)
RAS/IG:	Institute of Geography, Russian Academy of Sciences (RU)
RFBR:	Russian Foundation of Basic Research (RU)
Rainfall.NZ:	Rainfall.NZ (NZ)
SAT:	Societa Alpinisti Tridentini (IT)
SF:	Sezione forestale, Cantone Ticino (TI) (CH)
SGAA:	Servizio Glaciologico Alto Adige (IT)
SGL:	Servizio Glaciologico Lombardo (IT)
SMI:	Società Meteorologica Italiana (IT)
TCSM:	Tateyama Caldera Sabo Museum (JP)
TSHMRC:	Tien Shan High Mountain Research Center, Institute of Water Problems and Hydropower (KG)
TSU:	Tomsk State University (RU)
TSU/DG:	Department of Geography, Tomsk State University (RU)
Tarfala:	Tarfala Research Station, Stockholm University (SE)
TshMRC:	Department of Geography, Institute of Water Problems and Hydro Power (KG)
UACH:	Instituto de Ciencias Físicas y Matemáticas, Facultad de Ciencias, Universidad Austral de Chile (CL)
UBC:	University of British Columbia (CA)
UCant:	University of Canterbury (NZ)
UCant/DG:	Department of Geography, University of Canterbury (NZ)
UG/GRS:	Institute of Geography and Regional Science, University of Graz (AT)
UG/IRD:	Institute of Environmental Geosciences, CNRS, IRD, Grenoble-INP, Université Grenoble Alpes (FR)
UGA:	Université Grenoble-Alpes (FR)
UMSA:	Universidad Mayor de San Andrés (BO)
UNBC:	University of Northern British Columbia (CA)
UniBe:	University of Bern (CH)
UNIFR:	University of Fribourg (CH)
UNIPD/Dgsci:	Department of Geosciences, University of Padua (IT)

Abbreviation	Sponsoring Agency
UNIPD/TeSAF:	Department of Land, Environment, Agriculture and Forestry, University of Padua (IT)
UNTDF:	Universidad Nacional de Tierra del Fuego (AR)
UPV:	Departamento de Ingeniería del Terreno, Universidad Politécnica de Valencia (ES)
UPe:	University of Perugia (IT)
US/IES:	Institute of Earth Sciences, University of Silesia in Katowice (PL)
USGS:	United States Geological Survey (US)
USGS-F:	Alaska Science Center, Glaciology, U.S. Geological Survey (US)
UZH:	University of Zurich (CH)
VAW:	Laboratory of Hydraulics, Hydrology and Glaciology, ETH Zurich (CH)
VUB:	Vrije Universiteit Brussels (BE)
VUW:	Victoria University of Wellington (NZ)
WN:	Wald und Naturgefahren, Kanton Glarus (GL) (CH)

9 NATIONAL CORRESPONDENTS

(as of 2023)

AFGHANISTAN	Abeer Ahmad Sajood Earth Science Faculty, University of Kabul Polytechnic University's residential blocks Block No. 5, Apartment No. 8 AFGHANISTAN – Kabul E-mail: abeersajood@gmail.com
ARGENTINA/ ANTARCTICA	Pierre Pitte Instituto Argentino de Nivología, Glaciología y Ciencias Ambientales (IANIGLA) CCT CONICET Mendoza Casilla de Correo 330 Av. Ruiz Leal s/n Parque General San Martín ARGENTINA – 5500 Mendoza E-mail: pierrepitte@mendoza-conicet.gov.ar
AUSTRALIA/ ANTARCTICA	Ben Galton-Fenzi Australian Antarctic Division, Department of the Environment 203 Channel Highway AUSTRALIA – Kingston, Tasmania 7050 E-mail: Ben.Galton-fenzi@aad.gov.au
AUSTRIA	Andrea Fischer Institut für Interdisziplinäre Gebirgsforschung Österreichische Akademie der Wissenschaften Technikerstrasse 21 AUSTRIA – 6020 Innsbruck E-mail: andrea.fischer@oeaw.ac.at
BOLIVIA	Alvaro Soruco Instituto de Investigaciones Geológicas y del Medio Ambiente (IGEMA) Carrera de Ingeniería Geológica – Universidad Mayor de San Andres Calle 27, Cota Cota – P.O. 35140 BOLIVIA – La Paz E-mail: awsoruco@umsa.bo
BHUTAN	Phuntsho Tshering Cryosphere Services Devision National Center for Hydrology and Meteorology Royal Government of Bhutan PB no. 207 BHUTAN – Thimphu E-mail: ptshering@nchm.gov.bt
CANADA	Laura Thomson Department of Geography and Planning Queen's University Mackintosh-Corry Hall, Room E208 CANADA – Kingston, Ontario K7L 3N6 E-mail: l.thomson@queensu.ca

CHILE/ ANTARCTICA

Marius Schaefer
Instituto de Ciencias Físicas y Matemáticas
Campus Isla Teja
Universidad Austral de Chile
Edificio Emilio Pugín, Oficina 420
CHILE – Valdivia
E-mail: mschaefer@uach.cl

CHINA

Li Zhongqin
Tianshan Glaciological Station /
Cold and Arid Regions Environment and Engineering Research Institute (CAREERI)
Chinese Academy of Sciences (CAS)
260 West Donggang Road
P. R. CHINA – 730 000 Lanzhou, Gansu
E-mail: lizq@ns.lzb.ac.cn

COLOMBIA

Jorge Luis Ceballos Lievano
Instituto de Hidrología, Meteorología y Estudios Ambientales (IDEAM)
Subdirección de Ecosistemas e Información Ambientales
Calle 25 D No. 96 B - 70
COLOMBIA – Bogotá
E-mail: jceballos@ideam.gov.co

ECUADOR/ ANTARCTICA

Bolívar Ernesto Cáceres Correa
Programa Glaciares Ecuador
Instituto Nacional de Meteorología e Hidrología (INAMHI)
Iñaquito 700 y Corea
ECUADOR – 16 310 Quito
E-mail: bcaceres@inamhi.gob.ec

FRANCE

Delphine Six
Institut des Géosciences de l'Environnement (IGE)
54, rue Molière
BP 96
FRANCE – 38402 St-Martin-d'Hères Cedex
E-mail: delphine.six@univ-grenoble-alpes.fr

GEORGIA

Levan Tielidze
School of Natural Sciences and Medicine
Ilia State University
Cholokashvili Ave 3/5
GEORGIA – 0162 Tbilisi
E-mail: tielidzelevan@gmail.com

GERMANY

Christoph Mayer
Commission for Geodesy and Glaciology
Bavarian Academy of Sciences
Alfons-Goppel-Str. 11
GERMANY – 80539 München
E-mail: christoph.mayer@lrz.badw-muenchen.de

GREENLAND	Andreas Peter Ahlstrøm Department of Marine Geology and Glaciology The Geological Survey of Denmark and Greenland (GEUS) Øster Voldgade 10 DENMARK – 1350 Copenhagen K E-mail: apa@geus.dk
ICELAND	Hrafnhildur Hannesdóttir Icelandic Meteorological Office Bústaðavegi 9 ICELAND – 108 Reykjavík E-mail: hh@vedur.is
INDIA	Mohd Farooq Azam Discipline of Civil Engineering, Indian Institute of Technology Indore 310, POD 1D, Simrol, Indore, Madhya Pradesh ICELAND – 453552 E-mail: farooqazam@iiti.ac.in
INDONESIA	see AUSTRALIA
IRAN	Neamat Karimi Water Research Institute, Ministry of Energy Shahied Abbaspour Blvd., P.O. Box 16765-313 IRAN – Tehran E-mail: n.karimi@wri.ac.ir
ITALY	Carlo Baroni Università di Pisa Dipartimento di Scienze della Terra Via S. Maria 53 ITALY – 56126 Pisa E-mail: baroni@dst.unipi.it
JAPAN	Koji Fujita Department of Hydrospheric-Atmospheric Sciences (DHAS) Graduate School of Environmental Studies c/o Hydrospheric Atmospheric Research Center Nagoya University JAPAN – Nagoya 464 8601 E-mail: cozy@nagoya-u.jp
KAZAKHSTAN	Igor Severskiy Institute of Geography Ministry-Academy of Sciences of the Republic of Kazakhstan Pushkin Street 99 KAZAKHSTAN – 480 100 Almaty E-mail: iseverskiy@gmail.com

KENYA	Rainer Prinz Institute of Atmospheric and Cryospheric Sciences University of Innsbruck Innrain 52f AUSTRIA – 6020 Innsbruck E-mail: rainer.prinz@uibk.ac.at
KYRGYZSTAN	Ryskul Usubaliev Central Asian Institute of Applied Geosciences (CAIAG) Timur Frunze Str. 73/2 KYRGYZSTAN – 720027 Bishkek E-mail: r.usubaliev@caiag.kg
MEXICO	Hugo Delgado-Granados Instituto de Geofísica Universidad Nacional Autónoma de México Circuito Exterior, C. U. Coyoacán MEXICO – México D. F. 04510 E-mail: hugo@geofisica.unam.mx
MONGOLIA	Otgonbayar Demberel Institute of Earth Science and Technology Department of Geography Khovd University MONGOLIA – Khovd aimag, Jargalant soum E-mail: icecore_ot@yahoo.com
NEPAL	Sharad P. Joshi International Centre for Integrated Mountain Development (ICIMOD) GPO Box 3226, Khumaltar, Lalitpur NEPAL – Kathmandu E-mail: Sharad.Joshi@icimod.org
NEW ZEALAND/ ANTARCTICA	Brian Anderson Antarctic Research Centre Victoria University of Wellington PO Box 600 NEW ZEALAND - Wellington 6140 E-mail: brian.anderson@vuw.ac.nz
NORWAY Mainland	Hallgeir Elvehøy Norwegian water resources and energy directorate (NVE) P.O. Box 5091, Majorstua NORWAY – 0301 Oslo E-mail: hae@nve.no
NORWAY Svalbard	Jack Kohler Norwegian Polar Institute (NPI) Fram Centre P.O. Box 6606, Langnes NORWAY – 9296 Tromsø E-mail: jack.kohler@npolar.no

PAKISTAN

Ali Ghazanfar
Head Water Resources Section
Global Change Impact Studies Center (GCISC)
NCP Complex, Quaid-i-Azam University Campus
PAKISTAN – Islamabad
E-mail: ghazanfar.ali@gcisc.org.pk

PERU

Luzmilla Rosario Dávila Roller
Instituto Nacional de Investigación en Glaciares y
Ecosistemas de Montaña (INAIGEM)
122 Juan Bautista, Huaraz
PERU – Ancash
E-mail: ldavila@inaigem.gob.pe

POLAND

Bogdan Gadek
University of Silesia
Institute of Earth Sciences
60 Bedzinska St.
POLAND – 41 200 Sosnowiec
E-mail: bogdan.gadek@us.edu.pl

RUSSIA

Victor V. Popovnin
Moscow State University
Geographical Faculty
Leninskiye Gory
RUSSIA – 119 991 Moscow
E-mail: begemotina@hotmail.com

SPAIN/
ANTARCTICA

Guillermo Cobos
Departamento de Ingeniería del Terreno ETSICCP
Universidad Politécnica de Valencia
Camino de Vera s/n, Edificio 4I
SPAIN – 46022 Valencia
E-mail: gcobosc@trr.upv.es

SWEDEN

Per Holmlund
Department of Physical Geography and Quaternary Geology
University of Stockholm
SWEDEN – 106 91 Stockholm
E-mail: pelle@natgeo.su.se

SWITZERLAND

Matthias Huss
Department of Geosciences
University of Fribourg
Chemin du musée 4
SWITZERLAND – 1700 Fribourg
E-mail: matthias.huss@unifr.ch

TAJIKISTAN

Abdulkhamid Kayumov
State Scientific Institution «Center for Research of Glaciers
of the Academy of Sciences Tajikistan»
Ispechac-2
TAJIKISTAN – 734019 Dushanbe
E-mail: abdkaumov@mail.ru

TANZANIA	see KENYA
UGANDA	see KENYA
UK/ANTARCTICA	James M. Lea School of Environmental Sciences University of Liverpool UK – Liverpool E-mail: j.lea@liverpool.ac.uk
USA	Mauri Pelto Nichols College 129 Center Road USA – Dudley MA 01571 E-mail: mspelto@nichols.edu
UZBEKISTAN	Gulomjon Umirzakov National University of Uzbekistan Universitet 3 UZBEKISTAN – 100174 Tashkent E-mail: g.umirzakov@nuu.uz